Twenty Seventh Edition

Photovoltaics International

THE TECHNOLOGY RESOURCE FOR PV PROFESSIONALS

Imec Large-area n-PERT cells: Raising the efficiency beyond 22% by selective laser doping
Fraunhofer ISE Development of bifacial n-type solar cells: Status and perspectives
PI-Berlin Potential-induced degradation of thin-film modules: Prediction of outdoor behaviour
ISHF Ion implantation as an enabling technique for the fabrication of back junction back-contact cells within a lean process flow
CSEM Lamination process and encapsulation materials for glass-glass PV module design
SPREE Precursors for enabling higher efficiency silicon wafer solar cells
USPVMC Diamond wire sawing for PV – short and long-term challenges

First Quarter, March 2015

www.pv-tech.org

Photovoltaics International
Twenty Seventh Edition
2015

JA SOLAR

www.jasolar.com

Harvest the Sunshine

Premium Cells, Premium Modules

JA Solar Holdings Co., Ltd.

NO.36, Jiang Chang San Road, ZhaBei, Shanghai 200436, China

Tel: +86 (21) 6095 5888 / 6095 5999 Fax: +86 (21) 6095 5858 / 6095 5959 Email: sales@jasolar.com; market@jasolar.com

Photovoltaics International

Published by:
Solar Media Ltd.,
5 Prescot Street,
London E1 8PA, UK
Tel: +44 (0) 207 871 0122
Fax: +44 (0) 207 871 0101
E-mail: info@pv-tech.org
Web: www.pv-tech.org

Publisher: Tim Mann

Head of Content: Ben Willis
Deputy Head of Content: John Parnell
Commissioning Editor: Adam Morrison
Sub-Editor: Steve D. Brierley
Senior News Editor: Mark Osborne
Reporters: Andy Colthorpe
Design: Tina Davidian
Production: Daniel H Brown, Sarah-Jane Lee

Sales Director: David Evans
Account Managers: Adam Morrison,
Graham Davie, Lili Zhu

Cover image: A silicon wafer undergoing laser doping for the creation of a selective front surface field.
Image courtesy of imec, Leuven, Belgium

Printed by Buxton Press
Photovoltaics International
Twenty Sixth Edition
First Quarter 2015
Photovoltaics International is a quarterly journal published in February, May, August and November.

Distributed in the USA by Mail Right International, 1637 Stelton Road B4, Piscataway, NJ 08854.

ISSN: 1757-1197

USPS Information
USPS Periodical Code: 025 313

Periodicals Postage Paid at
New Brunswick, NJ
Postmaster: Send changes to:
Photovoltaics International,
Solar Media Ltd., C/o 1637 Stelton Road, B-4, Piscataway, NJ 08854, USA

Foreword

Now that the PV industry has unquestionably entered a new growth phase, all eyes are on which technologies will win through into the mainstream of PV manufacturing. PERC, n-type, p-type bifacial, heterojunction – all have become familiar terms in the ever-growing constellation of solar cell technologies. The question is which will offer manufacturers what they are looking for in improving efficiencies and cutting costs.

With the upturn now well in motion, *Photovoltaics International* has begun tracking the cell and module expansion plans announced by the major manufacturers. In this issue of the journal we publish the second instalment in what will now become a series (p.17).

Among the many interesting trends highlighted in this unique industry resource is the prevalence of PERC cell technology in manufacturers' future plans. According to our analysis, a significant majority of the c-Si cell capacity expansion plans made public since last year have included PERC technology.

One might almost be tempted to say that PERC is now a mainstream technology as manufacturers seek better efficiencies through existing production lines. If this is the case, the question then arises: what comes after PERC?

Another two promising technologies that are currently the subject of much endeavour in the R&D world are PERC's close cousins - passivated emitter and rear locally diffused – PERL - and passivated emitter rear totally diffused – or PERT – cells. Both offer a number of benefits that go above and beyond those offered by PERC.

On p.45 of this issue, researchers from Belgium's imec describe their n-PERT programme, specifically how they have used laser doping processes to push efficiencies past 22%. Using this process, the team hope to go even further, with an efficiency of 22.5% already in their sights.

The theme is taken up by scientists from Fraunhofer ISE, who on p.61 present a paper detailing their work in the development of bifacial n-type PERT cells. The peak conversion efficiency achieved by the Fraunhofer team using such technology currently stands at around 19.9%, but their paper sets out methods by which they believe much higher efficiencies could feasibly be achieved – of 22% and even as high as 24%.

Despite the promising advances described in these and other contributions to the latest *Photovoltaics International*, this issue ends on a cautionary note with a report on the winding up of the Sophia project (p.94). This four-year programme, which ended in January, was funded by the European Commission with the express aim of improving the coordination of the many research activities going across the continent in the field of PV research.

Although in many ways the project was a great success, a two-day series of events to mark its end saw some heated debate about the future *raison d'être* of PV research in Europe when the continent's solar industry is in such a state of decline. While no firm answers were offered to this multi-faceted question, the prognosis was not all doom and gloom: Sophia will morph into the so-called Cheetah programme, which will carry on much of its predecessor's good work. It's clear that those at the vanguard of European solar R&D aren't going to give up without a fight.

Ben Willis
Head of Content
Solar Media Ltd

Photovoltaics International

Photovoltaics International's primary focus is on assessing existing and new technologies for "real-world" supply chain solutions. The aim is to help engineers, managers and investors to understand the potential of equipment, materials, processes and services that can help the PV industry achieve grid parity. The Photovoltaics International advisory board has been selected to help guide the editorial direction of the technical journal so that it remains relevant to manufacturers and utility-grade installers of photovoltaic technology. The advisory board is made up of leading personnel currently working first-hand in the PV industry.

Editorial Advisory Board

Our editorial advisory board is made up of senior engineers from PV manufacturers worldwide. Meet some of our board members below:

Prof Armin Aberle, CEO, Solar Energy Research Institute of Singapore (SERIS), National University of Singapore (NUS)

Prof Aberle's research focus is on photovoltaic materials, devices and modules. In the 1990s he established the Silicon Photovoltaics Department at the Institute for Solar Energy Research (ISFH) in Hamelin, Germany. He then worked for 10 years in Sydney, Australia as a professor of photovoltaics at the University of New South Wales (UNSW). In 2008 he joined NUS to establish SERIS (as Deputy CEO), with particular responsibility for the creation of a Silicon PV Department.

Dr. Markus Fischer, Director R&D Processes, Hanwha Q Cells

Dr. Fischer has more than 15 years' experience in the semiconductor and crystalline silicon photovoltaic industry. He joined Q Cells in 2007 after working in different engineering and management positions with Siemens, Infineon, Philips, and NXP. As Director R&D Processes he is responsible for the process and production equipment development of current and future c-Si solar cell concepts. Dr. Fischer received his Ph.D. in Electrical Engineering in 1997 from the University of Stuttgart. Since 2010 he has been a co-chairman of the SEMI International Technology Roadmap for Photovoltaic.

Dr. Thorsten Dullweber, R&D Group Leader at the Institute for Solar Energy Research Hamelin (ISFH)

Dr. Dullweber's research focuses on high efficiency industrial-type PERC silicon solar cells and ultra-fineline screen-printed Ag front contacts. His group has contributed many journal and conference publications as well as industry-wide recognized research results. Before joining ISFH in 2009, Dr. Dullweber worked for nine years in the microelectronics industry at Siemens AG and later Infineon Technologies AG. He received his Ph. D. in 2002 for research on Cu(In,Ga)Se2 thin-film solar cells.

Julia Hamm, president and CEO, Solar Electric Power Association (SEPA)

SEPA is an educational non-profit organization dedicated to helping utilities integrate solar power into their energy portfolios. Prior to leading SEPA, Julia Hamm worked as a senior associate at ICF International where she supported the US Environmental Protection Agency with implementation of its ENERGY STAR programme. She holds a Bachelors of Science in Business Management from Cornell University.

Yong Liu, Chief Operating Officer and Chief Technology Officer, JA Solar

Yong Lui has more than 15 years of operation management experience at semiconductor wafer and solar cell manufacturing facilities. Prior to joining JA Solar, he served as fab director at Semiconductor Manufacturing International Corporation (SMIC), responsible for running three 12-inch wafer foundry fabs, which were the most advanced wafer fabs in China. Mr. Liu received his master's degree in solid state chemistry and bachelor's degree in solid state physics from the University of Science and Technology of China in 1992 and 1990, respectively.

Florian Clement, Head of Group, MWT solar cells/printing technology, Fraunhofer ISE

Dr. Clement received his Ph.D in 2009 from the University of Freiburg. He studied physics at the Ludwigs-Maximilian-University of Munich and the University of Freiburg and obtained his diploma degree in 2005. His research is focused on the development, analysis and characterization of highly efficient, industrially feasible MWT solar cells with rear side passivation, so called HIP-MWT devices, and on new printing technologies for silicon solar cell processing.

Sam Hong, Chief Executive, Neo Solar Power

Dr. Hong has more than 30 years' experience in solar photovoltaic energy. He has served as the Research Division Director of Photovoltaic Solar Energy Division at the Industry Technology Research Institute (ITRI), and Vice President and Plant Director of Sinonar Amorphous Silicon Solar Cell Co., the first amorphous silicon manufacturer in Taiwan. Dr. Hong has published three books and 38 journal and international conference papers, and is a holder of seven patents. In 2011 he took office as Chairman of Taiwan Photovoltaic Industry Association.

Matt Campbell, Senior Director, Power Plant Products, SunPower

Matt Campbell has held a variety of business development and product management roles since joining the SunPower, including the development of the 1.5MW AC Oasis power plant platform, organized SunPower's power plant LCOE reduction programmes, and the acquisition of three power plant technology companies. Campbell helped form a joint venture in Inner Mongolia, China for power plant project development and manufacturing. He holds an MBA from the University of California at Berkeley and a BBA in Marketing, Finance, and Real Estate from the University of Wisconsin at Madison.

Ru Zhong Hou, Director of Product Center, ReneSola

Ru Zhong Hou joined ReneSola as R&D Senior Manager in 2010 before being appointed Director of R&D in 2012. Before joining ReneSola he was a researcher for Microvast Power Systems, a battery manufacturer. His work has been published in numerous scientific journals. He has a Ph.D. from the Institute of Materials Physics & Microstructures, Zhejiang University, China.

The future of solar is us.

Suntech-Be Unlimited!

Learn more at: ***www.suntech-power.com***

SUNTECH
BE UNLIMITED

Contents

inter solar
connecting solar business

DISCOVER THE WORLD OF INTERSOLAR

Intersolar Europe | Munich
Intersolar North America | San Francisco
Intersolar South America | São Paulo
Intersolar India | Mumbai
Intersolar China | Beijing
Intersolar Summits | Worldwide

Discover the World's Leading
Exhibition Series for the Solar Industry
www.intersolarglobal.com

Contents

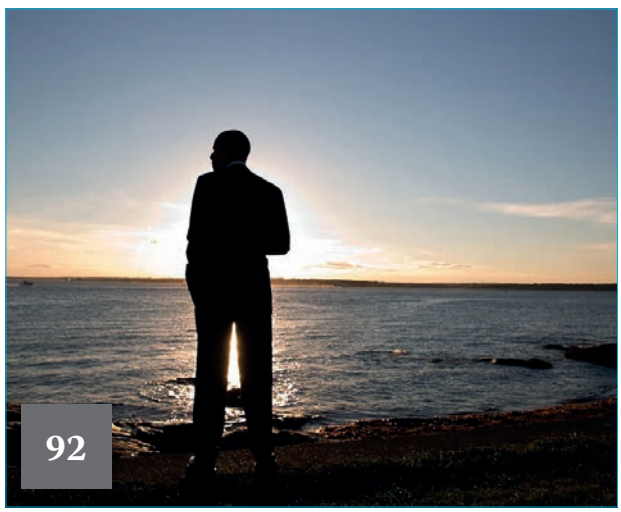

Fab & Facilities

News

Patchy recovery for PV equipment suppliers - SEMI

The latest figures from global microelectronics industry body SEMI suggest a stumbling recovery for PV equipment suppliers worldwide.

According to SEMI's latest analysis, PV equipment bookings and billings both fell in between the second and third quarters of 2014. Billings decreased to US$264 million in Q3, up 36% on the same quarter last year but down 17% on Q2. Third quarter bookings stood at US$157 million, 71% higher than Q3 2013 but down 33% on Q2 2014.

The quarterly book-to-bill ratio remained below parity at 0.6. Since the beginning of 2012, the book-to-bill ratio has only been above 1 once – in the first quarter of 2014. SEMI noted that Q3 2014 equipment billings fell in all regions except Europe, though Asia is still the largest regional market with more than 80% of total PV equipment billings.

Source: Meyer Burger

PV tool manufacturers saw a patchy recovery in 2014, according to SEMI.

Upgrades and expansions

SunEdison considers fully integrated PV manufacturing site in India

Major PV energy provider, SunEdison, has added Gujarat, India, to the list of potential sites for its plans to become a fully integrated PV manufacturer.

The US-based fabless photovoltaics energy provider (PVEP) said in a statement in January that it had signed a memorandum of understanding (MoU) with Indian conglomerate, Adani Enterprises, to establish a joint venture (JV) fully integrated (polysilicon to module) manufacturing cluster in Mundra, Gujarat at a cost of around US$4 billion. SunEdison has a similar exploratory MoU for a new manufacturing base in Saudi Arabia.

Talesun building 500MW integrated PV plant in Thailand

Chinese PV manufacturer Zhongli Talesun has officially started construction of a 500MW integrated solar cell and modules assembly plant in the Thai-China Industrial Park in Rayong, Thailand. Talesun said that the production plant would be fully automated and employ advanced processing technology to produce high-efficiency solar cells and modules with production expected to start in October 2015.

According to Wang Baixing, chairman of state-owned Zhongli Sci-Tech Group, the company's majority owner, the production plant in Thailand would service plans to invest RMB15 billion (US$2.4 billion) in more than 1GW of PV projects in the country over the next three years.

India's Waree Energies to expand capacity to 1GW by summer

Waaree Energies, one of India's largest PV module manufacturers, is significantly adding capacity to meet demand. Having already expanded capacity to 500MW it now plans to double that to 1GW in the run up to summer.

Waaree said that it had recently completed a 250MW module assembly expansion phase at its plant Surat, Gujarat, taking nameplate capacity to 500MW. The company claimed that as a result of the expansion it had become the largest single location for PV module manufacturing in India. However, Waaree noted that recent plans by the Indian government to raise the target of PV installations to 100GW by 2022 as well as demand from countries such as the UK and Europe in general as well as Japan and countries in Africa meant it would further expand capacity to 1,000MW by June.

Moser Baer completes two-year manufacturing technology upgrade

Indian PV manufacturer and project developer, Moser Baer Solar has said that a strategy announced back in January 2012 to vastly improve its competitive position in the industry had been completed.

Competition from China and industry overcapacity had originally forced Moser Baer Solar to curtail production and seek ways to upgrade its c-Si solar cell and a-Si thin-film technologies to offer higher performance products.

Deploying thin-film deposition techniques garnered from the acquisition of a Royal Philips subsidiary, OM&T a specialist in blue-ray optical processes in 2007, Moser Baer Solar said in early 2012 that it would upgrade its solar cell processes using metal and intrinsic layer semiconductor technology (MIST) to achieve average cell conversion efficiencies of 21%. It would therefore join the few cell producers that were producing conversion efficiencies above 20%.

Jobs

German module manufacturer Solar Fabrik enters administration

Solar-Fabrik, one of the last remaining PV module manufacturers still in German ownership filed for insolvency, but under self-administration, at the local court of Freiburg.

The company said that the insolvency proceedings were due to liquidity issues it had projected could occur in the course of the second quarter of 2015, without providing further details. Solar-Fabrik noted that it was not suffering from any form of over-indebtedness and was not insolvent. Solar-Fabrik Wismar, a subsidiary of the company, was also said to have filed for insolvency under self-administration at the same court.

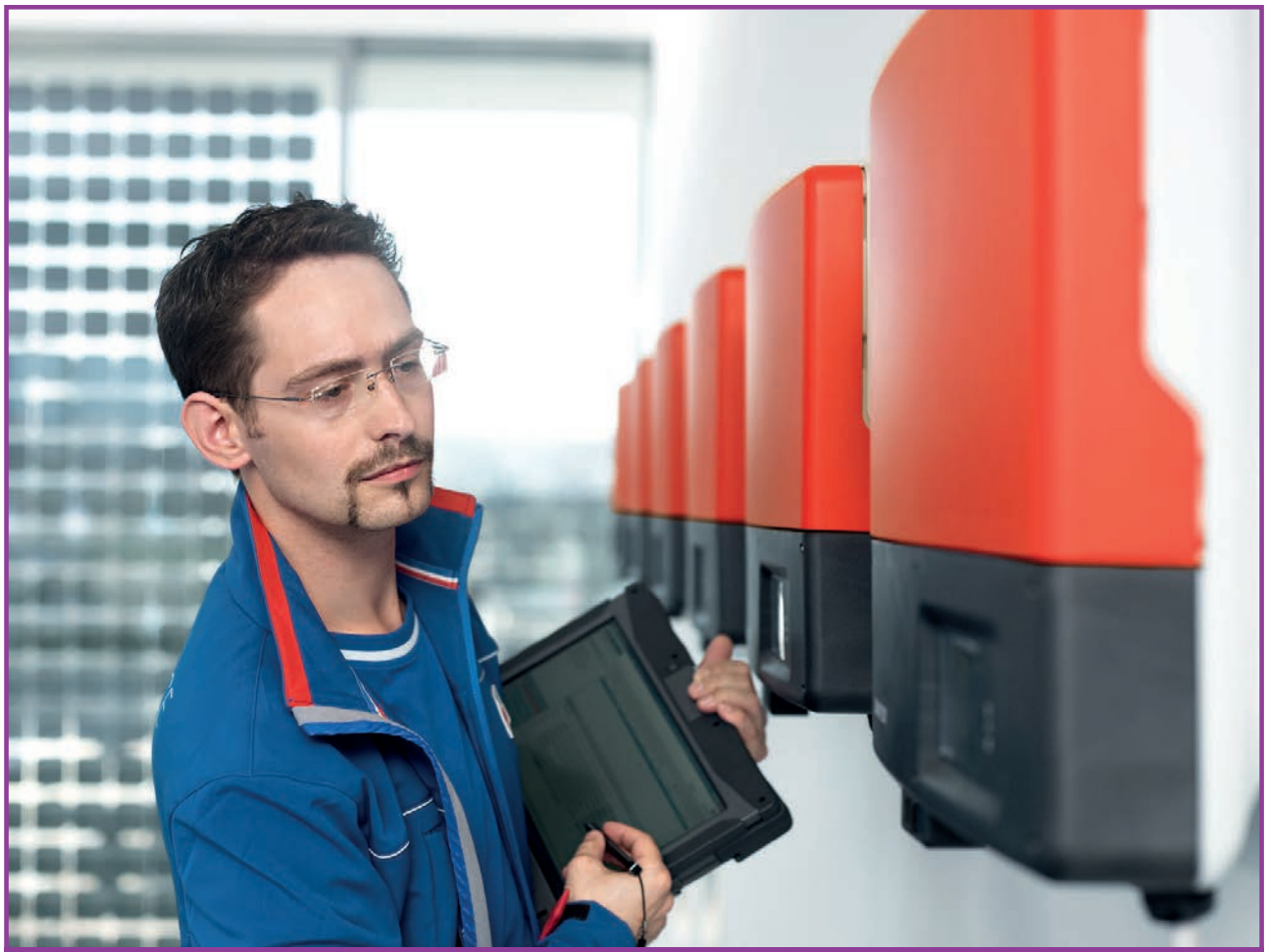

Source: SMA Solar

SMA has been forced to increase the number of staff layoffs this year by 1,000

SMA Solar to shed 1,000 jobs and one board member

Major PV inverter manufacturer, SMA Solar Technology, is slashing a further 1,000 jobs, primarily in Germany, due to lower expected sales in 2015 from its traditional German and European markets. SMA Solar had previously announced around 600 full-time job cuts in a bid to return to profitability.

The company noted that a total of 1,600 job cuts would be implemented by the end of June 2015. The company said that around 1,300 full-time jobs in Germany and approximately 300 full-time positions in international locations would be cut. SMA Solar had 4,667 full-time employees at the end of 2014. It also trimmed its management board down to four members.

Labs get certified

Trina lab secures 'first ever' TÜV power measurement cert

Trina Solar has claimed its State Key Laboratory Testing Center has become the first institute to attain TÜV Rheinland's Power Measurement Uncertainty Assessment Service ("UAS") Certificate.

The certificate authenticates the facility's on-site power measurements. All products assessed at the centre will now carry the TÜV Rheinland certification mark. Trina's processes, equipment and staff carrying out testing conform with both TÜV and International Electrotechnical Commission (IEC) standards.

"The PV industry is facing fierce competition. Modules verified by an objective third party greatly enhance customer confidence and increase sales," said Wei Zhou, VP of Trina Solar's quality department. "With the continuing

Source: Trina Solar

Trina Solar's Testing Center has received a TÜV Rheinland certification for its on-site power measurements.

Source: JA Solar

China's tier-one module producers were sold out in Q1 2015, IHS said.

development of solar power in China, ensuring the quality of solar power plants is paramount. TÜV Rheinland's recognition of our internal power measurement system assures our partners and customers of the reliability and quality of our modules."

ReneSola's PV testing lab given witness testing certification by UL

The Underwriters Laboratories (UL) has approved ReneSola's PV testing lab to undertake supervized product testing under its Witness Testing Data Program (WTDP). The WTDP certification enables ReneSola's PV testing laboratory in Jiangsu, China to potentially bring products to market sooner.

"This UL certification reflects our longstanding commitment to quality and the world-class level of our technical facilities," said Dr. Bill Hou, ReneSola's product centre director. "By working with experienced UL staff in our own laboratory, we will not only ensure that our award-winning PV products meet all applicable quality and performance standards, but will also help us to deliver those products to our worldwide sales and distribution centres more quickly."

Market

Solar R&D needs 'systemic shock' to avert death of European PV

Europe's approach to research and innovation in photovoltaics needs "systemic" change if the continent is to avoid seeing its solar manufacturing industry entirely wiped out in the coming years.

That was the stark warning issued by Vincent Bes, chief executive of Photowatt, one of Europe's few remaining integrated PV manufacturers, at a gathering in January of leading figures in PV R&D at France's INES solar institute in Chambery.

Bes was speaking a day after Hanwha Q CELLS announced the closure of its last plant in Germany and the transition of its remaining production operation to Malaysia. Citing the Q CELLS example, Bes said that without a "systemic shock" to the way Europe's PV R&D infrastructure is organised, the continent faced the real prospect of losing all its integrated PV manufacturing capability to Asia.

"We won the first battle, which was to create a solar industry," Bes said. "We lost the second battle and China won everything – not because they were smarter than us, just because they were richer than us and will continue to be. In the next battle, if we want to survive, why don't we merge all the research centres in Europe? There are billions spent [on PV R&D] every year, but if there is no industry, what is the point? There is no point."

For a full account of the symposium at which Bes was speaking, see the Market Watch section, p.94.

SolarCity expects 1GW solar module production target to be reached in early 2017

SolarCity said that it expects tool install to begin at its first 1GW integrated PV module assembly plant in early 2016, despite construction being slowed due to heavy snow falls in Buffalo, New York State.

SolarCity, the largest residential PV installer in the US also noted that it still expected to reach full annualized capacity of 1GW in early 2017.

On the technology front, SolarCity noted that it had completed the migration of Silevo's high-efficiency monocrystalline cells to larger 156mm x 156mm wafer size, up from 125mm x 125mm sized wafers, typically used for monocrystalline solar cells.

Chinese tier-one PV module suppliers sold out in Q1 – IHS

According to market research firm IHS, Chinese tier-one PV module suppliers were mostly sold out in the first quarter of 2015 due to strong demand from markets such as China, Japan and the UK as well as in South and Central America.

IHS noted that the overhang of PV projects in China was also playing a key factor in maintaining high demand for modules in the first quarter.

"We have heard from suppliers and buyers about the expected shortage of Chinese tier-one modules in Q1," said Jessica Jin, analyst for solar at IHS. "After a demand surge in the fourth quarter of 2014, Chinese tier-one module suppliers decreased their inventory significantly. Considering the Chinese New Year occurs in the first quarter, companies won't run their capacity in full production, either."

Precursors for enabling higher-efficiency silicon wafer solar cells

Bram Hoex, School of Photovoltaic and Renewable Energy Engineering (SPREE), University of New South Wales (UNSW), Sydney, Australia

ABSTRACT

The manufacturers of silicon wafer solar cells are constantly looking into cost-effective ways to increase the efficiency of their solar cells. Most of these enhancements result from incremental improvements and can be achieved by optimizing existing processes. However, it is widely recognized that in order to further improve the silicon wafer solar cell efficiency, new solar cell architectures are required. This will in turn require new manufacturing processes, which will typically involve new production equipment and consumables. New consumables can play an important role in the applicability or success of a new process step; in this paper a specific focus will be on the precursors used for the deposition of surface passivation films, such as silicon nitride and aluminium oxide.

Introduction

Table 1 gives a short, non-exhaustive summary of new (for silicon wafer PV) precursors that either have been recently introduced or are under serious consideration for inclusion in silicon wafer solar cell manufacturing processes. Most of these precursors are hazardous (e.g. toxic or pyrophoric) and thus require careful consideration before being allowed in pilot or high-volume manufacturing. These consumables, however, are not new to high-volume manufacturing in other sectors or even in PV. For example, trimethyl aluminium (TMA) is widely used in the chemical and semiconductor industries, such as for the synthesis of III–V compound semiconductors; phosphine (PH_3) and diborane (B_2H_6) are extensively used for the manufacturing of thin-film transistor (TFT) displays as well as for thin-film silicon solar cells.

The requirements of silicon wafer solar cell manufacturing, however, are different from those of, for example, the semiconductor industry. The profit margins in silicon wafer PV are currently (and are expected to remain) very low, and there is consequently a strong cost pressure on the entire supply chain.

> "The requirements of silicon wafer solar cell manufacturing are different from those of the semiconductor industry."

Precursors are generally available in various grades, where the lower-quality grades are typically significantly cheaper than their higher-quality-grade counterparts. The grade of the precursor is usually related to the purity level, with the lower grades having higher impurity levels. One development that is often seen is the introduction of 'solar-grade' precursors which have a significantly lower price than the 'semiconductor-grade' precursors. These precursor grades are developed by suppliers, such as Air Liquide, AkzoNobel and The Linde Group, in close collaboration with industry, research institutes or academic partners, as will also be seen later in this paper in the case of silane and TMA.

The kinds of impurity that can be tolerated are also highly dependent on the actual process or type of equipment that is used. For example, in the case of ion implantation it makes a big difference whether a mass-analysed or a non-mass-analysed system is used. Non-mass-analysed ion implanters (i.e. basically all currently available commercial ion implanters for silicon wafer solar cells) cannot discriminate between impurities on the basis of a difference in atomic mass and will consequently also introduce undesired impurities into the wafer. In the case of aluminium oxide deposition, the difference between using atomic layer deposition (ALD) or plasma-enhanced chemical vapour deposition (PECVD) is significant. ALD is in

Cell technology	Material	Most common precursors
Passivated emitter and rear contact (PERC), or Al local back-surface field (Al-LBSF) solar cells	AlO_x	TMA
	SiO_x	SiH_4 and N_2O or OCTMS
	SiN_x	SiH_4 and NH_3
Ion-implanted solar cells	P dopant	PH_3
	B dopant	BF_3 or B_2H_6
Heterojunction solar cells	a-Si:H	SiH_4 and H_2
	B doping	TMB or B_2H_6 (heavily diluted)
	P doping	PH_3
	Transparent conductive oxide (TCO)	ITO target
		DEZ, TMA, TMGa, B_2H_6

Table 1. Precursors recently introduced or under consideration for use in solar cell manufacturing processes.

essence a low-temperature chemical vapour deposition (CVD) process and thus more strongly dependent on the reactivity of the molecules used, whereas PECVD employs highly reactive plasmas, which are considerably less selective.

The remainder of this paper will go into more detail on the precursor-related research that has been done for silicon nitride and aluminium oxide, with a focus on the application to silicon wafer solar cells.

Silicon nitride deposition

The main chemistry used for PECVD of silicon nitride in silicon wafer PV is based on silane (SiH_4) and ammonia (NH_3). Both these gases are hazardous: silane is a pyrophoric gas and ammonia is an irritating and flammable gas. Consequently, there have been extensive efforts to replace these gases by alternative precursors or deposition methods that are less hazardous. Physical vapour deposition (predominantly sputtering) is a commonly used method in other industries for the deposition of silicon nitride films. In the case of silicon wafer solar cells, however, silicon nitride not only serves as an anti-reflection coating but also has to provide bulk and surface passivation: hence the sputtering process cannot directly be transferred from other industries.

Fraunhofer ISE and Applied Materials have spent significant effort in optimizing the silicon nitride sputtering process for silicon wafer solar cells, as reported by Wolke et al. in 2004 [1]. The results obtained at that time were reasonably good and the process was consequently commercialized by Applied Materials on their ATON platform, with a number of systems being sold to the PV industry. The level of bulk and surface passivation, however, was typically found to be lower than that of its PECVD counterparts, and the sputtering process did not therefore gain significant traction in the PV industry. Oerlikon is currently the only company that offers a system for the sputter deposition of silicon nitride for silicon wafer solar cells [2], with the vast majority of the silicon wafer PV industry still using PECVD for the deposition of silicon nitride films.

Some work has been done on replacing silane by an alternative that is less hazardous but can still meet the performance and cost targets of the PV industry. In 2009 Khang et al. [3] published the results of a study in which a non-pyrophoric Si precursor made by the company Sixtron was used for the deposition of a carbon-containing silicon nitride film. The solar cell efficiency results at that time were similar to those achieved by silicon nitride, and the process was tested on a pilot-scale level by various solar cell manufacturers. It is not clear, however, whether this precursor has actually been used in high-volume manufacturing. Hoex et al. [4], in 2006, also tested an alternative silane precursor for the deposition of PECVD silicon oxide films. Even though the performance was reasonable on dedicated test structures, the films did not perform as well in actual solar cell devices, and the process was consequently not transferred to the PV industry [5].

Various researchers have been looking at reducing the cost of ammonia, or at even using nitrogen gas as an alternative nitrogen source. ISC Konstanz in collaboration with Air Liquide investigated the impact of the ammonia precursor quality and the filling level of the cylinder on multicrystalline silicon wafer solar cell performance [6]. They found that the precursor grade could easily be reduced without impacting the solar cell efficiency. In the following year they reported some additional information regarding long-term stability, and it was determined that long-term stability was not affected, provided the grade of the ammonia was sufficiently high [7]. Typical industrial-grade ammonia was found to be insufficiently pure, while the intermediate grade demonstrated similar performance to that of semiconductor-grade ammonia and could therefore be used for solar cell manufacturing.

Hong et al. [8] from Eindhoven University of Technology investigated the deposition of silicon nitride using nitrogen gas instead of ammonia along with the expanding thermal plasma technology that was later commercialized by OTB Engineering (later OTB Solar and now part of the Meyer Burger Group). In that study it was found that the level of bulk passivation was lower when nitrogen was used instead of ammonia as a nitrogen precursor, and the ammonia process was eventually implemented in commercial systems.

Aluminium oxide

Aluminium oxide was first investigated in the late 1980s by Hezel and Jaeger [9], who demonstrated reasonable levels of surface passivation on undiffused silicon surfaces. Interest was rekindled in 2006 by the work done by Agostinelli et al. [10] and Hoex et al. [11]. Aluminium oxide is particularly interesting because of its intrinsic negative fixed charge, which makes it an ideal candidate for the passivation of p-type c-Si surfaces [12]. This was also quickly demonstrated at the solar cell device level on p-type passivated emitter and rear contact (PERC) and n-type passivated emitter and rear locally diffused (PERL) solar cells [13,14]. The original experiments were all performed using ALD to deposit the aluminium oxide film; however, very quickly it was shown that more conventional PECVD and sputtering could also yield aluminium oxide films with an adequate level of surface passivation [15,16]. ALD and PECVD used TMA as the aluminium precursor, while sputtering uses a solid aluminium target as the aluminium precursor.

The first technology that was transferred to the pilot level was PECVD by the company Roth & Rau (now part of the Meyer Burger Group) [17]. The biggest challenges of transferring the aluminium oxide process to the PV industry were the pyrophoric nature of TMA and the absence of a standard gas-delivery system. The PV industry was obviously used to handling pyrophoric gases, as almost all silicon wafer solar cell producers use silane as a silicon precursor for the deposition of their silicon nitride films. However, TMA is a liquid at room temperature: as a consequence, some sort of delivery system is required that converts the liquid TMA to its gaseous form for subsequent use in the PECVD or ALD process.

Schematics of the various delivery systems are shown in Figs. 1–3. In all cases, the gas line between the gas-delivery system and the reactor is heated to prevent condensation of the TMA in the gas line. All gas flows are controlled by a mass flow controller (MFC), and the liquid TMA flow in the direct injection system is controlled by a liquid flow controller (LFC).

"The biggest challenges of transferring the aluminium oxide process to the PV industry were the pyrophoric nature of TMA and the absence of a standard gas-delivery system."

Bubbler systems (Fig. 1) are typically used to evaporate TMA in a research environment or even in semiconductor manufacturing, but the gas-flow requirements for PV are unfortunately not compatible with bubbler systems. In addition, bubbler systems experience significant downtime during canister changes.

The next possible solution is the *vaporizer system*, which basically consists of a liquid-delivery system and a vaporizer, as shown schematically in Fig. 2. The vaporizer contains a controlled volume of TMA kept at an elevated temperature and thus supplies a pure precursor gas that can be controlled by an MFC. Subsequently this pure precursor gas is mixed with a desirable flow of carrier gas and transported to the process chamber through a heat-traced line (to prevent condensation). The advantage of this system is that the precursor flow can be independently controlled from the carrier flow, unlike in the case of the bubbler system; moreover, higher precursor flows can be obtained. One of the main downsides of the vaporizer system is that there is a significant amount of liquid TMA in the liquid-delivery system as well as the vaporizer, which obviously poses more of a challenge from a risk-management point of view.

The more recent systems use the *direct injection method* (Fig. 3), whereby the liquid TMA flow is controlled by an LFC and subsequently evaporated and mixed in a controlled evaporator mixer (CEM) unit. In this way, a large amount of liquid TMA is present in only one location, which is easier to manage from a safety point of view.

A schematic of what a factory-wide TMA-delivery system could look like is shown in Fig. 4. The two TMA vessels (one in service and one in standby to allow for continuous operation) are kept in a dedicated liquid-delivery room. The liquid TMA is then transported via small-diameter (double-contained) pipes to the various production tools.

The discussion above illustrates an important 'challenge' that is often neglected when introducing new technologies to the PV industry: even though the precursor is intensively used in other industries, the actual implementation in high-volume PV manufacturing is not just a simple copy-and-paste, especially when the precursor introduces a new hazard category (e.g. a liquid pyrophoric) to the factory. In the case of aluminium oxide, most equipment companies developed their own 'unique'

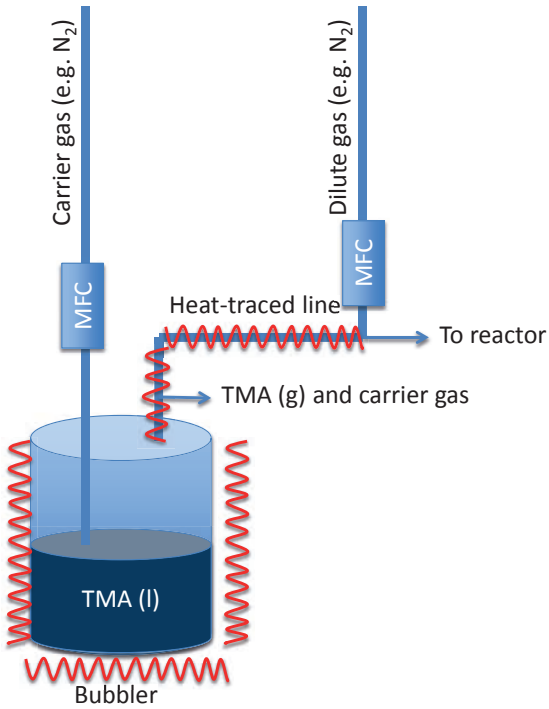

Figure 1. The easiest solution for converting liquid TMA (l) to gaseous TMA (g) is a bubbler system, whereby the liquid TMA canister is heated and a carrier gas is 'bubbled' through the TMA liquid. A mixture of carrier gas and TMA exits from the top of the bubbler system; this mixture is then mixed with another inert gas to dilute the precursor to the desired concentration.

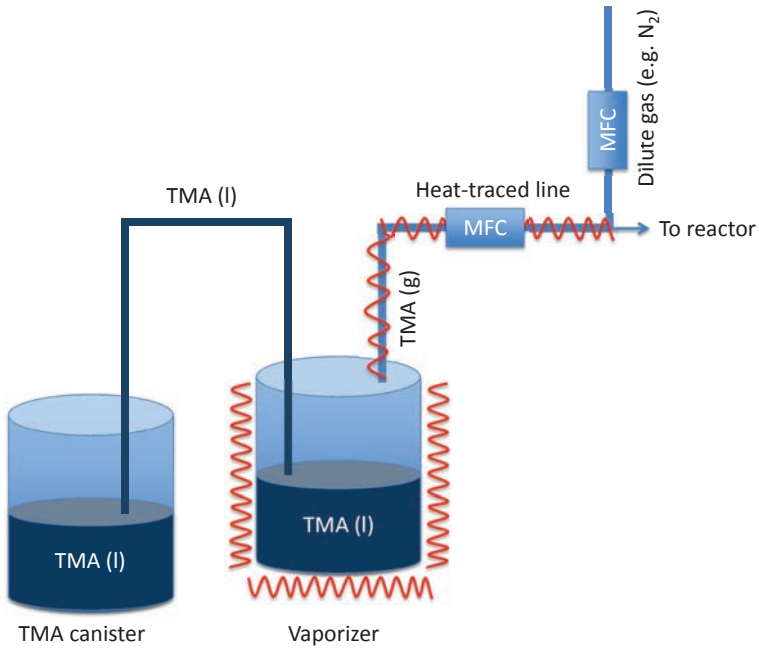

Figure 2. The vaporizer system for converting liquid TMA to gas is more advanced than the bubbler system. Here, a so-called 'vaporizer' is kept at an elevated temperature and allows the extraction of a pure TMA gas, which is then mixed with a carrier gas.

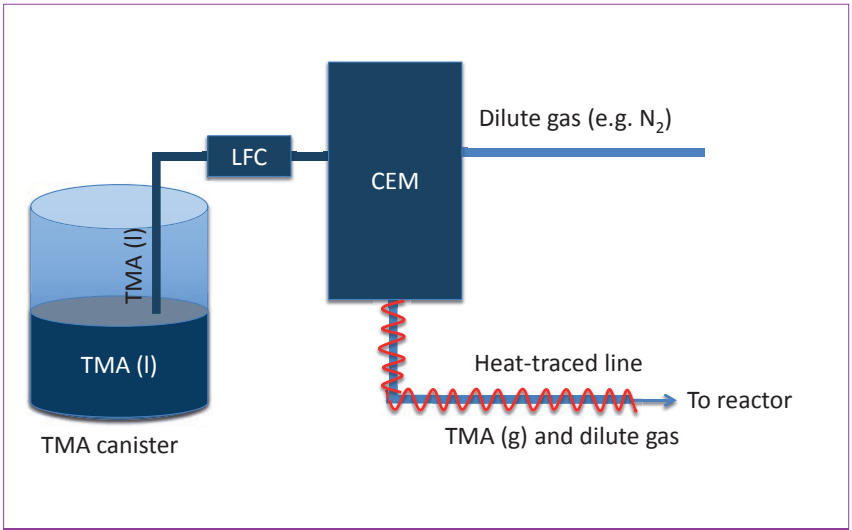

Figure 3. The most commonly used way of converting liquid TMA to gas is the direct injection method, whereby the TMA liquid flow is controlled and then converted to TMA gas in a controlled evaporator mixer (CEM) unit.

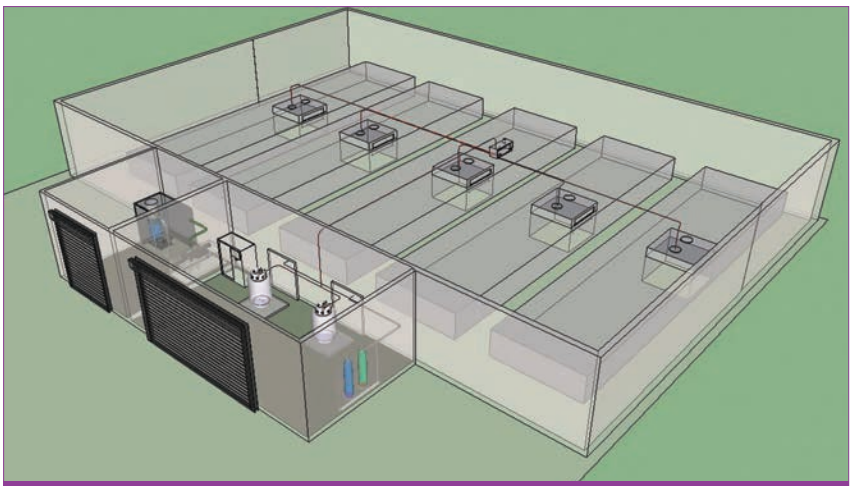

Source: The Linde Group

Figure 4. Schematic illustration of a factory-scale TMA-delivery system.

solutions, which often underwent modifications when transitioning from pilot-scale to high-volume manufacturing. In the author's view, it would have been better if the equipment companies had quickly agreed on a 'standard' and had only differentiated on the production equipment side. This would have also allowed further cost reductions, as a significant portion of the cost of TMA is associated with the canister and the transport. Fortunately, the PV sector can benefit from existing safety training that is available from the precursor suppliers, as liquid pyrophorics are widely used in other industries; for example AkzoNobel has a dedicated 'Metal Alkyls Safety Lab' in Deventer (The Netherlands), where personnel from equipment suppliers or solar cell manufacturers can receive (partly hands-on) training.

Another significant concern in the initial stages was the fact that TMA is a fairly expensive precursor. The price level of the TMA that is conventionally used in the semiconductor industry is prohibitively high for PV, even when only very thin aluminium oxide layers of thicknesses in the range 10–30nm are required. In order to produce semiconductor-grade TMA, various purification steps have to be executed to bring the contamination level down to an acceptable level. It was quickly established that the requirements for solar are not that stringent, since the TMA is not used for the fabrication of an active material. Hence, various companies have been releasing so-called 'solar-grade TMA' that meets the performance and cost targets of the PV industry.

Eindhoven University of Technology, in collaboration with Air Liquide, showed that aluminium oxide films grown using solar-grade TMA demonstrate a similar level of surface passivation performance to that of layers grown using semiconductor-grade TMA on a lab-scale ALD reactor [18]. The Solar Energy Research Institute of Singapore (SERIS), in collaboration with AkzoNobel and SoLayTec, reported similar results on an industrial-scale ALD reactor [19,20]; the deposited layers were investigated in great detail and no significant difference in performance or composition could be detected.

It is expected that the precursor suppliers can reduce costs even further by selective purification of TMA, thereby focusing on, for example, the most detrimental impurities (e.g. metals), while disregarding inert or non-reactive impurities, which are not harmful to the process and thus do not need to be removed. Similar work has been carried out by The Linde Group in the case of thin-film silicon solar cells [21].

Research groups are currently also working on alternatives to TMA for the deposition of aluminium oxide. Eindhoven University of Technology, in collaboration with Air Liquide, have shown that dimethylaluminium isopropoxide (DMAI) can be used instead of TMA as a precursor for the deposition of Al_2O_3 [22]. DMAI has a low pyrophoricity compared with TMA; the properties of the aluminium oxide films grown using DMAI were comparable to those of the aluminium oxide films grown using TMA for higher deposition temperatures. The paper by Pots et al. [22] also presents a good overview of the various aluminium precursors that could be used for ALD of aluminium oxide.

In contrast to silicon nitride, which is the standard front-side anti-reflection coating, there are alternatives to aluminium oxide for use in, for example, PERC or local back-surface field solar cells. And some companies decide, on the basis of the standard industrial practice of hierarchy of hazard control, that the risk level associated with TMA is too high; consequently, a substitute solution is implemented, even when the technical performance is slightly lower and the cost are potentially higher.

> "It is very important to consider precursors in the early stages of technology development in order to avoid delays in the later stages of technology deployment."

Conclusion

Universities, institutes and companies are making very good progress in the development of new high-efficiency silicon wafer solar cells. The success of these developments depends not only on the performance of these new solar cell designs but also on the availability of the whole supply chain required to mass produce these new solar cells. This paper has specifically looked at the precursor part of the supply chain for silicon nitride and aluminium oxide. Especially in the case of aluminium oxide, it is clear that this part of the supply chain is essential for the success of the technology, and it might still take a while before the ideal solution is found. This paper has also highlighted that it is very important to consider precursors in the early stages of technology development in order to avoid delays in the later stages of technology deployment.

Acknowledgements

The author would like to thank J. Hong (Air Liquide), A. Allegro (AkzoNobel), G. de Kok (AkzoNobel), J.-C. Cigal (The Linde Group), F. Lin (SERIS) and N. Nadakumar (SERIS) for their valuable contributions to this work. This research is partly supported by the National Research Foundation, Prime Minister's Office, Singapore, under its Energy Innovation Research Program (EIRP Award No. NRF2011EWT-CERP001-018).

References

[1] Wolke, W. et al. 2004, "SiN:H anti-reflection coatings for c-Si solar cells by large scale inline sputtering", *Proc. 19th EU PVSEC*, Paris, France, p. 419.

[2] Oerlikon 2009, "SOLARIS coating system improves production of crystalline solar cells", Media Release [available online at http://www.oerlikon.com/ecomaXL/files/oerlikon_Oerlikon_Systems_Mediarelease_Solaris_EN_09-12-03.pdf].

[3] Kang, M.H. et al. 2009, "The study of silane-free SiC_xN_y film for crystalline silicon solar cells", *J. Electrochem. Soc.*, Vol. 156, No. 6, p. H495.

[4] Hoex, B. et al. 2006, "High-rate plasma-deposited SiO_2 films for surface passivation of crystalline silicon", *J. Vac. Sci. Technol. A*, Vol. 24, No. 5, p. 1823.

[5] Hoex, B. 2008, "Functional thin films for high-efficiency solar cells", Ph.D. dissertation, Eindhoven University of technology, The Netherlands.

[6] Madec, A. et al. 2009, "Impact of NH_3 grade used for PECVD of a-SiN_x:H on silicon solar cell performance", *Proc. 24th EU PVSEC*, Hamburg, Germany, p. 1315.

[7] Madec, A. et al. 2010, "ARC deposition with various NH_3 grades: Impact on c-Si solar cell performance", *Proc. 25th EU PVSEC*, Valencia, Spain, p. 1635.

[8] Hong, J. et al. 2003, "Bulk passivation of multicrystalline silicon solar cells induced by high-rate-deposited (> 1nm/s) silicon nitride films", *Prog. Photovolt.: Res. Appl.*, Vol. 11, No. 2, p. 125.

[9] Hezel, R. & Jaeger, K. 1989, "Low-temperature surface passivation of silicon for solar cells", *J. Electrochem. Soc.*, Vol. 136, No. 2, p. 518.

[10] Agostinelli, G. et al. 2006, "Very low surface recombination velocities on p-type silicon wafers passivated with a dielectric with fixed negative charge", *Solar Energy Mater. & Solar Cells*, Vol. 90, No. 18–19, p. 3438.

[11] Hoex, B. et al. 2006, "Ultralow surface recombination of c-Si substrates passivated by plasma-assisted atomic layer deposited Al_2O_3", *Appl. Phys. Lett.*, Vol. 89, No. 4, p. 3.

[12] Hoex, B. et al. 2007, "Excellent passivation of highly doped p-type Si surfaces by the negative-charge-dielectric Al_2O_3", *Appl. Phys. Lett.*, Vol. 91, No. 11, p. 3.

[13] Benick, J. et al. 2008, "High efficiency n-type Si solar cells on Al_2O_3-passivated boron emitters", *Appl. Phys. Lett.*, Vol. 92, No. 25, p. 3.

[14] Schmidt, J. et al. 2008, "Surface passivation of high-efficiency silicon solar cells by atomic-layer-deposited Al_2O_3", *Prog. Photovolt.: Res. Appl.*, Vol. 16, No. 6, p. 461.

[15] Miyajima, S. et al. 2008. "Hydrogenated aluminium oxide films deposited by plasma enhanced chemical vapor deposition for passivation of p-type crystalline silicon", *Proc. 23rd EU PVSEC*, Valencia, Spain, p. 1029.

[16] Li, T.T. & Cuevas, A. 2009, "Effective surface passivation of crystalline silicon by rf sputtered aluminum oxide", *physica status solidi (RRL)*, Vol. 3, No. 5, p. 160.

[17] Roth & Rau [http://www.roth-rau.de].

[18] Dingemans, G. & Kessels, W.M.M. 2010, "Recent progress in the development and understanding of silicon surface passivation by aluminum oxide for photovoltaics", *Proc. 25th EU PVSEC*, Valencia, Spain, p. 1083.

[19] Lin, F. et al. 2013, "Excellent surface passivation of silicon at low cost: Atomic layer deposited aluminium oxide from solar grade TMA", *Proc. 39th IEEE PVSC*, Tampa, Florida, USA, p. 1268.

[20] Nandakumar, N. et al. 2013, "Silicon surface passivation by Al_2O_3 films grown by spatial atomic layer depositions using low-cost precursors", *Proc. 28th EU PVSEC*, Paris, France, p. 1105.

[21] Szych, P. et al. 2012, "Impact of relevant gas impurities on thin-film silicon solar cell performance", *Proc. 27th EU PVSEC*, Frankfurt, Germany, p. 2101.

[22] Potts, S.E. et al. 2012, "Plasma-enhanced and thermal atomic layer deposition of Al_2O_3 using dimethylaluminum isopropoxide, $[Al(CH_3)_2(\mu\text{-}OiPr)]_2$, as an alternative aluminum precursor", *J. Vac. Sci. Technol. A*, Vol. 30, No. 2, p. 021505.

About the Author

Dr. Bram Hoex graduated in applied physics from Eindhoven University of Technology in 2003. He received a Ph.D. in 2008, for which his research focused on the development of processes and materials for improving solar cell efficiency by the reduction of electronic and optical losses. After several years as group leader and director at the Solar Energy Research Institute of Singapore (SERIS), part of the National University of Singapore, he joined the School of Photovoltaic and Renewable Energy Engineering (SPREE) in the faculty of engineering at UNSW in 2015.

Enquiries

Bram Hoex
School of Photovoltaic and Renewable Energy Engineering (SPREE)
UNSW, Sydney
2052 Australia

Tel: +61432222450
Email: b.hoex@unsw.edu.au
Website: www.engineering.unsw.edu.au/energy-engineering/

Quarterly analysis of PV manufacturing capacity expansion plans

Mark Osborne, senior news editor, *Photovoltaics International*

ABSTRACT
In edition 26 of *Photovoltaics International* the rebirth of PV manufacturing capacity expansions in 2014 was analysed; this covered announcements on a global basis from a wide range of companies and included thin film and dedicated solar cell and module assembly lines, as well as integrated cell and module assembly lines. Because of the current level of capacity expansion announcements, a roughly quarterly analysis of such plans will be undertaken during 2015.

December 2014 review

The initial review of PV manufacturing capacity expansion plans in 2014 ran from January 2014 to November 2014; an analysis of announcements made in December will therefore be given first, and then a final tally provided for the year.

In December 2014 a total of seven companies announced expansion plans, primarily for integrated cell/module lines; this was especially noteworthy, as the majority were not Tier 1 c-Si manufacturers. A total of 1110MW of new c-Si solar cell capacity was announced, of which 300MW were classified as dedicated cell capacity. Because the majority of the announcements were for integrated lines, a total of 1160MW of c-Si module assembly line capacity was announced, which therefore closely matched the cell capacity expansions in December.

After four months of dormant thin-film activity, Hanergy Thin Film announced it would build a dedicated 300MW plant in China for the production of flexible CIGS thin-film substrates. Toolmaker Beijing Jing Cheng, a Hanergy Group subsidiary, was said to be providing the production lines for the facility, which would be in Changde, Hunan province. The new production facility would be built by the provincial government, with construction expected to be completed in June 2016.

Hanergy's plans, however, were not the largest announced in the last month of 2014; that honour goes to Bharat Heavy Electricals Ltd (BHEL), which announced plans to build an integrated c-Si plant with a nameplate capacity of 500MW, although this would be ramped in unspecified phases. BHEL was responding to India's plans for 100GW of PV installations by 2022, but as will be shown later in this paper, February 2015 marked a significant flurry of manufacturing capacity pledges in India based on the country's new targets.

Credit: SCHMID Group

Figure 1. SCHMID's laser process for PERC solar cells.

On a technological level the announced expansion by ERDM Solar, based in Mexico, is interesting, as the company plans to expand existing solar cell and module capacity from 60MW to 170MW through employing equipment and turnkey production supplier SCHMID's bifacial multi-busbar technology. ERDM Solar expects to ramp the new 110MW (two lines) expansion in the third quarter of 2015.

SCHMID was also busy in forming a partnership with Pekintas Group to build a 200MW turnkey c-Si cell and module manufacturing facility in Russia for start-up company Solar Systems. Financial details have not been disclosed, but Solar Systems was said to have been established by Chinese shareholder Amur-Sirius in 2014. Production is planned to begin in the second quarter of 2016.

Final 2014 roundup

On a monthly basis December's combined 1760MW of announcements were in line with those in January, February, May and June, while the peak months of the year clearly turned out to be March (3480MW) and November (4938MW), as seen in Fig. 2.

This should not come as a surprise, because the two peak months for announcements primarily included major expansions from leading Tier 1 PV manufacturers. Indeed, looking back over these specific companies, Trina Solar, JinkoSolar, JA Solar and Canadian Solar are noteworthy, as these were the fastest-growing Tier 1 producers on the basis of PV module shipments in 2014.

"The first and fourth quarters of 2014 generated the most activity for capacity expansion announcements."

2014 quarterly trends

On a quarterly basis it is clear that the first quarter (6.79GW) and fourth quarter (7.64GW) of 2014 generated the most activity for capacity expansion announcements, with significantly higher numbers than in the middle quarters of the year (Fig. 3).

Historically, the first quarter of a given year has always been recognized as a key quarter for capacity expansions, especially given that the majority of Tier 1 PV manufacturers are publicly listed and during this quarter will announce full-year financial results and guidance for the year ahead. From that perspective the first quarter of 2014 can be regarded as following historical trends.

The surprise, however, is the high number of announcements in the fourth quarter of 2014. Clearly, as already noted, some of the fastest-growing companies were responsible for further expansion announcements in the fourth quarter, and predominantly announced in November when reporting on the third-quarter financial period. This

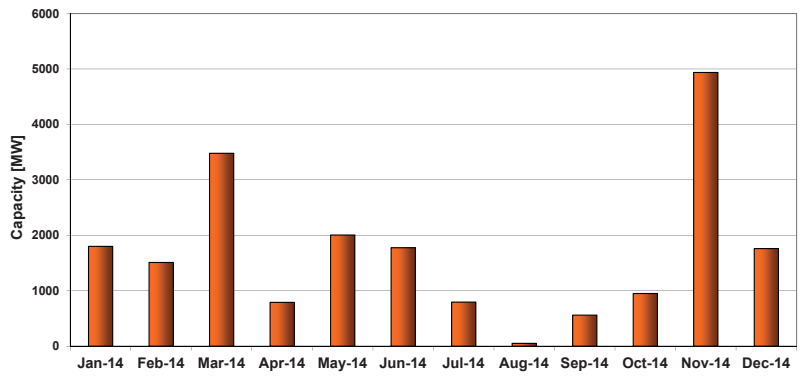

Figure 2. Cell/module manufacturing capacity expansions announced in 2014 by month.

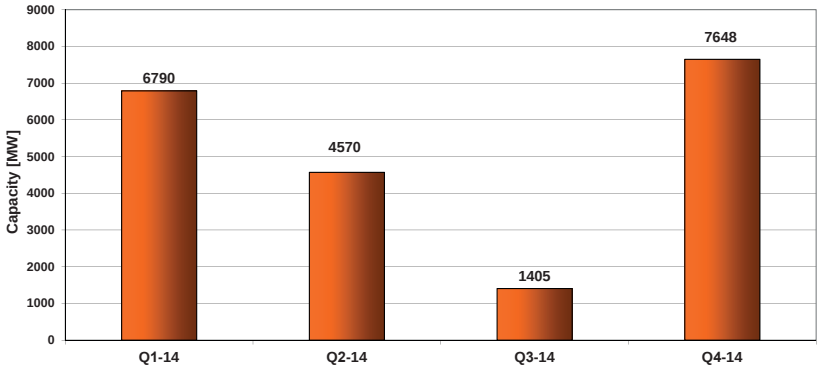

Figure 3. Cell/module manufacturing capacity expansions announced in 2014 by quarter.

Company	Announcement date	Manufacturing location	New nameplate capacity [MW]	Production/product type
Ascent Solar	Jan-14	Suqian, Jiangsu province, China	25	flex CIGS thin film
Solar Frontier	Jan-14	Tohohu, Japan	150	CIS thin film
Hanergy Solar	Jan-14	Caofeidian, Hebei province, China	600	CIGS thin film
TSMC	Feb-14	Taiwan	80	CIGS thin film
First Solar	Mar-14	Malaysia	200	CdTe thin-film upgrades
Stion Corp	Jun-14	Hattiesburg, Mississippi, USA	100*	CIGS thin-film module assembly
Siva Power	Jul-14	Silicon Valley, California, USA	CIGS pilot line	CIGS thin-film pilot line
SoloPower	Jul-14	Portland, Oregon, USA	75	flex CIGS thin film
First Solar	Nov-14	Perrysburg, Ohio, USA	178	CdTe thin-film modules
First Solar	Nov-14	Malaysia	350	CdTe thin-film module lines upgraded and recommissioned
Hanergy Thin Film	Dec-14	Changde, Hunan province, China	300	integrated flex CIGS thin-film plant
			Total 2058	

* Estimated

Table 1. Thin-film capacity expansion announcements in 2014.

Imagine you have up to **30%** more electricity yield.

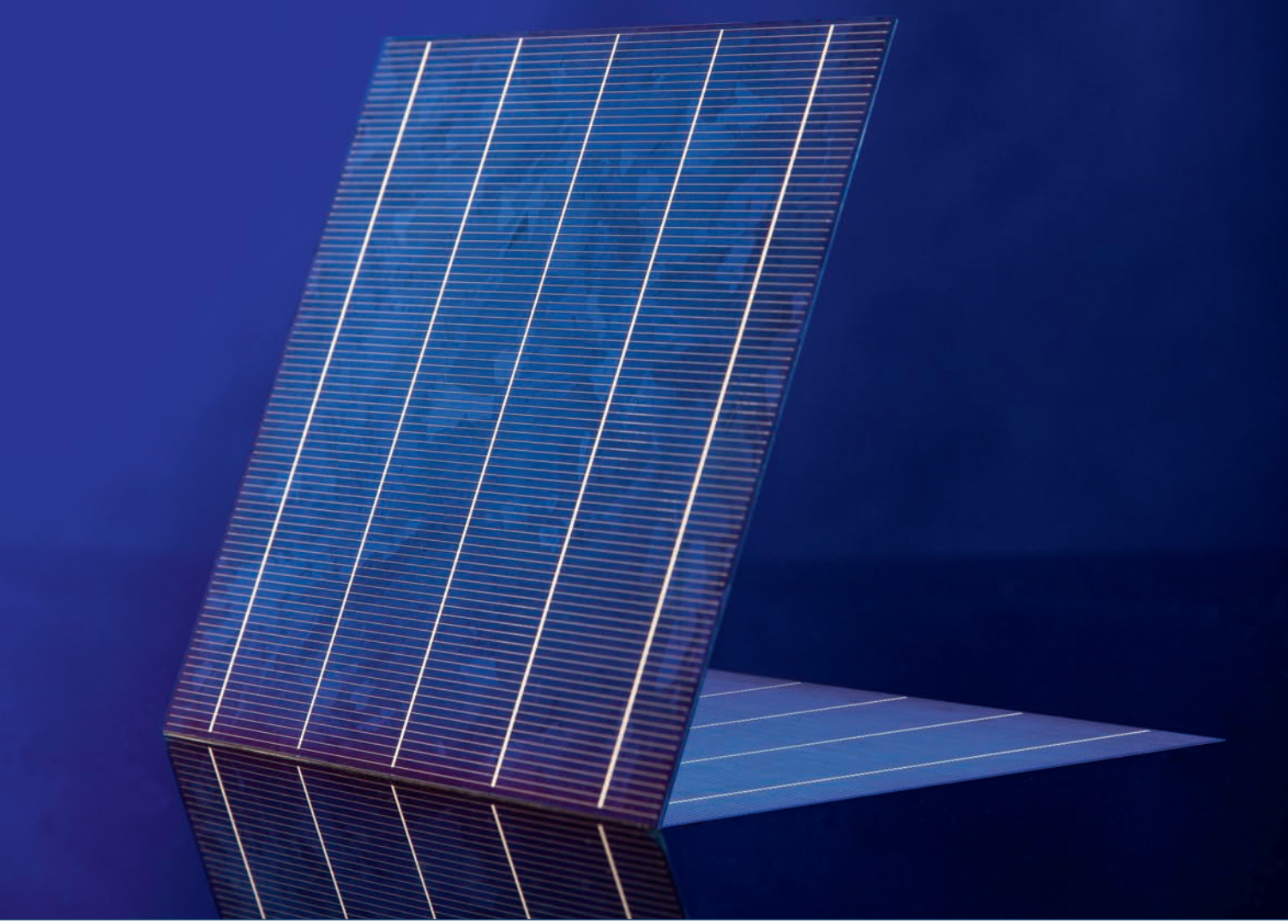

Expect Solutions. **GEMINUS.**

The SCHMID's GEMINUS bifacial cell technology enables low manufacturing costs of multi and mono bifacial cells featuring over 30% more energy yield (kWh/kWp)*. It combines outstanding manufacturing simplicity based on standard tools with highest efficiencies on all common p-type based material. The resulting multi crystalline based bifacial module operates at efficiency equivalents of over 18% and hence has a 7-10 USc BOS advantage as in comparison to current monofacial multi modules.

*Gain in energy depending on rear side illumination and module mounting.

was also supported by a relatively strong December from non-Tier 1 manufacturers.

Thin-film revival

Hanergy's 300MW announcement in December topped off a revival year for thin-film technologies. In total just over 2GW of new capacity expansions were announced in 2014, dominated by Hanergy's two separate CIGS thin-film plans for three of its acquired companies, totalling 900MW (Table 1).

Second was the return of CdTe leader, First Solar, which announced expansions and efficiency upgrades totalling 728MW at its plants in the USA and Malaysia. However, on a technology product basis, planned CIGS (including CIS) expansions exceeded 1230MW.

PERC cells lead c-Si capacity expansions

Another revival in 2014 was related to dedicated c-Si solar cell capacity expansions, also notable because the majority of expansions deployed PERC cell technology, as higher efficiency cells become a key path to product differentiation and offer the potential for lowering the cost per watt. Total dedicated c-Si solar cell expansions announced in 2014 topped 5GW, while the figure reached 7.86GW when integrated cell/module expansions are included (Table 2).

Another aspect of the revival in solar cell expansions was the scale rather than the number of companies announcing dedicated mono c-Si expansions. Although some PV manufacturers switched some production lines to mono production in the course of the year, these were not technically new capacity expansions.

Yingli Green may have touted technical developments and the adoption of new technologies, such as ion implantation to produce its n-type mono Panda cells, but the company has not added any new capacity in 2014. Only SolarCity, Canadian Solar, Mission Solar, Shaanxi Youser, SolarWorld and Suniva announced dedicated mono c-Si expansions in 2014, totalling almost 2GW of the combined 7.86GW of solar cell announcements.

> "PV module capacity expansions continued to gain momentum in 2014."

Module assembly leads capacity plans

PV module capacity expansions continued to gain momentum in 2014, with c-Si announcements reaching 11.9GW. As with solar cell expansions, major Tier 1 PV manufacturers dominated. However, new entrants such as SolarCity and a number of regionally small-scale players, certainly played a part in bulking-up the final tally (Table 3).

Africa (320MW) and Latin America (450MW) are notable, as they are clearly emerging downstream markets, and some specific countries – such as South Africa and Brazil – have local content rules.

January 2015 full of ambition

Early in January, major US-based fab-less photovoltaics energy provider (PVEP) SunEdison decided to add Gujarat in India to the list of potential sites in its eventual aim to become a fully integrated PV manufacturer. The company had signed a memorandum of understanding (MoU) with Indian conglomerate Adani Enterprises to establish a joint-venture (JV) fully integrated (polysilicon-to-module) manufacturing cluster in Mundra, Gujarat, at a cost of around US$4bn.

Company	Announcement date	Manufacturing location	New nameplate capacity [MW]	Production/product type
Hanwha Q CELLS	Jan-14	Cyberjaya, Malaysia	204	c-Si PERC cell
JinkoSolar/Topoint	Jan-14	China	500	multi c-Si cell
Solland Solar	Feb-14	Heerlen, Holland	50	multi c-Si cell
Trina Solar	Mar-14	China	500	multi c-Si cell
JA Solar	Mar-14	China	300	c-Si cell
Hanwha SolarOne	May-14	China	200	c-Si cell
Canadian Solar/ GCL-Poly	May-14	Funing, Jiangsu province, China	1200	c-Si cell
Indosolar	Jun-14	India	250	multi c-Si selective emitter cell
Shaanxi Youser	Jul-14	China	380	multi c-Si cell
Hareon Solar	Sep-14	China	100*	c-Si PERC cell
TS Solartech	Sep-14	Malaysia	20*	multi c-Si cell
Canadian Solar	Nov-14	Funing, China	400	mono c-Si PERC cell
JA Solar	Nov-14	China	600	multi c-Si cell
Rolta Group	Dec-14	Mumbai, India	300	multi c-Si cell
		Dedicated	Total 5004	
		Incl. integrated	Total 7860	

* Estimated

Table 2. Dedicated solar cell capacity announcements in 2014.

Company	Announcement date	Manufacturing location	New nameplate PV module capacity [MW]	Production/ product type
JinkoSolar/Topoint	Jan-14	China	100	multi c-Si module assembly
JA Solar/Powerway	Jan-14	Port Elizabeth, South Africa	150	multi c-Si module assembly
ELIFRANCE	Feb-14	La Talaudière, France	20*	multi c-Si module assembly
EL.ITAL	Feb-14	Avellino, Italy	20*	multi c-Si module assembly
Pure Energy Generation	Feb-14	Marechal, Brazil	70	multi c-Si module assembly
Wuxi Suntech	Feb-14	Wuxi, China	1000	multi c-Si module assembly
REC Solar	Feb-14	Singapore	120	multi c-Si module assembly
Vitec Global Solar	Mar-14	Otawara City, Tochigi Prefecture, Japan	80	multi c-Si module assembly
Trina Solar	Mar-14	China	1000	multi c-Si module assembly
Canadian Solar	Mar-14	China	400	multi c-Si module assembly
JA Solar	Mar-14	China	1000	c-Si module assembly
Jabil Circuits	Apr-14	Kwidzyn, Poland	240	multi c-Si module assembly
REC Solar	Apr-14	Singapore	300	multi c-Si module assembly
Solargiga/Jinzhou Yangguang	Apr-14	China	170	mono c-Si module assembly
Hanwha SolarOne	May-14	China	500	multi c-Si module assembly
Green Panel Technology Jurawatt Tunisie	May-14	Tunis, Tunisia	30	multi c-Si module assembly
Tata Solar	May-14	Bangalore, India	75	c-Si module assembly
Hanplast	Jun-14	Poland	85	Meyer Burger's 'SmartWire' module assembly
Gintung Energy	Jun-14	Taiwan	150	c-Si module assembly
Kyocera	Jun-14	Japan	200	c-Si module assembly
Suniva	Jul-14	Saginaw, Michigan, USA	200	n-type mono module assembly
BYD	Jul-14	Sao Paulo, Brazil	20*	c-Si module assembly/ R&D
Tecnova Renovables/Sky Solar	Aug-14	Paysandú, Uruguay	50	c-Si module assembly
Grupo IUSA	Sep-14	Mexico	50–200	c-Si module assembly
SolarTech	Sep-14	Riviera Beach, Florida, USA	80+	Meyer Burger's 'SmartWire' module assembly
Hanwha Q CELLS	Oct-14	Cyberjaya, Malaysia	800	c-Si PERC/module assembly
SunPower	Nov-14	Cape Town, South Africa	160	n-type mono module assembly
Canadian Solar	Nov-14	Changshu and Luoyang plants, China	500	mono/multi c-Si PERC modules
JA Solar	Nov-14	China	600	multi c-Si module assembly
Hanwha SolarOne	Nov-14	South Korea	250	multi c-Si module assembly
JinkoSolar	Nov-14	China	200	multi c-Si module assembly
JinkoSolar	Nov-14	China	640–800	c-Si PERC/module assembly
Bharat Heavy Electricals Ltd (BHEL)	Dec-14	Maharashtra, India	500	integrated c-Si cell/module lines
PSC Solar Industries	Dec-14	Warewa, Nigeria	10	multi c-Si module assembly
tenKsolar	Dec-14	Thailand	50–100	multi c-Si module assembly
ERDM Solar	Dec-14	San Andrés Tuxtla, Mexico	110	integrated c-Si bifacial cell/module lines
Solar Systems	Dec-14	Alabuga, Russia	200	integrated c-Si cell/module lines
Rolta Group	Dec-14	Mumbai, India	240	multi c-Si module assembly
* Estimated			Total 10,700	

Table 3. Dedicated c-Si module capacity expansion announcements in 2014.

However, despite the worldwide headlines proclaiming the MoU to be a done deal, the statement from SunEdison included a caveat that a decision on progressing with the MoU would only be made after it had conducted a feasibility study, without giving any timelines. Therefore, as SunEdison had already touted similar potential manufacturing deals in Saudi Arabia and China in 2014, the India plans will prudently not be included in the database until more concrete proposals have been announced, and such announcements will be classified as mere pledges for now.

On a more solid basis, China-based PV manufacturer Jetion Solar said that as part of its success in Thailand's PV market, it expected to have a 200MW cell and module facility operational in May 2015. PV module assembly manufacturing consultancy specialist J.v.G. Thoma said mid-month that it would supply a 70MW turnkey production line to start-up company Renovasol in Brazil and would be responsible for the complete toolset as well as certification, training and ramp-up. Module production is expected to start sometime in 2015.

Hanwha Q CELLS (to be merged with sister company Hanwha SolarOne and retain the Q CELLS name) said it will be closing down all solar cell and module manufacturing production in Germany; 230MW of solar cell nameplate capacity and 130MW of PV module capacity will be relocated to its main production facility in Cyberjaya, Malaysia. The company announced plans last year to add new capacity in Malaysia during the year, so the production capacity relocation has been included as added capacity, with the intention of highlighting for future reference actual nameplate capacity figures for what will be Hanwha Q CELLS' only manufacturing facility in Malaysia at this time.

Indonesian state-owned electronics firm PT Len Industri plans an integrated solar cell and module assembly plant in the country, confirming reports that go back to 2012, when proposals were said to target a 60MW capacity. Funding for the project has remained an issue, however.

India-based PV module assembly manufacturer Surana Solar is to start solar cell production in March 2015, having previously acquired two production lines from shuttered manufacturer Schott Solar in Germany. In 2013 Surana Solar had planned to acquire two solar cell lines, each having an annual nameplate capacity of 55MW, to integrate into its existing module assembly lines with a capacity of 40MW.

In total, 440MW of new capacity were announced in January, compared with 1.8GW announced in the first month of 2014. The key difference was the lack of announcements from major Tier 1 suppliers. Only 110MW of dedicated solar cell capacity were announced during the month, while integrated capacity totalled 260MW. Dedicated module assembly expansions totalled 70MW, but no thin-film announcements were made.

February 2015 capacity plans full of pledges

As noted earlier, India has significantly raised its PV installation target to 100GW by 2022. In mid-February, India's Prime Minister, Narendra Modi, and Minister of State for power, Piyush Goyal, attended the first government-backed event to kick-start investment in Modi's plans. This led to significant 'pledges' by India's PV manufacturers to expand production in line with the downstream targets. In total the capacity expansion pledges by at least 12 local firms exceeded 41GW. However, as they do not represent planned or announced expansions, the pledges should be treated with caution, similarly to the comments made about SunEdison's 'ambition' for establishing its first production facility in India. On the basis of several actual announcements of capacity expansions in India that have been driven by India's new PV targets, developments will nevertheless be closely monitored and reported as they happen.

Key capacity plans announced by mid-February include SolarPark Korea's proposals to expand its module capacity to 1.2GW, up from its current capacity of 600MW. LG Electronics is planning to spend around US$145m on expanding its capacity by around 200MW for its n-type monocrystalline cells and modules; the capital expenditure plans would be undertaken by the end of July 2015. Chinese PV manufacturer Zhongli Talesun has officially started construction of a 500MW integrated solar cell and module assembly plant in the Thai–Chinese Industrial Zone in Rayong, Thailand. Talesun said that the production plant would be fully automated and employ advanced processing technology to produce high-efficiency solar cells and modules; production is expected to start in October 2015.

Waaree Energies, one of India's largest PV module manufacturers, is significantly adding capacity to meet demand, having already expanded capacity to 500MW, and is planning to double that to 1GW over the next four months. Waaree recently completed a 250MW module assembly expansion phase at its plant in Surat, Gujarat, taking nameplate capacity to 500MW. The company claimed that as a result of the expansion it had become the largest single location for PV module manufacturing in India. In November 2014 Waaree said it was working with GT Advanced Technologies (GTAT) on incorporating its new Merlin cell metallization and interconnection technology into its existing module production lines.

In total, 2.39GW of new capacity announced in February 2015 were logged, compared with around 1.5GW announced in the second month of 2014. The key differentiator was the large expansions by SolarPark Korea, Waaree and Zhongli Talesun. Dedicated solar cell capacity expansion announcements in the month totalled 300MW, while integrated capacity announcements were 800MW. In the case of module assembly expansions, dedicated capacity totalled 765MW, while integrated capacity was 1.3GW. No thin-film announcements were made in February.

> "Capacity expansion announcements in the first two months of 2015 are in line with those for the same period last year."

Conclusion

Capacity expansion announcements in the first two months of 2015 are in line with those for the same period last year. However, the majority of announcements were from Tier 2 and start-up suppliers, and the absence of major Tier 1 suppliers may be due to looming full-year financial results in March, which is expected to generate another wave of expansions.

In the next quarterly report full details of Tier 1 announcements and a full quarterly analysis will be presented. As part of the analysis, an assessment of expected manufacturing capacity ramps from over a full year's worth of announcements will also be included, in order to understand supply and demand dynamics.

Materials

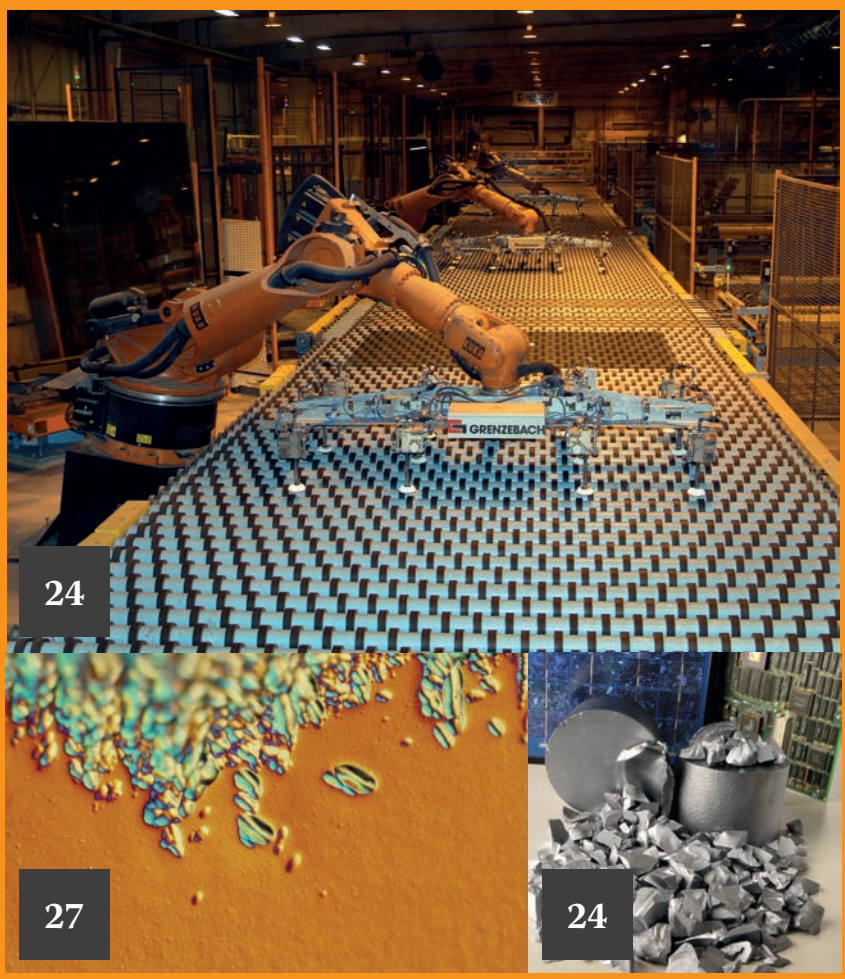

Hubert Seigneur[1,2,3], Andrew Rudack[1,4], Joseph Walters[1,2,3], Paul Brooker[1,2,3], Kristopher Davis[1,2,3], Winston V. Schoenfeld[1,2,3], Stephan Raithel[5], Shreyes Melkote[6], Steven Danyluk[6,7], Thomas Newton[7], Bhushan Sopori[8], Stephen Preece[9], Igor Tarasov[10], Sergei Ostapenko[10], Atul Gupta[11], Gunter Erfurt[12], Bjoern Seipel[12], Oliver Naumann[12], Ismail Kashkoush[13] & Franck Genonceau[14]

[1]c-Si U.S. Photovoltaic Manufacturing Consortium (PVMC), Orlando, FL, USA; [2]Florida Solar Energy Center (FSEC), Cocoa, FL, USA; [3]University of Central Florida (UCF), Orlando, FL, USA; [4]SEMATECH, Albany, NY, USA; [5]SEMI Europe, Berlin, Germany; [6]Georgia Institute of Technology, Atlanta, GA, USA; [7]Polaritek Systems, Atlanta, GA, USA; [8]National Renewable Energy Laboratory (NREL), Golden, CO, USA; [9]Process Research Products, Trenton, NJ, USA; [10]Ultrasonic Technologies, Wesley Chapel, FL, USA; [11]Suniva, Norcross, GA, USA; [12]SolarWorld, Hillsboro, OR, USA; [13]Akrion Systems, Allentown, PA, USA; [14]Applied Materials, Cheseaux, Switzerland.

News

Effective polysilicon capacity dampens 2015 downstream deployment forecast

Source: REC Silicon

Polysilicon shipment estimates suggests end-market demand in 2014 was lower than many had forecasted.

Based on the SEMI trade association's polysilicon shipment data as well as REC Silicon's own estimates, a total of 271,000MT of polysilicon was shipped in 2014, suggesting between 42GW to 43GW of PV modules were produced last year.

REC Silicon said during a February earnings call that the polysilicon shipment data indicates that the global end-market demand was therefore lower than many forecasts had anticipated. Tore Torvund, president and CEO of REC Silicon, said effective polysilicon capacity is expected to reach around 284,000MT by the end of the first-half of 2015.

With further effective capacity coming on stream this year, that total was expected to increase to around 321,000MT. REC Silicon's Kurt Levens noted that such levels of effective polysilicon capacity would support PV module production of around 50GW to 55GW in 2015. However, anywhere within this range could lead to periods of tight supply, depending on inventory levels in the supply chain.

Plants and production

REC Silicon to shift poly sales beyond China

US-based polysilicon producer REC Silicon is planning to attempt to shift its current FBR-based (fluidized bed reactor) polysilicon production sales away from China over tariff duty uncertainties and the eventual ramp of its JV FBR-base plant in China in 2017.

REC Silicon noted in an earnings call to discuss fourth quarter 2014 results that despite record quarterly production of FBR silicon it was forced to heavily discount polysilicon prices to the Chinese market, resulting in a 12% ASP decline, compared to the third quarter of 2014. The company also noted that it encountered weaker than expected FBR silicon demand starting in November, which also contributed to pricing pressure, while overall demand for the year remained as modelled and meant polysilicon prices were up around 20% for the year.

LDK to restart poly production

As a precursor to restarting polysilicon production, China-based LDK Solar has said it had completed a US$70 million upgrade to its plant in Mahong, Jiangxi.

LDK Solar said that its hydrochlorination re-engineering project had led to the production of trichlorosilane (TCS) during its first production run at the end of December, 2014.

The in-house production of TCS enables full-loop polysilicon production that can significantly lower production costs of the Siemens-based process. LDK Solar stopped polysilicon production several years ago as the average selling price (ASP) of polysilicon fell below average production costs due to overcapacity and weak market demand. The company also exited bankruptcy during February.

Hemlock to shutter Tennessee poly plant

Polysilicon producer Hemlock Semiconductor is to close its facility in Clarksville, Tennessee, due to what it said were ongoing adverse market conditions and problems stemming from international trade disputes.

The company's US$1.2 billion plant has never fully opened, having been mothballed since January 2014, and will now close altogether.

The company said some of the site's approximately 50 staff would either be offered other opportunities with Hemlock or its parent firm, Dow Corning, or receive severance packages.

Although recent successive quarterly results had painted a picture of recovering sales and revenue for Hemlock, the company said that under current market conditions it was unable to justify keeping the site open.

Market

RENA acquired by Swiss private equity firm

Insolvent PV equipment and wet processing specialist, RENA, has been acquired by Swiss private equity firm, Capvis for an undisclosed sum.

RENA had recently said it had received new orders in the fourth quarter of 2014 totalling €30 million (US$34 million) and that management had been working with major creditor groups on the restructuring strategy, which it said was progressing well.

In a financial statement, RENA said that it had received enquiries from a number of companies interested in the business but the deal with Capvis provided the best opportunities for the company.

EU reopens solar glass trade case with China

The European Commission has reopened its investigation into solar glass imports for China after a request from EU ProSun Glass.

In May the commission announced anti-dumping duties of 42.1% on Chinese manufacturers with some firms that cooperated given lower rates ranging from 17.15% to 39.3%. According to a filing in the official journal of the European Union on Friday, EU ProSun Glass, led

by manufacturer, Interfloat, has shown sufficient evidence that dumping margins extended beyond the level observed in the original investigation and that the positive impact for EU firms has been insufficient.

The EU must act on the results of the latest investigation within nine months. Module manufacturer SolarWorld which backed the original case, distanced itself from the new one.

GCL-Poly abandons wafer business sell-off

Leading Chinese polysilicon and wafer manufacturer, GCL-Poly, has abandoned plans for the US$1.3 billion sale of its wafer business. The company said in a statement to the Hong Kong Stock Exchange that it had decided to maintain its position as a "leading polysilicon and wafer manufacturer".

GCL-Poly announced the sale in early November 2014 as a measure to help ease its debt situation, and an agreement was signed later that month with various investors, including Jiangsu Golden Concord Energy, GCL's parent company. The sale had been expected to ease the company's debt to equity ratio from 146.5% to 38.8%.

But in its statement, GCL said the board had decided termination of the sale would be in the best interests of the company's shareholders, without giving further detail. In its latest quarterly figures, GCL reported that sales from both its polysilicon and wafer businesses were booming. Wafer sales for 2014 were predicted at around 13GW.

Sales updates

OCI reports 17% increase in polysilicon sales in 2014

Korean polysilicon producer, OCI, has reported a 17% increase in polysilicon sales in 2014 as its plants run at full capacity. OCI reported that its Basic Chemical division, which includes its polysilicon operations, had reached sales of KRW583 billion (US$526.4 million approx) in the fourth quarter of 2014 and total sales for the full-year of KRW2,107 billion (US$1.9 billion).

The company noted that operating its polysilicon production plants at full capacity, cost reductions, as well the benefits of relatively flat ASPs in 2014 had helped to return the division to profitability. The company noted that it was accelerating the mechanical completion of its P3 plant, phase nine debottlenecking, which is scheduled for completion during the second quarter of 2015, a quarter earlier than previously guided.

OCI noted that it expected an additional US$2/kg cost reduction (10%) from the P3.9 debottlenecking when fully operational. The P3.9 debottlenecking would provide a further 10,000MT of polysilicon capacity. However, plans to add new plant capacity announced several years ago remain on hold.

OCI said that it was targeting to achieve a global market share of polysilicon sales of 17% in 2015 on the back of continued strong demand for PV and expected global polysilicon demand to be in the range of 310,000MT.

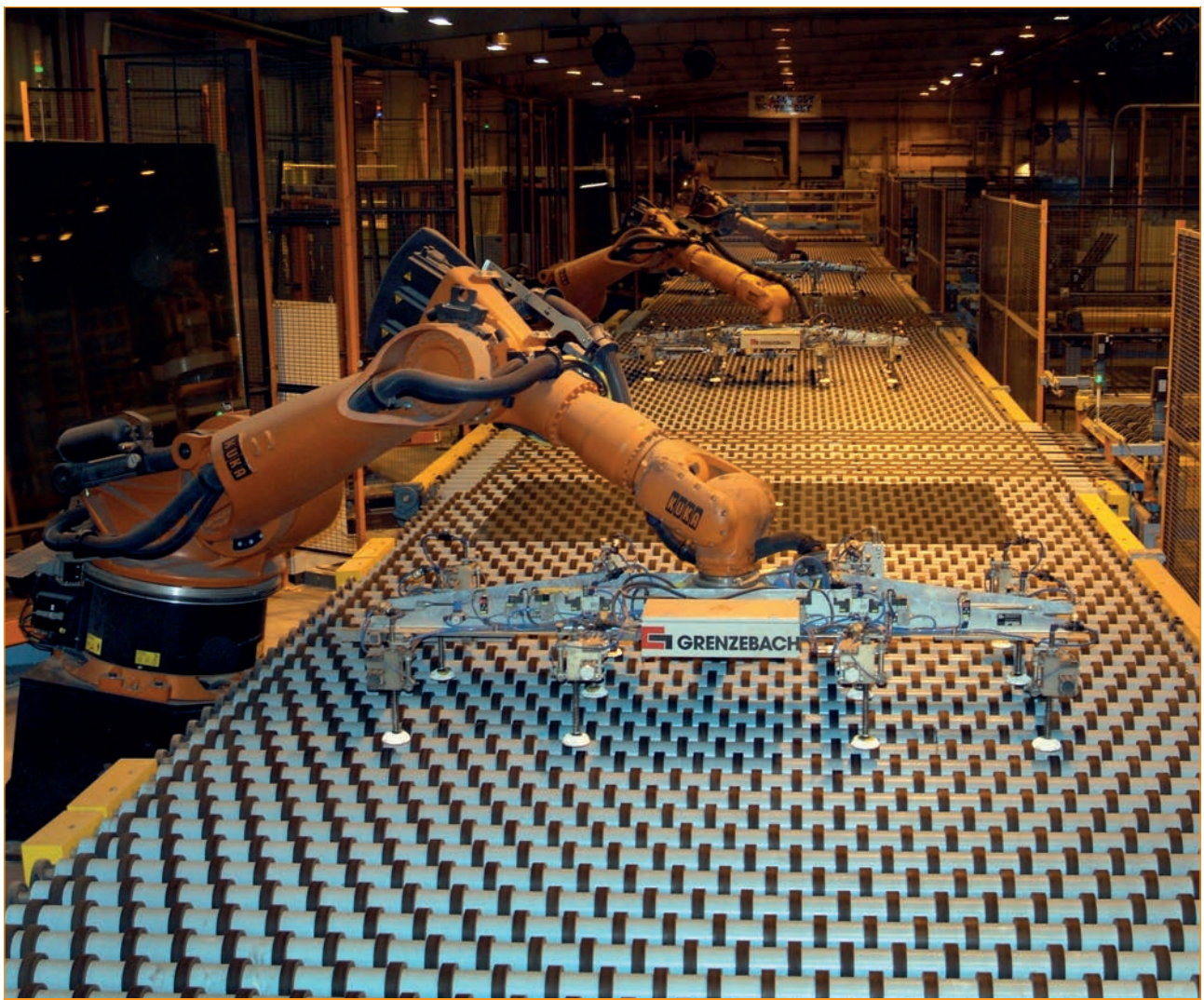

Source: AGC

The EC is to reopen a previous investigation into Chinese solar glass imports.

Hemlock's polysilicon sales hold firm in 2014

Dow Corning, majority owner of Hemlock Semiconductor, the largest polysilicon producer in the US, reported fourth quarter 2014 sales of US$1.68 billion, a 5% increase compared to the fourth quarter of 2013. However, the company reported a significant decline in net income in the quarter of US$37 million, a 66% decline. In the full year, sales increased by 9% and net income by 36%.

Hemlock was said to have increased its sales performance in the year. J. Donald Sheets, Dow Corning's CFO said: "Our Polysilicon segment, the Hemlock Semiconductor Group, continued its strong performance in 2014 despite the lack of progress in resolving the US and China trade disputes plaguing the solar industry. The fourth quarter decision to permanently close Hemlock Semiconductor's Clarksville site, while difficult, will ultimately strengthen Dow Corning's financial performance by eliminating the significant costs associated with maintaining the site." Sheets was referring to the decision to close its major polysilicon plant expansion at a greenfield site in Clarksville, Tennessee (see p.18).

GET full year sales 18% above 2013

Taiwan's largest solar wafer producer, Green Energy Technology (GET), reported unaudited full-year 2014 revenue of approximately NT$15,359 million (US$480 million), an 18% increase over 2013. The company noted that wafer production capacity utilization remained above 95% in December.

Around 60% of wafer sales are generated from Taiwan solar cell producers, which have seen sales decline in recent months after recovering form anti-dumping rulings in the US.

GET said that it was planning to cooperate further with high-end customers in different market regions to broaden its customer base. The company retains 2GW of in-house capacity and 700MW of capacity from strategic partnerships. The company's January results were up 16.7% on December last year.

Wacker's polysilicon sales increase in 2014

Wacker has reported that preliminary sales for its polysilicon division in the fourth quarter of 2014 topped €262 million (US$296 million), up 5% from the prior year period, but declined slightly quarter on quarter.

Wacker noted that its polysilicon plants remained at full capacity in the quarter, due to continued strong demand and stable ASPs that remained significantly higher than the prior year period. EBITDA growth for polysilicon was €89 million (US$100.6 million) in the fourth quarter, 25% higher than in the prior year period and up slightly from €87.9 million (US$99.4 million) in the previous quarter. Wacker said there was no special income from retained advance payments or damages relating to terminated customer polysilicon supply contracts in the fourth quarter.

The company continues to invest in new polysilicon capacity expansions with its first US-based production plant nearing completion. Wacker noted that capital expenditures amounted to €572 million (US$647 million) in 2014, up from €504 million (US$570 million) in the previous year, with the majority of spending attributed to its polysilicon site in Charleston, Tennessee. Total preliminary 2014 polysilicon sales reached €1.04 billion (US$1.18 billion), compared to €924.4 million (US$1.05 billion) in 2013.

Hemlock's sales held firm in 2014 despite ongoing trade disputes.

Source: Hemlock Semiconductor

Diamond wire sawing for PV – Short- and long-term challenges

Hubert Seigneur[1,2,3], Andrew Rudack[1,4], Joseph Walters[1,2,3], Paul Brooker[1,2,3], Kristopher Davis[1,2,3], Winston V. Schoenfeld[1,2,3], Stephan Raithel[5], Shreyes Melkote[6], Steven Danyluk[6,7], Thomas Newton[7], Bhushan Sopori[8], Stephen Preece[9], Igor Tarasov[10], Sergei Ostapenko[10], Atul Gupta[11], Gunter Erfurt[12], Bjoern Seipel[12], Oliver Naumann[12], Ismail Kashkoush[13] & Franck Genonceau[14]

[1]c-Si U.S. Photovoltaic Manufacturing Consortium (PVMC), Orlando, FL, USA; [2]Florida Solar Energy Center (FSEC), Cocoa, FL, USA; [3]University of Central Florida (UCF), Orlando, FL, USA; [4]SEMATECH, Albany, NY, USA; [5]SEMI Europe, Berlin, Germany; [6]Georgia Institute of Technology, Atlanta, GA, USA; [7]Polaritek Systems, Atlanta, GA, USA; [8]National Renewable Energy Laboratory (NREL), Golden, CO, USA; [9]Process Research Products, Trenton, NJ, USA; [10]Ultrasonic Technologies, Wesley Chapel, FL, USA; [11]Suniva, Norcross, GA, USA; [12]SolarWorld, Hillsboro, OR, USA; [13]Akrion Systems, Allentown, PA, USA; [14]Applied Materials, Cheseaux, Switzerland.

ABSTRACT

A shift from free-abrasive/steel wire sawing to fixed-abrasive diamond wire sawing is expected to take place in the PV cell manufacturing industry, with 2018 being the anticipated pivotal point for market dominance. This shift is due to several key advantages of diamond wire sawing, such as higher throughput, less wire per wafer, no slurry and the possibility of kerf recycling. However, in order for diamond wire sawing to realize its promise as the next-generation workhorse for the slicing of silicon PV wafers, inherent fundamental challenges must be properly identified and successfully addressed by the PV industry. As a first step to increasing the current collective understanding of the critical needs/challenges of diamond wire sawing, the c-Si programme of the U.S. PVMC held a workshop on July 8th, 2014 in San Francisco, California. One of the key products of this workshop was an extensive list of short- and long-term challenges. This article expands on some of the most important challenges identified at the workshop through the collective discussions and dialogue among a variety of PV industry experts and stakeholders.

Introduction

Unlike loose abrasive sawing, where abrasives are dispensed within the slurry and pushed against an ingot using a moving steel wire, fixed-abrasive sawing makes use of diamond wire consisting of a steel wire core onto which diamond particles are plated using a metal, usually nickel. Fig. 1 shows the anatomy of a diamond wire – steel core, metal coating and embedded diamond particles. There are several key advantages of diamond wire sawing: higher throughput is achievable, less wire is required per wafer, there is no slurry, and kerf recycling is possible. In addition, diamond wire sawing is expected to result in lower total thickness variation (TTV) of the wafer and in reduced metal contamination of the Si surface [1,2]. Reports also indicate that saw damage depths are lower with diamond wire sawing than with slurry-based sawing [1,3]. As a result, there has been a significant gain in momentum for diamond wire sawing.

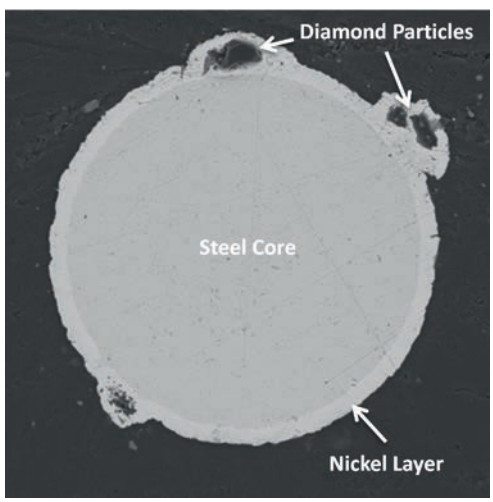

Figure 1. Scanning electron microscope (SEM) image of a diamond wire cross section, showing the core and the metal coating with embedded diamonds.

> "There has been a significant gain in momentum for diamond wire sawing."

However, diamond wire saws have been shown to decrease the breakage force for c-Si wafers by as much as a half, because of the formation of elongated cracks on the silicon surface during sawing [4]. The surfaces of slurry-sliced wafers tend to have more pits, while diamond-wire-sliced wafers exhibit scratches. The difference between the surfaces of diamond-wire-based and slurry-based cut silicon is due to the different cutting mechanisms. For slurry-based sawing, the accepted mechanism is the 'rolling-indenting' model, where SiC particles roll across the surface and carve out sections of silicon. In contrast, diamond wire sawing tends to cut silicon wafers by 'plastic ploughing' and 'brittle chip-off' methods [3].

As a result, the surface morphology of diamond-wire-sawn wafers has far-reaching effects, both technological and economical, down the value chain; these must be identified and addressed for diamond wire sawing to be prevalent by 2018. This article identifies the key challenges of diamond wire sawing from the perspective of diamond wire

manufacturers, coolant manufacturers, diamond wire saw manufacturers, metrology manufacturers, solar cell manufacturers and academic researchers.

Current outlook

The aim of the SEMI International Technology Roadmap for Photovoltaic (ITRPV) is to inform suppliers and customers about expected technology trends in the field of crystalline silicon (c-Si) PV and to add to discussions on required improvements and standards. The objective of the roadmap is not to recommend detailed technical solutions for identified areas of improvement, but to emphasize to the PV community the need for improvement and to encourage the effort to identify comprehensive solutions.

The fifth edition of the ITRPV (2014) [5] was jointly prepared by 28 leading international c-Si solar cell manufacturers, module manufacturers, silicon producers, wafer suppliers, PV equipment suppliers and production material providers, as well as PV research institutes. It covers the entire PV value chain, from crystallization, wafering and cell manufacturing to module manufacturing and PV systems. Significant parameters set out in earlier editions are reviewed along with some new ones, and discussions about emerging trends in the PV industry are reported. The following outlined topics specifically focus on diamond wire sawing.

Materials – crystallization and wafering

A significant improvement in cost reductions in the wafering process is expected as a consequence of the introduction of diamond wire sawing, especially for monocrystalline Si (mono-Si) wafers. Diamond wire sawing is expected to become widespread for mono-Si wafering; however, the field is open with regard to multicrystalline Si (mc-Si) wafering. Other new wafer-manufacturing techniques, especially kerfless technologies, are not expected to gain notable market shares, because of the maturity of the established sawing technologies. Fig. 2 shows the expected share of wafering technologies in volume production. The roll-out of diamond wire sawing technology requires a synchronization with cell process development.

Processes – technology

A challenging parameter is the kerf loss from slurry-based and diamond-wire-based technologies, as shown in Fig. 3. Kerf loss must decrease in order to achieve reductions in wafer thickness and silicon consumption.

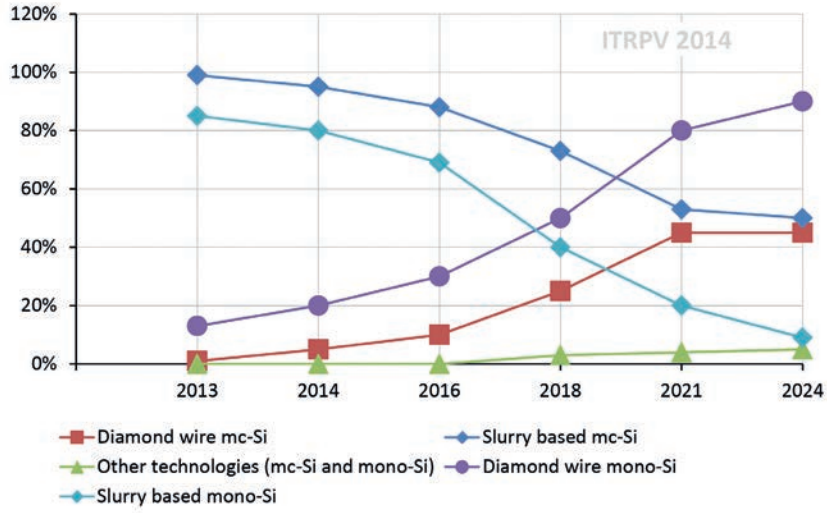

Source: SEMI PV [5]

Figure 2. Respective market share of wafering technologies for mono- and mc-Si.

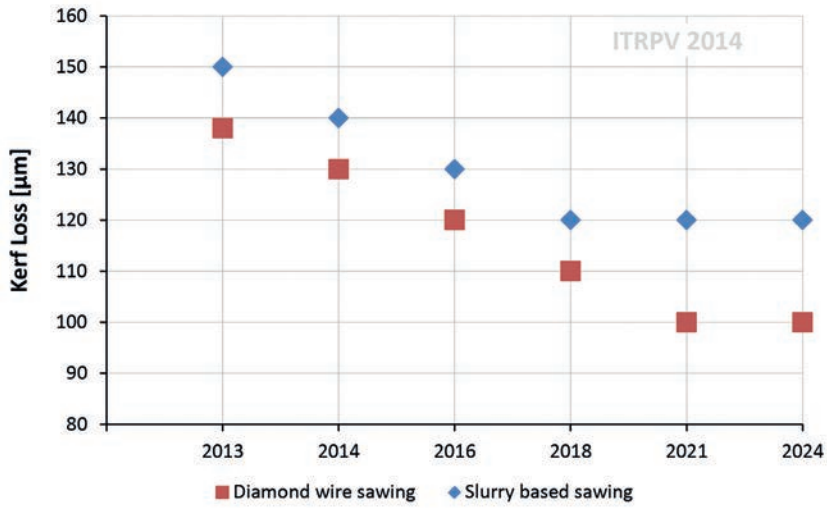

Source: SEMI PV [5]

Figure 3. Prediction for kerf-loss reduction trend.

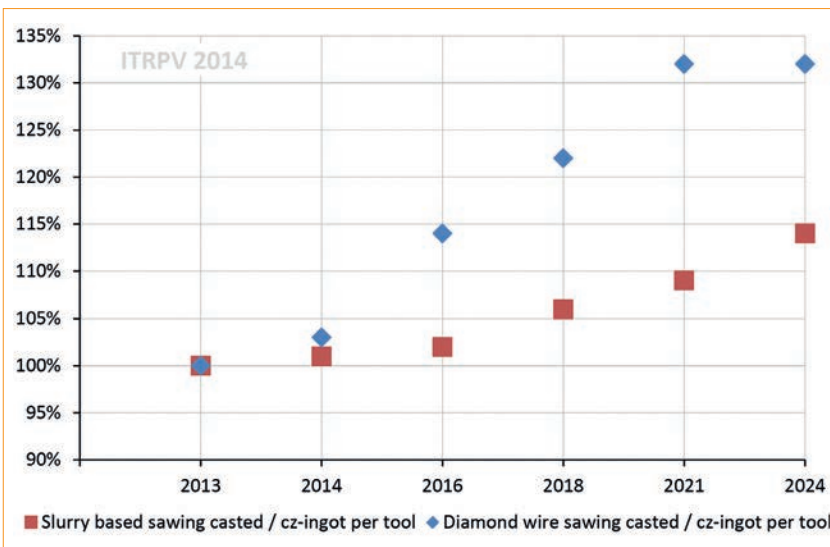

Source: SEMI PV [5]

Figure 4. Throughput per tool for diamond wire and slurry-based wafer sawing.

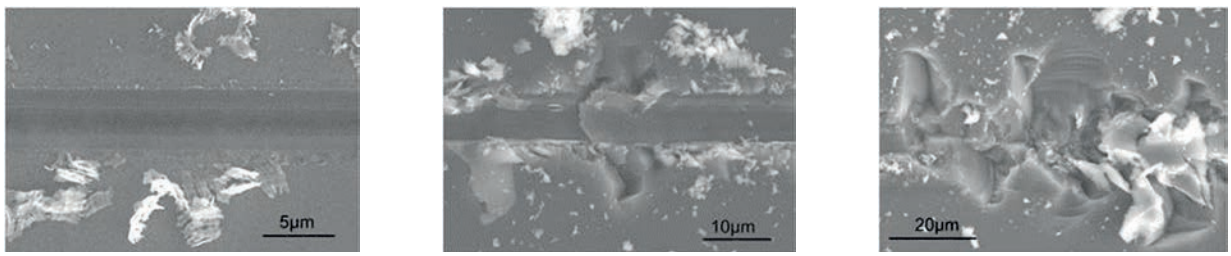

Figure 5. Scratch topography in diamond scribing of (111) mono-Si at different depths: (a) d_s= 0.12µm ductile cut; (b) d_s= 0.72µm ductile-brittle cut; (c) d_s= 1.23µm brittle cut [6,7].

Additional cost savings are expected from the introduction of diamond wire sawing processes as discussed above. Comparing the predictions of wafer thickness and kerf-loss trends beyond 2018, it is unclear if it is economically feasible to have a kerf-loss amount that is greater than the wafer thickness itself.

"Kerf loss must decrease in order to achieve reductions in wafer thickness and silicon consumption."

Processes – manufacturing

Fig. 4 shows that diamond wire sawing throughput is expected to grow steadily over the next few years, along with the expected appearance of new tools and processes accelerated by the introduction of this technology to the market. Slurry-based wire sawing will continue to improve its throughput over the coming years, but new developments, such as structured wires, demonstrate promising and significant throughput improvements.

Short-term challenges

Increase understanding of the diamond-wire-cutting process in order to reduce damage

Unlike the traditional slurry wire sawing process, which removes material through a combined rolling and indenting action of the SiC abrasives on silicon, the material removal in diamond wire sawing is characterized by a combination of two-body abrasion and indentation mechanisms. Consequently, the surface morphology of a diamond-wire-sawn wafer is distinctly different from a slurry-sawn wafer in that it exhibits clear evidence of ductile-mode cutting in the form of horizontal striations (or saw marks) interspersed with localized regions of brittle fracture.

It is well known that brittle materials such as silicon and other ceramics can exhibit pseudo-plastic (or ductile) behaviour under certain loading conditions that are induced by a combination of the cutting parameters (e.g. ingot/wire feed and speed) and grit geometry. This is the same behaviour that is responsible for the ductile saw marks visible on diamond-wire-sawn wafers. In theory, if the abrasive shape and cutting conditions can be controlled to promote ductile mode cutting behaviour at all points of interaction between the diamond abrasives and silicon, then a damage-free (or crack-free) surface can be achieved. This, in turn, can yield wafers that are mechanically much stronger than those obtained using current wire sawing technology. This section highlights the need and methods for further improving our fundamental understanding of the diamond wire sawing process and related surface/subsurface damage in order to further reduce damage.

Low-speed diamond-scribing studies using idealized indenter (or 'grit') shapes designed to elucidate the fundamental physics of material removal and associated surface/subsurface damage in silicon have shown that ductile-mode cutting behaviour is obtained at very small depths of cut (equivalent to the

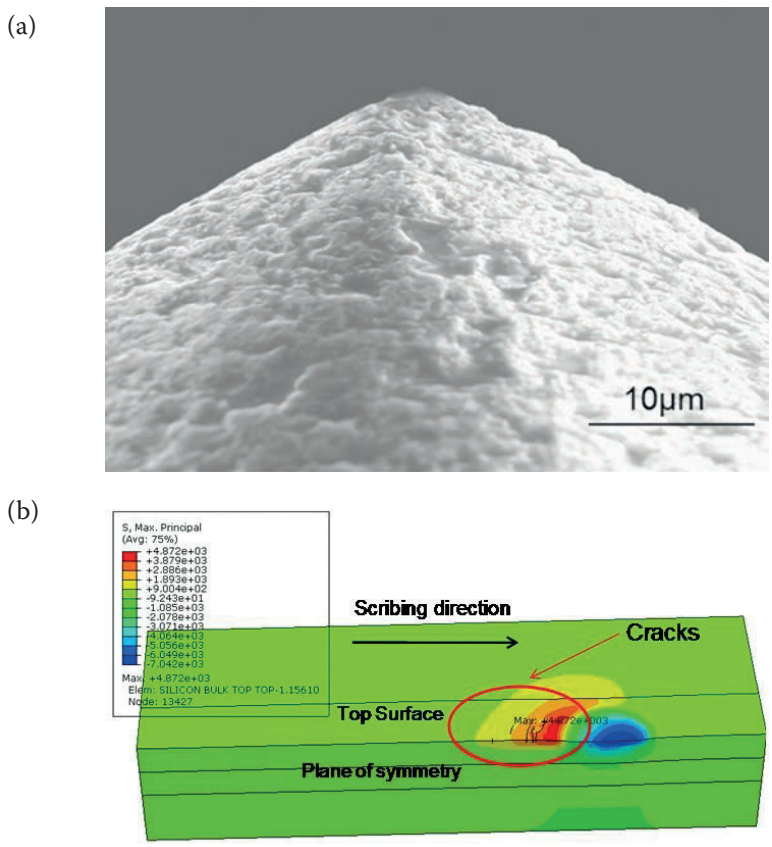

Figure 6. (a) SEM image of 'sharp'-tipped diamond scriber; (b) associated simulated stress state and surface cracking [6].

ingot/wire feed in wire sawing) (see Fig. 5). These studies also show that the abrasive shape plays a major role in determining the surface and subsurface cracking behaviour of the material. Specifically, the stress state produced in silicon during grit–material interaction is strongly influenced by the grit shape, and certain stress states (corresponding to the grit shape) cause ductile-to-brittle transition at lower depths of cut, leading to surface and/or subsurface cracking behaviour.

Fig. 6 shows an example of the simulated stress state and associated surface cracking for an idealized diamond indenter with a 'sharp' tip. Surface and subsurface cracking can also be 'delayed' by lowering the coefficient of friction between the diamond abrasive and the silicon [6], which can be accomplished in practice by suitably engineering the water-based cutting fluid used in diamond wire sawing.

At present, the industry use of diamond wire sawing is mostly limited to the production of mono-Si wafers, for which the process is economical. However, given the microstructural complexity of multicrystalline silicon (arising from the presence of grain boundaries, higher density of dislocations, carbide/nitride inclusions, etc.), the process is not economical for the wafering of multi-Si. Diamond-scribing experiments aimed at understanding the influence of some of the aforementioned crystal defects on the cutting characteristics of multicrystalline silicon suggest that local dislocation density variations (both within the grain and at the grain boundary) cause local mechanical property variations, which lead to local variations in the cutting characteristics and the resulting surface morphology [8,9]. Further work on this material is needed.

Accurately characterize surface and subsurface damage

The surface/subsurface damage produced by diamond wire cutting is the result of stress induced by the diamond particles, the wire, and the dynamics of cutting; the latter includes microcleavage of silicon by diamond chips, forward and reverse movement of the wire, and wobbling and vibrations of the wafer/ingot during cutting. The damage to the silicon lattice is in the form of:

1. Dislocations that remain 'frozen in' close to the surface, because the dislocation propagation velocity at the cutting temperature is very low.
2. Phase transformations (into amorphous silicon, and several possible phases of crystalline silicon).
3. Microcracks.
4. Lattice distortions that do not have accompanying dislocations.

It is important to accurately determine how far these defects reach into the wafer.

Angle polish method

The most common technique for determining surface damage is to angle polish a small section of wafer, followed by defect etching. To do this, a section of a wafer is mounted on a bevelled chuck and typically polished at 10° using progressively decreasing grit size and a final chemical mechanical polish (CMP). The CMP step ensures that the angle-polished region does not have any damage that can interfere with defect delineation by chemical etching.

Fig. 7 shows an optical microscope image of a defect-etched/angle-polished sample from a diamond-wire-sawn wafer: it shows the vicinity of the original as-cut and the angle-polished regions. The as-cut surface itself is very heavily dislocated, and some of the dislocations penetrate deep below the surface into the polished region. It should be pointed out that waviness of the unpolished region is due to the roughness of the cut surface. The maximum depth of damage is 5.6μm.

The angle-polishing/defect-etching process detects the mechanical manifestations of the damage and is influenced by surface roughness. Identifying the demarcation between as-cut and polished regions is subjective.

Effective minority-carrier lifetime method

A new method that uses an electronic property (surface recombination velocity – SRV) has been developed and recently modified for use with detection using the measurement of minority-carrier lifetime. This technique is based on measuring the effective minority-carrier lifetime τ_{eff} as a function of depth. The procedure consists of removing thin layers from the wafer surfaces by chemical etching and measuring the minority-carrier lifetime after each etch

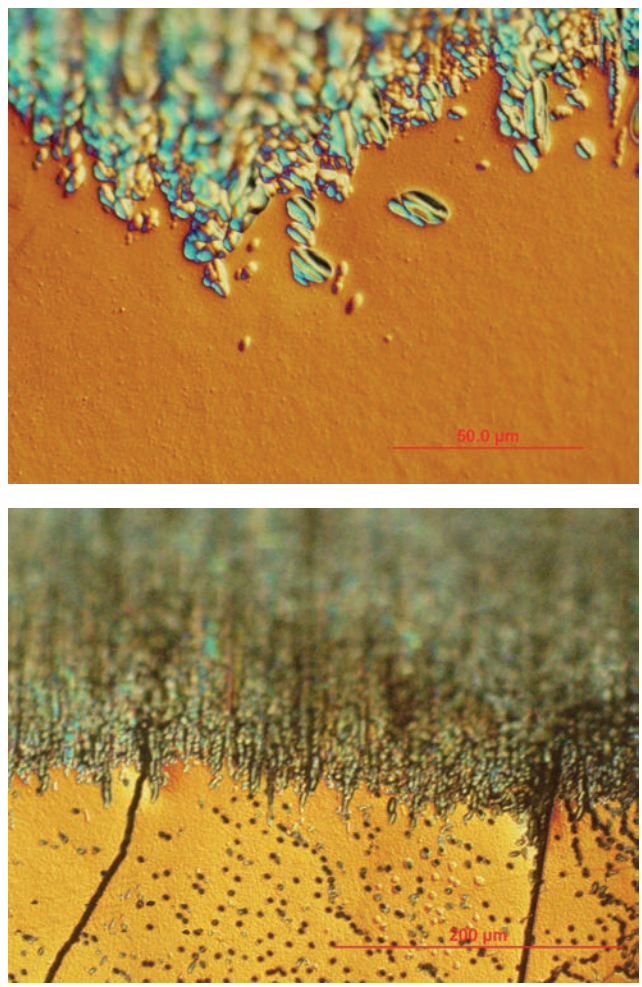

Figure 7. 10° angle-polished and defect-etched (using Sopori etch) diamond-wire-cut silicon samples, showing damage penetration into the bulk: (a) mono-Si wafer; (b) multi-Si wafer.

step. The effective lifetime increases as the thickness is removed and reaches a constant value; the thickness removed when the lifetime reaches the peak value is the damage depth. This new method is very accurate and has many advantages, including the fact that it can be easily adapted in a solar cell facility.

Fig. 8 shows a plot of the measurements of lifetime vs. thickness per side removed for a diamond-wire-sawn wafer. It is seen that there is a rapid increase in lifetime for etched depths below 3μm, followed by a gradual increase from ~3μm to ~5μm, and the lifetime then begins to drop. Since the decrease in surface recombination velocity (S) for S < 50cm/s has only a small effect on increasing τ_{eff} (especially for low lifetimes), this increase is small; τ_{eff} then decreases because wafer thickness is reduced. Because S is very sensitive to damage, the highest lifetime (at around 5μm) implies the damage is fully removed. This new method is very versatile and has many advantages, including:

1. It can determine the average damage depth over a large area, which is more appropriate for solar cell fabrication.

2. The measurement system is readily available in most solar cell laboratories.

3. It can be applied to wafers that have significant surface roughness (e.g. diamond-wire-sawn wafers).

Infrared polariscopy method

Residual stresses in the starting wafers and the finished cells can affect the electrical behaviour of devices, as well as eventually leading to the fracture and failure of cells [10,11]. One source of residual stress is sawing. Sawing generates damage in the form of plasticity and cracks on both sides of the wafer surface, and it is the interaction of the dislocations, cracks and other defects that leads to stress [12]. This stress is referred to as *residual stress*, since it exists without any externally applied loads. The level of this residual stress varies over the surface and can easily reach or exceed typical stresses imparted by wafer handling. Residual stress varies with the sawing conditions, such as the type of sawing used (diamond wire vs. slurry), the entry point of the wire, the feed rate and the speed of the wire [13]. This surface damage and the associated residual stress can be removed by etching, but to effectively do so requires an understanding of how the residual stress is produced, its magnitude, its sign (tensile or compressive) and its depth into the wafer.

There are a few suitable techniques available for measuring residual stress; of these, near-infrared (NIR) digital photoelasticity is attractive because of its simplicity, accuracy, sensitivity to localized stress, and full-field, non-contact nature. This technique can generate, in a matter of seconds, full-wafer residual stress maps with an accuracy of 1MPa and at a spatial resolution of just 20μm^2. In NIR digital photoelasticity, polarized light is transmitted through a birefringent material, such as a silicon wafer, as pictured in Fig. 9. As the polarizing optics are rotated to known angles, a digital camera can record the relative phase retardation of the polarized light at each point in the wafer; this retardation can then be associated with the localized residual stress by using well-established techniques. Specifically, the stress measured by this technique is the maximum shear stress. However, the maximum shear stress alone is not sufficient for capturing the true nature of the stresses due to sawing conditions: an additional image-processing algorithm must be applied in order to determine the normal stress components oriented to the wafer edges. To accomplish this task, unique algorithms were developed to extract the normal stress maps, which play a key role in understanding the relation of the sawing conditions to other characteristics of the cells and, of course, to possible failure of the wafers.

As an example, consider the residual stress values shown in Fig. 10, obtained for an as-sawn Cz silicon wafer: Fig. 10(a) shows the maximum shear stress plot, and Fig. 10(b) and (c) show the separated normal stress components. In Fig. 10(a) and (b), note the presence of curvature lines caused by wire sawing. Although some sawing damage is visible in the maximum shear stress map in Fig. 10(a), the x-direction normal stress component seen in Fig. 10(b) clearly indicates significant tensile stresses perpendicular to the sawing direction. By leveraging this measurement technique, both the sawing and the

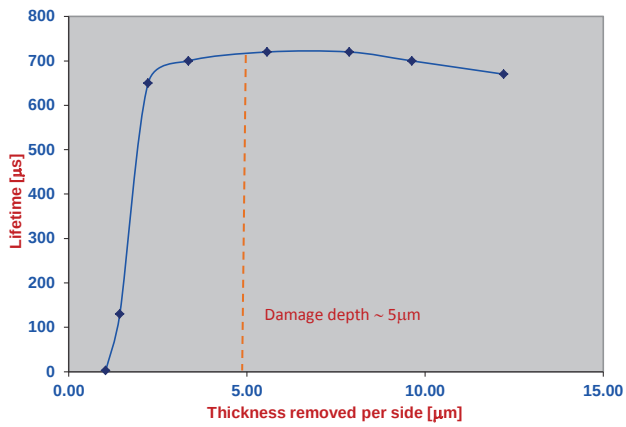

Figure 8. Measured lifetime as a function of depth for a diamond-wire-sawn wafer. The damage depth determined by this technique (4.8μm) agrees very well with the average depth resulting from the angle-polishing/defect-etching technique.

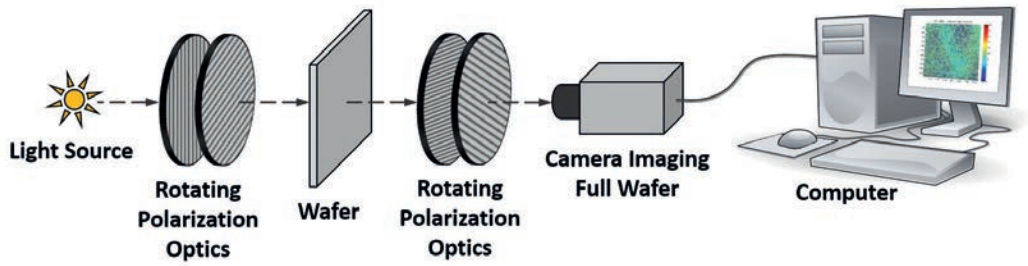

Figure 9. Schematic of the imaging technique used to generate full-field stress maps with NIR digital photoelasticity.

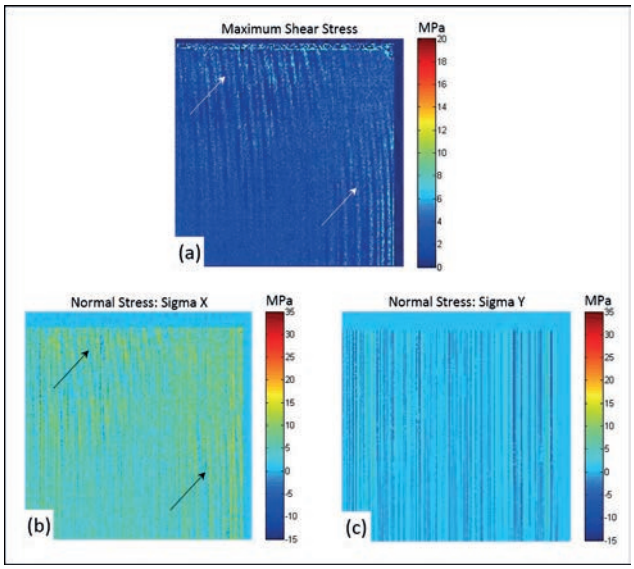

Figure 10. Stress plots of a Cz silicon wafer, generated through NIR digital photoelasticity: (a) maximum residual shear stress; (b) normal stress component σ_x; (c) normal stress component σ_y.

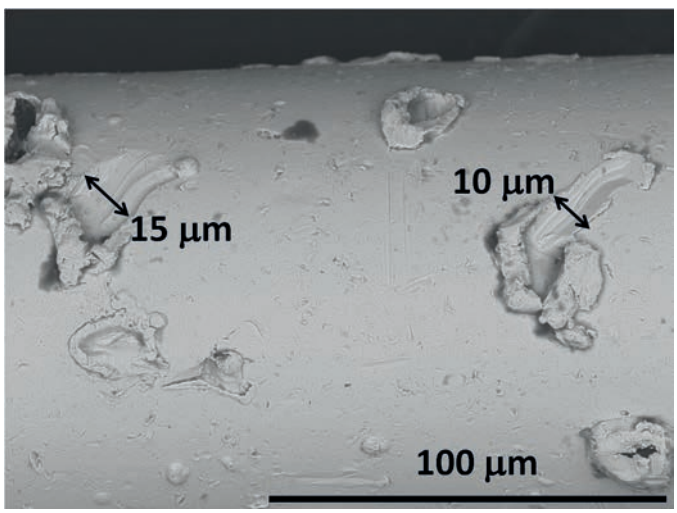

Figure 11. Diamond pull-out.

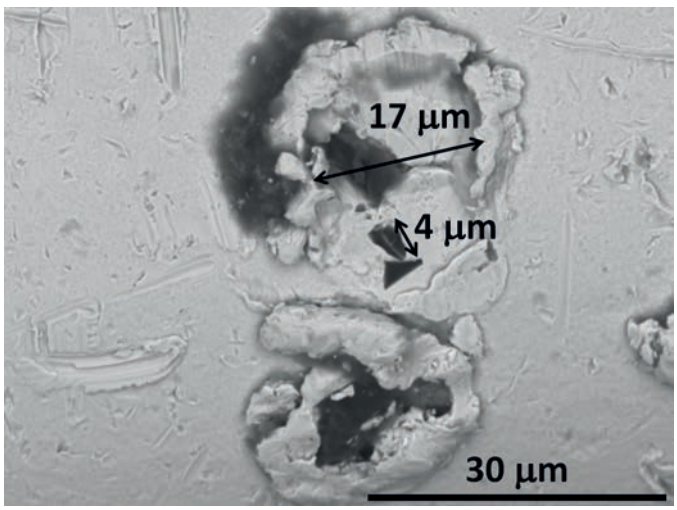

Figure 12. Diamond fracture.

etching process of the wafer can be monitored and optimized.

"The identification of failure modes and wear mechanisms will help increase the wire durability and material lifetime, and may also reduce wire consumption."

Identify failure modes and wear mechanisms

Diamond wire wear and failure during silicon wafer slicing is influenced by a number of factors, including the properties of the diamond wire and its components (steel core, diamond particles, plating metal), wire saw parameters, mechanical properties of the silicon, and coolant chemicals used to aid slicing [14–17]. The identification of failure modes and wear mechanisms will help increase the wire durability and material lifetime, and may also reduce wire consumption.

Diamond wire and components

The diamonds employed in diamond wire saws are attached to the surface of steel cores by means of electroplated nickel; thus, the adhesion of the diamonds depends on the quality of the electroplated metal. Furthermore, the friability of the diamonds will play a crucial role in the diamonds' ability to abrade the silicon. Higher friability will lead to less abrasion and could increase wafer surface damage. SEM images of used diamond wires demonstrate several wear mechanisms of the wires.

First, as mentioned, diamond adhesion to the wire can be poor. As shown in Fig. 11, diamonds can be 'pulled out' of the wire, clearly damaging the wire surface, and possibly damaging the wafer too. Not all pull-outs, however, are accompanied by scratches, as also evidenced by Fig. 11. The hole at the top clearly had a diamond at one time, but this has become detached during use. Factors that influence a diamond pull-out could be manufacturing based or application based. In terms of manufacturing, the effectiveness of the electroplating process in adequately attaching the diamonds will play an important role in retaining the wire's abrasion. However, the speed and force of the wire on the ingot will quite likely also play a role, as will the extent to which the wire is used. The more the wire is used, the less nickel there is surrounding the diamonds and the greater the chances are of diamond pull-outs.

Another wear mechanism of diamond wire is diamond fracturing: in this mechanism, the diamond size is reduced to less than 5µm (see Fig. 12). At this size, the diamonds will again be removed from the wire and the abrasiveness will decrease. This mechanism is a function of the choice of diamond, and should be considered when manufacturing diamond wire.

Some ex situ testing revealed that the adhesion between the steel core and metal coating can be a challenge. In these tests, a wire was drawn in tension until it failed, at which point the fractured ends were examined by SEM. At times, the wires showed some separation between the core and coating, suggesting some adhesion issues (see Fig. 13). The extent to which this failure mode impacts wire performance in the field is unknown.

The surface of the wire also points to the wire dynamics during cutting. Several wires were examined after slicing wafers, and it was observed that scratches were present over the surface. It was also observed that the scratches extended along the length of the wire and in several directions (Fig. 14). These scratches could be the result of diamond or silicon particles damaging the surface of the wire. It is recognized that the nickel surface is much softer than silicon, so the damage to the wire is probably more than what would be observed on the wafer. However, it does indicate to some extent the types of particle that are present during diamond wire wafer slicing.

Wire saw parameters and mechanical properties of the silicon

Numerous wire saw parameters were evaluated during slicing experiments with 156mm silicon ingots. It was concluded that, within typical setting ranges, fresh wire feed rate into the web had the largest effect on wire wear. Diamond wire specifications were fixed, with a core wire diameter of 120µm and electroplated diamond particles in the range 10–20µm; hence there were no significant variations in wire properties that might affect wear. Three different 156mm silicon ingots were sliced:

- Ingot A: monocrystalline Cz p-type boron-doped silicon with <100> orientation.
- Ingot B: monocrystalline MCz p-type boron-doped silicon with <100> orientation.
- Ingot C: p-type multicrystalline silicon.

The slicing coolant for all experiments was Aquaslice, diluted at 2% in city water.

Slicing was performed using a Takatori WSD-K2 R&D-scale diamond wire saw, which allowed the number of wires in the web to be varied from 1 to 29. In most cases, six wires were used, generating five wafers per experiment. Fresh wire feed rate was varied from 1.0m/min to 2.5m/min; typical slicing time was 260min and hence the total wire use per experiment varied between 260 and 650m. Wire tension and speed were kept constant at 20N and 600m/min respectively.

Wire wear was determined by measuring the diameter of the wire at 50m intervals before and after each experiment and expressed as a percentage of the original wire diameter. Wire wear was normalized to percentage of slicing completion; this allowed experiments in which the wire broke during slicing to be compared with successfully completed experiments. A means of comparing wire wear measured under various conditions was required: a wire-to-silicon contact ratio was therefore developed and defined as

$$\frac{\textit{Amount of wire used}\ [\mathrm{m}]}{\textit{Cut depth}\ [\mathrm{mm}] * \textit{Number of wires in web}} \quad (1)$$

Higher values of this ratio can represent low numbers of wires or high wire feed rates, or both; lower values represent high numbers of wires in the web or low wire feed rates, or both.

Normalized wire wear vs. wire-to-silicon contact ratio results for ingots A, B and C are plotted in Fig. 15. As expected, wire wear increased with decreasing wire-to-silicon contact ratio. Apart from single-wire conditions, the wear for ingot B was considerably higher than for ingot A, implying that the MCz silicon was more difficult to slice than

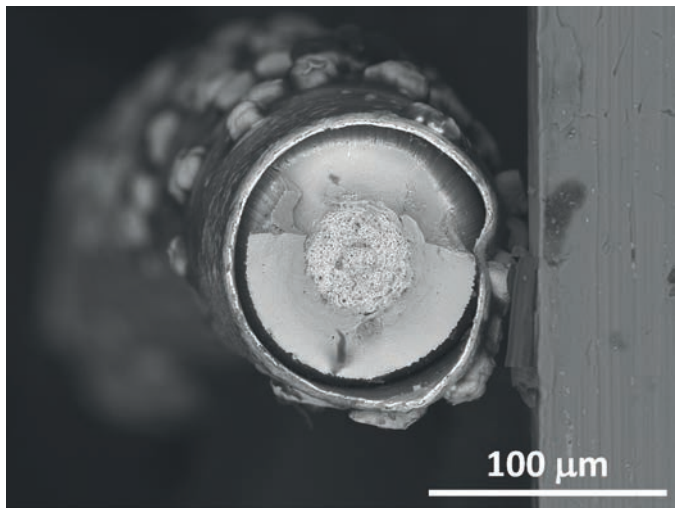

Figure 13. SEM cross section of an ex situ failed wire.

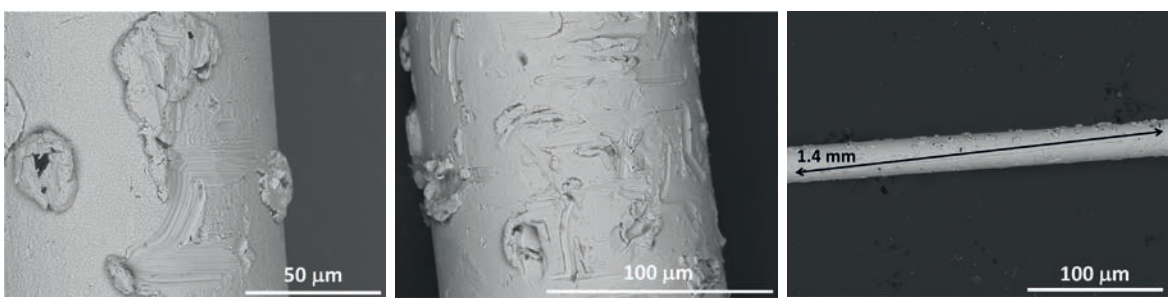

Figure 14. Several scratch directions on used wires.

Cz silicon. These results correlate well with measured Vickers hardness values of 532kg/mm^2 and 658kg/mm^2 for ingots A and B respectively. Vickers hardness data were not obtained for ingot C (multicrystalline); however, the slicing of ingot C appeared to cause wire wear somewhere between that for the MCz ingot B and for the Cz ingot A.

"There is a need for real-time inspection of the diamond wire for quality control during diamond wire production and/or for process control during silicon wafering."

Implement non-destructive inspection metrology for diamond wire

There is a need for real-time inspection of the diamond wire for quality control during diamond wire production and/or for process control during silicon wafering (e.g. real-time monitoring of the level of wear of diamond wire during sawing). This section describes novel solutions for an in-line and non-destructive inspection of diamond wire. However, the in-line implementation of these metrology techniques dictates that they operate at certain speeds and within harsh environments.

Optical inspection system

A new optical inspection system capable of detecting defects – down to a few microns in size – that are only on the surface of diamond wires moving at speeds of up to 10m/s was recently reported [18]. This novel non-contact metrology relies on four high-speed cameras that can take 10,000 images per second and process them in real time. An obvious concern is the maintenance of the optics in the harsh wafering environment.

Resonant vibrations of the diamond wire

Another approach, which can be applied at the back-end of diamond wire production and diamond wire silicon wafering, is based on the resonant vibrations (RVs) of the diamond wire. Fundamentally, this method assesses the diamond wire mechanical quality using the physics of a vibrating string, by agitating the diamond wire segment by a non-contact actuator and measuring an RV curve with a non-contact acoustic probe in a selected frequency range. Characteristics of the resonance curve – peak frequency, bandwidth and amplitude – allow a fast non-destructive characterization of the diamond wire quality.

The RV method was initially demonstrated on a stationary diamond wire sample and then expanded to a moving diamond wire, which is a model of a real-time wafering process. The following experimental data validated the RV approach:

- The RV frequency measured on new and used samples of diamond wire from the same vendor shows a shift on the used samples.
- The RV frequency gradually shifts with

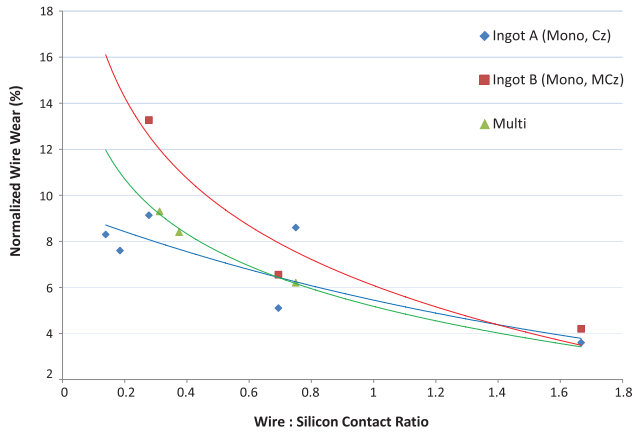

Figure 15. Effect of wire-to-silicon contact ratio on normalized wire wear. (Note: on the basis of a typical fresh wire diameter of 144µm, maximum wire wear (all diamonds lost) would be around 17%.)

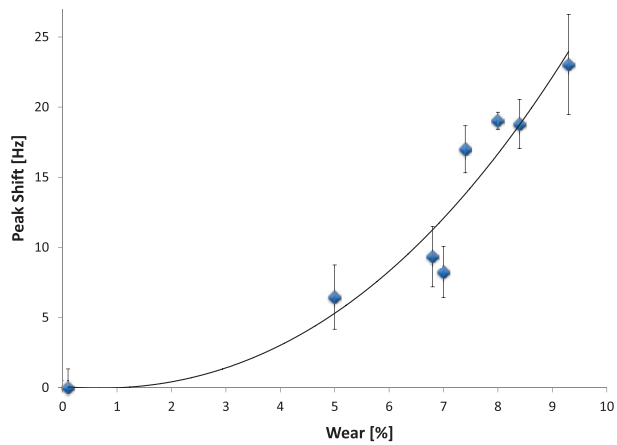

Source: UST/UCF

Figure 16. RV vs. wear in % of wire diameter. The error bars represent standard deviations for three samples from each diamond wire.

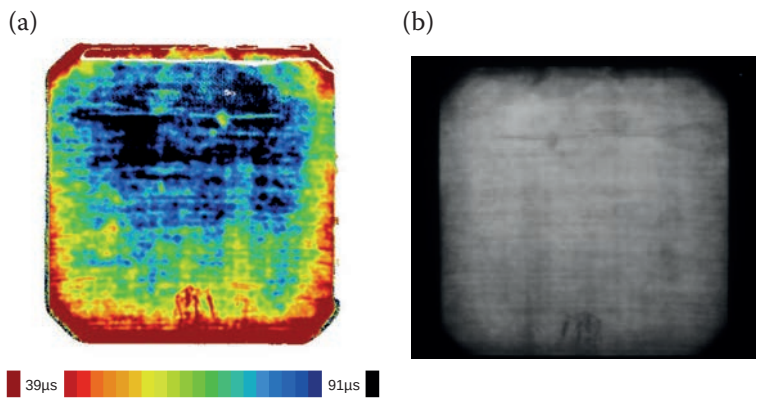

Figure 17. (a) Minority-carrier lifetime and (b) PL maps of a diamond-wire-cut wafer after etching a thin layer from the surfaces in order to sufficiently lower the SRV to enable the making of the maps. (Note the taper in the damage profile, with higher damage towards the bottom edge.)

increasing metal plating thickness.

- The RV frequency is reduced with increased density of the diamond particles.
- A correlation exists between the percentage of diamond wire wear and the shift in RV frequency (see Fig. 16).

The RV method is able to detect internal flaws below the surface of the diamond wire components (core, metal layers, etc.) and is compatible with the harsh wafering environment. Theoretically, it has been determined that the characteristics of the resonance curve do not change at speeds upwards of 500m/s, which makes it a viable candidate for monitoring diamond wire during sawing as the wire speed continues to scale up.

Impact of diamond-wire-sawn wafers on solar cell manufacturing

The surface properties of diamond-wire-sawn wafers and slurry-sawn wafers are different, which impacts the entire solar cell production process. Chemical etching of mono-Si wafers by NaOH- or KOH-based solutions is extensively being used for texturing to reduce the surface reflectance and for providing very effective light trapping of wafer-based Si solar cells. The etching is typically done using KOH solutions in a concentration range of 30–40%, at 70ºC. Under these conditions, texturing occurs because the etch rate in the <100> direction is very high compared with that in the <111> direction, causing exposure of the (111) faces and a concomitant formation of pyramids. The texturing of (100) wafers reduces the reflectance to about 10%, which can be further lowered by an anti-reflection coating. It is known that texturing of wafers works well only in the presence of surface damage; this is very fortunate because it allows texturing to be combined with the surface damage removal step, yielding a uniform texture on slurry-cut wafers.

However, the surface roughness of diamond-sawn wafers is greater than that of slurry-cut wafers, and the wafer surfaces exhibit striations, which can interfere with texturing. Fig. 17 illustrates the damage and surface roughness effects in a diamond-wire-sawn wafer. Fig. 17(a) is a minority-carrier lifetime map of a wafer, which was chemically etched to remove a thin layer of the damaged surface (to enable lifetime and photoluminescence – PL – measurements); the regions of lower lifetime correspond to higher damage. Fig. 17(b) is a PL map of the same wafer, confirming the effect of striations.

Fig. 18 is a reflectance map of a standard diamond-cut, textured wafer, showing a modulation in the reflectance because of the surface morphology generated by diamond cutting and retained through texturing. This results in a non-uniform texture whose effect is estimated to degrade cell efficiency by at least 0.5% abs. To process diamond-wire-sawn wafers, production lines developed for slurry-sawn wafers need to be adapted. Hence, it is expected that improving the texturing of the sawn wafers can recover the loss in cell efficiency, and will also simplify cell processing (such as metallization).

It has been shown that diamond-wire-sawn wafers have thicker oxide layers than slurry-sawn wafers, and that the surface layer also contains significant amounts of amorphous silicon [19]. These layers have an impact on the wet-chemical processes used for saw damage removal and texturization. It has been reported that the etch rate of amorphous silicon is slower by a factor of 30 in the (001) surface [20], thereby increasing valuable processing time in order to achieve the target wafer surface condition. Moreover, thicker oxide layers might act as a masking layer during texturization, which leads to lower light trapping when compared with slurry-sawn wafers. An example is shown in the SEM image in Fig. 19. When subjected to the same texturization process, the diamond-wire-sawn wafer still has untextured regions, while the slurry-sawn wafer is fully textured.

Long-term challenges

Reduce kerf loss below 80µm

As the solar industry continues to move to higher-efficiency cell performance, it is also focusing on ways to reduce wafer cost, which is still a big portion of the module cost. The main cost contributor is the silicon and can be split into wafer-thickness and kerf-loss categories. While the industry looks to save on cost, wafer manufacturers are investigating ways of reducing wafer thickness and kerf loss.

Kerf loss is determined by the wire core size used by the slicing technology. The limitation for reducing the wire core with slurry-slicing technology is around 110µm; however, with diamond-wire-slicing technology the wire core can be reduced further. The diamond wire core used today is around 100µm, with the trend moving to less than 70µm within the next two years. The use of such a thin wire core, however, introduces key technical challenges: one of these is that, as the wire core diminishes, so does its intrinsic breaking load. The breaking-load curve limitation is illustrated in Fig. 20.

As shown in Fig. 20, a 70µm wire core should have a working tension of around 8N, with a breaking load of 15N, while a 120µm wire core can operate at 25N and have a breaking load of 45N. This provides only a 7N safety margin to operate a 70µm wire core below its physical limitation, while the safety margin is 20N for a 120µm wire core. Consequently, both the working-tension control accuracy and the pulley-inertia management must be improved to accommodate the wire limitation.

The wire management of a new wire saw platform will have to include

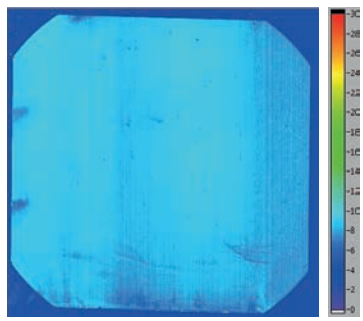

Figure 18. A reflectance map of a textured wafer, showing previous striations after texture etching. (Note: there are other 'marks' on the textured wafer from the holder.)

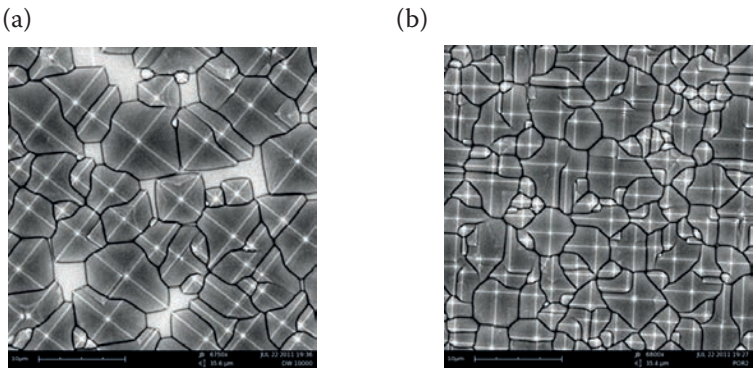

Figure 19. SEM of the texture for (a) a diamond wire cut, and (b) a slurry-based cut.

highly accurate tension control, a low-inertia pulley system, and an innovative cutting movement designed to optimize cutting pressure and silicon removal. These features will compensate for the thin wire core limitations and optimize the slicing trade-offs in terms of cutting feed rate and diamond wire usage. A kerf-loss reduction of 20µm achieved by using a thinner wire core would yield significant silicon cost savings and therefore wafer cost savings. The new wire saw platform addresses these key technical challenges by supporting improvements – such as an innovative cutting motion, accurate wire-tension control and low-inertia pulley systems – resulting in higher wafer quality.

Enable diamond-wire-sawn wafer thickness below 140µm

Another big opportunity for lowering wafer cost is by decreasing wafer thickness. The current monocrystalline wafer thickness is around 180µm, which represents around 60% of the silicon cost. The goal is to drive the wafer thickness below 140µm; at today's cost, a reduction of 40µm can represent a saving of around $0.10 per wafer. This cost reduction can help drive the adoption of monocrystalline advanced cell structures, such as interdigitated back contact (IBC) solar cells and heterojunction (HJT) silicon-based solar cells. An additional, and potentially more critical, motivation for reducing wafer thickness concerns cell efficiency. There is an optimal wafer thickness for which the best cell efficiency can be obtained: according to studies, this is approximately 50µm [21].

However, there exist barriers to producing ultrathin wafers, so an intermediate step is to first reduce wafer thickness from 180µm to 140µm. Even for this level of reduction, there are still barriers, including:

1. At the saw level – motorization, gluing and singulation.
2. At the cell level – mechanical yield and wafer handling.
3. At the module level – stringing and tabbing thermal effects, leading to mechanical and electrical yield issues.

At the saw level, cutting ultrathin wafers with ultrathin kerf loss will require an increase in machine power: the more wafers to cut, the more power required (based on the cutting forces) to remove the silicon materials from the cutting channel. The gluing step will also need to be improved, as the cross section of the wafer reduces the area holding the wafers by the glue. The saw must be equipped with an advanced wafer box to prevent wafers falling during the cut when wafer thickness drops below 180µm. In addition, an innovative cutting motion can improve wafer strength and will therefore help wafer handling as wafer thickness is further reduced. For example, it was recently reported by Applied Materials that a technology called OS2 (oriented synchronized slicing) can increase wafer strength by 6%.

Automatic singulation may be required for handling the emerging fragile ultrathin wafers. Eventually, the singulation can be integrated with the saw to minimize broken wafers and optimize mechanical yield. Cells produced from wafers of thickness below 140µm will require soft handling to prevent breakage, which leads to a mechanical yield issue. It is a well-known fact that the force required to break a wafer decreases as the wafer becomes thinner, while the wafer flexibility increases. In order to accommodate lower thicknesses, screen printers must allow for advanced handling schemes. At the module level, to minimize mechanical yield loss, new and innovative modelling structures, such as the backsheet with back-side cell structures, need to be introduced.

All the above factors are slowing down the rate of industry adoption of wafers below 140µm.

"Increased collaboration on a technical wafer-cost roadmap will be crucial in order to help the industry achieve further cost reductions."

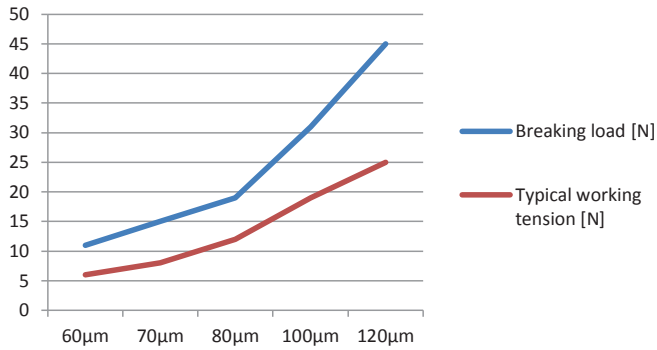

Figure 20. Breaking-load curve limitation.

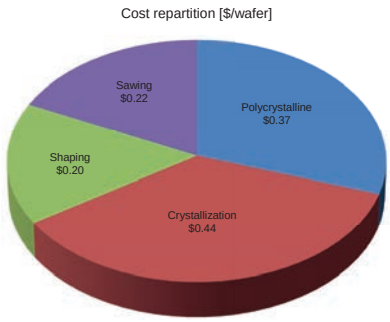

Source: Applied Materials

Figure 21. Monocrystalline wafer cost breakdown.

Enable a wafer price below $0.70/wafer

Increased collaboration on a technical wafer-cost roadmap will be crucial in order to help the industry achieve further cost reductions, at both cost per watt and manufacturing cost per wafer levels. This wafer-cost roadmap should take into account several major inputs in order to reduce the wafer-slicing cost. Different aspects – such as polycrystalline, crystallization, wafer-slicing conversion and consumables costs – can be evaluated separately or in combination. This section discusses a roadmap and the associated challenges for achieving a wafer price below $0.70 and a levelized cost of electricity (LCOE) below $0.06/kWh.

Barriers to achieving under $0.70/wafer

Today's cost of a multicrystalline wafer (156mm × 156mm) is in the neighbourhood of $0.90, against $1.20 for a monocrystalline wafer of the same size. The industry has been able to drastically reduce the multicrystalline wafer cost over the last decade by introducing high-efficiency multicrystallization techniques (higher material efficiency), lowering the wafering cost (leveraging cost of consumables)

and implementing production-scale manufacturing accompanied by market consolidation. These improvements are reaching their limits for multicrystalline wafers; however, there is still room for significant improvements in the case of monocrystalline wafers. A breakdown of the monocrystalline wafer cost is given in Fig. 21.

Improvements are being made in the following areas:

- Polycrystalline cost reduction through the implementation of advanced fluidized bed reactor technology.
- Crystallization cost reduction through the use of continuous Czochralski processes (lower electricity and crucible costs).
- Wafer-slicing conversion costs at the saw level, boosting productivity, lowering wire consumption, decreasing kerf loss, and optimizing pitch for silicon saving. (Slicing-conversion cost benefits are also possible from a consumables perspective; for example, improvements in diamond wire manufacturing can lead to lower diamond wire pricing.)
- Enabling thinner wafers within the next two or three years will also be part of the wafer cost saving equation.

Assuming the industry overcomes the related challenges, and is able to introduce these advanced technologies, Table 1 shows a path to reducing the cost of monocrystalline wafers to less than $0.70.

Impact of wafer cost on cell price and LCOE

A fundamental factor driving the adoption of PV as a viable energy source is the reduction in the LCOE produced from PV. The LCOE target for PV to be competitive with the alternatives has to take into account many complex factors (including site location, module cost and efficiency, climate, interest rates, logistics, balance of systems (BOS) costs, land costs, etc.). In the USA an LCOE target of $0.06/kWh is generally believed to be a critical threshold for PV to be a viable alternative to traditional sources of energy. Two of the critical factors (module cost and module efficiency) influencing the LCOE are directly controlled by a PV (cell and module) manufacturer.

As an example, Fig. 22 shows, for a generic location in the USA (Atlanta, Georgia, with 4.66kWh/m^2/day of average daily insolation), the sensitivity of the LCOE to module efficiency and module cost under two different BOS cost assumptions. As can be seen from the shape of the LCOE contours in Fig. 22(a) and (b), the module cost becomes a more significant factor in moving to a lower LCOE either when the module efficiency is improved (contours become more vertical on the upper halves of the charts) or when the overall system costs are reduced, as evidenced from a comparison of Fig. 22(b) and Fig. 22(a). This implies that, in order to move the LCOE towards the $0.06/kWh value, it would be necessary to significantly reduce module costs, which comprise wafer costs, wafer-to-cell conversion costs and cell-to-module conversion costs. The costs for all three of these components need to be cut through reductions in the bill of materials for wafers (polysilicon costs, consumables, etc.), cells (reduced use of Ag and chemicals in cell fabrication), and modules (lower-cost encapsulant, thinner glass, etc.), as well as through reductions in processing costs. The latter is achievable by means of larger-scale and fully integrated operations through further consolidation of PV manufacturing and improvements in processing equipment (higher throughputs, lower cost of ownership).

Cheaper wafers can significantly impact the module costs and thus help lower the LCOE. In particular, the current average costs of monocrystalline wafers of ~$1.10 to $1.30 equates to a contribution of approximately $0.25/Wp to the module cost. A reduction in wafer price to ~$0.70 (enabled through a wafer thickness reduction in order to increase the wafer yield per ingot) will translate into a module cost reduction of approximately 42%, or $0.104/Wp, in module costs. This further translates into an LCOE reduction of $0.005/kWh, as can be seen from Fig. 22(a) and (b), which is a significant move towards grid parity.

> "For diamond wire sawing to overtake loose-abrasive/slurry-based sawing, short- and long-term challenges need to be successfully addressed."

Conclusion

Wire sawing is expected to continue to be the workhorse of the PV industry for slicing silicon ingots into wafers with thicknesses less than 200µm, although various disruptive kerfless wafering technologies are being developed.

Cost component	2014 (slurry)	2016 (diamond wire)	2018 (diamond wire)
Wafer thickness [µm]	180	163	140
Wire diameter [µm]	110	80	60
Kerf loss [µm]	150	100	70
Pitch [µm]	330	263	210
Theoretical wafer yield [wafers/kg]	53 (19g/wafer)	66 (15g/wafer)	83 (12g/wafer)
Productivity [MW/year]	11.8	14.3	12.7
DW usage [m/wafer]	-	1.3	1.44
Yield [%]	95	98	98
TTV [µm]	< 30	< 20	< 15
Est. cost (poly) [$/wafer]	0.37	0.25	0.22
Est. cost (cryst.) [$/wafer]	0.44	0.27	0.19
Est. cost (shaping) [$/wafer]	0.20	0.12	0.09
Est. cost (sawing) [$/wafer]	0.22	0.17	0.16
Total est. cost [$/wafer]	1.23	0.88	0.66

Source: ITRPV, Applied Materials

Table 1. Monocrystalline (156mm × 156mm) cost roadmap, illustrating that a wafer cost under $0.70 is possible.

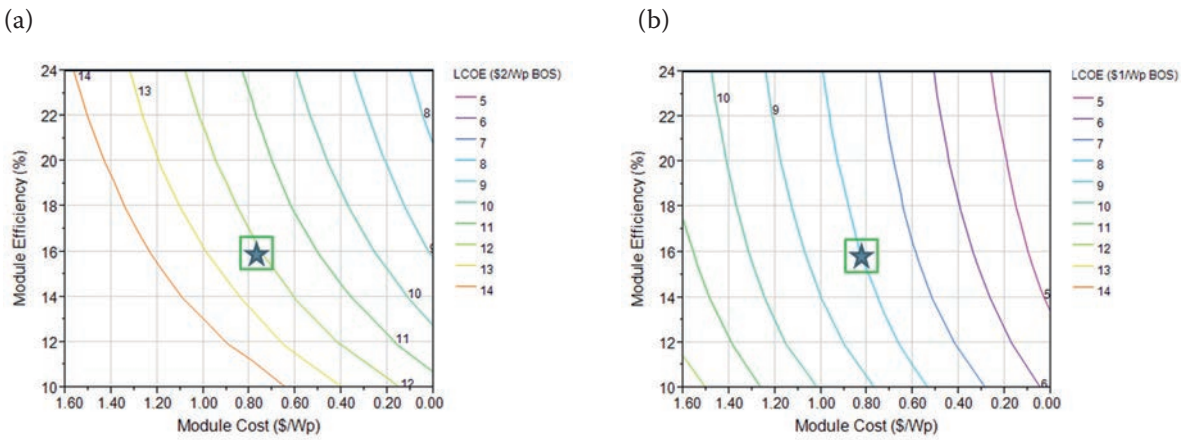

Figure 22. LCOE contours for Atlanta, Georgia, as a function of module efficiency and cost under two different cost assumptions: (a) BOS costs of $2/Wp; (b) BOS costs of $1/Wp. The inner box represents mainstream modules available on the market and their costs to the installers. LCOE calculations were performed using the system advisor model (SAM) program from NREL [22] with the following parameters: system lifetime = 30 years; performance derate = 20%; average inflation = 2.5%; real discount = 8%; loan term = 10 years; weighted average cost of capital (WACC) = 7.69%; no investment tax credits (ITC), with 50% of the total BOS costs scaled with efficiency.

Today, most companies in this industry use a loose-abrasive/slurry-based slicing process as opposed to the promising fixed-abrasive diamond wire approach. However, most industry roadmaps predict an increase in market share for diamond wire sawing for both mono- and multicrystalline silicon. For diamond wire sawing to overtake loose-abrasive/slurry-based sawing, short- and long-term challenges need to be successfully addressed. Moreover, the interdependency of the challenges dictates a resolution through a collaborative methodology and industry consensus.

References

[1] Bye, J.-I. et al. 2011, "Industrialised diamond wire wafer slicing for high efficiency solar cells", *Proc. 26th EU PVSEC*, Hamburg, Germany.

[2] Lanz, M. & Richter, A. 2011, "Comparison of diamond wire and slurry sawn wafers with respect to cell manufacturing and performance", *Proc. 26th EU PVSEC*, Hamburg, Germany.

[3] Cai, E. et al. 2011, "Characterization of the surfaces generated by diamond cutting of crystalline silicon", *Proc. 26th EU PVSEC*, Hamburg, Germany.

[4] Bidiville, A. et al. 2010, "Diamond wire wafering: Wafer morphology in comparison to slurry sawn wafers", *Proc. 25th EU PVSEC*, Valencia, Spain.

[5] SEMI PV Group Europe 2014, "International technology roadmap for photovoltaic (ITRPV): Results 2013", 5th edn (March) [available online at http://www.itrpv.net/Reports/Downloads/].

[6] Wu, H. & Melkote, S.N. 2012, "Study of ductile-to-brittle transition in single grit diamond scribing of silicon: Application to wire sawing of silicon wafers, *J. Eng. Mater. & Tech.*, Vol. 134, p. 041011.

[7] Wu, H. & Melkote, S.N. 2012, "Effect of crystallographic orientation on ductile scribing of crystalline silicon: Role of phase transformation and slip", *Mater. Sci. & Eng. A*, Vol. 549, pp. 200–205.

[8] Wu, H. & Melkote, S.N. 2013, "Effect of crystal defects on mechanical properties relevant to cutting of multicrystalline solar silicon, *Mater. Sci. Semicon. Proc.*, Vol. 16, pp. 1416–1421.

[9] Kumar, A. et al. 2014, "Relationship between macro and micro-scale mechanical properties of photovoltaic silicon wafers, *Proc. 29th EU PVSEC*, Amsterdam, The Netherlands, pp. 769–772.

[10] He, S. et al. 2006, "Residual stresses in polycrystalline silicon sheet and their relation to electron-hole lifetime", *Appl. Phys. Lett.*, Vol. 89, pp. 111909–111909-3.

[11] Seidensticker, R.G. & Hopkins, R.H. 1980, "Silicon ribbon growth by the dendritic web process, *J. Cryst. Growth*, Vol. 50, pp. 221–235.

[12] Möller, H.J. et al. 2005, "Multicrystalline silicon for solar cells", *Thin Solid Films*, Vol. 487, pp. 179–187.

[13] Yang, C. et al. 2013, "On the residual stress and fracture strength of crystalline silicon wafers", *Appl. Phys. Lett.*, Vol. 102, pp. 021909–021909-5.

[14] Clark, W.I. et al. 2003, "Fixed abrasive diamond wire machining – Part I: Process monitoring and wire tension force", *Int. J. Mach. Tools & Manufac.*, Vol. 43, pp. 523–532.

[15] Lee, C.M. 2012, "Cooling Device for Diamond-Wire Cutting System", Patent application US 20120167733 A1.

[16] Peguiron, J. et al. 2014, "Reducing wire wear by mechanical optimization of equipment in diamond-wire wafering", Meyer Burger PV production article.

[17] Youssef, K. et al. 2013, "Effect of oxygen and associated residual stresses on the mechanical properties of high growth rate Czochralski silicon", *J. Appl. Phys.*, Vol. 113, pp. 133502–133502-6.

[18] Carl, D. 2014, "Wire inspection: As fast as a world-class sprinter", Press Release (April) [http://www.fraunhofer.de/en/press/research-news/2014/april/wire-inspection.html].

[19] Bidiville, A. et al. 2009, "Diamond wire-sawn silicon wafers – From the lab to the cell production", *Proc. 24th EU PVSEC*, Hamburg, Germany, pp. 1400–1405.

[20] Noritaka, K. et al. 2005, "Etch stop of silicon surface induced by tribo-nanolithography", *Nanotechnology*, Vol. 16, p. 1411.

[21] Bowden, S. 2009, "From the Valley of Death to the Golden Decade: Crystalline silicon solar cells from 10 to 100 microns", *Proc. 19th Worksh. Cryst. Si. Sol. Cells & Mod.*, Vail, Colorado, USA, pp. 192–195.

[22] Blair, N.D. et al. 2014, System Advisor Model (SAM), National Renewable Energy Laboratory (NREL), Golden, Colorado, USA [https://sam.nrel.gov/].

About the Authors

Dr. Hubert Seigneur is the c-Si feedstock/wafering programme manager at the U.S. PVMC, where his role involves overseeing projects and activities relating to new wafering methodologies, thin-wafer platforms and crack mechanics.

Andrew Rudack serves as the operations manager for SEMATECH's participation in the crystalline silicon programmes of the U.S. PVMC in Orlando and Albany. He is responsible for opening the SEMATECH EUV Resist Test Center in Albany.

Joe Walters is the programme director of the certification of solar energy systems for FSEC, and also holds the position of quality manager for the ISO 17025 accredited test facility at this location.

Dr. Paul Brooker is an assistant professor in solar technologies research at FSEC, and also an assignee to the PVMC, where he has assisted in identifying failure modes and wear mechanisms for diamond wires used in silicon wafer slicing.

Kristopher Davis is the c-Si programme manager for the c-Si branch of the PVMC in Orlando, Florida. He has a B.S. in electrical engineering and an M.S. in optics and photonics, both from the University of Central Florida.

Dr. Winston Schoenfeld is director of c-Si at PVMC as well as director of the solar technologies research division of FSEC at UCF. He has authored/co-authored more than 110 journal publications in various fields.

Stephan Raithel is director of PV in Europe and MD at SEMI Europe, Berlin. In his role as director of PV, he facilitates and leads the combined industry effort in writing an International Technology Roadmap for PV.

Dr. Shreyes Melkote is Morris M. Bryan, Jr., Professor of Mechanical Engineering at Georgia Tech and also serves as Associate Director of the Georgia Tech Manufacturing Institute.

Dr. Steven Danyluk is founder and CEO of Polaritek Systems, former director of the Manufacturing Research Center at Georgia Tech, and an expert in sensor and metrology system development.

Thomas Newton is director of product development at Polaritek. His expertise is in simplifying and deploying complex technology in a manner suitable for the industrial user.

Dr. Bhushan Sopori is a principal engineer at NREL. A solar energy researcher with more than 30 years' experience, he has contributed more than 315 journal papers, meeting abstracts, books, patents and copyrights.

Dr. Stephen Preece is director of R&D at Process Research Products, focusing on developing diamond wire coolants for slicing PV and electronics-grade silicon. He has a Ph.D. in inorganic chemistry from the University of Southampton.

Dr. Igor Tarasov is a researcher and software developer at Ultrasonic Technologies Inc. He received his Ph.D. in electrical engineering from the University of South Florida.

Dr. Sergei Ostapenko is president and CEO at Ultrasonic Technologies. With over 20 years' experience leading R&D projects involving solar silicon, he specializes in defect diagnostics and characterization using ultrasonic technology.

Dr. Atul Gupta is director of product development/R&D at Suniva, where his primary responsibilities include the development and execution of the company's product development roadmap through adoption of innovative technologies that enable higher performance at a lower cost.

Dr. Gunter Erfurt is MD of SolarWorld Innovations GmbH. An engineer and physicist, he has a Ph.D. in experimental physics and 10 years' experience in PV.

Dr. Bjoern Seipel is a senior scientist at SolarWorld and a professor of physics at Portland State University. He has a Ph.D. in applied mineralogy from the University of Tuebingen and eight years' experience in PV R&D.

Oliver Naumann works at SolarWorld Innovations, where he is responsible for the technological development of diamond wire wafering. He graduated in mechanical engineering from Dresden University of Applied Sciences.

Dr. Ismail Kashkoush is vice president of technology at Akrion Systems, where he is responsible for managing the process engineering and technology department. He received his Ph.D. in engineering sciences from Clarkson University.

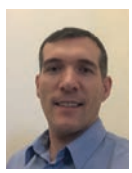

Franck Genonceau is global product manager for wafering solutions systems in the solar products division at Applied Materials and responsible for product strategy, development and marketing. He has a B.S. in mechanical engineering from Polytech Orléans and an M.B.A. from ESM.

Enquiries

Hubert P. Seigneur
PVMC
12354 Research Parkway
Suite 210
Orlando
FL 32826
USA

Tel: +1 407 823-6151
E-mail: hubert.seigneur@uspvmc.org
Website: www.uspvmc.org
www.fsec.ucf.edu, www.ucf.edu

Cell Processing

www.pv-tech.org

News

Taiwan's Motech and Topcell to merge

Taiwan-based solar cell producers, Motech Industries and Topcell Solar International (TSI), have announced plans to merge operations, potentially creating the largest merchant solar cell producer, with around 3GW of capacity.

Motech said in statement that it would be the surviving company post-merger after agreement by both company boards on December 26 2014. The merger is expected to close in early July 2015.

"After Motech's merger, its solar cell production capacity will hit 3GW, which is the largest professional solar cell maker that focus on manufacturing solar cells," said, Jason Huang, research manager of EnergyTrend, a research division of TrendForce. "Globally, it trails slightly behind the vertically integrated Hanwha SolarOne and Yingli, with 3.28GW and 3.2GW solar cell production capacity respectively. Following the industry development trend of larger enterprises remaining strong, production capacity expansion is also beneficial to price negotiations other than steadily leading in technology and quality, making it one of the essential factors of maintaining supply chain competitiveness," added Huang.

Source: Wikimedia Commons

Motech and Topcell solar Internatinoal are to merge to create one of the world's largest merchant cell producers.

Manufacturer updates

Taiwan cell producers ship record 10GW in 2014 but issues loom - EnergyTrend

According to market research firm, EnergyTrend, Taiwan-based solar cell producers shipped more than 10GW of cells in 2014, despite the impact of US anti-dumping duties. The new shipment record is 20% higher than was achieved in 2013, according to EnergyTrend, a fact attributed to an increase in actual shipments but also increases in solar cell conversion efficiency gains in the year.

Neo Solar Power's (NSP) cell shipments accounted for 22% of total annual shipments, while Motech and Gintech's shipments accounted for 16% and 15%, respectively. As such, the three leading Taiwanese cell producers accounted for 53% of the total shipments in 2014.

However, EnergyTrend sees some looming issues facing Taiwanese cell producers in 2015. Firstly, the loss of sales to Chinese PV module manufacturer's after the latest US anti-dumping duties, which have resulted in a drastic decline in orders for the cell producers.

Secondly, EnergyTrend believes the impact from the loss of sales to China will filter through after the first quarter of 2015, as well as a reduction in production due to Taiwan cell producers planning to move some production lines overseas to counter the US duties and regain Chinese customers business.

Thirdly, Taiwanese cell makers should increase their monocrystalline cell production capacities in order to match the production of modules with higher wattages as well as developing new sales channels and markets.

NSP's solar cell sales plummet in January

The largest merchant solar cell producer, Neo Solar Power (NSP), reported a dramatic drop in sales for January 2015. NSP reported sales of NT$1,508 million (US$47.9 million) in January, 2015, compared to NT$2,877 million (US$89.86 million) in December 2014.

The company had reported a record sales month in December after its project developer subsidiary General Energy Solutions (GES) sold a US project for US$26 million. However, extracting the one off PV project revenue gain, NSP had normal solar cell related sales of around US$63.8 million, equating to a sales decline of around 6% in December, 2014, compared to the previous month.

Taiwan-based market research firm, EnergyTrend recently warned of several challenges facing Taiwanese solar cell producers in 2015. These included the loss of sales to Chinese PV module manufacturer's after the latest US anti-dumping case and the need to relocate some production overseas to avoid US import duties and regain custom from China, which would impact revenue streams during the transition.

Solartech Energy's solar cell sales increased 37.9% in 2014

Taiwanese solar cell producer, Solartech Energy Corp, reported flat sales for January 2015, compared to the previous month. Solartech reported sales of NT$826 million (US$26.1 million), up 0.48% from the previous month but still ahead of the steep decline in the middle of last year due to the impact of pending US anti-dumping duties. Full-year 2014 sales topped NT$9,686 million (US$306.7 million), an increase of 37.9% from 2013.

Gintech's solar cell sales fall nearly 30% in January

After a strong recovery in solar cell shipments at the end of 2014, Taiwan-based cell producer, Gintech Energy, reported a 29.8% month-on-month sales decline for January 2015. Gintech's almost 30% fall in sales follows Neo Solar Power's dramatic drop in sales for January. Gintech reported sales in

Source: Neo Solar Power

Neo Solar Power saw a dramatic drop in sales in January.

January of NT$1,109 million (US$35.17 million), down from NT$1,580 million (US$49.69 million) in the previous month.

Motech's PV product sales jump over 13% in January

Taiwan-based PV manufacturer Motech Industries has reported a 13.4% jump in sales for the month of January, continuing a recovery in sales which slumped in July and August last year due to the US anti-dumping case. The company reported sales in January that reached NT$1,710 million (US$54.4 million), compared to US$33 million in December 2014. Unaudited sales for 2014 were NT$20,024 million (US$625.8 million), compared to NT$ 21,350 million in 2013. Motech is planning to merge with Topcell Solar International (TSI), potentially creating the largest merchant solar cell producer, with around 3GW of production capacity (see above).

Tools and upgrades

LG Electronics investing US$145 million to expand n-type mono cell capacity

LG Electronics is planning to spend around US$145 million on expanding its capacity for its n-type monocrystalline cells and modules, according to reports.

The company was said to have announced the plans in financial filings to the Korean stock exchange. The reports claimed that the capital expenditure plans would be undertaken by the end of July 2015. No details regarding capacity expansion figures were provided in the reports. US anti-dumping duties have already pushed Korean-owned Hanwha SolarOne to establish its first 200MW production plant in Korea to supply non-Chinese produced cells/module to the US market, avoiding duties on its products made at its main manufacturing plant in China.

Despatch Industries supplies 10 solar cell firing furnaces to single customer

PV equipment specialist, Despatch Industries, said in January it had sold 10 firing furnaces to a leading solar cell producer, marking a milestone that all of the top-10 largest solar cell producers are now using its furnace technology.

"The top-10 manufacturers account for over 40% of all the crystalline solar

Source: Despatch Industries

Despatch Industries reported in January a sale of 10 of its firing furnaces to an unnamed cell producer.

cells produced worldwide," noted Ellen Cheng, general manager of Solar Business for Despatch Industries. "Despatch continues to be the global leader and supplier of firing furnaces for the industry, holding a 75% market share through 2014."

Despatch noted that its 'CF Series Firing Furnace' had been the workhorse for many solar cell producers for post-metallization processes, while its more recent Safire Firing Furnace with DriTech Dryer could deliver 0.1% absolute improvement in overall cell efficiency.

MegaCell and RCT Solutions to collaborate on multicrystalline bi-facial solar cells

Italian specialist solar cell producer MegaCell and turnkey equipment and technology supplier, RCT Solutions are collaborating on establishing a pilot production line for multicrystalline bi-facial solar cells. Currently, MegaCell is operating an 80MW n-type solar cell plant in Carmignano di Brenta, Italy.

The collaboration entails technical co-development and licence agreement with RCT Solutions, which will be a precursor to offering turnkey bi-facial solar cell production lines. The new pilot line is expected to be operational in the first quarter of 2015.

Records

China's HT-SAAE touts record n-type PERT solar module efficiency

China state-owned aerospace firm, Shanghai Aerospace Automobile Electromechanical Co (HT-SAAE), has revealed verified record solar module efficiencies for both n-type PERT (passivated emitter, rear totally diffused) and p-type multicrystalline modules.

HT-SAAE said in January that TUV Rheinland had verified that its 60-cell (n-type PERT) modules employing 156mm x 156mm commercial monocrystalline wafers achieved peak output power (Pmax) of 335.6Wp. HT-SAAE claims this to be a new industrial record.

In tandem, HT-SAAE said that TÜV Rheinland had verified 156mm x 156mm commercial P-type multicrystalline wafers in a standard 60-cell format to achieved peak output power of 310.5Wp.

Zhang Zhongwei, CTO of HT-SAAE said: "HT-SAAE has spent half a century gaining abundant experience in the photovoltaic industry. With R&D as its starting engine and lean production as the core competency, HT-SAAE has realised remarkable quantity of high quality projects worldwide."

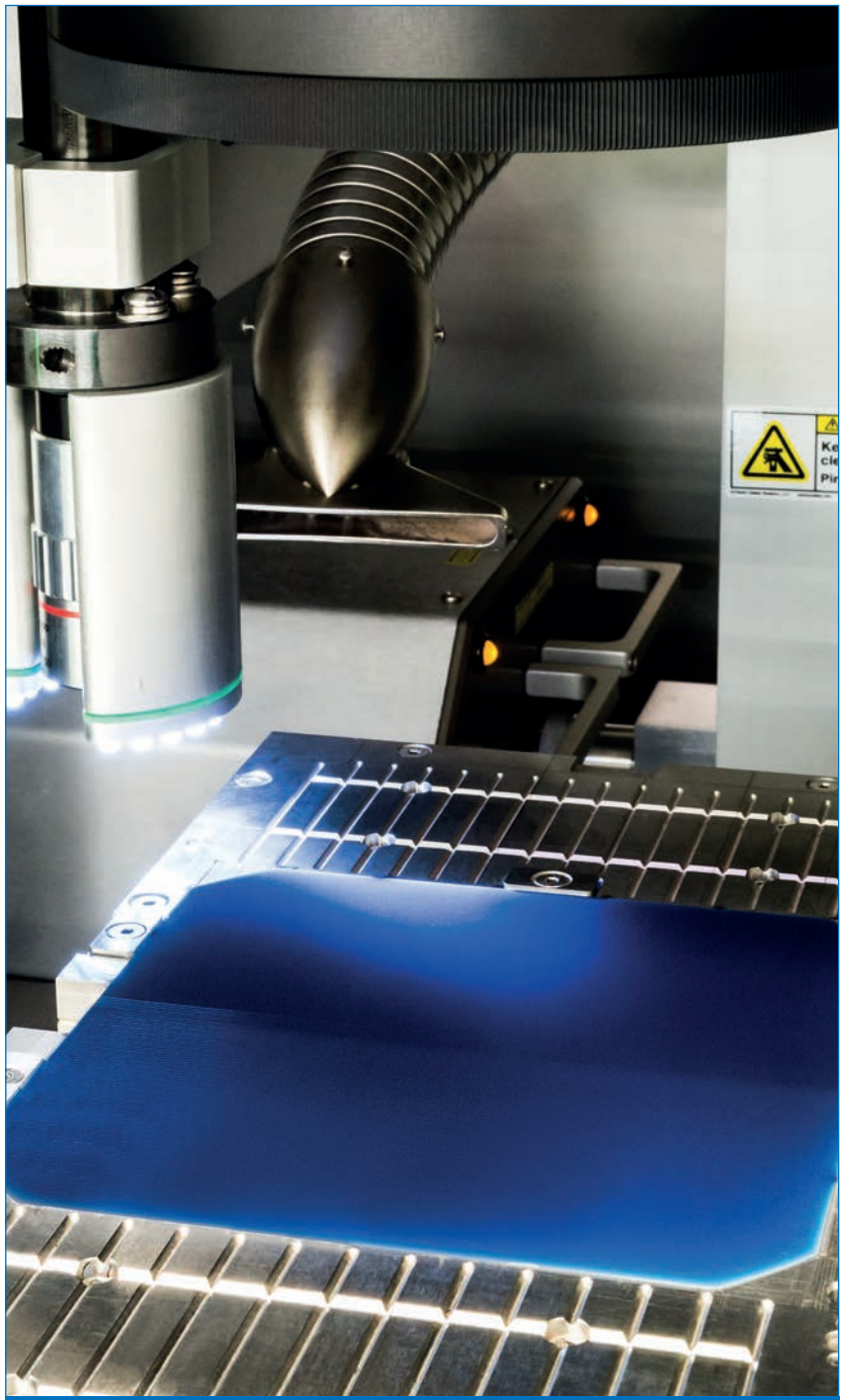

Source: Imec

Imec has achieved a record for its n-type mono-Si n-PERT cell using laser doping.

Imec pushes commercially ready n-PERT solar cell conversion efficiency record 22%

European R&D facility, imec, has achieved new solar cell record efficiency for its n-type, monocrystalline n-PERT (passivated emitter, rear totally diffused) process using commercial-sized wafers and processing equipment.

Imec said that a conversion efficiency of 22.02% was achieved and was calibrated at ISE CalLab and features an open-circuit voltage (Voc) of 684mV, a short-circuit current (Jsc) of 39.9 mA/cm2, and 80.7% fill factor (FF).

"Our new developments further confirm the potential of n-type PERT cells for next-generation highly efficient silicon solar cells" said Filip Duerinckx, manager of imec's n-PERT technology platform.

Reiterating n-PERT's commercial credentials, imec highlighted that the record efficiencies were obtained by incorporating a selective front surface field through laser doping, which generated improved open circuit voltage and short circuit current (see imec's paper, p.45).

Product Reviews

MacDermid

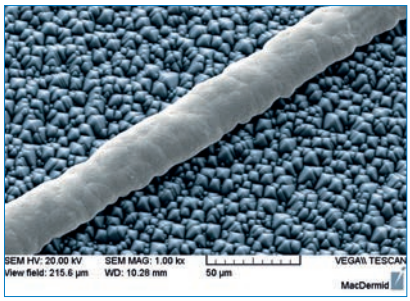

MacDermid's HELIOS plating solution replaces silver paste with narrow copper grid conductors

Product Outline: MacDermid's HELIOS nickel, copper and silver wet chemical plating solution produces 30µm fingers and 4N pull strengths, while reducing costs by US$0.06/cell.

Problem: The decreasing cost of producing silicon solar cells has put pressure on whether conventional screen-printed silver paste can to serve the industry's future needs. In addition, printing and sintering silver limits the ability to implement thinner wafers and more efficient cell designs, due to physical and thermal stresses. To address these challenges, PV roadmaps call for copper grid conductors. Until now, copper conductors suffered adhesion loss, plated on the ARC, and required huge, expensive plating equipment.

Solution: Narrow copper conductors, allowing 50% more light capture, are formed in a three-step process. A pico second UV laser ablates the ARC, exposing the silicon. An inline conveyorized plating tool deposits 1µm of nickel, 10-15µm of copper and 0.2µm of silver, using ultra-fast electrodeposition. The HELIOS metal grid is quickly annealed, achieving adhesion similar to paste printed conductors. The nickel achieves a full-area contact to silicon, and the copper reaches conductivity unachievable with paste.

Applications: Mono- and multicrystalline silicon cell conductor formation.

Platform: Specialized laser patterning is available from MacDermid's partner in Germany, scalable to 50 or 100MW installations. Conductors are plated using MacDermid's new HELIOS chemical systems, at extremely high deposition rates, very high purity, and virtually zero plated stress, according to the company.

Availability: Currently available.

Intevac

Intevac's 'ENERGi' ion implant system offers competitive alternative to POCl3 diffusion process

Product Outline: Intevac's 'ENERGi' ion implant system employs a continuous flux ion source system designed to meet industry roadmaps and is extendible to enable advanced cell designs and increased efficiency requirements.

Problem: For standard front contact Ag paste cell manufacturing there is a trade-off between a low contact resistance versus low phosphorus concentration in the emitter. While front Ag pastes have improved, allowing for higher sheet resistance emitters (lower peak concentration resulting in high Voc), obtaining the full benefit of new pastes, or the benefits of advanced non-paste metallization, requires the ability to tailor phosphorus profiles beyond what is possible with a single step POCl3 diffusion.

Solution: ENERGi provides high productivity and competitive costs (< US$0.8/W) for industrial high efficiency phosphorus and boron doping requirements. The system has the capability to enable advanced metallization paste requirements with appropriate surface concentration and junction depth. A simple annealing process fully recrystallizes the silicon through solid phase epitaxial regrowth, leaving behind no defects.

Applications: Phosphorus and boron doped layers.

Platform: The unique, patented ion source allows for a small footprint (24m2) and high throughput. High beam current is maintained even at low implant energies for phosphorus and boron doping. The ENERGi implantation system has processed millions of production wafers and has demonstrated >99.97% wafer yield, improved efficiency and tighter efficiency binning, and can achieve 3000wph, according to the company.

Availability: Currently available.

Tempress

High Density POCl3 platform from Tempress provides improves uniformity and high efficiencies

Product Outline: Tempress, a subsidiary of Amtech, has developed an alternative atmospheric process called 'High Density POCl3' (Phosphorus Diffusion). The HD system benefits from the throughput advantage of small pitch, back-to-back, and long flatzone, while using improved chemistry and hardware upgrades to provide excellent uniformity and high efficiencies.

Problem: POCl3 is a simple and well-known process that controls the formation of the emitter and defines the interface with the contacts. However, the drive to higher cell efficiencies places increasingly stricter process control requirements for the POCl3 process, notably emitter resistivities, lower surface concentrations and better uniformities.

Solution: With the HD-POCl3 diffusion process, Tempress has focused on process innovation to increase throughput without the drawbacks (high cost/high maintenance) of complex low pressure systems. The HDPOCl3 platform is said to enable emitter formation at around 35% lower cost per watt compared to the conventional atmospheric POCl3 systems, and >10% lower cost per watt compared to low pressure processing.

Applications: POCl3 diffusion process.

Platform: The HD-POCl3 platform contains improvements in furnace hardware, process gas chemistry and recipe structure. The five-stack HD POCl3 system is fully designed to process >3200 wph. The furnace comes with an integrated automation system employing a six-axis robot that allows that loading/unloading of a full HD POCl3 load of 1,000 wafers in under 15 minutes.

Availability: Currently available.

Imec's large-area n-PERT cells: Raising the efficiency beyond 22% by selective laser doping

Monica Aleman, Angel Uruena, Emanuele Cornagliotti, Aashish Sharma, Richard Russell, Filip Duerinckx & Jozef Szlufcik, imec, Leuven, Belgium

ABSTRACT

This paper presents the main features of imec's n-PERT (passivated emitter rear totally diffused) cells, which have achieved independently confirmed efficiencies of 22%. A special focus is given to the selective front-surface field formation by laser doping, which – combined with imec's front-plating sequence and the excellent rear-surface passivation by Al_2O_3 on the boron-diffused emitters – has enabled very high voltages (close to 685mV) to be realized on large-area n-type Cz material.

Introduction

The PV module market is currently dominated by standard screen-printed aluminium back-surface field (Al-BSF) silicon solar cells, which represent about 90% of total silicon solar cell production. Although their fabrication is simple and robust, there is a downside in that the typical conversion efficiency of Al-BSF cells is limited to values of around 19% as a result of various technological limitations, including:

- Strong Auger recombination at the front junction, because of the high surface doping level required by the screen-printing pastes for good electrical contact.
- Reduced optical response on the rear, because of parasitic absorption in the metal.
- Poor passivation of the Al-BSF on the rear side.

These cells also suffer from wafer bowing due to the different thermal expansion coefficients of silicon and aluminium.

> "Typical conversion efficiency of Al-BSF cells is limited to values of around 19%."

With the continuous fall in module prices and the increasing influence of the balance of system cost on the levelized cost of electricity (LCOE), there is a growing desire for high-efficiency modules – hence the worldwide interest in passivated emitter and rear cell (PERC) technology, which enables higher efficiencies than Al-BSF cells to be achieved. PERC cells use dielectrics on the rear side, improving both the rear passivation and the optical response. The electrical contacts are locally formed by opening small areas in the dielectrics. Industrial manufacturing of PERC cells on p-type material has already been in place for several years at companies such as Sunrise and Hanwha Q CELLS. Although Schott Solar have shown efficiencies of up to 21% to be achievable on large-area devices [1], an average of 20.4% is expected for the high-volume production by Trina Solar [2]. Passivated emitter and rear locally diffused (PERL) and passivated emitter rear totally diffused (PERT) structures are also of great interest in R&D: whereas the first enables even higher efficiencies (up to 25% on a lab scale), the second can be produced using current production lines without introducing too many changes.

At imec a process flow is under development with which we have already achieved 22% efficiency with

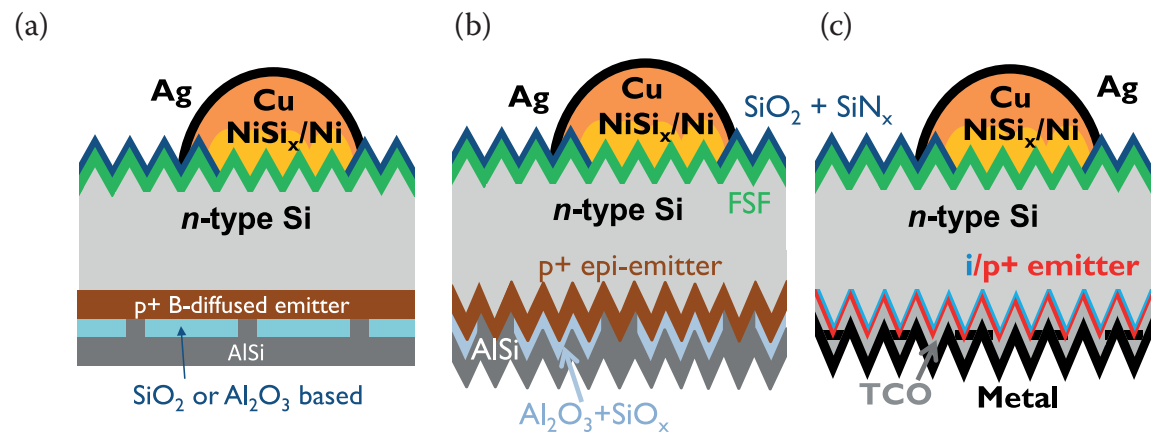

Figure 1. Schematics of n-Si rear-junction concepts under study at imec: (a) diffusion route; (b) epitaxial route; (c) hybrid route.

large-area, back-junction n-PERT cells. This research activity began by combining the best of imec's p-type PERC and n-type IBC platforms. For the front-side metallization of n^+ surfaces from the p-type PERC platform, imec's know-how was put to use in laser patterning and plating. The high-quality rear-junction formation by boron diffusion and the rear passivation by thermal oxidation on n-type substrates originated from the IBC platform.

Fig. 1(a) shows a schematic of imec's first devices, which are constructed on large-area, commercially available, n-type Cz-Si wafers with a typical base resistivity in the range 3–5Ωcm. The front surface is textured with random pyramids formed in an alkaline solution. Minority carriers are shielded from the front surface by a diffused front-surface field (FSF), which is passivated by a thin thermal oxide coated with a plasma-enhanced chemical vapour deposition (PECVD) silicon nitride as an anti-reflection coating (ARC). Contact openings on the front are created by laser ablation, followed by a Ni/Cu/Ag plating sequence.

On the rear side, three different process flows are evaluated; the flows differ in the methods used to fabricate the p^+ junction. The diffused baseline, which acts as a reference (see Fig. 1(a)), relies on BBr_3 diffusion to create the rear emitter and on dielectric passivation, based on either a thermal SiO_2 or an Al_2O_3/SiO_x coating. Laser ablation is used to define the rear-contact pattern, while physical vapour deposition (PVD) by sputtering of Al is used to form the back-side contact.

Another flow consists of the epitaxial growth of the rear emitter (Fig. 1(b)). This route allows a simplified process sequence and more freedom in the design of the emitter doping profile, resulting in very low emitter dark saturation current densities (J_{0e}). More information for this cell type can be found in Recaman et al. [3].

The final flow makes use of an a-Si i/p^+ heterojunction emitter (Fig. 1(c)), thereby enabling a 1D current flow on the rear surface with excellent J_{0e} values due to the passivated contact structure. More details can be found in Tous et al. [4].

This paper will concentrate more on the characterization and cell results obtained for the diffused emitter route, although all details relating to the front-surface optimization are equally applicable to the other process flows, since they all share the front-side processing.

Features of imec's n-PERT cells

Material

The choice of phosphorus-doped Cz wafers has several advantages. The bulk of this material is less sensitive than p-type wafers to iron and other metallic impurities. For many common metallic impurities, the capture cross section for electrons is greater than that for holes. The smaller capture cross section for n-type substrates results in a higher bulk lifetime (and longer diffusion length). Additionally, phosphorus-doped wafers do not suffer from the light-induced degradation typically observed with boron-doped substrates. Moreover, even though the current price of n-type Si is higher than for p-type Si, it is expected that, with the increase in n-type Si production, prices will even out because of economies of scale. This is expected to happen, as the International Technology Roadmap for Photovoltaics (ITRPV) predicts an increase in the share of n-type Si wafers in the market, mainly for high-efficiency devices [5].

A potential disadvantage of cells based on n-type silicon wafers, grown with the standard Czochralski method, is the wide resistivity range found in a typical phosphorus-doped ingot (due to the low segregation coefficient of phosphorus in silicon). Although imec's n-PERT devices typically use 3–5Ωcm material, dedicated experiments have shown that similar efficiencies (±0.1%) are obtainable for base resistivities in the range 2–10Ωcm, with small but opposite trends for the short-circuit current and the open-circuit voltage as a function of the base resistivity.

Front contacts

As mentioned earlier, plating is applied for the front-side metallization; this enables a self-aligned contact formation, where the metal is selectively deposited in the laser-patterned areas. The plating sequence for the front side is as follows. First, a light-induced plating (LIP) step is performed for nickel and copper deposition. Ni is used to improve the contact formation to the FSF and to protect the wafer from Cu diffusion. Next, copper electroplating is carried out to increase the finger thickness, so that a higher line conductivity can be achieved. The contacts are finally finished with a very thin 'flash' Ag coating (~100nm) to prevent copper oxidation. All these steps are performed in a single inline plating tool.

A metallization scheme based on copper plating has several advantages. First of all, copper prices per kilo equate to only 1% of Ag prices and are less susceptible to fluctuation; the influence on the final cell/module price is therefore much smaller. The features of the plated fingers are also narrower than those of printed cells (enabling more light to come into the device). Moreover, the use of Ni facilitates the contact formation in areas with a surface doping concentration as low as $10^{19}cm^{-3}$, which is an order of magnitude smaller than the surface doping concentration typically required by standard screen-printing pastes. The implementation of such lightly doped profiles on the front represents an improved spectral response (particularly for the short-wavelength region), because of the lower Auger recombination in the diffused FSF, which has a favourable effect on both the current and the voltage. In addition, the response in the IR region of the spectrum is improved as well, because of a reduction in free-carrier recombination (FCA) due to the lower doping of the FSF. In other words, the use of nickel-plated contacts for the front metallization allows higher voltages and currents to be achieved for two-side contacted cells.

Rear junction

A rear-junction device presents several advantages over the front-junction cells on n-type material:

- The front side can be easily contacted with a well-developed metallization process based on Ni/Cu plating on n^+ surfaces patterned by laser ablation. The cell layout (n^+ front/p^+ rear) is the same as that for current p-type PERC cells, enabling it to be adopted by industry more quickly.
- There is a negligible impact on cell performance because of the retrograde boron profile (compared with a front-junction cell).
- Since the bulk has the same polarity as the FSF, it also contributes to the majority-carrier flow on the front. The front design can be further optimized while still keeping the same lateral resistance: either the number of front fingers compared with a front-junction device (see Fig. 2) is reduced (which would lower the shadowing and recombination losses), or the total front doping concentration is reduced (which would also reduce the front recombination).

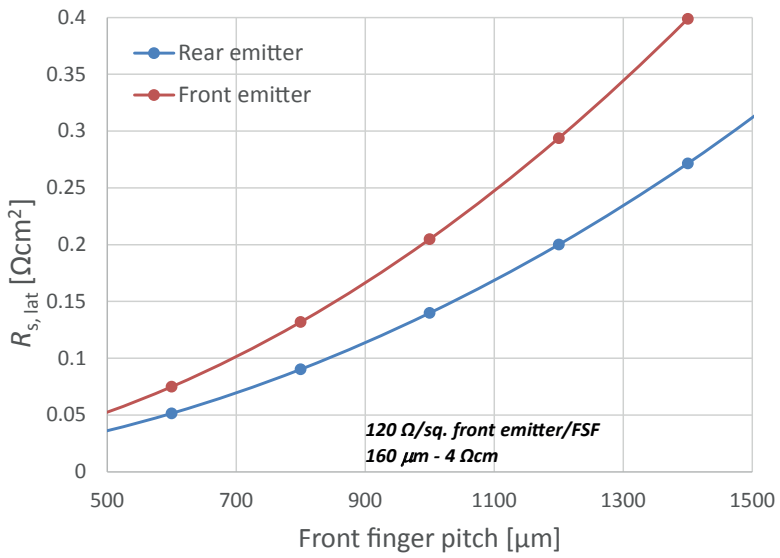

Figure 2. Simulation of the lateral series resistance as a function of the front pitch for front-junction and rear-junction cells. For the simulation a 160µm-thick cell on 4Ωcm material with a front FSF/emitter doping of 120Ω/sq. was assumed [6].

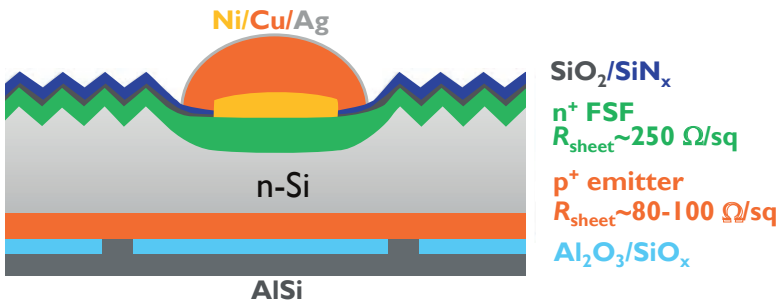

Figure 3. Schematic of imec's n-PERT cell, featuring a laser-doped and plated FSF, and a boron-diffused emitter and Al_2O_3/SiO_x dielectric stack on the rear. Record efficiencies of up to 22% have been demonstrated with this cell.

Rear passivation

In the first imec devices the rear-side passivation was delivered by a ~100nm-thick thermal oxide layer grown during a wet-oxidation step. J_0 values of 25–30fA/cm² were achieved on the standard boron-diffused emitter, featuring a sheet resistance between 90 and 100Ω/sq.

It has already been shown that Al_2O_3 layers result in lower saturation current densities than thermal oxide passivation [7]. With the replacement of the silicon oxide passivation by an aluminium oxide layer, the passivated $J_{0,rear}$ goes down to 14fA/cm² [6]. The thin Al_2O_3 coating is capped with a PECVD SiO_x layer to improve the rear optical response [8]; the PECVD deposition of the SiO_x does not, however, have any detrimental impact on the passivation quality of the Al_2O_3. For more information on this subject see Cornagliotti et al. [6].

Front-surface field

Most of the carrier generation occurs on the front side. The minority carriers have to travel through the wafer thickness to reach the rear junction; consequently, these devices are very sensitive to the front-surface recombination. An optimal FSF needs to deliver a good shield against Shockley-Read-Hall recombination while fulfilling two different conditions: a light doping on the non-contacted areas in order to keep the Auger recombination as low as possible, and a deep, heavily doped profile on the contacted area in order to achieve a good and well-passivated electrical contact.

A single diffused FSF (R_{sheet} ≈ 120Ω/sq.) was first implemented. To enable a good electrical contact with nickel, and avoid a heavily doped surface, a compromise in the profile design had to be made; passivated J_0 values are around 50fA/cm² for this profile. The impact of the laser-ablation process on the front-side recombination was characterized, and it was observed that shallower junctions suffer from a stronger laser-induced degradation [9]. For imec's process in particular, this resulted in a $J_{0,laser}$ greater than 5000fA/cm² – in other words, a total front recombination $J_{0,front}$ greater than 100fA/cm² after the laser treatment, with an implied V_{oc} of around 668mV (assuming a J_{sc} of 39.5mA/cm²).

> "Selective laser doping is an excellent technological alternative, with strong potential for forming local junctions in industrial environments."

Selective laser doping

To overcome FSF limitations, a more sophisticated front design based on the selective junction formation by laser doping was developed and implemented in imec's process flow (Fig. 3). Selective laser doping is an excellent technological alternative, with strong potential for forming local junctions in industrial environments. A commercial spin-on dopant (SOD) is spin coated over a surface, and a deep junction is formed through quasi-continuous wave laser doping. In imec's devices a phosphorus-containing SOD is applied on top of the silicon nitride ARC to create an n^{++}-doped area, during which narrow lines ~10µm wide and over 2µm deep are locally formed. The profile characteristics depend on the laser power and speed [10].

As can be seen in Fig. 4, the front-side pyramids are flattened during laser doping; this behaviour is not observed for laser-ablated samples. The SOD residues are removed in a short HF dip. The laser damage generated during laser doping is subsequently annealed in a belt furnace anneal (BFA) [11]; this anneal also enables the formation of a good electrical contact on the rear and the passivation of the different doped regions [12].

After the BFA, the cells are plated following the sequence presented earlier. The use of selective laser

ASYS SOLAR

Laser Contact Opening

Inline System

Laser Island

Contact Opening (LCO) of All Dielectric Layers

- Unique to the market: fully integrable into metallization lines
- High-precision: market-leading repeatability of wafer positioning
- Throughput of up to 3600 cph on dual lane

ASYS SOLAR Laser Solutions

ASYS offers laser systems for different processes. All laser systems are based on a platform concept. They provide proven quality and can be upgraded easily. In combination with an ASYS loader and unloader, the systems can be transformed into laser islands (single lane / dual lane). For some processes they can also be integrated directly into the metallization line.

ASYS GmbH
Benzstrasse 10, 89160 Dornstadt, Germany

www.asys-solar.com

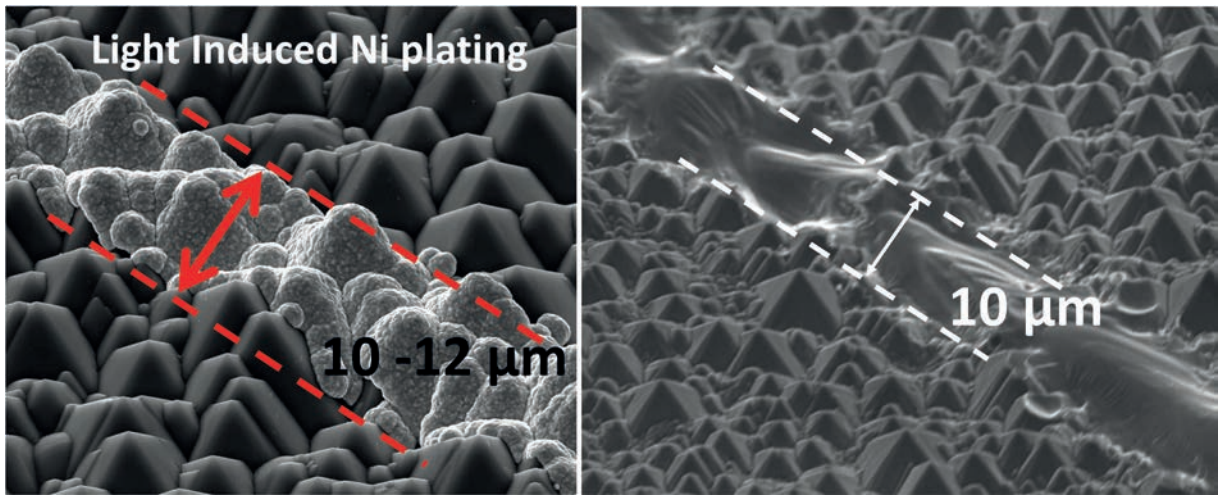

Figure 4. SEM images showing the surface finishing on the front side for (a) a laser-ablated and nickel-plated device, and (b) a laser-doped cell.

Process flow	R_{sheet} FSF [Ω/sq.]	FSF patterning	Rear passivation	J_{sc} [mA/cm^2]	V_{oc} [mV]	*FF* [%]	Efficiency [%]
1	120	Laser ablation	SiO_2	39.4	668	80.9	21.3*
2	120	Laser ablation	Al_2O_3	39.1	677	81.3	21.5**
3	250	Laser doping	Al_2O_3	39.9	684	80.7	22**

*Internal measurements; **Measurements performed at FhG ISE CalLab.

Table 1. *I–V* results from imec's n-PERT devices after the implementation of the specified optimized features.

doping and metal plating is the optimal combination for a simple process for high-efficiency contact formation. The final width of the front fingers after plating is between 25 and 30µm wide.

Thanks to the use of selective laser doping, a higher resistive FSF is integrated in the devices (R_{sheet} ≈ 250–300Ω/sq.). The passivated J_0 for this lightly doped FSF is ~25fA/cm^2. After laser doping and annealing, $J_{0,laser}$ values below 3000fA/cm^2 were measured; this results in an implied V_{oc} of more than 690mV.

Cell results

Table 1 summarizes imec's top-efficiency cells obtained over the past two years with a diffused n-PERT structure, along with their main differences. All the process flows have the following in common: n-type Cz wafers with a thickness around 160µm and a base resistivity between 3 and 5Ωcm were used to manufacture the devices. The front side is textured with an alkaline solution, resulting in random pyramids with a front reflection down to 9.5% at 700nm (before ARC). The front dielectrics consist of a thin thermal oxide used for the passivation of the FSF, and a PECVD SiN_x layer used as the ARC. The standard diffused rear emitter implemented in all the flows features an R_{sheet} of ~90–100Ω/sq. The rear dielectrics are patterned by laser ablation, and a 2µm PVD AlSi layer is used as a rear electrode. Finally, after laser patterning and metallizing the front of the cells, the edges are isolated for carrying out the electrical characterization.

Flow 1 was based on thermal oxide passivation on both front and rear surfaces, single diffusion for the FSF formation, and laser ablation for the front-side patterning. Average efficiencies over 21% were achieved with this sequence; the V_{oc} was limited to ~668mV by both the front and the rear recombination.

The use of Al_2O_3 as the rear passivation in flow 2 led to increases in V_{oc} and *FF*, which in turn led to a 0.2% abs. increase in efficiency compared with that for the SiO_2 passivated reference. The optimization of the FSF (by combining it with selective laser doping), the Al_2O_3 passivation on the rear emitter, and the improved front optics and an optimized front metallization collectively resulted in a record, independently confirmed efficiency of 22%.

The expected increase in implied V_{oc} observed for the high-resistivity emitter with selective laser doping is also seen for the devices from flow 3. The increase in J_{sc} results from a combination of different aspects: the optimization of the ARC and texturing steps, the improved blue response with the lightly doped FSF, and a modification of the front-metallization pattern. Further experiments are necessary to understand the decrease in *FF* for flow 3 as compared to flow 2.

Other paths to achieving even higher efficiencies are under investigation – for example a modification of the front metallization through the implementation of SmartWire Connection Technology [13].

Light-induced degradation (LID)

Using the devices corresponding to flow 2 in Table 1, the impact of the light illumination on the n-PERT devices was evaluated and compared

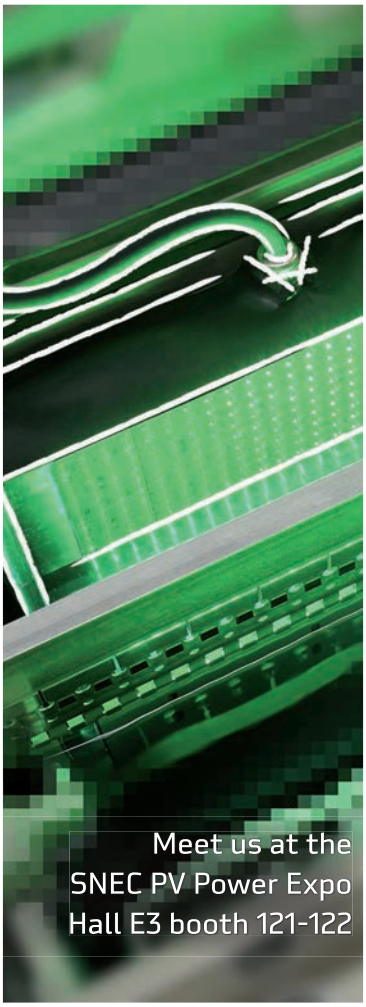

Besi

Meco Equipment Engineers B.V.

Marconilaan 2
5151 DR Drunen
The Netherlands

T: +31 416 384 384
meco.sales@besi.com

Meco Plating Equipment

metallization for high efficiency solar cells

Crystalline solar cells:

- Proven efficiencies:
  > 20.5% on p-type; > 22.0% on n-type
- > 65% reduction of metallization costs
- Inline process up to 3,000 wph
- Allows standard module assembly
- Life tested according to IEC61215
- P-type, n-type, bifacial, HIT, MWT, IBC

CIS & CIGS thin film solar cells:

- Electrochemical deposition of Cu, In, Ga
- Atmospheric process: no vacuum required
- > 15.9% on module level
- 100% utilization of precious metals such as Indium and Gallium
- > 20% lower Cost-of-Ownership

www.besi.com

SPECTRE High Throughput PECVD

294 wafers per load; 1800 wafers per hour
PID-free solution without efficiency penalty available
Process flexibility; stacked/graded layers

TEMPRESS AMTECH GROUP

InPassion ALD

Superior passivation with spatial ALD
Modular system up to 5000 wph

TEMPRESS.NL THE NETHERLANDS

INTEGRATED PERC SOLUTION

High Throughput rear side passivation
Post Deposition Anneal (PDA) integrated in SiNx deposition step
Hight efficiency through superior passivation

Visit us at **SNEC 2015**
Booth E3-330

with a p-type PERC reference. It was observed that after 12h of illumination at one sun, the n-PERT cells did not show any signs of degradation, whereas the p-type PERC reference cells showed a loss of ~3mV in V_{oc} and 2% in *FF*. It is therefore confirmed that imec's n-PERT devices do not suffer from LID.

"Independently confirmed efficiencies of 22% have been achieved for large-area devices with imec's current process flow."

Conclusion

The main features of imec's n-PERT cells have been presented in this paper. An optimization of the main features of the devices on test structures has been demonstrated and the devices evaluated at the cell level. Of particular interest was the combination of the selective junction formation by laser doping and the self-aligned front metallization by Ni/Cu plating. Independently confirmed efficiencies of 22% have been achieved for large-area devices with imec's current process flow, and a clear path towards realizing 22.5% has been described.

References

[1] Metz, A. et al. 2014, "Industrial high performance crystalline silicon solar cells and modules based on rear surface passivation technology", *Solar Energy Mater. & Solar Cells*, Vol. 120, Part A, pp. 417–425.

[2] Osborne, M. 2015, "Trina solar starts PERC technology volume production", News Report (Jan. 19th) [http://www.pv-tech.org/news/trina_solar_starts_perc_technology_volume_production].

[3] Recaman, M. et al. 2014, "Opportunities for silicon epitaxy in bulk crystalline silicon photovoltaics", *Proc. 29th EU PVSEC*, Amsterdam, The Netherlands.

[4] Tous, L. et al. 2015, "Process simplification in large area hybrid silicon heterojunction solar cells", *Proc. 5th SiliconPV*, Konstanz, Germany.

[5] SEMI PV Group Europe 2014, "International technology roadmap for photovoltaic (ITRPV): Results 2013", 5th edn (Mar.) [http://www.itrpv.net/Reports/Downloads/].

[6] Cornagliotti, E. et al. 2014, "Large area n-type c-Si solar cells featuring rear emitter and efficiency beyond 21%", *Tech. Digest 6th WCPEC*, Kyoto, Japan.

[7] Hoex, B. et al. 2007, "Excellent passivation of highly doped p-type surfaces by negative-charge-dielectric Al_2O_3", *Appl. Phys. Lett.*, Vol. 91, p. 112107.

[8] Duerinckx, F. et al. 2014, "Quantifying internal optical losses for 21% n-Si rear junction cells", *Proc. 29th EU PVSEC*, Amsterdam, The Netherlands.

[9] Aleman, M. et al. 2014, "Reducing front recombination losses to improve the efficiency of rear junction Cu-plated n-Si cells", *Proc. 29th EU PVSEC*, Amsterdam, The Netherlands.

[10] Hallam, B. et al. 2013, "Deep junction laser doping for contacting buried layers in silicon solar cells", *Solar Energy Mater. & Solar Cells*, Vol. 113, pp. 124–134.

[11] Hallam, B. et al. 2014, "Hydrogen passivation of laser-induced defects for silicon solar cells", *IEEE J. Photovolt.*, Vol. 4, No 6, pp. 1413–1420.

[12] Uruena, A. et al. 2015 [forthcoming], "Beyond 22% large area n-type silicon solar cells with front laser doping and a rear emitter", *Proc. 30th EU PVSEC*, Hamburg, Germany.

[13] Meyer Burger 2014, "SmartWire Connection Technology", White Paper [http://www.meyerburger.com/en/media/downloads/publications/].

About the Authors

Monica Aleman received her mechanical engineering degree in Venezuela in 2003 and her Ph.D. in microelectronics in 2013 from Freiburg University, Germany. She has worked on Si solar cells since 2004 and first focused on front metallization while at Fraunhofer ISE. Monica has been at imec since 2009, where her main interest is the development of high-efficiency n-type cells.

Angel Uruena is a silicon PV research scientist at imec, where he focuses on the development of n-type solar cells. He obtained a B.Sc. in telecommunications and an M.Sc. in electronics in 2004 and 2007 respectively, from the University of Valladolid. Angel then received his Ph.D. in electrical engineering in 2013 from KU Leuven.

Emanuele Cornagliotti received his M.Sc. in 2006 from the Politecnico of Torino, Italy, and his Ph.D. in electrical and electronic engineering in 2011 from KU Leuven, Belgium. Since 2007 Emanuele has been a researcher at imec, working on the development of industrial silicon solar cells, with a focus on process integration.

Aashish Sharma received his B.Sc. in physics from Jacobs University Bremen in 2010 and his M.Sc. in optics and photonics from Karlsruhe Institute of Technology in 2012. Aashish is currently pursuing a Ph.D. at imec and KU Leuven, working on high-efficiency n-PERT c-Si solar cells.

Richard Russell received a bachelor's in physics from the University of Exeter, England, and a master's in physics from the University of Dundee, Scotland. Between 1990 and 2010 he worked for BP Solar, mainly on Ni/Cu-metallized laser-grooved buried contact cells. In 2011 Richard joined imec, where he leads copper-based metallization activities within the iPERx platform.

Filip Duerinckx leads the iPERx platform in the silicon photovoltaics group at imec. He received his M.Sc. in engineering from KU Leuven, Belgium, in 1994, followed by his Ph.D. in 1999. Filip's current focus is on performance and economic aspects of n-type PERx silicon solar cells.

Jozef Szlufcik received his M.Sc. and Ph.D. degrees, both in electronic engineering, from the Wroclaw University of Technology, Poland. He joined imec in 1990 as head of research on low-cost crystalline silicon solar cells, and then from 2003 to 2012 held the position of R&D and technology manager at Photovoltech, Belgium. Jozef is currently the director of the photovoltaics department at imec.

Enquiries

Monica Aleman
imec
Kapeldreef 75
B-3001 Leuven
Belgium

Tel: +32 16 28 78 55
Email: Monica.Aleman@imec.be

Ion implantation as an enabling technique for the fabrication of back-junction back-contact cells within a lean process flow

Robby Peibst[1], **Agnes Merkle**[1], **Udo Römer**[1], **Bianca Lim**[1], **Yevgeniya Larionova**[1], **Rolf Brendel**[1], **Jan Krügener**[2], **Eberhard Bugiel**[2], **Manav Sheoran**[3] & **John Graff**[3]

[1]Institute for Solar Energy Research Hamelin (ISFH), Emmerthal, Germany; [2]Institute of Electronic Materials and Devices, Leibniz Universität Hannover, Germany; [3]Applied Materials, Gloucester, Massachusetts, USA

ABSTRACT

Ion implantation offers significant process simplification potential for the fabrication of back-junction back-contact (BJBC) solar cells. First, the number of high-temperature steps can be reduced to one when applying a co-annealing process which includes an in situ growth of a silicon oxide passivation layer. Second, the implanted regions can be patterned in situ by utilizing shadow masks. ISFH's results from evaluating both aspects are reported in this paper. With fully ion-implanted, co-annealed and laser-structured small-area cells, efficiencies of up to 23.41% (20mm × 20mm designated area) have now been achieved. It is shown that the excellent recombination behaviour of 156mm × 156mm BJBC cells patterned in situ implies a potential for realizing efficiencies greater than 23%; however, back-end issues have so far limited the efficiency to 22.1% (full-area measurement). Ion implantation can also be utilized for the doping of BJBC cells with carrier-selective junctions based on polycrystalline silicon. The current status of ISFH's work in this direction is presented.

Introduction

High energy conversion efficiencies are currently becoming more and more important, since the increasing amount of balance of system (BOS) cost has to be offset [1]. Since its proposal in 1977 [2], the back-junction back-contact (BJBC) solar cell continues to be extensively investigated as a promising high-efficiency concept. The absence of optical shading from front-side metallization is considered the main advantage of BJBC solar cells, compared with double-side contacted cells. However, the recent progress achieved with more standard-type, potentially industrially feasible double-side contacted cells (e.g. > 21% efficiency for fully screen-printed p-type PERC cells [3,4]) puts pressure on the BJBC cell concept. Either the BJBC cell needs to be realized using a process flow that is as lean as that for double-side contacted cells, or additional process complexity has to be offset by additional benefits, in particular significantly higher energy conversion efficiencies. With regard to the first aspect, ion implantation can serve as an 'enabling technology', yielding a significant simplification of the BJBC front-end process. (The 'front end' of a BJBC cell process includes wafer cleaning, formation of doped regions and passivation.)

While ion implantation had already been investigated in the 1980s for PV applications [5–7], it regained significant research interest in 2010 [8] for two main reasons: first, high-current implanter tools became available, which were capable of the high throughput required in PV; and second, the capability for in situ patterning via shadow masks offered a potentially cost-effective way to form local doped regions. Although the latter aspect was first evaluated for the formation of selective emitters for double-side contacted cells [8], it was quickly applied to the fabrication of BJBC cells [9–11]. Efficiencies of up to 22.4% [9] for 5-inch industrial BJBC cells, and up to 22.1% [11] for 6-inch cells, were already demonstrated in 2012/2013; these efficiencies have very likely been limited by back-end issues. (The 'back end' of a BJBC cell process includes creation of contact openings and rear-side metallization.)

On a small area, industrial ion-implanted BJBC cells with 'conventional' (non-carrier-selective) junctions have demonstrated efficiencies of 23.41% [12]. BJBC cells with carrier-selective junctions have recently achieved record efficiencies of 25% and above [13–15]. In situ patterned ion implantation can also be utilized in the case of carrier-selective junctions based on polycrystalline Si, in particular.

In this paper important aspects relating to junction formation based on ion implantation for both monocrystalline and polycrystalline Si will first be presented. ISFH's current BJBC cell results will then be reported in the second part of the paper.

Junction formation

Doping of monocrystalline silicon by ion implantation

The ionized dopants are accelerated to energies of several keV and implanted into the c-Si wafer, where they transfer their energy by nuclear and electronic interactions to the Si lattice. Eventually, the dopants form an as-implanted profile, peaking at the projected range of a few tens of nanometres, while many Si atoms are driven out of their former lattice sites and thus become Si self-interstitials. This crystal damage must be annealed and the implanted dopants have to be incorporated into the silicon lattice ('dopant activation') by high-temperature treatment.

In microelectronics, it is important to activate a major part of the dopants while maintaining a shallow doping profile: thus, only 'spike' anneals of a few seconds' duration are performed. These short annealing steps typically

do not yield a complete annealing of the crystal damage.

"It is of utmost importance to sufficiently anneal the crystal damage in order to minimize recombination losses."

By contrast, shallow doping profiles are neither required nor desirable for junctions in solar cells; rather, it is of utmost importance to sufficiently anneal the crystal damage in order to minimize recombination losses. Thus, longer annealing processes are required in PV than in microelectronics.

For boron (^{11}B) implants, which do not yield an amorphization of the surface for typical doses, the annealing of the crystal damage is not trivial [16]. During the first phase of the annealing process, the Si self-interstitials agglomerate to extended defects – first {311} clusters, which later evolve to dislocation loops [17]. The dislocation loops are very stable and only dissolve at temperatures above 900°C through the emission of Si atoms towards sinks, such as the wafer surface. Nevertheless, as first demonstrated by Benick et al. [18], it is possible to achieve recombination current densities as low as those for BBr_3 diffusion, indicating an almost complete annealing of implant-induced damage.

By comparing advanced process simulations [19] and experimental results, the thermal budget required for a sufficient annealing of boron implants was evaluated [20]. It was found that for an annealing temperature of 1050°C, durations of ~20min are required. For even higher annealing temperatures, which might be achievable with halogen-lamp-based rapid thermal processing (RTP), the annealing time can be significantly reduced (e.g. to 1min at 1200°C [20]). The good news regarding this rather high thermal budget is that the resulting doping profiles are completely determined by boron diffusion rather than by the shape of the as-implanted profile (Fig. 1(a)). Therefore, it is not necessary to precisely control the implant energy, which offers the possibility of simplifying and reducing the cost of PV implant tools.

There are several promising approaches to reducing the required temperature budget of the annealing process. For example, BF_2 instead of elementary boron can be utilized as the implant species: in this case, the wafer surface is amorphized, and the subsequent solid phase epitaxy supports the annealing process [21]. Alternatively, crystal defects can be restricted very close to the wafer surface by using low implant energies of down to 1keV [22]. After an incomplete annealing, e.g. at 950°C, the remaining defects can be removed by an etch-back of several tens of nanometres of Si [22]. The disadvantage of this approach is that it is not compatible with an in situ growth of a silicon oxide passivation layer during the annealing process. With this passivation scheme, emitter recombination current densities J_{0e} almost as low as with Al_2O_3 passivation were achieved (Fig. 1(b)). The fact that the J_{0e} values obtained with boron implants and subsequent annealing are comparable to the best reported in the literature for BBr_3-diffused boron emitters [23,24] shows the excellent annealing quality (Fig. 1(b)).

Phosphorus implants typically yield an amorphization of the wafer surface for doses above $10^{15}cm^{-2}$ [25]. Solid phase epitaxy takes place during the annealing process and removes a major part of the crystal damage. Thus, the annealing of phosphorus implants does not require temperatures as high as those in the case of boron implants. Annealing temperatures of around ~850°C are sufficient, which are comparable to those for a $POCl_3$ diffusion.

For BJBC fabrication, however, it

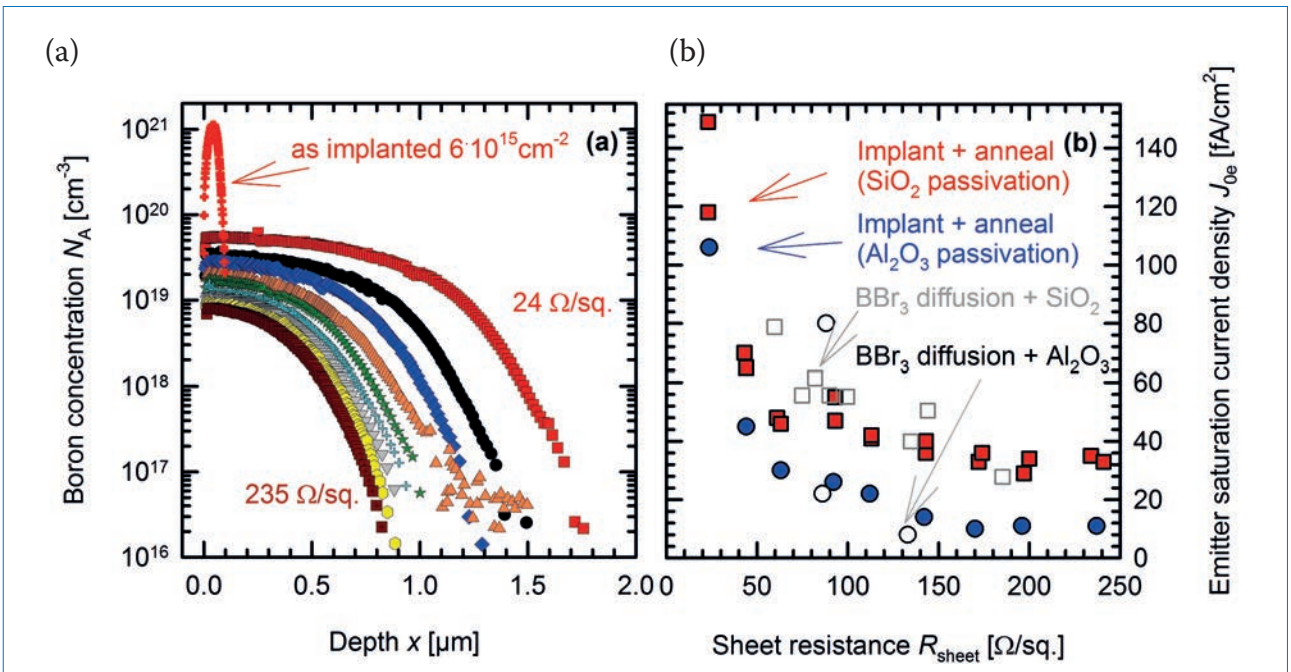

Figure 1. (a) Electrochemical capacitance-voltage (ECV) profiles of different boron emitters after implant and annealing. The implant dose is varied from $4{\cdot}10^{14}cm^{-2}$ to $6{\cdot}10^{15}cm^{-2}$, while the implant energy is kept constant at 10keV. For the highest dose, the as-implanted profile according to TRIM (transport of ions in matter) process simulation is shown. (b) Emitter saturation current densities for the emitters shown in (a). Different passivation schemes are compared – in situ grown SiO_2 and ALD-Al_2O_3. (Solid symbols refer to the authors' data for implanted and annealed samples, whereas open symbols refer to literature data for BBr_3-diffused emitters, according to Slade et al. [23] and Richter et al. [24].)

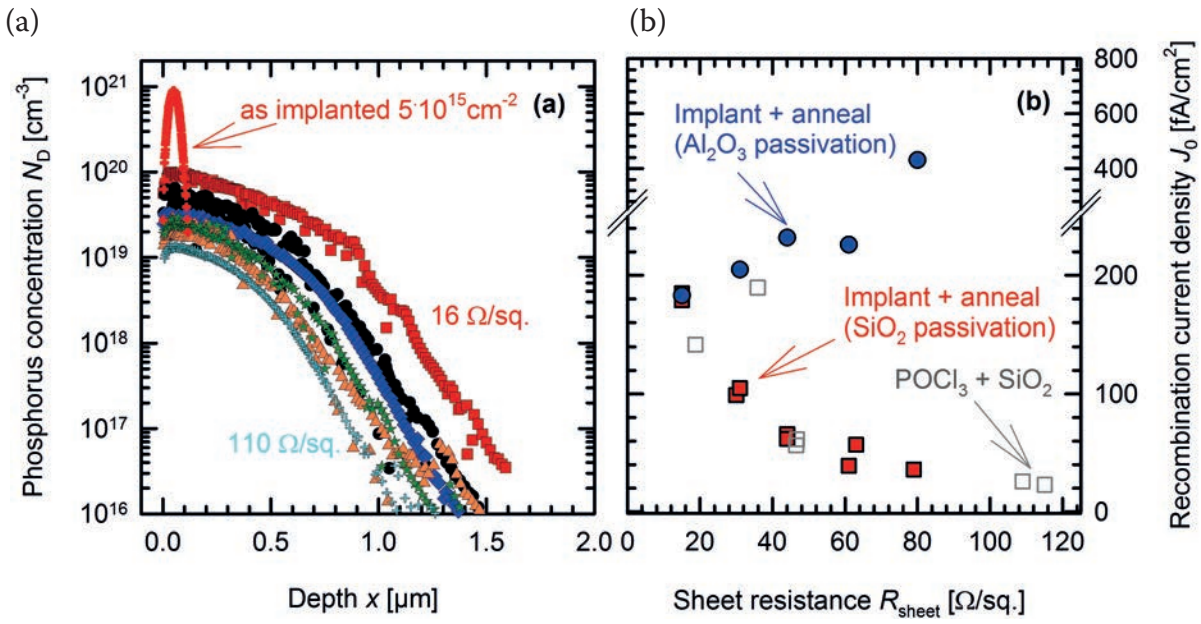

Figure 2. (a) ECV profiles of different phosphorus BSFs after implant and annealing. The implant dose is varied from 5·10^{14}cm^{-2} to 5·10^{15}cm^{-2}, while the implant energy is kept constant at 35keV. For the highest dose, the as-implanted profile according to a TRIM process simulation is shown. (b) Recombination current densities for the BSFs shown in (a). Different passivation schemes are compared – in situ grown SiO$_2$ and ALD-Al$_2$O$_3$. (Solid symbols refer to the authors' data for implanted and annealed samples, whereas open symbols refer to literature data for POCl$_3$ diffused and oxidized n$^+$ regions, according to Cuevas et al. [27].)

is desirable to anneal both implants in one co-annealing step. Obviously, the co-annealing temperature is determined by the requirements of the boron implant anneal, for example >20min at 1050°C (see above); thus, the resulting shape of the phosphorus-doping profiles is quite different from that of the POCl$_3$-diffused n$^+$ region (Fig. 2 (a)). As for boron, the as-implanted profile shape has almost no impact on the final doping profile.

> "For BJBC fabrication it is desirable to anneal both implants in one co-annealing step."

For screen-print metallization, the surface doping concentrations – ranging from 1·10^{19}cm^{-3} to 1·10^{20}cm^{-3} for sheet resistances from 109Ω/sq. down to 16Ω/sq. – seem quite low. With state-of-the-art Ag pastes, however, low specific contact resistances could possibly be achieved for these phosphorus profiles. In the case of metallization based on physical vapour deposition (PVD), specific contact resistances well below 1mΩcm^2 are achievable for these surface doping concentrations [26]. For silicon oxide passivation grown in situ during the annealing process, the J_0 values are comparable to the best reported in the literature [27] for POCl$_3$ diffusion and subsequent thermal oxidation (Fig. 2(b)). On the other hand, for Al$_2$O$_3$ passivation deposited by ALD (atomic layer deposition), the passivation achieved on the implanted back-surface field (BSF) regions (Fig. 2(b)) is rather poor. For increasing sheet resistance, the recombination current density also increases, a behaviour that is reminiscent of unpassivated doped surfaces.

Doping of polycrystalline silicon by ion implantation

An emerging candidate for carrier-selective junctions, which provides excellent passivation in metallized regions ('passivated contacts') as well, is a stack consisting of the monocrystalline (c-) Si wafer, a thin interfacial silicon oxide, and a highly doped polycrystalline (poly-) Si layer [28–31]. Fig. 3 shows a transmission electron microscopy (TEM) cross-section image of such a poly-Si/c-Si junction in high resolution. Ion implantation is well suited to doping of the poly-Si top layer [32–35]. Recombination current densities of down to 1fA/cm^2 after phosphorus implantation were recently achieved, and of down to 4.4fA/cm^2 after boron implantation in poly-Si [35]. The compatibility with local doping methods, such as ion implantation, might be the main advantage of poly-Si/c-Si junctions [14,15] for BJBC solar cell fabrication. However, it is fair to say that the current world record efficiency of 25.6% was achieved for a BJBC cell with carrier-selective junctions based on a-Si/c-Si heterojunctions [14].

A high-temperature anneal is required after implantation in the case of poly-Si/c-Si junctions as well. In contrast to implantation in monocrystalline Si, this annealing step is not necessary for the removal of implant-induced crystal defects. The poly-Si is anyway inherently highly defective. Since minority carriers are already blocked at the interface between the c-Si wafer and the interfacial oxide, recombination in the poly-Si is suppressed. Besides an electrical activation of the implanted dopants in the poly-Si, the high-temperature treatment also improves the passivation quality of the interfacial oxide and decreases the junction resistance [36]. The physical mechanism responsible for this improvement, however, is still under debate. One possible hypothesis is self-organized structural changes in the interfacial oxide, which might even lead to the formation of local pinholes [37,38]. In Fig. 3, it is at least obvious that the interfacial oxide thickness spatially varies between ~2 and ~4nm

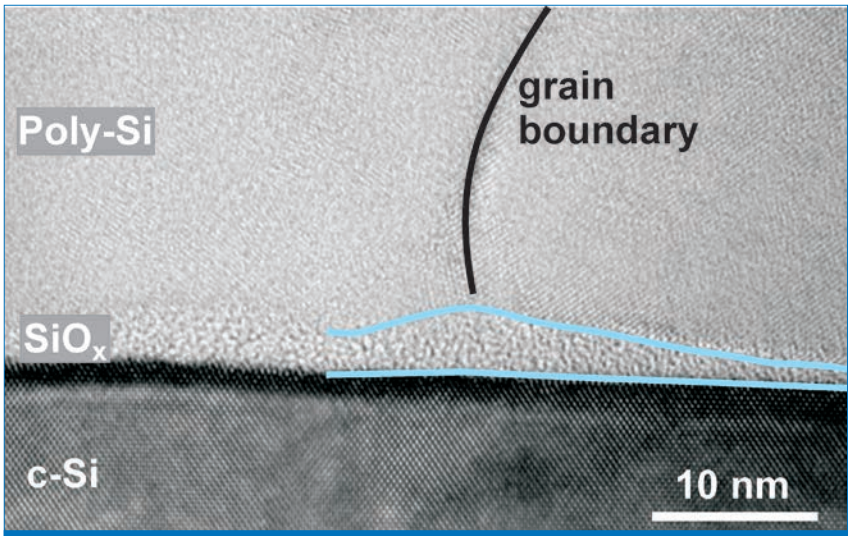

Figure 3. TEM cross-section image in high resolution, showing a poly-Si/c-Si junction with thermally grown interfacial oxide. The poly-Si was doped by phosphorus ion implantation, and received a subsequent high-temperature anneal. The variable thickness of the interfacial oxide is highlighted. The recombination current density of this sample is 1fA/cm².

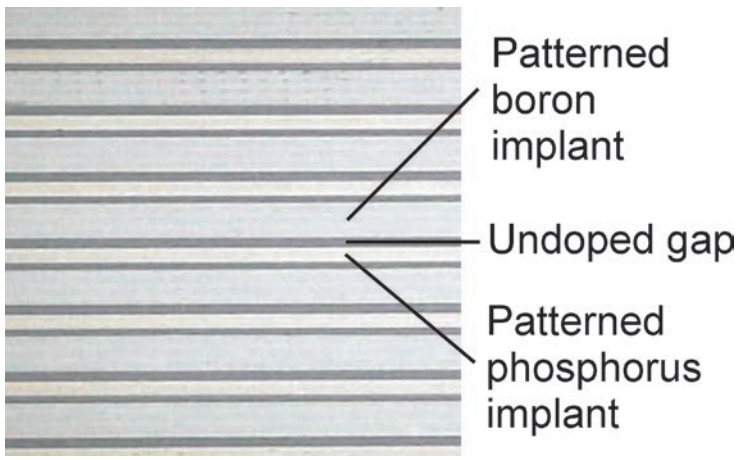

Figure 4. Optical microscope image of a wafer after two subsequent masked implant steps. The wider fingers were boron implanted using the first mask, and the narrower fingers were phosphorus implanted using the second mask. A narrow region was left intentionally undoped between both fingers. The images show the excellent implant-to-implant alignment.

after a high-temperature treatment of the complete stack, while the interfacial oxide itself was presumably grown with a uniform thickness in a short thermal oxidation. Pinholes might not be resolvable in TEM, because pinhole areal density is low. In any case, the temperature budget has to be adapted to the specific interfacial oxide [36] rather than to the implant conditions. Therefore, the optimum temperatures are typically lower than those required for the annealing of implant damage in c-Si: for wet-chemically grown oxides, temperatures of ~800–900°C are sufficient [36,39]. Temperatures that are too high certainly result in a perforation of the interfacial oxide and a significant increase in recombination current densities [36].

Depending on the poly-Si thickness, it might be challenging to accommodate the entire as-implanted profile in the poly-Si without damaging the interfacial oxide [32]; low implant energies are therefore required. Furthermore, it may be beneficial to utilize fairly heavy implant species with a low projected range – for example BF_2 instead of elementary boron, and arsenic instead of phosphorus.

The implant dose also affects the quality of the poly-Si/c-Si junction [32,35]. Interestingly, this is not only because of a different band bending (a different field effect passivation), but also because the passivation quality of the interfacial oxide is affected. For higher doses, a significant diffusion of dopants from the poly-Si into the c-Si occurs [32,35]. The optimum implant dose is different for boron and phosphorus, and depends on the thickness of the poly-Si.

> "One of the main advantages of ion implantation for BJBC solar cell fabrication is its capability of in situ patterning."

In situ patterning

One of the main advantages of ion implantation for BJBC solar cell fabrication is its capability of in situ patterning. Two approaches are possible:

1. One implant, for example the boron implant for emitter formation, could be performed all over the entire cell rear side. Only the second implant, for example the phosphorus implant for BSF formation, needs to be masked. The choice of appropriate implant parameters yields a local overcompensation of boron by phosphorus in the BSF regions ('counter-doping') [39].

2. Both implants could be masked. An undoped gap region can be maintained between emitter and BSF regions.

Although the first concept does not require implant-to-implant alignment, and therefore appears to be the simplest approach, implant-to-implant alignment is nevertheless feasible using state-of-the-art PV implanters, such as the SOLION XP tool from Applied Materials. Fig. 4 shows an optical microscope image of an implanted BJBC cell precursor. The wider finger was implanted with a first mask, and the narrower finger was implanted in a second step with another mask.

For implantation in monocrystalline Si, the first (counter-doping) concept works very well [39]. Although implanted n^+ and p^+ regions are in direct contact, the excellent annealing quality prevents a poor recombination behaviour due to trap-assisted tunnelling or to generation–recombination processes in the space charge region.

For implantation in poly-Si, the situation is different as a result of the inherently high defect density in the

poly-Si [35]. Thus, it is beneficial to leave an undoped region between the emitter and BSF fingers; this is possible with implant-to-implant alignment, corresponding to the second concept mentioned above.

Cell results

To achieve high energy conversion efficiencies in BJBC solar cells, it is important to form excellent p-n (high–low) junctions between the emitter (BSF) and the base, and to apply a rear-side passivation scheme which adequately passivates both polarities – emitter and BSF – as well as the p-n junction meander between these regions. The latter aspect is of particular importance for small BSF indices, which are necessary in order to minimize lateral transport losses of majority carriers in the Si bulk. In this case, the p-n junction meander length is fairly large. For these reasons, in situ grown silicon oxide passivation seems to perform better than ALD Al_2O_3 rear-side passivation [12], although the latter provides slightly better passivation quality on the emitter regions.

Fig. 5 shows the recombination behaviour (measured by photoconductance decay) of a 156mm × 156mm BJBC cell precursor after implantation, annealing and passivation. For this cell precursor, patterning is performed in situ via shadow masks in accordance with the counter-doping concept (see previous section). All three implants – phosphorus implant over the entire cell front side for front-surface field formation, boron implant over the entire cell rear side for emitter formation, and masked phosphorus implant on the cell rear side for BSF formation – are annealed within one co-annealing step that includes an in situ growth of a silicon oxide passivation. The high implied open-circuit voltage of 696mV and the high implied pseudo fill factor of 84.35% demonstrate the excellent quality of the ion-implantation-based front-end processing.

To estimate the efficiency potential, the following assumptions are made: a recombination current density in the metallized regions, $J_{0,met}$, of 1000fA/cm² for both polarities; a total metallized area fraction of 3.5% (PVD-based metallization); and an 'internal' series resistance (including the contributions from the base, emitter, FSF and BSF, as well as the specific contact resistance) of 0.3Ωcm². (The last of these values originates from numerical device simulations.) Accordingly, V_{oc} will decrease by 10mV upon contact opening and metallization, and the fill factor will

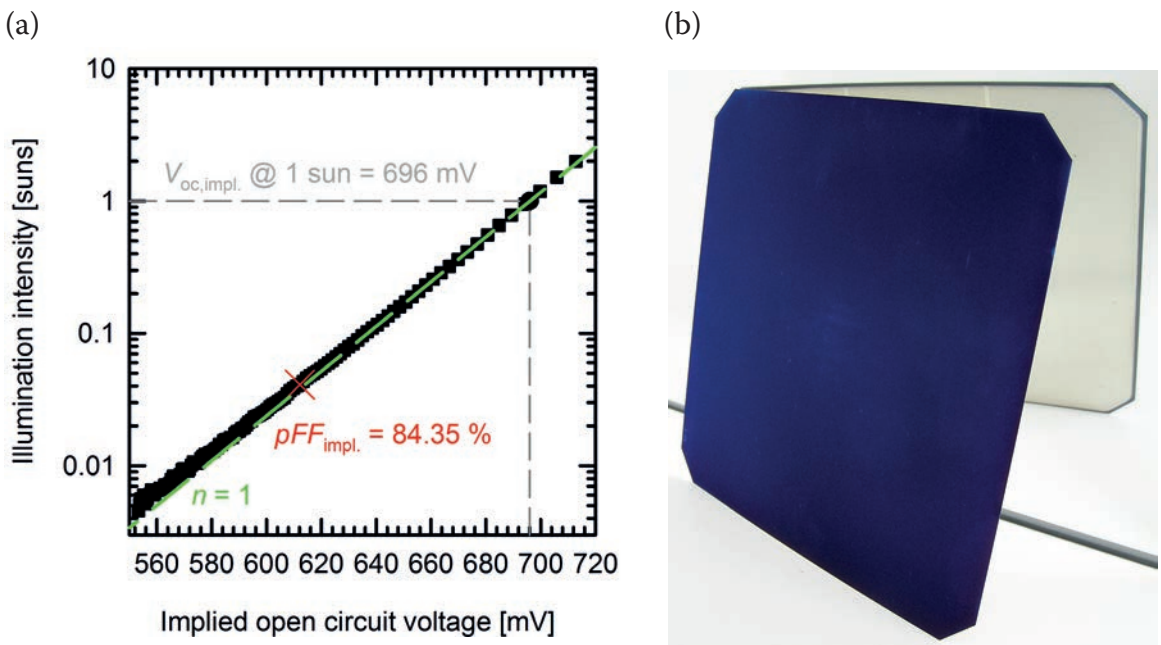

Figure 5. (a) Recombination behaviour of a 156mm × 156mm BJBC cell precursor after front-end (implantation, annealing, passivation) processing, as determined by photoconductance decay measurements. The high implied open-circuit voltage of 696mV and the high implied pseudo fill factor of 84.35% are indicated. The slope of the green dashed line corresponds to an ideality factor of one. (b) Photograph of a finished BJBC cell.

	Measurement	A [cm²]	η [%]	J_{sc} [mA/cm²]	V_{oc} [mV]	FF [%]
Large-area industrial BJBC conventional junctions	Full area	241*	22.1*	41.6*	676.2*	78.8*
Small-area industrial BJBC conventional junctions	Designated area	3.97**	23.41 ±0.47**	41.26 ±0.78**	692.8 ±2.4**	81.91 ±0.53**
Small-area industrial BJBC hybrid – conventional p^+ emitter, n^+ poly-Si BSF	Designated area	3.97*	22.2*	40.7*	690.6*	78.8*

*In-house measurement, **Independently confirmed by F-ISE CalLab

Table 1. ISFH's current record ion-implanted BJBC cells.

be 82.8%. For a short-circuit current density of 41.6mA/cm^2, the efficiency potential of this cell precursor is 23.6%.

ISFH's best cell result achieved so far on an industrial 156mm × 156mm BJBC cell, however, is 22.1%, as seen in Table 1. ('Industrial' denotes the absence of any pure laboratory techniques, such as photolithography: for example, besides in situ patterned ion implantation and co-annealing including in situ growth of silicon oxide passivation, contact openings are laser ablated, and metallization is performed using a high-throughput inline Al evaporation tool.) The main difference from the estimate of potential performance given earlier is the rather low fill factor of 78.5%. The fill factor loss is caused by resistive losses and an inhomogeneous potential distribution implied by the non-optimized rear-side metallization [40]. This back-end issue is independent of the junction formation method.

In order to screen out the back-end issue, small-area BJBC cells were also fabricated, which were measured on the designated area [12]. Here, co-annealing was also applied, including an in situ growth of oxide passivation, as well as laser ablation for contact opening formation. To allow a flexible evaluation of different device geometries, the doped regions were patterned by laser structuring rather than by shadow-masking the implant. The current record efficiency of 23.41% corresponds (to the authors' knowledge) to the highest value reported so far for a fully ion-implanted cell. This efficiency level can be transferred to large-area cells by utilizing an optimized, busbar-less rear-side metallization scheme, such as a simplified two-layer metallization [41].

For BJBC cells with poly-Si/c-Si junctions, significantly higher efficiencies are expected [33]: according to numerical device simulations, efficiencies above 25% are feasible. However, it will be necessary to adapt many process steps, such as the local laser ablation of a dielectric rear-side reflector on the rather thin poly-Si layer [42]. Because of these challenges, the best in-house measured efficiency for a small-area BJBC cell with n^+ poly-Si BSF regions and a conventional boron emitter is only 22.2% (Table 1). Nevertheless, a significant improvement is expected once the emitter has also been realized via a poly-Si/c-Si junction, and all related process issues have been resolved.

> "For ion-implanted BJBC cells with poly-Si/c-Si junctions, efficiencies of the order of 25% appear to be feasible."

Conclusions

Ion implantation can be utilized for the formation of excellent junctions in monocrystalline Si, as well for the doping of polycrystalline Si for emerging carrier-selective poly-Si/c-Si junctions. For boron and phosphorus implantation in monocrystalline Si and subsequent co-annealing, recombination current densities as low as the best reported in the literature for diffusion-based junctions were achieved.

In the case of BJBC cells with conventional junctions, since both polarities – the n^+ doped BSF and the p^+ doped emitter, as well as the p-n junction meander in between both regions – have to be passivated, silicon dioxide seems to be the best rear-side passivation scheme. This passivation layer can be grown in situ during the annealing process. The capability for in situ patterning is the main advantage of ion implantation for BJBC cell fabrication, resulting in significant process simplification potential. It is possible to mask just the second implant for a local overcompensation of the first implant, or to mask both implant steps, with an excellent implant-to-implant alignment.

For BJBC cells with conventional junctions in monocrystalline Si, the excellent recombination behaviour after the implant-based front-end processing indicates an efficiency potential well above 23%. With small-area BJBC cells, this potential is almost fully exploited, with a current record efficiency of 23.4%. For large-area cells, however, the back-end issues have been limiting up to the present moment: the highest efficiency obtained so far for an industrial 156mm × 156mm BJBC cell is therefore 22.1%, but further optimization of the rear-side metallization could greatly improve this result. For ion-implanted BJBC cells with poly-Si/c-Si junctions, efficiencies of the order of 25% appear to be feasible.

Acknowledgements

Major parts of this work were funded by the European Union's Seventh Program for research, technological development and demonstration under Grant Agreement No. 608498 (HERCULES), as well as by the German Federal Ministry for Economic Affairs and Energy under Grant 0325478 (SIMPLIHIGH). We thank our former colleagues from Bosch – D. Stichtenoth, T. Wütherich, C. Schöllhorn and A. Grohe – for their contributions to the development of the large-area BJBC cells. We also thank A. Klatt, T. Friedrich, H. Kohlenberg, S. Mau, D. Sylla and T. Neubert for their help with sample processing, and B. Wolpensinger for her help with the TEM measurements.

References

[1] SEMI PV Group Europe 2014, "International technology roadmap for photovoltaic (ITRPV): Results 2013", 5th edn (March) [http://www.itrpv.net/Reports/Downloads/].

[2] Lammert, M.D. et al. 1977, "The interdigitated back contact solar cell: Silicon solar cell for use in concentrated sunlight", *IEEE Trans. Electron Dev.*, Vol. 24, p. 337.

[3] Hannebauer, H. et al. 2014, "21.2%-efficient fineline-printed PERC solar cell with 5 busbar front grid", *physica status solidi (RRL)*, DOI: 10.1002/pssr.201409190 (also ISFH press release, April 10th [www.isfh.de]).

[4] Verlinden, P.J. et al. 2014, "Strategy, development and mass production of high-efficiency crystalline silicon PV modules", *Tech. Dig. WCPEC-6*, Kyoto, Japan (also Trina press release, Nov. 17th [www.pv-tech.org]).

[5] Minucci, J.A. et al. 1980, "Tailored emitter, low-resistivity, ion-implanted silicon solar cells", *IEEE Trans. Electron Dev.*, Vol. 27, No. 4, pp. 802–806.

[6] Spitzer, M.B. et al. 1984, "High-efficiency ion-implanted silicon solar cells", *IEEE Trans. Electron Dev.*, Vol. 31, pp. 546–550.

[7] Wood, R.F. et al. 1987, "Excimer laser-processed oxide-passivated silicon solar cells of 19.5-percent efficiency", *IEEE Electron Dev. Lett.*, Vol. 8, No. 5, pp. 249–251.

[8] Low R. et al. 2010, "High efficiency selective emitter enabled through patterned ion implantation", *Proc. 35th IEEE PVSC*, Honolulu, Hawaii, USA, pp. 001440–001445.

[9] Mo, C.B. et al. 2012, "High efficiency back contact solar cell via ion implantation", *Proc. 27th EU PVSEC*, Frankfurt, Germany.

[10] Grohe, A. et al. 2012, "High-efficient ion implanted back contact cells for industrial application", *Proc. 27th EU PVSEC*, Frankfurt, Germany.

[11] BOSCH Solar Energy 2013, Press Release (Aug.) [www.solarserver.de, www.pv-magazine.de].

[12] Merkle, A. 2014, "High efficient fully ion-implanted, co-annealed

and laser-structured back junction back contact solar cells", *Proc. 29th EU PVSEC*, Amsterdam, The Netherlands.
[13] Smith, D.D. et al. 2014, "Toward the practical limits of silicon solar cells", *IEEE J. Photovolt.*, Vol. 4, No. 6, pp. 1465–1469.
[14] Masuko, K. et al. 2014, "Achievement of more than 25% conversion efficiency with crystalline silicon heterojunction solar cell", *IEEE J. Photovolt.*, Vol. 4, No. 6, pp. 1433–1435.
[15] Nakamura, J. et al. 2014, "Development of heterojunction back contact Si solar cells", *IEEE J. Photovolt.*, Vol. 4, No. 6, pp. 1491–1495.
[16] Florakis, A. et al. 2012, "Simulation of the anneal of ion implanted boron emitters and the impact on the saturation current density", *Energy Procedia*, Vol. 27, pp. 240–246
[17] Avic, I. 2002, "Loop nucleation and stress effects in ion-implanted silicon", Ph.D. dissertation, University of Florida, Gainesville, USA.
[18] Benick, J. et al. 2010, "Very low emitter saturation current densities on ion implanted boron emitters", *Proc. 25th EU PVSEC*, Valencia, Spain, pp. 1169–1173.
[19] Wolf, F.A. et al. 2014, "Modeling the annealing of dislocation loops in implanted c-Si solar cells", *IEEE J. Photovolt.*, Vol. 4, No. 3, pp. 851–858.
[20] Krügener, J. et al. 2015, "Electrical and structural analysis of crystal defects after high-temperature rapid thermal annealing of highly boron ion-implanted emitters", *IEEE J. Photovolt.*, Vol. 5, No. 1, pp. 166–173.
[21] Krügener, J. et al. 2015 [forthcoming], "Ion implantation of boric molecules for silicon solar cells", *Proc. 5th SiliconPV Conf.* and *Sol. Energy Mater. Sol. Cells*.
[22] Müller, R. et al. 2014, "Defect removal after low temperature annealing of boron implantations by emitter etch-back for silicon solar cells", *physica status solidi (RRL)*, Vol. 1–4, DOI 10.1002/pssr.201409469.
[23] Slade, A. 2003, "Boron tribromide sourced boron diffusions for silicon solar cells", Ph.D. dissertation, University of New South Wales, Sydney, Australia.
[24] Richter, A. et al. 2013, "Boron emitter passivation with Al_2O_3 and Al_2O_3/SiN_x stacks using ALD Al_2O_3", *IEEE J. Photovolt.*, Vol. 3, No. 1, pp. 236–245.
[25] Keys, P.H., 2001, "Phosphorus-defect interactions during thermal annealing of ion implanted silicon", Ph.D. dissertation, University of Florida, Gainesville, USA.
[26] Schroder, D.K. 1984, "Solar cell contact resistance – A review", *IEEE Trans. Electron Dev.*, Vol. 31, No. 5, pp. 637–647.
[27] Cuevas, A. et al. 1996, "Surface recombination velocity of highly doped n-type silicon", *J. Appl. Phys.*, Vol. 80, pp. 3370–3375.
[28] Lindholm, F.A. et al. 1985, "Heavily doped polysilicon-contact solar cells", *IEEE Electron Dev. Lett.*, Vol. 6, No. 7, pp. 363–365.
[29] Borden, P. et al. 2008, "Polysilicon tunnel junctions as alternates to diffused junctions", *Proc. 23rd EU PVSEC*, Valencia, Spain, pp. 1149–1152.
[30] Feldmann, F. et al. 2014, "Passivated rear contacts for high-efficiency n-type Si solar cells providing high interface passivation quality and excellent transport characteristics", *Solar Energy Mater. & Solar Cells*, Vol. 120, pp. 270–274.
[31] Brendel, R. et al. 2013, "Recent progress and options for future crystalline silicon solar cells", *Proc. 28th EU PVSEC*, Paris, France, pp. 676–690.
[32] Feldmann, F. et al. 2014, "Ion implantation into amorphous Si layers to form carrier-selective contacts for Si solar cells", *physica status solidi (RRL)*, Vol. 8, pp. 767–770.
[33] Peibst, R. et al. 2014, "Building blocks for back-junction back-contacted cells and modules with ion-implanted poly-Si junctions", *Proc. 40th IEEE PVSC*, Denver, Colorado, USA, pp. 0852–0856.
[34] Reichel, C. et al. 2014, "Interdigitated back contact silicon solar cells with tunnel oxide passivated contacts formed by ion implantation", *Proc. 29th EU PVSEC*, Amsterdam, The Netherlands, pp. 487–491.
[35] Römer, U. et al. 2015, "Ion implantation for poly-Si passivated back-Junction back-contacted solar cells", *IEEE J. Photovolt.*, DOI: 10.1109/JPHOTOV.2014.2382975.
[36] Römer, U. et al. 2014, "Recombination behavior and contact resistance of n^+ and p^+ poly-crystalline Si / mono-crystalline Si junctions", *Solar Energy Mater. & Solar Cells*, Vol. 131, pp. 85–91.
[37] Wolstenholme, G.R. et al. 1987, "An investigation of the thermal stability of the interfacial oxide in polycrystalline silicon emitter bipolar transistors by comparing device results with high-resolution electron microscopy observations", *J. Appl. Phys.*, Vol. 61, pp. 225–233.
[38] Peibst, R. et al. 2014, "A simple model describing the symmetric I–V characteristics of p polycrystalline Si / n monocrystalline Si, and n polycrystalline Si / p monocrystalline Si junctions", *IEEE J. Photovolt.*, Vol. 4, No. 3, pp. 841–850.
[39] Feldmann, F. et al. 2014, "Tunnel oxide passivated rear contacts as an alternative to partial rear contacts", *Solar Energy Mater. & Solar Cells*, Vol. 131, pp. 46–50.
[39] Römer, U. et al. 2013, "Counterdoping with patterned ion implantation", *Proc. 39th IEEE PVSC*, Tampa, Florida, USA, pp. 1280–1284.
[40] Schinke, C. et al. 2012, "Contacting interdigitated back-contact solar cells with four busbars for precise current–voltage measurements under standard testing conditions", *IEEE J. Photovolt.*, Vol. 2, No. 3, pp. 247–255.
[41] Schulte-Huxel, H. et al. 2014, "Two layer metallization and module integration of point-contacted solar cells", *Energy Procedia*, Vol. 55, pp. 361–368.
[42] Römer, U. 2014, "Ion-implanted poly-Si / c-Si junctions as a back-surface field in back-junction back-contacted solar cells", *Proc. 29th EU PVSEC*, Amsterdam, The Netherlands, pp. 1107–1110.

About the Authors

Robby Peibst received his diploma degree in technical physics in 2005 from the Ilmenau University of Technology in Germany. In 2010 he received his Ph.D. from the Leibniz University of Hanover, with a thesis on germanium-nanocrystal-based memory devices. He joined ISFH in 2010 and has led the emerging c-Si technologies group since 2013. His research focuses on techniques for producing high-efficiency silicon solar cells.

Agnes Merkle studied physics at the University of Bucharest, Romania, where she specialized in biophysics. She joined ISFH in 1995, carrying out research and development work on several high-efficiency solar cell concepts. Her current research focuses on the development of n-type back-junction back-contact solar cells.

Udo Römer received his diploma degree in physics in 2010 from the Justus-Liebig-Universität Giessen in Germany. Since 2010 he has been working toward his Ph.D. with Fraunhofer ISE. His work focuses on the development and understanding of passivated polysilicon contacts for monocrystalline silicon solar cells.

Bianca Lim studied physics at Freie Universität Berlin and did her Diploma thesis at Hahn-Meitner-Institut, Berlin. She then joined ISFH to work on a doctorate on boron-oxygen-related recombination centres in silicon, receiving her Ph.D. (Dr. rer. nat.) from Leibniz Universität Hannover in 2011. She is currently in charge of a project at ISFH that involves simplified processes for local doping and n-type PERT silicon solar cells.

Yevgeniya Larionova studied physics and received her Ph.D. in optics (laser physics) from V.N. Karazin Kharkov National University in Ukraine. From 2002 to 2007 she worked as a research scientist in the Optics Department at Physikalisch-Technische Bundesanstalt (PTB, Braunschweig, Germany). Since 2007 she has been a research scientist at ISFH, working on development and efficiency improvement of silicon solar cells.

Rolf Brendel is the scientific director of ISFH. He received his Ph.D. in materials science, for which he researched infrared spectroscopy, from the University of Erlangen. In 2004 he joined the Institute of Solid State Physics of the Leibniz University of Hanover as a full professor. His main research focuses on the physics and technology of crystalline silicon solar cells.

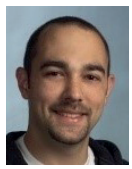

Jan Krügener received his diploma and Ph.D. degrees in electrical engineering from the Leibniz University of Hanover, where he is currently an associate researcher in the Institute of Electronic Materials and Devices. His research focuses on the fabrication and characterization of advanced high-efficiency silicon solar cells.

Manav Sheoran received his Ph.D. in physics from Georgia Institute of Technology in Atlanta, USA, in 2009, his thesis work for which focused on the development of high-efficiency solar cells through design optimization and hydrogen passivation of defects. Since 2011 he has been with Applied Materials-Varian Semiconductor in Gloucester, USA, where he is currently the leader of the team working on ion-implanted IBC solar cells.

John Graff is director of Solar Cell Technology at Applied Materials, Inc. He joined Applied through its acquisition of Gloucester USA-based Varian Semiconductor Equipment Associates, where he was principal scientist and leader of the ion-implantation group responsible for IBC solar cells. Dr. Graff earned his Ph.D. in electrical engineering from Boston University in 2003, with a research focus on high-brightness visible LEDs.

Enquiries
Dr. Robby Peibst
Institut für Solarenergieforschung Hameln (ISFH)
D-31860 Emmerthal
Germany

Tel: +49 (0) 5151 999 633

Email: r.peibst@isfh.de
Webpage: www.isfh.de

Development of bifacial n-type solar cells at Fraunhofer ISE: Status and perspectives

Sebastian Mack, Elmar Lohmüller, Philip Rothhardt, Sebastian Meier, Sabrina Werner, Andreas Wolf, Florian Clement & Daniel Biro, Fraunhofer Institute for Solar Energy Systems (ISE), Freiburg, Germany

ABSTRACT

This paper reports on the status of large-area, 156mm, bifacial, n-type passivated emitter and rear totally diffused (n-PERT) solar cells, which feature full-area homogeneous doped regions on the front and rear sides. The fabrication process includes either two separate gas-phase diffusion processes with sacrificial diffusion barrier layers, or a sophisticated co-diffusion approach, in which a deposited stack of borosilicate glass (BSG) and silicon oxide acts as a dopant source during back-surface field (BSF) formation in a tube furnace. Thus, the co-diffusion approach reduces the number of required high-temperature processes to one, which significantly streamlines the process sequence. It is shown that by implementing two deposition phases during the BSF diffusion process, it is possible to separately control both the depth and the surface concentration of the BSF. The use of a tailored BSG source allows low recombination and specific contact resistance values on both the front and rear sides, resulting in peak conversion efficiencies of 19.9%. A discussion on the recombination at the emitter–metal interface completes the paper, and several paths to driving the conversion efficiency towards 22% are outlined.

Introduction

During the last few years, n-type wafers and solar cells have been receiving more attention. The inherent advantages of n-type doped Czochralski-grown silicon (Cz-Si) wafers over p-type Cz-Si wafers are the absence of light-induced degradation (LID) [1], a reduced sensitivity against metal contaminations [2] – in particular iron – and a longer minority-carrier lifetime. The price of n-type Cz-Si wafers, however, is currently about 16% higher than that of p-type Cz-Si wafers [3], but this gap could become smaller in the future.

Compared with solar cells made from p-type silicon wafers, where the aluminium back-surface field (Al-BSF) cell and the passivated emitter and rear cell (PERC) are by far the two most dominant architectures, there are more concepts under investigation for cells made from n-type silicon. Both heterojunction with intrinsic thin layer (HIT) [4] and back-contact back-junction (BC-BJ) [5,6] solar cells are known for their high conversion efficiencies. Other promising cell concepts include rear-emitter structures, formed by either diffusion [7–10] or alloying a screen-printed aluminium layer [11,12], and the passivated emitter and rear locally diffused (PERL) [13] or passivated emitter and rear totally diffused (PERT) cells [14–16]. Also under consideration are n-type metal-wrap-through (n-MWT) solar cells [17,18].

Some of the above-mentioned architectures feature a rear surface that is only partially metallized, which makes them potentially interesting for bifacial applications. With adaptations of the module layout, an additional energy yield of the order of 20% has been reported [19,20], at almost no additional cost; this is certainly one of the reasons why the ITRPV roadmap forecasts a market share increase for n-type solar cells from 5% in 2013 to almost 40% in 2024 [21]. In addition, it is worth mentioning that bifacial solar cells are developed not solely for n-type substrates, but also for p-type wafers [22,23]. For an overview of bifacial systems and recent progress in this field, see Kopecek et al. [24].

This paper reports on the status of bifacial n-PERT solar cells and R&D activities at Fraunhofer ISE. After a presentation of a fabrication process with sequential diffusion processes, this process is simplified by an implementation of the compact co-diffusion approach, in which a deposited borosilicate glass acts as a dopant source for emitter formation during a gas-phase diffusion process for back-surface field formation. The properties of the diffusion process as well as of the doping profiles produced are characterized, and saturation current densities and specific contact resistance values are reported. One dedicated section addresses the recombination at the emitter–metal interface and describes ways to reduce that particular contribution to the overall recombination.

Sequential diffusion approach

In the reference process for the fabrication of bifacial H-pattern cells, 156mm n-type Cz-Si wafers with a base resistivity between 3 and 6Ωcm are used. After random pyramid formation in alkaline solution, the boron emitter and the phosphorus BSF are formed by two sequential tube-furnace diffusion processes using boron tribromide (BBr_3) and phosphorus oxychloride ($POCl_3$) as dopant sources. Obviously one has to ensure selective doping of each side during this sequence, and this is accomplished by the use of sacrificial dielectric diffusion barrier layers, applied prior to each diffusion.

As BBr_3 diffusion takes place at temperatures considerably higher than those for $POCl_3$ diffusion, it was decided to perform the BBr_3 diffusion first, in order to minimize profile changes during the second high-temperature step [25]. A clear advantage of this approach is the possibility of optimizing each diffusion process separately, at least to a large extent. A disadvantage is the use of two high-temperature processes; this could possibly affect the minority-carrier lifetime in the bulk, as well as putting some cost pressure on the process sequence.

After the second diffusion process and glass removal, a dielectric stack of aluminium oxide (Al_2O_3) and silicon nitride (SiN_x) is deposited by plasma-

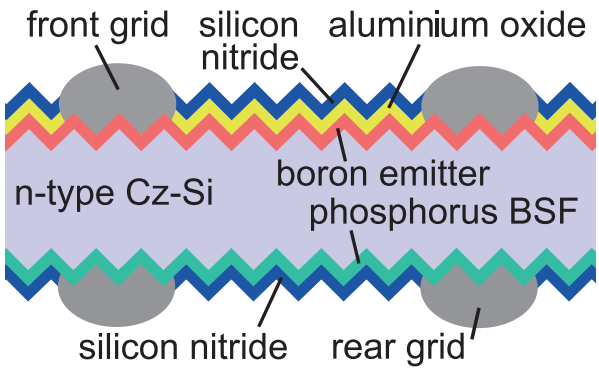

Figure 1. Schematic cross section of a bifacial n-PERT solar cell with an H-pattern grid on both the front and back sides.

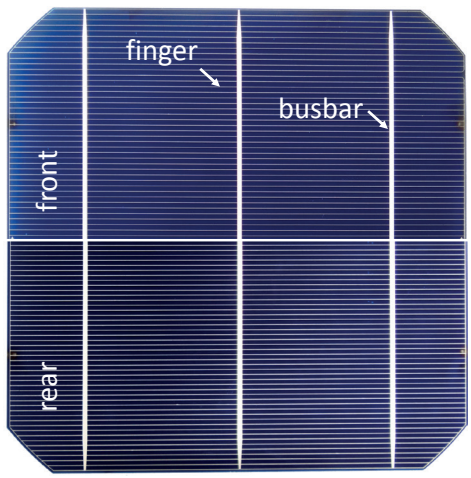

Figure 2. Photographs of the front and back sides of a bifacial n-type solar cell with an H-pattern grid. The cell layout is suited to bifacial applications, for example in glass–glass modules or in modules with transparent backsheets.

enhanced chemical vapour deposition (PECVD) on the front side, whereas on the rear side a single PECVD-SiN_x layer is deposited. Front-contact formation is realized by screen printing a AgAl paste, whereas a Ag paste is used on the rear side. After contact firing, laser edge isolation ensures the electrical insulation between the front and rear sides.

Fig. 1 shows a schematic cross section of a bifacial n-PERT solar cell in a standard H-pattern layout; the top and bottom views are illustrated in the photograph in Fig. 2. Conversion efficiencies of 19.7%, measured in a cell tester on a white and non-conductive foil, have been achieved using the sequential diffusion approach.

Simplified process sequence using co-diffusion

As discussed above, in the fabrication of the investigated H-pattern bifacial solar cells it is necessary to provide doping profiles of different polarities on the front and rear sides of the device. Although this can be achieved, for example, by applying diffusion barriers and two subsequent gas-phase diffusion processes, it would be more convenient to restrict the dopant formation to one side of the sample and perform only one high-temperature step.

"The co-diffusion approach investigated at Fraunhofer ISE permits a largely independent adjustment of boron and phosphorus doping profiles."

(a)

- Alkaline texture
- BSG + SiO_x deposition by APCVD
- $POCl_3$ Co-diffusion
- PSG/BSG etching
- ALD Al_2O_3 deposition (4nm) on boron emitter
- PECVD SiN_x (70nm) on front
- PECVD SiO_xN_y/SiN_z on rear
- Dual print front (Ag busbars and AgAl fingers)
- Double print rear (Ag)
- Contact firing
- Laser edge isolation

(b)

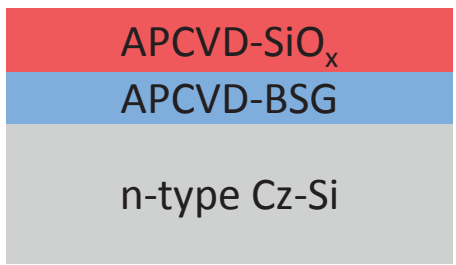

Figure 3. (a) Process flow for the fabrication of bifacial n-PERT solar cells. After BSG/SiO_x dielectric layer stack deposition, co-diffusion takes place in a $POCl_3$ diffusion process. (b) Schematic cross section of the samples before co-diffusion in a $POCl_3$ atmosphere.

Recently, more attention has especially been given to ion implantation [26–28] and diffusion from deposited doped glasses [29–34]. Both require a subsequent high-temperature step for respectively dopant activation and drive-in. One approach is to implant or cap both sides of the wafer and perform one thermal treatment in an inert gas or in an atmosphere with a low oxygen content [35]. Both co-annealing and co-diffusion significantly streamline the process sequence, but the degree of freedom for independent control of the doping profiles is reduced, as the dose for each dopant type can only be chosen in advance and cannot be adjusted during the thermal process. The ups and downs of both process sequences have already been nicely summarized by Lim et al. [36]. The co-diffusion approach investigated at Fraunhofer ISE, which combines the diffusion from a deposited glass with that from a gas-phase diffusion process, overcomes the above-described limitation, since it permits a largely independent adjustment of boron and phosphorus doping profiles.

For the fabrication of co-diffused bifacial large-area n-PERT solar cells, denoted CoBiN (co-diffused bifacial n-type) [32], n-type Cz-Si wafers with an edge length of 156mm and a base resistivity of 3Ωcm are used; the process flow is depicted in Fig. 3(a). A layer stack of borosilicate glass (BSG) and silicon oxide (SiO_x), deposited by atmospheric pressure chemical vapour deposition (APCVD) (in cooperation with SCHMID Group), is used as a dopant source for emitter formation during BSF formation in a $POCl_3$ atmosphere (see Fig. 3 (b)), in the standard phosphorus tube-furnace diffusion system that is widely used today in the PV industry. Other groups have also successfully applied the boron source by alternative methods, such as PECVD [29,30,33], spin-on [37] or inkjet printing [35]. Recently, Mitsubishi reported the use of an APCVD-BSG layer for emitter formation in bifacial n-PERT solar cells as well, yielding conversion efficiencies above 21% [31].

After front-surface passivation with an Al_2O_3 layer in an inline atomic layer deposition (ALD) tool, the SiN_x anti-reflection coating and the silicon oxynitride (SiO_xN_y)/SiN_z rear-passivation stack are deposited by PECVD. In this experiment, the front contact has been formed by dual printing (printing the busbars and fingers in different process steps), where Ag paste is applied for the floating busbar and AgAl paste for the fingers. Both the front AgAl fingers and the subsequently printed rear Ag fingers are formed by print-on-print (double-printing) technology, using the same grid and paste for each printing step twice. Contact firing and laser edge isolation complete the process sequence.

Solar cells fabricated with the CoBiN process sequence have demonstrated conversion efficiencies of up to 19.9% (see Table 1) on a reflecting, conductive chuck (calibrated measurements at Fraunhofer ISE CalLab PVCells); these values are similar to those reported by other authors [30,36,38]. Measurements taken on a black, non-conductive chuck yield a conversion efficiency of only 19.5%, which highlights the impact of the measurement conditions on the conversion efficiency in the case of bifacial cells.

Böscke et al. [16] have reported that measurements on a non-reflective,

Measurement chuck	V_{oc} [mV]	J_{sc} [mA/cm²]	*FF* [%]	η [%]	R_p [kΩcm²]
Black, non-conductive	647	38.3	78.7	19.5	19
Golden, conductive	648	38.8	79.0	19.9	19
Combined	648	38.8	78.7	19.8	19

Table 1. *I–V* data of large-area bifacial n-type co-diffused CoBiN solar cells, extracted from calibrated measurements at Fraunhofer ISE CalLab PVCells. The parallel resistance R_p is determined from a measurement in an industrial cell tester.

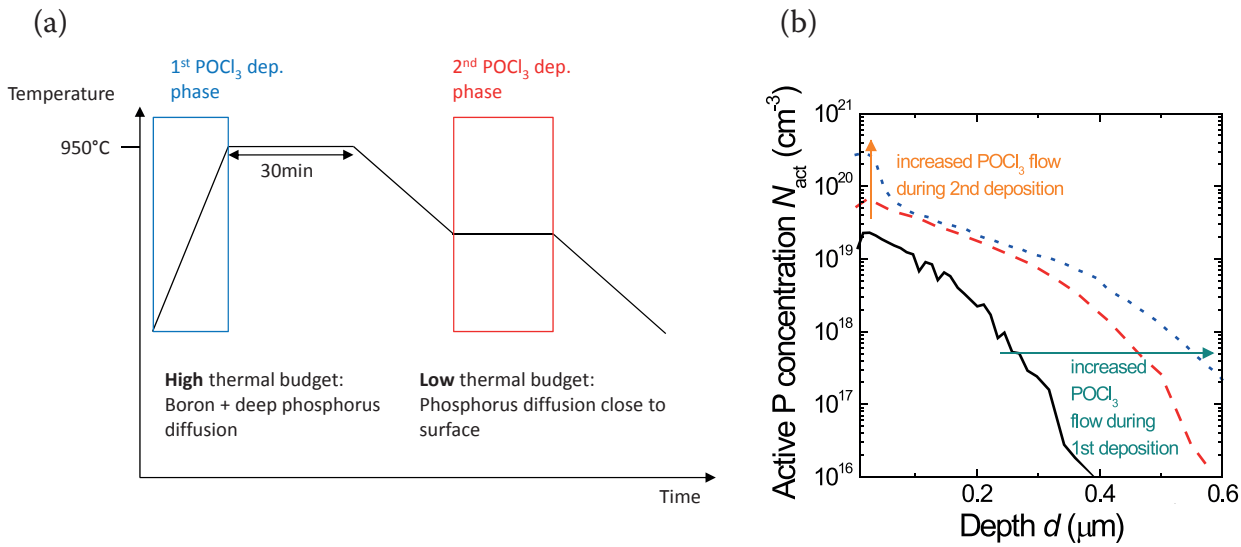

Figure 4. (a) Temperature–time profile of the $POCl_3$ diffusion process, highlighting two deposition phases, which allows independent control of the depth and surface concentration of the phosphorus doping profile. Drive-in of the boron emitter out of the APCVD-BSG/SiO_x stack takes place during the first deposition step at 950°C. (b) The resulting phosphorus profiles, measured by electrochemical capacitance voltage (ECV) profiling on alkaline saw-damage-etched surfaces.

non-conductive chuck show a decrease in both J_{sc} and *FF* compared with a reflective, conductive chuck. Since no norm yet exists relating to how bifacial cells or modules should be measured, the calculation of a combined efficiency has been proposed, which includes V_{oc} and J_{sc} from the measurement on the reflective chuck and *FF* from the measurement on the non-conductive chuck. This results in a combined efficiency of 19.8% for Fraunhofer ISE cells.

When measuring bifacial n-PERT solar cells, it is important to look not only at the forward current but also at the reverse bias stability; as several authors have shown, this might be a bigger challenge for these cells than for p-type cells [15,28,39].

Layer and doping profile properties

In the $POCl_3$ co-diffusion process developed at Fraunhofer ISE, with a temperature–time profile depicted in Fig. 4(a), the use of different deposition phases makes it possible to separately control the depth and surface concentration of the BSF. The $POCl_3$ flow in the first deposition phase controls the depth of the phosphorus BSF; in addition, the temperature of 950°C allows the drive-in of the boron out of the pre-deposited BSG source.

> "The use of different deposition phases makes it possible to separately control the depth and surface concentration of the BSF."

Changes in the $POCl_3$ bubbler gas flow during the second deposition phase, towards the end of the process, affect the surface concentration of the doping profile (see Fig. 4(b)); the profile can be tailored to achieve a low specific contact resistance between the phosphorus BSF and the screen-printed Ag contacts. Thus, an independent manipulation of BSF depth and surface concentration is possible in a single process, while the BSG composition and thermal budget of the process control the boron doping profile.

Fig. 5 shows the specific contact resistance ρ_c and dark saturation current density $J_{0,BSF}$ of phosphorus BSFs for variations in the $POCl_3$ gas flow in the second deposition phase. The contacts have been formed by the screen printing of Ag paste followed by contact firing. As expected from the diffusion profile, transfer length method (TLM) measurements reveal low ρ_c values, between 2mΩcm² and 4mΩcm², for a wide range of $POCl_3$ flow rates, when a second deposition phase is introduced.

The $J_{0,BSF}$ values shown in Fig. 5 were extracted in high-level injection on symmetric n-type Cz-Si samples with alkaline-textured surfaces after passivation by either a PECVD-SiN_x layer or a PECVD-SiO_xN_y/SiN_z stack and contact firing. For a flow rate of 200sccm, which was the lowest tested flow rate in this experiment, $J_{0,BSF}$ amounts to 125fA/cm² for a SiO_xN_y/SiN_z passivation stack. This flow rate (200sccm) is also used for BSF formation in Fraunhofer ISE solar cells. Fraunhofer ISE's $POCl_3$ process was recently enhanced to allow $J_{0,BSF}$ values below 100fA/cm², and the process time was shortened, while improving at the same time the sheet resistance homogeneity over the wafer.

The question arises as to whether the deposited BSG/SiO_x stack is really impervious to phosphorus and completely blocks the phosphorus diffusion from the gas phase. To address this point a secondary ion mass spectrometry (SIMS) was performed on shiny-etched wafers after layer deposition and $POCl_3$ diffusion; measurements of the respective atomic concentration in the dielectric layers as well as in the silicon wafer were taken. The results are shown in Fig. 6, with a proposed layer arrangement indicated above the graph.

At the surface of the samples, the $POCl_3$ from the atmosphere reacts with the bare SiO_x layer to form a phosphorus silicon glass (PSG). The high concentration gradient might lead to some phosphorus diffusion through the SiO_x and BSG layer, as highlighted by a P concentration of around $10^{17}cm^{-3}$ in the silicon wafer itself; however, that concentration is a few orders of magnitude below that of the boron concentration. Interestingly,

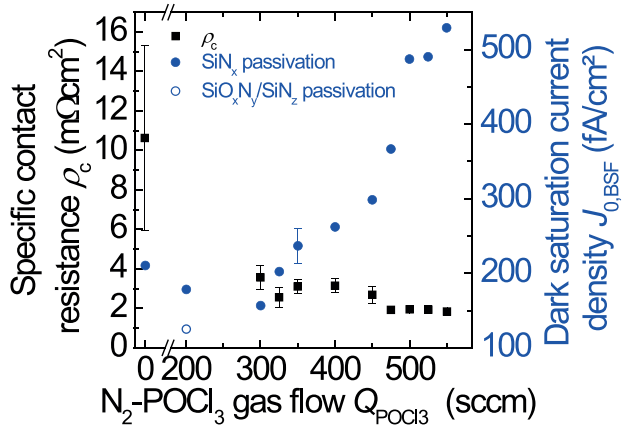

Figure 5. Specific contact resistance ρ_c and dark saturation current density $J_{0,BSF}$ of phosphorus-diffused BSFs for different $POCl_3$ gas flows. A PECVD-SiN_x layer or a SiO_xN_y/SiN_z stack was used for surface passivation.

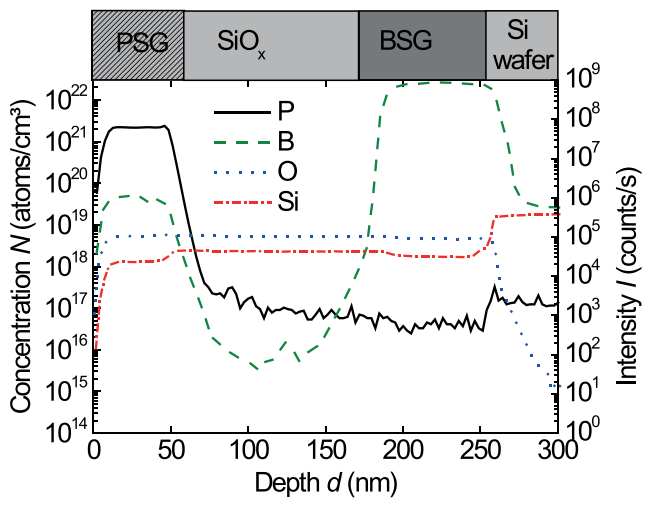

Figure 6. SIMS measurements of BSG/SiO_x layer stack after $POCl_3$ diffusion. The proposed sample structure is shown above the graph.

the high boron concentration gradient leads to a boron diffusion through the SiO_x layer into the PSG, resulting in concentrations above $10^{19}cm^{-3}$, whereas in the SiO_x layer itself a very low boron concentration of $10^{16}cm^{-3}$ is measured.

From the results it is concluded that, even if there might be some diffusion of phosphorus through the BSG/SiO_x stack, it will not negatively impact the boron diffusion profile; this is confirmed by identical boron doping profiles measured for diffusion processes with and without $POCl_3$ in the process atmosphere. Similar results are expected in the solar cell, where the dielectric stack is deposited on alkaline-textured surfaces.

The resulting boron emitter profiles themselves are characterized by a sheet resistance of 77Ω/sq. and J_{0e} = 57fA/cm², measured in high-level injection on symmetrically textured n-type Cz-Si samples after passivation by an Al_2O_3/SiN_x stack and activation of the passivation layers in a firing furnace. After a screen printing of AgAl paste and contact firing, TLM measurements yield ρ_c = 2mΩcm², which is similar in value to that of the diffused boron profiles from the gas phase.

Boron emitter metallization

Inherent in boron profiles that are suitable for screen-printed contacts using AgAl paste is a rather high recombination $J_{0e,met}$ at the semiconductor–metal interface. Values of $J_{0e,met}$ in the range 3500–4200fA/cm² have recently been reported [17,40], which might be the result of deep spike penetration of the AgAl paste into the wafer surface and emitter; these values are a couple of times higher than those seen for Ag pastes on the phosphorus BSF. Although the metallized area fraction A_{met} at the front of solar cells is only a few per cent, the J_0 contribution of the AgAl contacts is about two to four times higher than that of the passivated area J_{0e}. As a result, efforts to reduce A_{met} are being made.

One approach is dual printing of the AgAl front contact, where printing takes place in two separate steps and different pastes are used for the busbar and fingers. The implementation of floating Ag busbars in H-pattern cells thus reduces A_{met} of the AgAl paste from 5.8% to 3.4%, which in this case increases the open-circuit voltage V_{oc} by 7mV. However, the shaded-area fraction remains unchanged. Another approach is the integration of MWT structures, where moving the busbars from the front to the rear not only decreases A_{met} compared with contacting busbars, but also reduces shading.

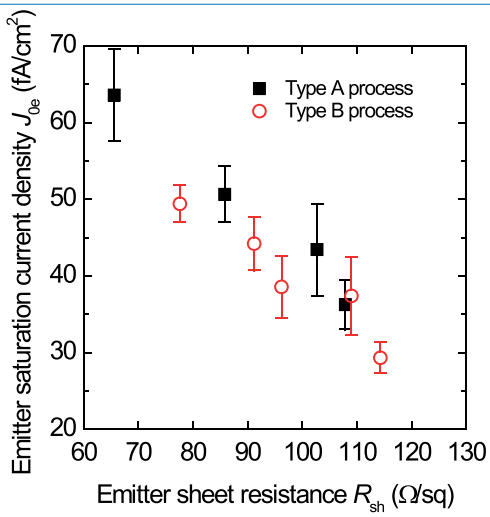

Figure 7. Emitter saturation current density J_{0e} plotted vs. the sheet resistance R_{sh} for symmetric, alkaline-textured, 10Ωcm, n-type Cz-Si wafers. The J_{0e} determination is performed in high-level injection after passivation with an Al_2O_3/SiN_x stack by PECVD and contact firing.

An alternative approach to reducing front-metallization-related recombination is an adaptation of the boron diffusion process. Edler et al. [40] have shown that increasing the profile depth while keeping the surface concentration unchanged is effective in reducing $J_{0e,met}$. This indicates a possible window for selective boron emitters, which might, however, be made obsolete by improvements in metallization pastes, as seen in the case of phosphorus emitters in the past. Adaptations of Fraunhofer ISE's BBr_3 diffusion process have made it possible to decrease J_{0e} by increasing the depth and reducing the surface concentration of the emitter profile to values down to 30fA/cm² on alkaline-textured surfaces (see Fig. 7). Here, the surfaces are passivated by a fired Al_2O_3/SiN_x layer stack, with 'Type A' and 'Type B' referring to different processes. Initial TLM measurements reveal specific contact resistance values in the low mΩcm² range for all 'Type A' processes using a commercially available AgAl paste; however, the $J_{0e,met}$ determination is still pending.

Another promising option for reducing $J_{0e,met}$ might also be the replacement of screen-printed contacts by plated Ni/Cu contacts, if process maturity is ensured; this could very likely be combined with an adaptation of the emitter profile as indicated above.

Conclusions

For the fabrication of bifacial n-PERT front-junction solar cells, a reference process has been established, which is based on two sequential diffusion processes and which allows conversion efficiencies of up to 19.7% in H-pattern cells, measured on a white, non-conductive foil. It has been shown that the detrimental impact of high front-contact recombination can be reduced by the implementation of floating Ag busbars, which increases V_{oc} by 7mV.

The process sequence has been further greatly simplified by substituting a co-diffusion process for the two sequential diffusion processes. An APCVD process forms the BSG/SiO_x stack for emitter formation on the front side of the samples, followed by a drive-in during BSF formation in a $POCl_3$ atmosphere. The $POCl_3$ diffusion process contains two deposition phases; this allows independent manipulation (to a large extent) of both depth and surface concentration of the BSF. Bifacial solar cells with a conversion efficiency of up to 19.9% have been fabricated with this CoBiN process. Further increases in conversion efficiency are expected in the near future through improvements to the $POCl_3$ diffusion process, adaptations of the BSG source and new metallization pastes.

The fact that $POCl_3$ diffusion furnaces are widely available and facilitate high throughput, as well as the similarities of the CoBiN process sequence to p-type PERC solar cell fabrication, reduces the barriers to industrial implementation.

"A TOPCon layer implementation could increase the conversion efficiency of bifacial n-PERT front-junction solar cells to over 22% in the near future."

Outlook

To address the high carrier recombination at the screen-printed AgAl emitter contact, it is planned to adapt Fraunhofer ISE's BSG source and $POCl_3$ diffusion process accordingly. Improved metallization pastes will be applied for the screen-printed contacts route, or, alternatively, fully plated contacts on both the front and the rear will be included. This will decrease not only $J_{0e,met}$ but also J_{0e} in the passivated regions and thus result in a higher open-circuit voltage. Simulations with Sentaurus Device indicate a conversion efficiency potential of over 22% for such cells.

Another option is to adapt the cell structure itself and include a polysilicon [41,42] or a TOPCon (tunnel oxide passivated contact) layer for a carrier-selective rear contact. With monofacial solar cells of size 2cm × 2cm with a planar rear side, the excellent passivation quality of the TOPCon layer has yielded open-circuit voltages of 715mV and conversion efficiencies greater than 24% [43]; a very good passivation quality on textured surfaces, however, has already also been demonstrated by Moldovan et al. [44], with a V_{oc} limit of 715mV. Since recombination in the BSF region is the second-highest loss factor after $J_{0e,met}$ in the CoBiN cell structure, a TOPCon layer implementation could increase the conversion efficiency of bifacial n-PERT front-junction solar cells to over 22% in the near future.

References

[1] Glunz, S.W. et al. 2001, "Minority carrier lifetime degradation in boron-doped Czochralski silicon", *J. Appl. Phys*, Vol. 90, pp. 2397–2404.

[2] Istratov, A.A., Hieslmair, H. & Weber, E.R. 1999, "Iron and its complexes in silicon", *Appl. Phys. A*, Vol. A69, pp. 13–44.

[3] PVInsights 2015, Solar Wafer Monthly Contract Price (9th Feb.) [http://pvinsights.com/].

[4] Masuko, K. et al. 2014, "Achievement of more than 25% conversion efficiency with crystalline silicon heterojunction solar cell", *IEEE J. Photovolt.*, Vol. 4, pp. 1433–1435.

[5] Franklin, E. et al. 2014, "Fabrication and characterization of a 24.4% efficient IBC cell", *Proc. 29th EU PVSEC*, Amsterdam, The Netherlands.

[6] Smith, D.D. et al. 2013, "SunPower's Maxeon Gen III solar cell: High efficiency and energy yield", *Proc. 39th IEEE PVSC*, Tampa, Florida, USA.

[7] Lim, B. et al. 2014, "n-PERT back junction solar cells: An option for the next industrial technology generation?", *Proc. 29th EU PVSEC*, Amsterdam, The Netherlands.

[8] Duerinckx, F. et al. 2014, "Quantifying internal optical losses for 21% n-Si rear junction cells", *Proc. 29th EU PVSEC*, Amsterdam, The Netherlands.

[9] Mertens, V. et al. 2013, "Large area n-type Cz double side contact back junction solar cell with 21.3% conversion efficiency", *Proc. 28th EU PVSEC*, Paris, France.

[10] Degans, H. 2015, "Imec demonstrates large area industrial crystalline silicon n-PERT solar cell with a record 22 percent efficiency", Press Release (Jan.) [http://www2.imec.be/be_en/press/imec-news/imec-22-percent-npert-solar-cell.html].

[11] Schmiga, C. et al. 2012, "Status and perspectives on n-type silicon solar cells with aluminium-alloyed rear emitter", *Proc. 27th EU PVSEC*, Frankfurt, Germany.

[12] Xi, X. et al. 2012, "High efficiency aluminum-rear-emitter n-type silicon solar cells with inline phosphorus diffusion process on the front surface", *Proc. 27th EU PVSEC*, Frankfurt, Germany.

[13] Steinhauser, B. et al. 2014, "Firing-stable PassDop passivation for screen printed n-type PERL solar cells based on a-SiN_x:P", *Solar Energy Mater. & Solar Cells*, Vol. 126, pp. 96–100.

[14] Tao, Y. et al. 2014, "20.7% efficient ion-implanted large area n-type front junction silicon solar cells with rear point contacts formed by laser opening and physical vapor deposition", *Progr. Photovolt.: Res. Appl.*, Vol. 22, pp. 1030–1039.

[15] Blévin, T. et al. 2014, "Development of industrial processes for the fabrication of high efficiency n-type PERT cells", *Solar Energy Mater. & Solar Cells*, Vol. 131, pp. 24–29.

[16] Böscke, T. et al. 2013, "Bifacial n-type cells with >20% front-side efficiency for industrial production", *IEEE J. Photovolt.*, Vol. 3, pp. 674–677.

[17] Lohmüller, E. et al. 2014, "The HIP-MWT+ solar cell concept on n-type silicon and metallization-induced voltage losses", *Proc. 29th EU PVSEC*, Amsterdam, The Netherlands.

[18] Guillevin, A. et al. 2014, "High efficiency n-type metal-wrap-through cells and modules using industrial processes", *Proc. 29th EU PVSEC*, Amsterdam, The Netherlands.

[19] Grunow, P. 2012, "Bifacial modules – Promises and challenges", bifipv-workshop, Konstanz, Germany.

[20] Van Aken, B.B. et al. 2014, "Relation between indoor flash testing and outdoor performance of bifacial modules", *Proc. 29th EU PVSEC*, Amsterdam, The Netherlands.

[21] SEMI PV Group Europe 2014, "International technology roadmap for photovoltaic (ITRPV): Results 2013", 5th edn (Mar.) [http://www.itrpv.net/Reports/Downloads/].

[22] Fertig, F. et al. 2014, "The BOSCO solar cell – A both sides collecting and contacted structure", *physica status solidi (RRL)*, Vol. 8, pp. 381–384.

[23] ERDM Solar/SCHMID Group 2014, "ERDM Solar and SCHMID Group announce the supply agreement for the world's first full GEMINUS bifacial turnkey cell and module manufacturing line with multi bus bar module technology", Press Release (Dec.) [http://www.schmid-group.com/en/press-%2B-news/press-releases/p180/erdm-solar-and-schmid-group-announce-the-supply-agreement-for-the-worlds-first-full-geminus-bifacial-turnkey-cell-and.html].

[24] Kopecek, R. et al. 2014, "Bifaciality: One small step for technology, one giant leap for kWh cost reduction", *Photovoltaics International*, 26th edn, pp. 32–45.

[25] Lohmüller, E. et al. 2013, "Depletion of boron-doped surfaces protected with barrier layers during $POCl_3$-diffusion", *Proc. 28th EU PVSEC*, Paris, France.

[26] Benick, J. et al. 2012, "Fully implanted n-type PERT solar cells", *Proc. 27th EU PVSEC*, Frankfurt, Germany.

[27] Kiefer, F. et al. 2014, "Influence of the boron emitter profile on V_{oc} and J_{sc} losses in fully ion implanted n-type PERT solar cells", *physica status solidi (a)*, DOI 10.1002/pssa.201431118, pp. 1–7.

[28] Böscke, T. et al. 2014, "Fully ion implanted and coactivated industrial n-type cells with 20.5% efficiency", *IEEE J. Photovolt.*, Vol. 4, pp. 48–51.

[29] Cabal, R. et al. 2009, "Investigation of the potential of boron doped oxide deposited by PECVD – Application to advanced solar cells fabrication processes", *Proc. 24th EU PVSEC*, Hamburg, Germany.

[30] Frey, A. et al. 2014, "N-type bi-facial solar cells with boron emitters from doped PECVD layers", *Proc. 29th EU PVSEC*, Amsterdam, The Netherlands.
[31] Nishimura, S. et al. 2014, "Over 21% efficiency n-type monocrystalline silicon photovoltaic cell with boron doped emitter", *Tech. Digest 6th WCPEC*, Kyoto, Japan.
[32] Rothhardt, P. et al. 2014, "Codiffused bifacial n-type solar cells (CoBiN)", *Energy Procedia*, Vol. 55, pp. 287–294.
[33] Wehmeier, N. et al. 2013, "Boron-doped silicon oxides as diffusion sources for simplified high-efficiency solar cell fabrication", *Proc. 28th EU PVSEC*, Paris, France.
[34] Rothhardt, P. et al. 2012, "Control of phosphorus doping profiles for co-diffusion processes", *Proc. 27th EU PVSEC*, Frankfurt, Germany.
[35] Keding, R. et al. 2014, "$POCl_3$-based co-diffusion process for n-type back-contact back-junction solar cells", *Proc. 29th EU PVSEC*, Amsterdam, The Netherlands.
[36] Lim, B. et al. 2014, "Simplifying the fabrication of n-PERT solar cells: Recent progress at ISFH", *Photovoltaics International*, 26th edn, pp. 46–54.
[37] Barth, S. et al. 2013, "Bifacial solar cells with highly efficient spin-on boron diffusion", *Proc. 28th EU PVSEC*, Paris, France.
[38] Cabal, R. et al. 2014, "20% PERT technology adapted to n-type mono-like silicon: Simplified process and narrowed cell efficiency distribution", *Proc. 29th EU PVSEC*, Amsterdam, The Netherlands.
[39] Lohmüller, E. et al. 2014, "Reverse bias behavior of diffused and screen-printed n-type Cz-Si solar cells", *IEEE J. Photovolt.*, Vol. 4, pp. 1483–1490.
[40] Edler, A. et al. 2014, "Metallization-induced recombination losses of bifacial silicon solar cells", *Progr. Photovolt.: Res. Appl.*, DOI: 10.1002/pip.2479.
[41] Römer, U. et al. 2014, "Ion-implanted poly-Si / c-Si junctions as a back-surface field in back-junction back-contacted solar cells", *Proc. 29th EU PVSEC*, Amsterdam, The Netherlands.
[42] Stradins, P. et al. 2014, "Passivated tunneling contacts to n-type wafer silicon and their implementation into high performance solar cells", *Tech. Digest 6th WCPEC*, Kyoto, Japan.
[43] Feldmann, F. et al. 2014, "Tunnel oxide passivated contacts as an alternative to partial rear contacts", *Solar Energy Mater. & Solar Cells*, Vol. 131, pp. 46–50.
[44] Moldovan, A. et al. 2014, "Simple cleaning and conditioning of silicon surfaces with UV/ozone surfaces", *Energy Procedia*, Vol. 55, pp. 834–844.

About the Authors

Sebastian Mack holds a diploma degree in physics from the University of Jena and a doctoral degree in physics from the University of Konstanz, Germany. For his doctoral thesis he investigated thermal oxidation processes for industrial high-efficiency PERC solar cells at Fraunhofer ISE. Sebastian is currently a postdoctoral researcher in the Thermal Processes / Passivated Solar Cells Group at Fraunhofer ISE, where his interests include high-temperature processing and process development for p- and n-type silicon solar cells.

Elmar Lohmüller studied physics at the University of Tübingen and at Nelson Mandela Metropolitan University, Port Elizabeth, South Africa. He received his diploma degree in 2010 and for his thesis worked at Fraunhofer ISE on the development of p-type MWT-PERC solar cells. Elmar is currently working on his dissertation, focusing on the development of n-type MWT solar cells.

Philip Rothhardt received a master's in physics from Humboldt University of Berlin, and a Ph.D., also in physics, in 2014 from the University of Freiburg, Germany. The work for his doctorate, carried out at Fraunhofer ISE, involved the development and characterization of co-diffusion processes for n-type solar cells.

Sebastian Meier studied physics at the University of Freiburg and at Pierre and Marie Curie University in Paris. In 2014 he received his diploma degree, the thesis work for which was carried out at Fraunhofer ISE on the development of bifacial n-type solar cells based on co-diffusion. He recently began working on his dissertation, focusing on the development of co-diffused bifacial n- and p-type solar cells.

Sabrina Werner studied physics at the University of Freiburg, Germany, receiving her diploma degree in 2011. Since then she has been working in the Photovoltaic Production Technology and Quality Assurance Division at Fraunhofer ISE. Her research interests include the improvement of high-temperature processes and passivated solar cells.

Andreas Wolf studied physics at the Technical University of Darmstadt and at the KTH Royal Institute of Technology in Stockholm. He received his Ph.D. from the Leibniz University of Hanover in 2007. Andreas is head of the Thermal Processes / Passivated Solar Cells Group at Fraunhofer ISE.

Florian Clement received his doctorate in 2009 from the University of Freiburg. He is currently head of the MWT Solar Cells and Printing Technology Group at Fraunhofer ISE, where his research interests include the development of highly efficient pilot-line-processed metal-wrap-through solar cells, as well as the development and evaluation of printing technologies.

Daniel Biro studied physics at the University of Karlsruhe, Germany, and at the University of Massachusetts Amherst, USA. He received his Ph.D. in the field of silicon solar cell diffusion technologies from the University of Freiburg in 2003. During 2004–2005 he coordinated the design and ramp-up of the production-oriented research platform PV-TEC and is currently head of the Thermal, PVD, and Printing Technology / Industrial Cell Structures Department at Fraunhofer ISE.

Enquiries

Fraunhofer Institute for Solar Energy Systems (ISE)

Heidenhofstr. 2
79110 Freiburg
Germany

Tel: +49 (0) 761 4588 0
Email: info@ise.fraunhofer.de

Website: www.ise.fraunhofer.de

Thin Film

News

Hanergy comes under spotlight from WSJ and FT

Both the Wall Street Journal (WSJ) and the Financial Times (FT) newspapers have recently attempted to delve into the financial and business operations of the Hanergy group of companies.

The driver for the scrutiny has been a combination of factors including the fact that its founder and majority shareholder Li Hejun was cited by Forbes as China's fifth richest man. This was primarily attributed to Hanergy's stock valuation (Hanergy Thin Film Power Group) after a massive 300% rise in the share price through 2014.

Interest in Hanergy seems to have been sparked by a detailed research note from renewables analyst Charles Yonts at independent investment firm CLSA, titled "Are they really that good? Hanergy: House of cards or card shark?"

Yonts, like the FT, highlighted that the majority of sales outside Hanergy's hydro-electric business have come from internal sales within the group in relation to its a-Si thin-film equipment sales, yet end product sales have been elusive.

Source: Hanergy

Hanergy has faced media scrutiny following the huge hike in its share price last year.

Hanergy's deals and orders

Hanergy reveals master supply agreement on thin-film products

Hanergy Thin Film Power (HTF) has revealed for the first time the planned thin-film product supply deals signed with Hanergy Group through 2017 for its downstream project business plans.

HTF said that Hanergy Group's master supply agreement to purchase PV modules in each financial year from 2015 to the financial year of 2017 included 1.5GW of a-Si/Si-Ge based thin-film modules.

HTF has been shipping, installing and qualifying equipment and automation systems for Hanergy Group in respect to its first two a-Si production plants through 2014. Hanergy Group is also planning to purchase 70MW of flexible CIGS thin-film modules and 80MW of conventional glass/glass CIGS thin-film modules under the master supply agreement.

Spire wins sun simulator order from Chinese thin-film firm

PV equipment and automation specialist Spire Corporation has secured a 'Spi-Sun Simulator 6013i SLP' order with an unnamed Chinese producer of large-area thin film modules.

Spire noted that the order was placed by a major Chinese thin-film module manufacturer with facilities in Europe, China and the US, which narrows it down to one company, Hanergy Thin Film Power.

The custom-made sun simulator was said to be used to accurately characterize the performance of large-area thin film modules. The design was also said to include an automation system that would allow a test area of 6 meters by 1.3 metres.

The Spi-Sun Simulator 6013i SLP is specifically designed for flexible thin-film substrates, suggesting it is for Hanergy's planned fab in China for CIGS thin-film substrates.

Source: Heliatek

Heliatek is looking to expand into Southeast Asia

Singulus to supply Hanergy CIGS equipment order in 2015

PV equipment specialist, Singulus Technologies, said in early February it had received contractually agreed payments for CIGS thin-film equipment believed to be for Hanergy's planned capacity expansions in China.

Singulus had originally signed an order it said was for €15 million worth of wet-chemical coating processing tools from an unidentified customer in China, later confirmed by the company to be with Hanergy Solar, now known as Hanergy Thin Film Power.

The order was for its second-generation TENUIS II platform used for buffer layer deposition.

Organic PV

Heliatek expanding OPV market opportunities to Southeast Asia

Germany-based OPV substrate manufacturer, Heliatek, has signed a business development agreement with Singapore-based vTrium Energy to grow its market in the region.

Source: Manz

Dieter Manz claims crystalline silicon technology will 'lose out' to CIGS thin-film technology as the market grows.

The organic PV producer is the first company to begin commercialization of large-area OPV solar films and has taken over the mantle of the main producer of OPV substrates since the bankruptcy of US-based Konarka Technologies in 2012.

The company has already established technology partners, such as AGC Glass Europe, and is currently ramping up its production for first reference and pilot projects, according to the company.

Dyesol to pay for novel glass substrate sealing technology

Thin-film OPV firm, Dyesol, is collaborating with Portuguese electrical engineering firm, EFACEC, on a novel laser-assisted, glass frit sealing technology for its solid-state DSC solar cells to provide 20-year plus sealing for its planned perovskite-based commercial PV products.

Dyesol said it would pay EFACEC €500,000 over a 15-month period and based on various development milestones. However, a further payment of €1.7 million over 24 months could be made by Dyesol on successful development of the technology as well as a further €2.8 million payable as a royalty pending the commercialization of the process in Dyesol's proposed solar panels and modules. The company reiterated that it was on schedule to produce demonstration prototype modules in 2016, leading to mass production in 2018.

Heliatek spearheading new BIOPV market

Heliatek has started integrating flexible OPV substrates on a PVC-based membrane used for air dome structures, opening up a new area of building-integrated organic PV (BIOPV), according to the company.

Heliatek said in January it had supplied its 'HeliaFilm' flexible thin-film substrates for a PVC-based membrane air dome in Berlin, Germany, for PARANET, an air dome manufacturer.

According to Heliatek, the substrate is attached with an integrated mounting on the outer shell on 50 square metres, in 2 x 2 metre squares. The total electrical output is 1.4kWp, typically providing around 5% of the annual energy demand of the air dome.

Dyesol confirms technology development partnership with UK's SPECIFIC innovation centre

Thin-film OPV firm, Dyesol has renewed its involvement with Swansea University in Wales and the Sustainable Product Engineering Centre for Innovative Functional Industrial Coatings (SPECIFIC) to develop and commercialize perovskite-based OPV thin-film products.

Dyesol had previously been involved in SPECIFIC with Tata Steel back in 2010, to develop and commercialize liquid-based dye sensitised thin-film coatings and laminates for steel roofing applications. The relationship with Tata Steel goes back to 2007. However, Tata Steel pulled-out of the programme in 2013. Dyesol recently noted in the FY Q1 results that its earlier generation OPV materials had "relatively poor performance in low light conditions" and that the European solar roofing markets were at an early stage of development.

Betting on thin-film

Thin-film will be tech of choice in a 100GW global PV market, says Manz

Dieter Manz, founder of equipment supplier Manz AG, claims that crystalline technology will "lose out" to thin-film as the global solar market grows and gears itself up to much larger scales of production.

Manz believes his company is right to back the growth of thin-film and in particular copper indium gallium selenide (CIGS) technologies for solar, predicting that the scope for cost reduction is greater in CIGS than for competing technologies.

Despite thin-film gaining some mainstream attention as the PV technology of choice for consumer sales through IKEA in Europe, for example, and large-scale solar development coming under fire in some markets such as the UK, which are moving towards increases in rooftop development instead, Manz remains convinced that utility-scale plants remain the biggest market for solar and biggest opportunity for CIGS.

City of Wuxi invests in Siva Power

CIGS thin-film start-up Siva Power has recently raised a total of US$10 million to fund its build of what it claims is the world's highest capacity co-evaporation source, the key tool for its claimed ultra-low cost CIGS modules.

Siva Power was recently awarded US$3 million in funding from the US Department of Energy (DOE) SunShot

Source: First Solar

First Solar has broken its own CdTe cell record with an efficiency of 21.5%.

Initiative to further develop its co-evaporation tool. The start-up is hoping that the construction and demonstration of the co-evaporation tool is the precursor to building its first 300MW CIGS module plant. Siva said that site selection analysis would be done in the US as well as overseas.

One of the new backers in the latest funding round was said to be the City of Wuxi, China, home to former major PV manufacturer Wuxi Suntech, now owned by Shunfeng.

First Solar still strong

First Solar pushes verified CdTe cell efficiency to record 21.5%

First Solar has announced it has set yet another world record for cadmium-telluride (CdTe) PV research cell conversion efficiency, achieving 21.5% efficiency certified at the Newport Corporation's Technology and Applications Center (TAC) PV Lab. According to First Solar the verified efficiency puts the company ahead of its own research cell roadmap.

Demonstrating that production-scale performance is keeping pace with record R&D advancements, First Solar has also announced its commercial modules have passed the Atlas 25+ certification following a series of long-term combined-stress environmental exposure tests. As with other records set in-house by the company, the cells used were said to have been fabricated at its Perrysburg, Ohio manufacturing factory and Research & Development Center using commercial-scale manufacturing equipment.

First Solar completes another half-gigawatt project in California

The 550MW Desert Sunlight project has been completed in California, earning the distinction of being the world's joint largest operational PV power plant. Developed and built by US PV energy provider, First Solar, Desert Sunlight equals the record set by another of First Solar's projects last year, the 550MW Topaz plant, also in California.

Details published by the California Independent System Operator (CAISO) records the two elements of the project as having entered into commercial operation on 5 December 2014. Located in Riverside County, Desert Sunlight is co-owned by NextEra Energy Resources, GE Energy Financial Services and Sumitomo Corporation of America.

Potential-induced degradation of thin-film modules: Prediction of outdoor behaviour

Thomas Weber & **Juliane Berghold**, PI Photovoltaik-Institut Berlin AG (PI-Berlin), Germany

ABSTRACT

The current standards (IEC 61646 and IEC 61730-2, and IEC 62804 draft for c-Si only) are clearly insufficient to guarantee satisfactory long-term stability and energy yield for thin-film modules, given that reports from the field, as well as from laboratory test results (beyond IEC testing), in some cases show significant degradation of IEC-certified modules. Accordingly, thin-film modules can also exhibit degradation effects, such as TCO corrosion and power degradation, because of potential-induced degradation (PID). This paper presents the results obtained for thin-film modules subjected to bias and damp-heat (BDH) conditions in both indoor and outdoor tests. In order to assess module lifetimes for different thin-film technologies with respect to PID, indoor- and outdoor-determined leakage currents are compared and analysed, taking into account weather data and results from accelerated ageing tests. Finally, on the basis of simulations and investigations for different installation locations, module lifetimes are estimated and discussed.

Introduction

Module producers certify their products in accordance with the established IEC 61646 and 61730-2 standards as minimum requirements. These standards, however, are clearly not sufficient, since field and laboratory test results for conditions exceeding the IEC requirements demonstrate in some cases unacceptable degradation of IEC-certified modules.

Potential-induced degradation (PID) is an effect which can be generated in the laboratory by applying negative or positive bias to the modules in the damp-heat test chamber: this will be referred to as a bias and damp-heat (BDH) procedure. The phenomenon of transparent conductive oxide (TCO) corrosion of silicon thin-film modules has been known for a long time and is well documented [1,2]. Degradation processes for all other thin-film technologies under negative BDH conditions have been identified as well [3,4], but they demonstrate different degradation mechanisms and fault patterns.

In general, the term 'PID' is used for c-Si [5] as well as for thin film (TF). However, TCO corrosion is one specific type of PID for TF and refers to visible delamination of the TCO layer (see Fig. 1). The development of a standard test for PID for c-Si is in progress, but no IEC-standard draft has yet been submitted for PID and thin-film technologies. The work reported in this paper aims to support the development of testing procedures for predicting the outdoor behaviour of thin-film modules and ties in with previous work [1–4,6]. However, the test sequence presented here allows a comparison of thin-film modules from different technologies and designs on the basis of their distinct leakage-current behaviours. Leakage currents are therefore measured and investigated in order to analyse their influence on power degradation and to

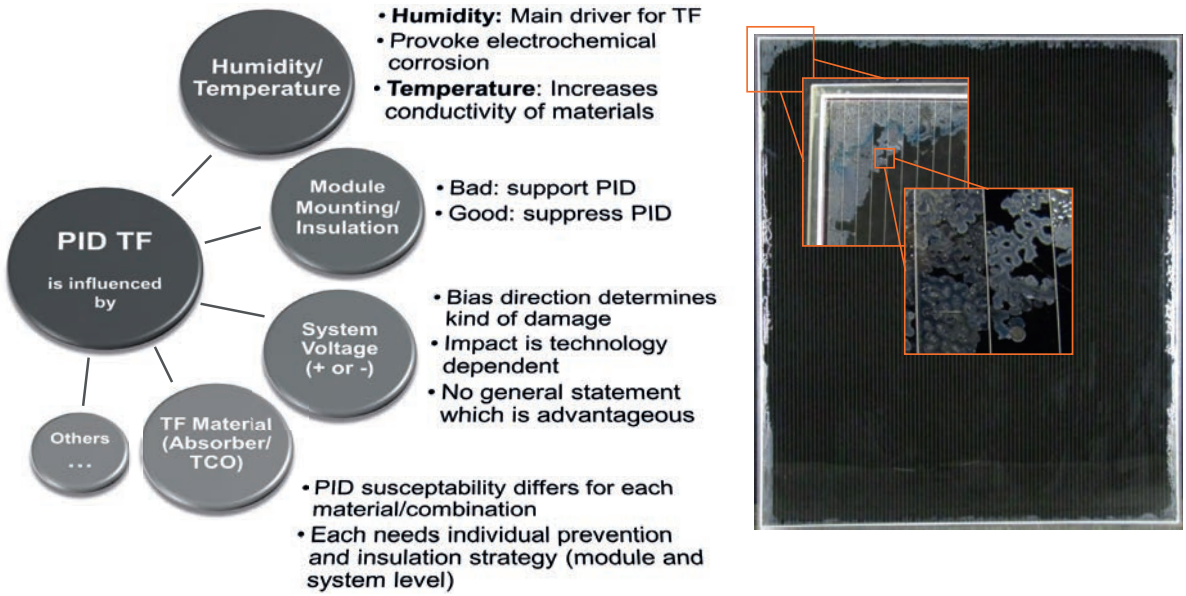

Figure 1. Some of the factors influencing PID of thin-film modules (left). A µc-Si module exhibiting TCO corrosion after a BDH test of duration 1000h and with a bias voltage of –1kV (right).

estimate module lifetimes by means of simulations after an accelerated ageing test. By simulating different weather conditions, it is possible to identify the lifetimes of the tested modules and to draw conclusions with regard to their outdoor behaviour. The main goal of this work can be summarized as the location-dependent prediction of power degradation potential by the determination of individual module leakage currents.

McMahon [7] describes what these failures can look like and presents possible failure mechanisms. Fig. 1 (left) summarizes the main drivers for PID of thin-film modules. Some of these drivers relate to influencing factors such as humidity, temperature and system voltage. Other factors, such as the mounting, have already been investigated [3,8]: it can be stated that a good mounting suppresses PID by keeping leakage currents low and away from sensitive module parts, such as the module edges. Further influencing factors are the choice of material and design – the semiconductor type or the production processes, for example. Fig. 1 (right) shows a µc-Si module that exhibits the well-known TCO corrosion after a 1000h, BDH test with a bias of –1kV; the corrosion begins at the edges of the module and progresses inwards.

Experiment design

In order to investigate in detail the PID effects for thin film and collect the necessary data for the simulation, several thin-film modules were tested in accordance with the test scheme depicted in Fig. 2. Three different thin-film technologies with corresponding industrial modules were investigated: A) CdTe, B) CIGS, and C) µc-Si. All modules were installed in accordance with their specifications in order to simulate 'realistic' leakage-current pathways in the experiment: this entailed the use of a clamp/laminate installation for the CdTe modules, a clamp/frame installation for the CIGS modules, and a back-rail mounting for the µc-Si modules.

The test scheme is divided into a sensitivity test (orange), a degradation analysis (grey) and a simulation (blue); at all stages, the parameters temperature, humidity and voltage were recorded and the distinct module leakage currents measured. Each module type was installed in the prescribed mounting manner and tested under positive and negative system voltages. The outdoor sensitivity test was performed in June 2013 at PI-Berlin's outdoor test site.

The main goal of the sensitivity analysis was to find for each parameter (range) – temperature (T), relative humidity (RH) and voltage (V) – a corresponding leakage current (LC), where $LC_{A,B,C} = f(T,RH,V)$. The I–V curves were recorded before and after each exposure. In contrast to c-Si standard technology, thin-film technologies need special preconditioning procedures, for which commonly agreed procedures and standards for the different technologies do not exist or are still the subject of studies [9,10]. Special preconditioning procedures were conducted, but are not discussed in detail in this paper: further results can be found elsewhere [8].

Next, the degradation analysis was performed using the results of an accelerated ageing experiment in the damp-heat chamber with applied bias voltages. Intermediate measurements, to determine in particular the power degradations, were conducted after 90, 200, 420, 670 and 940h. The outcome of this experiment is the module degradation determined for a certain charge flow (P), where $P_{A,B,C} = f(Q_{A,B,C})$ with

$$Q_{A,B,C}(t) = \int_0^t I_{A,B,C}(t)\,dt \qquad (1)$$

To obtain comparable results for each module, the charge flow $Q_{A,B,C}(P_{80})$ was determined (partly extrapolated) until the point where 80% of the initial power remained. Finally, all the datasets were fed into a simulation to predict the module lifetimes: this is described in a later section. For further details of the complete test procedure see Weber et al. [8].

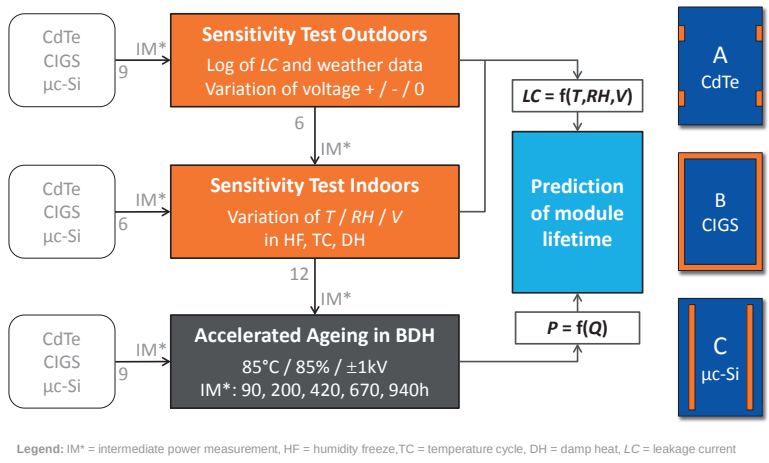

Figure 2. Schematic of the test procedure: sensitivity test (orange), accelerated ageing (grey), and simulation for the prediction of module lifetimes (light blue). Three module technologies (shown far right) were investigated.

Results

All the datasets obtained outdoors were analysed and mean values for the leakage current determined. A data-matrix was created from the results and also incorporated indoor sensitivity test results obtained by LC monitoring in a climate chamber test with varying parameters (outcomes of the orange boxes in Fig. 2). Exemplary values for LC measurements are presented in Fig. 3(b) for a CIGS module of type B biased at –1kV. Fig. 3(a) shows the total number of hours for which a parameter lies within typical ranges during one year in Berlin (for details see the simulation section below). The charge flow for each temperature range is calculated by multiplying LC and time (Equation 1), and can be seen in Fig. 3(c). By summing up all these values for a module, one obtains the specific annual charge flow, which will play an important role in the simulation of module lifetimes.

From an analysis of the daily leakage-current behaviours (not presented here), it was obvious that the highest leakage currents did not occur when the ambient conditions were highest, in other words when absolute humidity was high. The highest leakage currents were measured at times of low absolute humidity (mostly low temperatures with high relative humidity in morning-dew or rain situations). The impact of module-type design or mounting differences, however, cannot be extracted from such results. In general, leakage currents vary significantly, depending on polarity, ambient conditions and module design. (The last of these was not studied here – see Osterwald et al. [2], Gossla et al. [3] and Weber et al. [8]).

Module Temperature [°C]

Relative humidity *RH* [%]

(a) Hours in each parameter range

	< –10	–10-0	0-10	10-20	20-30	30-40	40-50	50-60	60-70	> 70
> 75	4	174	704	694	203	4	-			
65-75	-	7	155	274	237	29	-			
50-65	-	-	65	257	406	159	7	-	-	-
40-50	-	-	1	64	217	193	31	-	-	-
30-40	-	-	-	8	81	127	48	2	-	-
< 30	-	-	-	-	3	8	9	-	-	-

(b) Leakage current [µA], CIGS -1kV

> 75	*0.018*	*0.036*	0.057	0.117	0.084	*1.600*	-			
65-75	-	*0.036*	0.032	0.048	0.069	0.064	-			
50-65	-	-	0.014	0.021	0.034	0.032	0.047	-	-	-
40-50	-	-	0.007	0.009	0.016	0.017	0.021	-	-	-
30-40	-	-	-	0.004	0.008	0.011	0.012	0.017	-	-
< 30	-	-	-	-	0.004	0.005	*0.006*	-	-	-

(c) Transferred charge [As]

> 75	0.000	0.023	0.143	0.292	0.062	0.023	-			
65-75	-	0.001	0.018	0.047	0.059	0.007	-			
50-65	-	-	0.003	0.019	0.050	0.019	0.001	-	-	-
40-50	-	-	0.000	0.002	0.013	0.011	0.002	-	-	-
30-40	-	-	-	0.000	0.002	0.005	0.002	0.000	-	-
< 30	-	-	-	-	0.000	0.000	0.000	-	-	-

Time *t* [hours] × Current *LC* [µA] = Charge *Q* [As]

Figure 3. Illustration of charge calculation: (a) number of hours for which each temperature vs. relative humidity parameter range prevails for a statistical year in Berlin; (b) measured leakage currents (from sensitivity tests) representative of a CIGS module, indicated as mean values for each parameter range; (c) charge for each parameter range, calculated by multiplying time in (a) and current in (b).

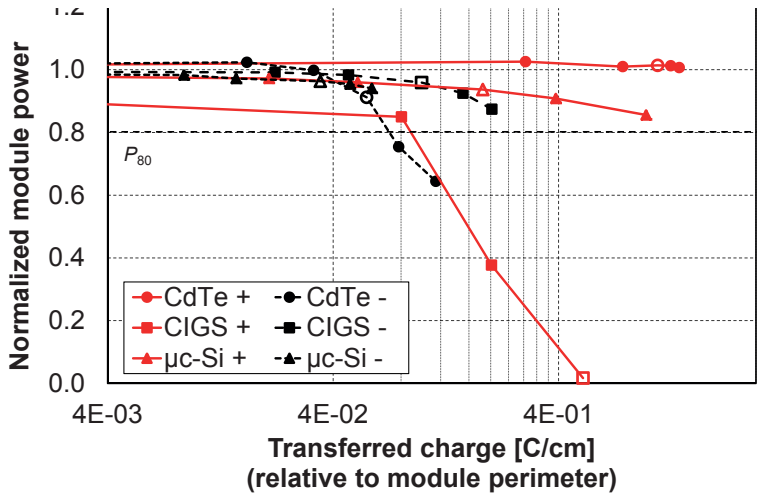

Figure 4. Degradation behaviour of the CdTe, CIGS and µc-Si modules tested in BDH conditions, as a function of the transferred charge relative to the module perimeter. One set of modules was tested under positive bias (red), the other under negative bias (black). Empty symbols indicate measurements after 420h.

The next step in the procedure was the determination of the degradation behaviour in an accelerated ageing test (see grey box in Fig. 2). The results are presented in Fig. 4 for modules tested in BDH only, and the power measurement was performed with no preconditioning. The graph shows the power drop as a function of the transferred charge flow. Also indicated is the P_{80} line, which represents a relative power of 80% of the initial value. Modules tested under positive voltages are labelled in red, and negative ones in black. Table 1 summarizes the power drops for each module after each resolved intermediate measurement time.

It is obvious that CdTe modules of type A with a positive bias (circles) remain unaffected, despite a high charge transfer; the same type under a negative bias degrades by 25% after 680h. CIGS modules of type B (squares) degrade slowly under a negative bias (13% after 940h), but very quickly under a positive bias (15% after 90h). The µc-Si modules of type C (triangles) are the most stable ones under both conditions: these modules degrade 14% after 940h under a positive bias, and 6% after 940h under a negative bias.

Comparing the results of one module type with another is difficult when the actual field degradation and leakage-current behaviour are excluded. As a consequence, it is not possible to derive the actual impact in the field for degraded modules. To do that, it is suggested to simulate the results of $P(Q)$ from Fig. 4 with the actual leakage currents measured in the field, as described in the next section. A particular value is therefore necessary – one which correlates the outdoor leakage currents (sensitivity tests: orange boxes in Fig. 2) with the leakage currents of the accelerated test (BDH test: grey box in Fig. 2). The interpolated and extrapolated $Q(P_{80})$ values representing the amount of charge up to the point where 80% of initial power remains were determined from the graph in Fig. 4 and are listed in Table 2.

	90	200	430	670	940
CdTe +	3%	1%	1%	1%	1%
CIGS +	–15%	–62%	–98%	–	–
µc-Si +	–3%	–4%	–6%	–9%	–14%
CdTe –	2%	0%	–9%	–25%	–36%
CIGS –	–1%	–2%	–4%	–7%	–13%
µc-Si –	–2%	–3%	–4%	–5%	–6%

Table1. BDH degradation in % after *x* hours.

Type	CdTe +	CdTe –	CIGS +	CIGS –	µc-Si +	µc-Si –
$Q(P_{80})$ [C/cm]	2.147	0.071	0.093	0.255	1.410	0.155

Table 2. Interpolated and extrapolated $Q(P_{80})$ values representing the amount of charge up to the point where 80% of initial power remains.

Among other factors, the results are influenced by the preconditioning before a power determination. Fig. 5 shows the results for the investigation of the influence of performing a preconditioning (PC) procedure. The results are shown for the case of CIGS modules of type B differing in two parameters. The first parameter is the use of a PC procedure, for which a combined light-soaking and pre-current-soaking method was used. The solid line in Fig. 5 indicates a PC was performed, whereas the dashed line means there was no PC (i.e. the module was fresh from the production line). The second parameter is the bias voltage of the accelerated ageing experiment. The results show that the preconditioning improves the power measurement by up to 12% (CIGS –: black line) and 40% (CIGS +: red line) for degraded modules. For the positive-biased module, the improvement increases with the level of degradation.

Simulation of module lifetimes

Simulations were carried out using a simple model. The assumption is that the PID and individual leakage-current behaviour of a thin-film module are correlated with its degradation in outdoor and indoor tests. Other degradation mechanisms, such as material degradation, are neglected.

The outdoor and indoor leakage currents determined under certain conditions were referenced to different parameter ranges in order to simulate the leakage currents over a whole year at different locations (for illustration of this step see Fig. 3). Weather data for Tokyo (Japan), Kuala Lumpur (Malaysia), Tucson (USA) and Berlin (Germany) were analysed for the parameter ranges shown in Figs. 3 and 6. The graphs in Fig. 6 show a relative distribution of the temperature and relative humidity; they were generated from the Meteonorm database and based on monthly values (station data), which were calculated for hourly values of all parameters using a stochastic model [11]. To obtain the module temperature T_{Module} from the outdoor temperature $T_{Outdoor}$, the following linear dependence was used:

$$T_{Module} = T_{Outdoor} + k * \frac{Irradiance}{Irradiance_{STC}} \quad (2)$$

where the irradiance at standard test conditions (STC) is 1000W/m^2, and k is a constant factor, which depends on the module installation set-up (k = 20°C for free standing, k = 30°C for roof integration with ventilation, k = 45°C for roof integration without ventilation). In this case, a free-standing

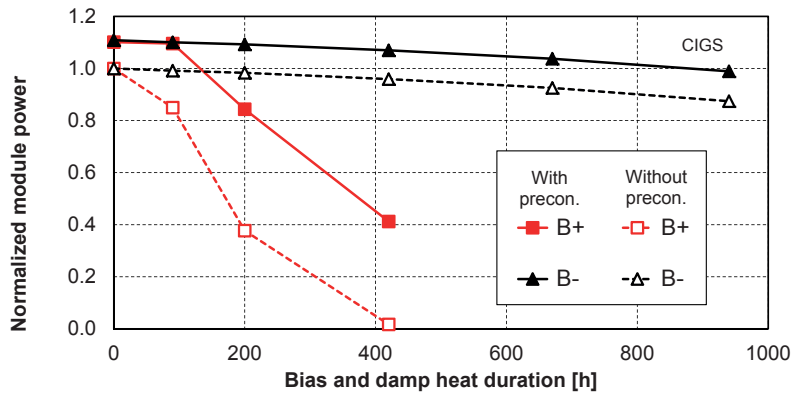

Figure 5. Power measurements for CIGS modules of type B with positive and negative PID-bias voltages, showing that module power can be influenced by preconditioning.

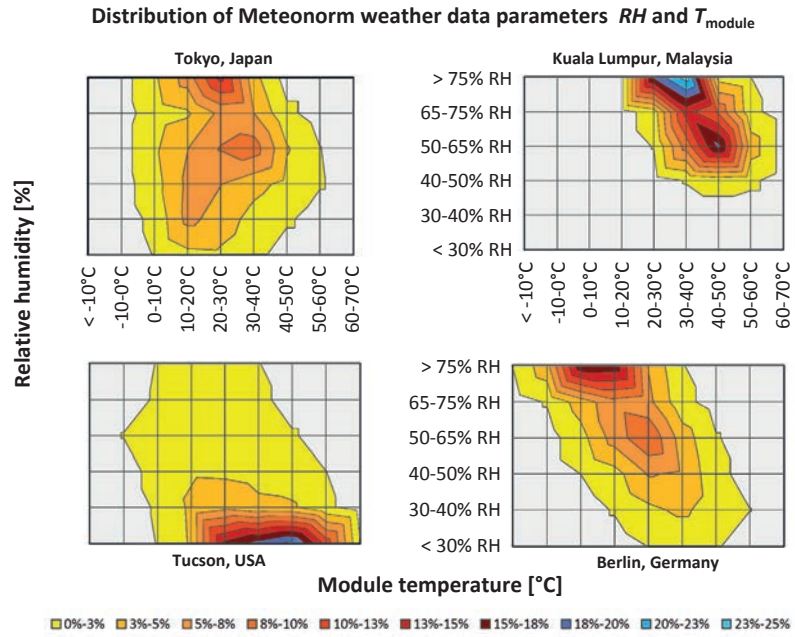

Figure 6. Meteonorm weather data analysed for Tokyo (Japan), Kuala Lumpur (Malaysia), Tucson (USA) and Berlin (Germany), showing the relative distribution of the temperature vs. humidity parameter ranges of interest.

plant was simulated [12]. It is only during the daytime that the modules operate under voltage and that leakage currents arise; therefore, only values with global irradiances above 5W/m^2 can be chosen, and the corresponding frequencies of occurrence allocated to the different parameter ranges.

To obtain the module lifetime (*LT*), the charge flows under +/– BDH conditions are divided by the annual charge flow Q_{annual} calculated from the weather and leakage-current data:

$$LT = \frac{Q(P_{80})}{Q_{annual}} \quad (3)$$

where Q_{annual} is determined from the outdoor-measured leakage currents, complemented by indoor-measured leakage currents under damp-heat, humidity–freeze and thermal-cycling conditions.

Fig. 7 summarizes the results of the simulation of lifetimes for the A, B and C module types under positive and negative bias conditions. In Fig. 7 (right) a classification of the results for evaluation purposes is suggested. For locations with a dry climate, such as Tucson, all investigated module types are very stable (LT >> 25 years), as Fig. 7 (left) demonstrates. CdTe + and µc-Si + are stable in all simulated locations, but short lifetimes (LT < 25 years) are indicated for CdTe – and µc-Si –. A humid and warm place, such as Kuala Lumpur, does not appear to be a suitable place to install the CIGS +/–, CdTe – and µc-Si – module types, whereas warm and dry climates seem to be very suitable for thin films from the PID point of view.

If the degradation results from the accelerated ageing test are compared with the simulated lifetimes, interesting results are obtained. Although the investigated CIGS module type degrades considerably and rapidly under a positive

Module	PID Module Lifetime (LT) [years] (module LT may be limited by other mechanisms)			
	Kuala Lumpur	Berlin	Tokyo	Tucson
CdTe +	83	166	183	362
CIGS +	9	41	37	127
µc-Si +	51	135	157	1659
CdTe –	3	8	10	31
CIGS –	13	141	77	637
µc-Si –	20	21	39	294

Classification of the Results [years]
LT < 25 → PID critical
25 < LT < 40 → PID likely uncritical
LT > 40 → no PID likely

Figure 7. Simulated module lifetimes with regard to PID for all investigated locations and module types (left), and suggested classification scheme for evaluation purposes (right).

bias, the module lifetime is significantly affected only in Kuala Lumpur, a hot and humid place; the other simulated locations result in long lifetimes. The same scenario can be seen for the µc-Si module type under a positive bias. The µc-Si – module exhibits no perceptible degradation in the accelerated BDH ageing test, although the lifetime simulation results in a 20% degradation in Berlin (after 21 years) and in Kuala Lumpur (after 20 years). If one takes other degradation effects into account this might become critical.

No degradation could be found with CdTe under a positive bias, which correlates to long lifetimes; the same was found for others.

To dramatically improve the effectiveness and reliability of accelerated ageing experiments and/or this simulation, it is necessary to correlate the degradation behaviour $P = f(Q)$ with the actual leakage currents occurring during realistic conditions in the field.

Given the actual problems associated with some TF module types in the field, it is suggested by some technology providers to install off-set boxes (for the application of a positive potential overnight) as a short-term solution in the case of identified PID issues in a solar installation. However, the results presented here might call into question the implementation of such an approach as a 'standard' solution, because it has been shown that not only can PID occur in negative bias conditions but it can also occur in positive bias conditions in certain cases.

"The leakage-current analysis and simulation results revealed a high humidity to be the main driver for PID of thin-film modules."

Conclusion

The results obtained for thin-film modules under BDH conditions in indoor and outdoor tests have been presented. The development of a standard test for PID for c-Si is in progress; however, for thin-film technologies an IEC-standard draft has not yet been submitted.

Leakage currents were measured and investigated in order to analyse their influence on power degradation and to estimate module lifetimes after an accelerated ageing test and simulation. A simple simulation model was presented and enabled the deduction of lifetimes by conducting an accelerated stress test. It is therefore important to determine outdoor leakage currents that are adjusted using results from indoor sensitivity tests for the simulation. Moreover, the simulation allowed lifetimes for different climate conditions to be distinguished. The leakage-current analysis and simulation results revealed a high humidity to be the main driver for PID of thin-film modules. On the other hand, warm and dry climates seem to be less critical for thin films in terms of PID.

The results of accelerated PID tests do not necessarily reflect the PID risk at a certain location (expressed by the module lifetime). For example, although module type C (µc-Si) exhibits negligible degradation under a negative bias in a BDH test, the simulated lifetime for Berlin – corresponding to a 20% power drop in 20 years – could become critical when other degradation mechanisms are taken into account. In contrast, the same module type under a positive bias exhibits heavy degradation in the PID test, but the simulated lifetimes are quite acceptable for moderate latitudes.

To sum up in one sentence, the simulation model developed for a worst-case analysis enables benchmarking, the identification of PID-sensitive modules, the determination of a location-specific suitability of a technology, and a statement to be made regarding the distinct advantage of a positive or negative system voltage.

References

[1] Mon, G.R. et al. 1985, "Electrochemical degradation of amorphous silicon photovoltaic modules", *Proc. 18th IEEE PVSC*, Las Vegas, Nevada, USA, p. 1142.

[2] Osterwald, C.R. et al. 2003, "Electrochemical corrosion of S_nO_2:F transparent conducting layers in thin-film photovoltaic modules", *Solar Energy Mater. & Solar Cells*, Vol. 79, pp. 21–33.

[3] Gossla, M. et al. 2010, "Leakage currents and performance loss of thin film solar modules", *Proc. SPIE*, San Diego, California, USA, Vol. 7773, p. 7773000.

[4] Lechner, P. et al. 2012, "Estimation of time to PID-failure by characterization of module leakage currents", *Proc. 27th EU PVSEC*, Frankfurt, Germany.

[5] Koch, S. et al. 2014, "Prediction Model for Potential Induced Degradation Effects on Crystalline Silicon Cells", *Proc. 29th EU PVSEC*, Amsterdam, The Netherlands.

[6] Weber, T. et al. 2010, "Electroluminescence on the TCO-corrosion of thin-film modules", *Proc. 25th EU PVSEC*, Valencia, Spain.

[7] McMahon, T.J. 2004, "Accelerated testing and failure of thin-film PV modules", *Prog. Photovolt.: Res. Appl.*, Vol. 12, pp. 235–248.

[8] Weber, T. et al. 2013, "Test sequence development for evaluation of PID on thin-film modules", *Proc. 28th EU PVSEC*, Paris, France.

[9] Gostein, M. & Dunn, L. 2011, "Light soaking effects on photovoltaic modules: Overview and literature review", *Proc. 37th IEEE PVSC*, Seattle, Washington, USA.

[10] Ferretti, N. et al. 2014, "Investigation of Preconditioning Procedures for Thin Film Modules", *Proc. 29th EU PVSEC*, Amsterdam, The Netherlands.

[11] Meteotest 2010, Meteonorm Version 6.0 – Handbook Parts I and II, Version 6.120 [http://meteonorm.com/].

[12] Valentin Software 2013, PV*SOL®Expert Version 6.0, "Design and simulation of photovoltaic systems" – Manual [http://www.valentin-software.com/en/news/product-news/release-6-pvsol-expert-6-0].

Acknowledgements

The authors thank the teams of PI-Berlin and PI-Solar for their support and discussions. This study was supported by a grant from the European Union in the European Regional Development Fund under contract number 10147955.

About the Authors

Thomas Weber studied environmental engineering at the University of Applied Science Berlin. He completed his diploma, with a topic of post-annealing treatments of silicon thin-film solar cells, at the Helmholtz Center Berlin. Since June 2008 he has been working as a project manager at PI-Berlin, specializing in TF PID and electroluminescence.

Juliane Berghold is head of the PV Technology and R&D Services business unit at PI Berlin AG. She received her Ph.D. in physical chemistry in 2002 and worked as a research associate on crystalline silicon thin-film technology at Helmholtz-Zentrum Berlin (HZB) until 2006.

Enquiries

Photovoltaik-Institut Berlin AG
Wrangelstr. 100
10997 Berlin, Germany

Tel: +49 30 814 52 64 111
Fax: +49 30 814 52 64 101
Email: weber@pi-berlin.com

PV Modules

Gianluca Cattaneo[1], Antonin Faes[1], Heng-Yu Li[1,2], Federico Galliano[1,2], Maria Gragert[3], Yu Yao[3], Rainer Grischke[3], Thomas Söderström[3], Matthieu Despeisse[1], Christophe Ballif[1,2] & Laure-Emmanuelle Perret-Aebi[1]

[1]CSEM, PV-Center, Neuchâtel; [2]Photovoltaics and Thin Film Electronics Laboratory (PV-Lab), Institute of Microengineering (IMT), Ecole Polytechnique Fédérale de Lausanne (EPFL), Neuchâtel; [3]Meyer Burger AG, Gwatt, Switzerland


79

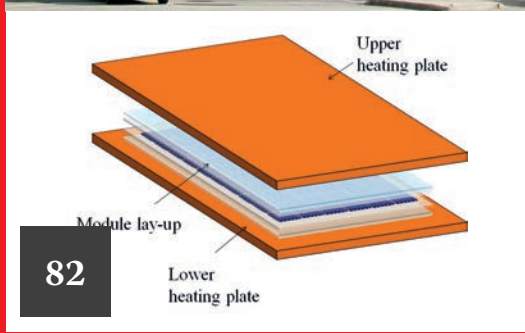

82

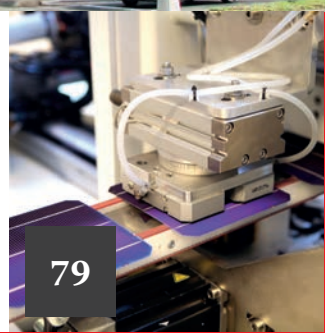
79

News

Trina Solar remains committed to supplying PV modules to US after ITC ruling

Trina Solar has said it will continue to meet demand for its PV modules in the US, despite the US International Trade Commission's (ITC) final determination on anti-dumping and countervailing duties issued in January, which led to the company receiving a final dumping tariff of 26.71% and a final subsidy tariff of 49.79%.

Trina Solar had been a mandatory respondent to both of the investigations regarding China. However the company noted that it expects the combined tariff to be reduced after the US Department of Commerce (DOC) completes its double-counting analysis.

By comparison, Yingli faces 52.13% AD rate and the China wide anti-subsidy of 38.72%. The AD rate for companies not assigned an individual level of tariff will be 165.04%. Taiwanese producers have been given an AD rate of 19.5% with the exceptions of Motech and Gintech who were assigned 11.45% and 27.55% respectively.

Source: Wikimedia Commons/loytoy

US ITC: Trina has remained defiant following confirmation by the commission of the latest round of US solar duties on Chinese imports.

US module news

SolarCity to house Silevo HQ in leased Solyndra factory

US installer and leasing company SolarCity appears to be stepping up its move towards vertical integration, with reports emerging that the company has leased a factory formerly occupied by Solyndra.

The California-based industry leader purchased solar module manufacturer, Silevo, in June last year. At the time, the company said it would open a facility in Buffalo, New York State, that could surpass 1GW production capacity within two years.

SolarCity chairman, Elon Musk and co-founders Lyndon and Peter Rive also said following the acquisition that "one or more significantly larger plants at order of magnitude greater annual production capacity" would follow shortly after.

Astronergy latest module manufacturer to reach new UL fire standards

Thin-film module manufacturer, Astronergy, has announced that it is the latest company to earn the UL1703 Certificate with Type1 fire performance.

The standard for fire performance will be rolled out nationally from 2016 with California having introduced it a year early. The certificate is necessary for a PV system to be given a Class A fire rating, now a requirement in California.

ReneSola, REC and PhonoSolar are among other manufacturers awarded the certificate already.

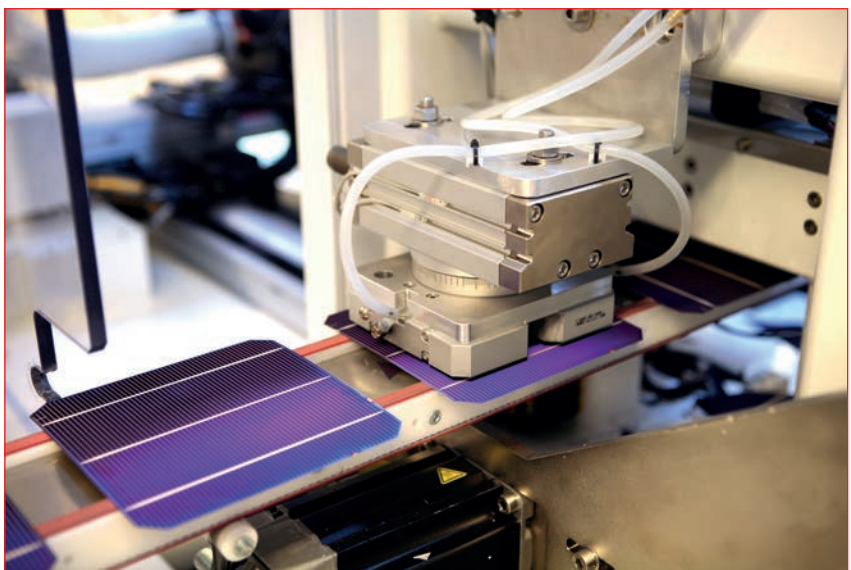

Source: Innotech Solar

Innotech Solar has acquired insolvent distributor, Energiebau Solarstromsysteme.

Mergers and acquisitions

Hanwha SolarOne changing name to Hanwha Q CELLS on merger completion

Hanwha SolarOne has completed the acquisition of Hanwha Q CELLS, which will result in Hanwha Q CELLS adopting the formal name Hanwha Q CELLS Co. Ltd. and trading on the NASDAQ under the symbol HQCL.

Terms of the deal were first revealed in December 2014 when it emerged Hanwha SolarOne would acquire all of its sister company's stock from Hanwha Solar Holdings in what amounts to a merger. The estimated value of the deal is US$1.2 billion. The combined entity will have a 3GW cell manufacturing capacity, which it claims makes it the largest cell producer in the world.

Innotech acquires insolvent Energiebau

Scandinavian-German module manufacturer, Innotech Solar, is to take ownership of insolvent German PV distributor, Energiebau Solarstromsysteme.

The wholesaler will become a wholly

owned subsidiary of Innotech with the new name of Energiebau Solar Power. Details of the transaction have not been disclosed by either company.

Founded in 1983, Energibau filed for insolvency at the end of October 2014 citing difficult market conditions. Innotech said the acquisition would enable it to expand its German and international sales activities through Energiebau's customer base. Energiebau founder and CEO Michael Schäfer said the deal would enable the firm to retain "a majority" of its current jobs.

Finance News

Struggling China Sunergy fails to maintain minimum US$15 million NASDAQ market value

Struggling small cap PV module manufacturer, China Sunergy (CSUN), has failed to comply with a second NASDAQ listing rule after its market value of publicly held shares (MVPHS) fell below the minimum threshold of US$15 million.

CSUN has been loss making since 2011 and has failed to release quarterly financial results since the second quarter of 2014, triggering the first NASDAQ notice of non-compliance. To comply, CSUN must establish a minimum of 10 consecutive business days of compliance with the US$15 million MVPHS within 180 days, a period which started at the end of January. The company last reported sales of US$62.7 million on module shipments of 140MW for the first quarter of 2014. Losses were US$14.6 million.

Shunfeng to post annual profit on increased solar cell and module shipments

China-based PV energy provider, Shunfeng International Clean Energy, expects to report a return to profitability for 2014 on the back of increased solar cell and module shipments and PV power plant electricity generation.

Preliminary figures reported by Shunfeng show solar cell shipments reached 863.4MW in 2014, a 79.7% increase from 480.5MW in the previous year. PV module shipment contributions from subsidiary, Suntech, were said to have reached 663.7MW in 2014, up from only 22MW in 2013, a 2,916.8% increase due to the acquisition of the company from receivership and the restart of module production.

However, module shipments were below previous guidance of 1.3GW to 1.5GW from a nameplate capacity of 2.4GW. Wuxi Suntech had 763MW of modules produced and registered in court filings in 2013.

Japan sales figures

Kyocera's solar module sales revenue weaker than expected

Japanese electronics firm Kyocera Corporation has said that steeper than expected PV module price declines in Japan, coupled to a halt in grid access applications by many utilities, led to solar sales declining in the fourth quarter of 2014.

Kyocera said that within its solar energy business sales decreased in the first nine months of the year, compared with the previous year, despite efforts to expand its PV module product range and reduce overall costs. Module price declines were said to have impacted margins within its Applied Ceramic Products Group, which houses its PV module business unit. The weakness in sales was said to have resulted in the company lowering its overall sales forecast for the financial year.

Panasonic increases HIT PV module sales in Japan

Panasonic reported a small increase in PV module sales in Japan in the third quarter of its fiscal year 2014 financial results. The electronics giant reported sales of its Eco Solutions division, which includes its PV modules business, were up 2% to ¥1,224.3 billion (US$10.4 million) from the prior year period.

Source: JA Solar

JA Solar has shipped over 100MW of modules to London-based solar EPC firm, Solarcentury, for its UK projects.

Source: REC Group

REC Solar has appointed a new chief executive after finalising its takeover by China National Bluestar.

Panasonic described PV module sales in Japan, primarily for the residential market as 'stable'.

Sharp to globalize energy solutions business on waning Japanese sales

Japanese electronics giant Sharp Corporation will streamline its Energy Solutions division, which includes its PV module and sales operations, while pushing its product solutions globally. Sharp reported that its Energy Solutions division fell to a US$14 million loss in its financial year third quarter, due primarily to a decline in sales of solar cells in Japan. Solar cell sales were 349MW in the third quarter, down from 537MW in the prior quarter, a 35.1% decline.

The overall decline in Energy Solutions sales was attributed to falling sales from its recently sold US PV project developer, Recurrent Energy, as well as from both residential and commercial PV business in Japan.

Order news

JA Solar ships 100MW to Solarcentury in 2014

Chinese PV manufacturer, JA Solar, has revealed that it shipped more than 100MW of solar modules to London-based solar developer, Solarcentury, in 2014.

Almost half of the shipped modules will be used at the company's Southwick solar farm, which Solarcentury expects to be connected to the grid before March 2015 in order to benefit from the renewable obligation scheme before it closes to projects above 5MW. The 49MW solar farm will become one of the UK's largest solar farms when it is completed.

WINAICO ships first 48 cell 230W 'HeatCap' modules to Japanese customers

Taiwan-based specialist PV module manufacturer WINAICO said it had starting shipping its recently launched 'HeatCap' modules to Japan.

WINAICO's 48-cell 230W, WST-230M6-H module is claimed to use the world's highest efficiency monocrystalline PERC technology, supplied by Taiwanese merchant cell producers with its in-house-developed, micro-crack-preventing 'HeatCap' technology with SiC (silicon carbide) that is claimed to reduce the risk of micro-crack formation in PERC cells. Module shipment quantities were not disclosed.

Gestamp's 42.5MW project in Honduras to get Trina Solar modules – power gen

Chinese tier-one manufacturer Trina Solar will supply PV modules to 'Marcovia Solar', a 42.5MW solar farm in Honduras which is scheduled to go online during the second quarter of this year. Gestamp Solar, headquartered in Spain, is developing the plant in Marcovia in the southern Choluteca region of the Central American country. Trina Solar will supply 160,000 of its high efficiency PC14-310W modules to Marcovia Solar, Gestamp's first plant in Honduras. The ground-mounted plant will also be fitted with 300 solar trackers and is expected to have an annual output of 93GWh.

Company news

LDK Solar exits bankruptcy proceedings

LDK Solar's chapter 15 bankruptcy proceedings as well as the chapter 11 bankruptcy proceedings in the US have been concluded with the majority of bondholders agreeing to a complex debt for stock swap and a convertible debt scheme due in 2018.

However, LDK Solar remains heavily debt laden with at least US$2 billion owed to a number of Chinese banks. Through two investment vehicles, the billionaire owner of Shunfeng, Zheng Jianming, has almost a 30% stake in LDK Solar.

REC appoints new CEO following Chinese takeover

PV module manufacturer, REC Solar, has appointed a new chief executive, Steve O'Neil. O'Neil will replace the firm's interim CEO, Martin Cooper, who resumes his position as chief financial officer. O'Neil takes the helm at a pivotal time for REC.

Last month, the company's shareholders signed off its planned acquisition by the Chinese conglomerate, China National Bluestar, and concurrent merger with fellow Norwegian firm, the silicon supplier Elkem. O'Neil has previously held the positions including senior vice president, China, and chairman of the TE Connectivity China Business Council at TE Connectivity, a global provider of sensor and connectivity hardware for various industries.

Lamination process and encapsulation materials for glass–glass PV module design

Gianluca Cattaneo[1], Antonin Faes[1], Heng-Yu Li[1,2], Federico Galliano[1,2], Maria Gragert[3], Yu Yao[3], Rainer Grischke[3], Thomas Söderström[3], Matthieu Despeisse[1], Christophe Ballif[1,2] & Laure-Emmanuelle Perret-Aebi[1]

[1]CSEM, PV-Center, Neuchâtel; [2]Photovoltaics and Thin Film Electronics Laboratory (PV-Lab), Institute of Microengineering (IMT), Ecole Polytechnique Fédérale de Lausanne (EPFL), Neuchâtel; [3]Meyer Burger AG, Gwatt, Switzerland

ABSTRACT

In the last few years PV technology has seen continuous improvements, with significant enhancements at the cell and module levels. In addition to the requirement of high efficiency, the long-term reliability of PV modules leads to proposals for innovative module concepts and designs. Meyer Burger has developed a low-temperature wire-bonding technology, known as SmartWire Connection Technology (SWCT), with the aim of offering a cost-effective solution for high-efficiency solar cells while minimizing cell-to-module losses. The introduction of this interconnection design immediately brings new challenges, especially in the selection of an appropriate encapsulant, which must ensure a good processability as well as the required long-term module reliability. The compatibility of the most cost-effective types of encapsulant currently available on the market was analysed in the study reported in this paper. Thermoplastic polyolefin encapsulants with water absorption less than 0.1% and no (or few) cross-linking additives have proved to be the best option for long-lasting PV modules in a glass-glass (GG) configuration. The development of a laminator having a symmetrical structure (two heating plates without any vacuum membrane) has also opened the door to fast lamination processes with cycle times under eight minutes.

Introduction

The majority of today's crystalline silicon (c-Si) PV modules are manufactured in accordance with a glass-backsheet (GBS) module lay-up: 3.2–4mm glass at the front and a polymer-based insulating backsheet (Fig. 1(a)). An aluminium frame is applied around the module to increase mechanical stability. The mono- or polycrystalline Si solar cells with busbars (BBs) are electrically connected with tinned copper ribbons using a high-temperature (T > 220°C) soldering process (Fig. 1(b)). The most popular encapsulant for this PV module design has long been (and still is) the copolymer ethylene vinyl acetate (EVA).

This type of module has been operational in the field for over 30 years, and several failures have been discovered, observed and investigated [1–3]. Failure mechanisms are often attributed to moisture penetration into the module through the backsheet and the bulk of the encapsulant. When subjected to water and/or ultraviolet (UV) radiation exposure, EVA decomposes to produce acetic acid, which accelerates metallization corrosion [4,5]. Under outdoor conditions, EVA suffers yellowing, browning and delamination, which cause considerable power loss. Fig. 2 shows a GBS PV module with an EVA encapsulant after 20 years' exposure on the roof of a building in Switzerland. Among the observed failures, there is clear evidence of delamination and yellowing, which lead to a total measured power loss of 15%. Potential-induced degradation (PID) has also been linked to EVA formulation and identified as a critical aspect of PV module system reliability [6].

As a response to the need for longer-lasting and higher-efficiency PV modules, significant improvements have been

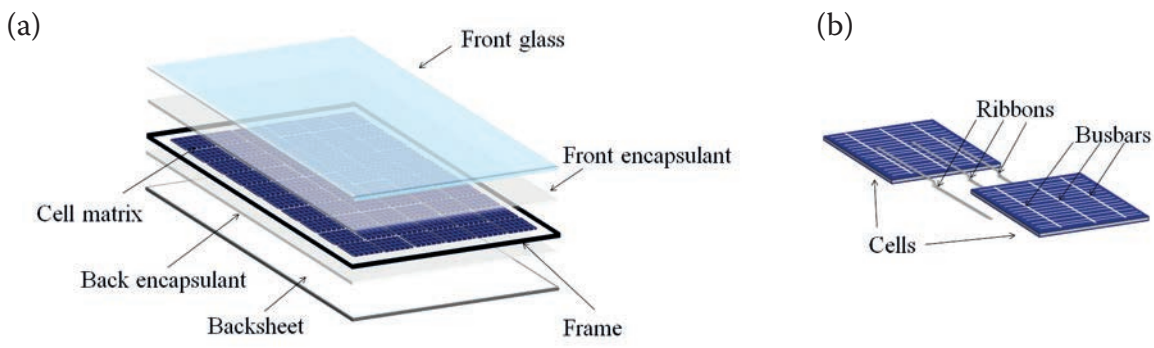

Figure 1. Standard c-Si PV modules: (a) GBS module lay-up; (b) ribbon connection technology for c-Si solar cells with BBs.

made at the cell and module levels in recent years. In addition, even if the dominance of EVA (>80% of the market share) remains currently uncontested, during the last few years (especially with the emerging cell technologies) non-EVA-based products have been proposed as an alternative encapsulant material.

The first step of the study entailed an analysis of the compatibility, in terms of lamination processability, of the most cost-effective types of encapsulant currently available on the market, with a PV module design based on a glass-glass (GG) lay-up and SmartWire Connection Technology (SWCT). The reliability of this specific module design was subsequently demonstrated.

"In terms of mechanical strength, a module design with two glasses of the same thickness is ideal."

PV module design: glass–glass lay-up and SWCT

Glass–glass lay-up

To ensure the mechanical stability of the PV modules and provide efficient protection to the cells and metallization, a GG module configuration is clearly the most appropriate solution (Fig. 3(a)). In terms of mechanical strength, a module design with two glasses of the same thickness is ideal; indeed, this symmetric configuration leads to a zero force in the photovoltaic cell, despite the external load forces (wind, snow) that can stress a PV module during its lifetime. This improved mechanical stability avoids the need for a metallic frame around the module, thus reducing the cost and, furthermore, the risk of PID. Moreover, if the polymer-based backsheet is replaced by a glass, the penetration of moisture into the module is drastically reduced, as it can only penetrate into the module from the edge area [7]. For an encapsulant with high water diffusivity, such as EVA, the typical equilibrium time needed by the water content to reach equilibrium conditions passes from days/weeks in the case of GBS, to years in the case of GG. The use of an encapsulant with a lower diffusivity and/or the use of an efficient edge sealant can further reduce the moisture ingress. This decrease in water vapour ingress has a direct positive impact on PV module reliability compared with that for a standard GBS lay-up.

Recent developments of thin, 2mm tempered glass have made GG design a more competitive solution, compared with 3 or 4mm GG modules (heavyweight) or standard GBS modules. In the case of bifacial cells, GG lay-up is clearly the best solution for exploiting the advantages of such cells in terms of energy yield [8]. In addition, instead of systems with framed modules, less-expensive mounting systems based on innovative techniques can be used

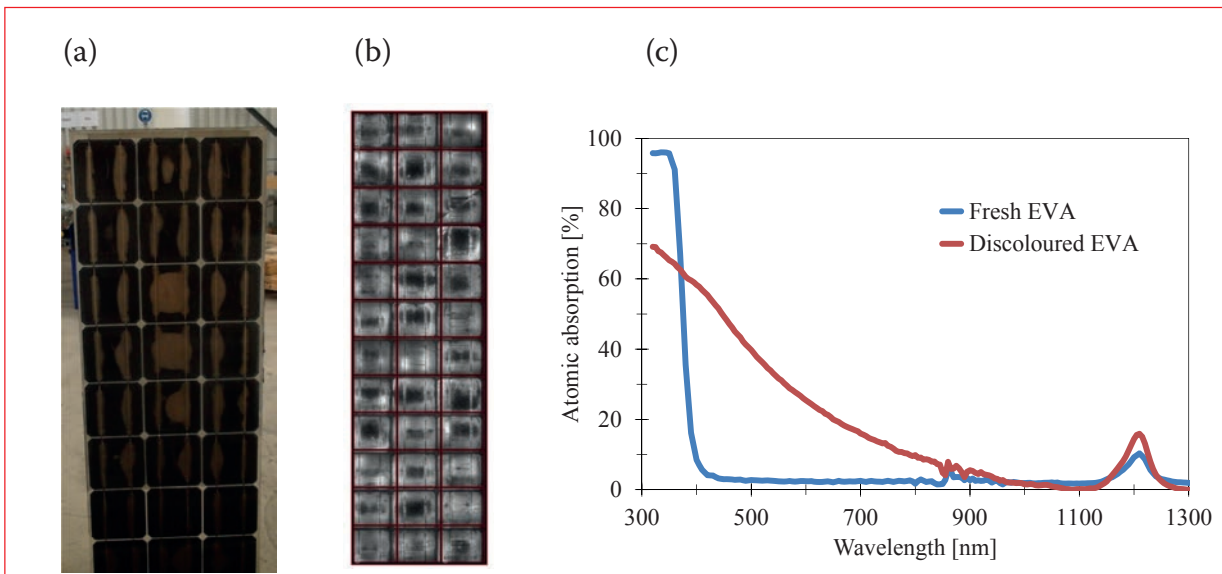

Figure 2. A solar module after 20 years' outdoor exposure on the roof of a building in Switzerland (power loss 15%): (a) delamination and yellowing; (b) electroluminescence image showing metallization corrosion; (c) absorption of the module's discoloured EVA, compared with fresh EVA.

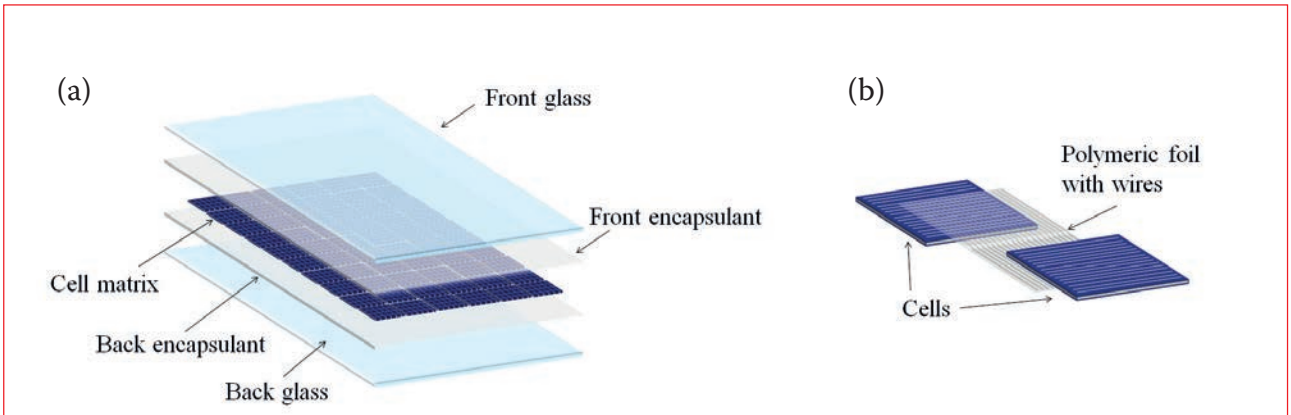

Figure 3. Novel PV module design: (a) GG module lay-up; (b) SWCT for c-Si solar cells without BBs.

[9]. The substitution of a thin glass for a thick one also increases the light transmission and speeds up the heat transfer, allowing a much shorter time for the lamination process.

SWCT

Today, high-efficiency solar cells – such as heterojunction technology (HJT), passivated emitter rear totally diffused (PERT) or interdigitated back-contact technology (IBC) – require special care, as the losses during photogenerated current transportation need to be reduced without sacrificing solar module reliability. SWCT, initially proposed by Day4 Energy [10] and now industrialized by Meyer Burger [11], is an effective alternative to standard BB and ribbon technology for realizing the highest possible benefits from these high-efficiency solar cells.

Typically, 18 copper-based wires, coated with a low-melting-point alloy, are used on both sides of the solar cell; the wires are embedded in a polymeric foil directly applied to the metallized cell (Fig. 3(b)). The soldering process takes place during the lamination process at temperatures typically below 165°C, thereby reducing the stress to the wafer. Compared with standard BBs and tinned copper ribbons, SWCT offers different advantages. The use of multiple wire connections allows the implementation of fine-line metallization on the cell (for the same ohmic loss), thereby reducing shadowing losses and economizing material costs, especially when expensive materials (such as silver paste) are used for metallization [12]. The large number of thin wires, compared with BB technology, is of even greater interest in the case of bifacial cells, for which a higher current (up to 20 to 30% more) has to be extracted, and for which metallic fingers are formed both on the front and on the back side. The cost saving is therefore higher thanks to the reduced resistive losses in the fingers, with the potential of using a low quantity of silver on both sides of the cell.

PV modules based on a module design with a 2mm-GG lay-up and SWCT were constructed using full-square 156mm × 156mm HJT bifacial cells produced by Choshu Industry Corporation [13] (nominal conversion efficiencies over 22% measured with GridTouch contacting technology developed by PASAN [14]). A maximum power of up to 311Wp_{front} (front-side illumination) resulted from module testing (Fig. 4); this value is unquestionably higher than that for standard c-Si cell PV modules. Furthermore, for installation above surfaces with good or high reflectivity, the energy yield of GG bifacial modules (kWh/kWp_{front}) is up to 15–30% higher than the energy yield of standard GBS monofacial modules (kWh/kWp), resulting in a significant reduction in the levelized cost of electricity (LCOE) [8].

> "The energy yield of GG bifacial modules is up to 15–30% higher than the energy yield of standard GBS monofacial modules."

Encapsulants overview

The rapid development of the PV market during the last few years has caused a substantial expansion of the encapsulant material market for photovoltaic applications [15–17].

For GG lamination, **polyvinyl butyral** (**PVB**) is a well-known thermoplastic (non-cross-linked) encapsulant. It has been used for a long time in architecture for safety-glass laminates, as well as in the PV industry for building-integrated photovoltaics (BIPV) and for thin-film technology with a GG configuration. One disadvantage of PVB is that it is very sensitive to hydrolysis because of high water uptake.

The durability of **EVA** is mainly influenced by the additive elements but has been considerably improved in recent years. Many solutions have been presented with regard to the degradation problem of yellowing, but other degradation reactions (acetic acid production) still remain for this type of encapsulant. The use of cross-linking additives in EVA encapsulants also creates issues in terms of both module processing time and material storage.

Liquid silicone demonstrates excellent resistance to oxygen, ozone and UV light, a wide temperature stability range, excellent transparency in the UV-visible range and low moisture uptake. Although very promising as an encapsulant material, silicone is only rarely used (e.g. extraterrestrial applications) owing to its high price and the need for special processing machines.

Encapsulants based on a

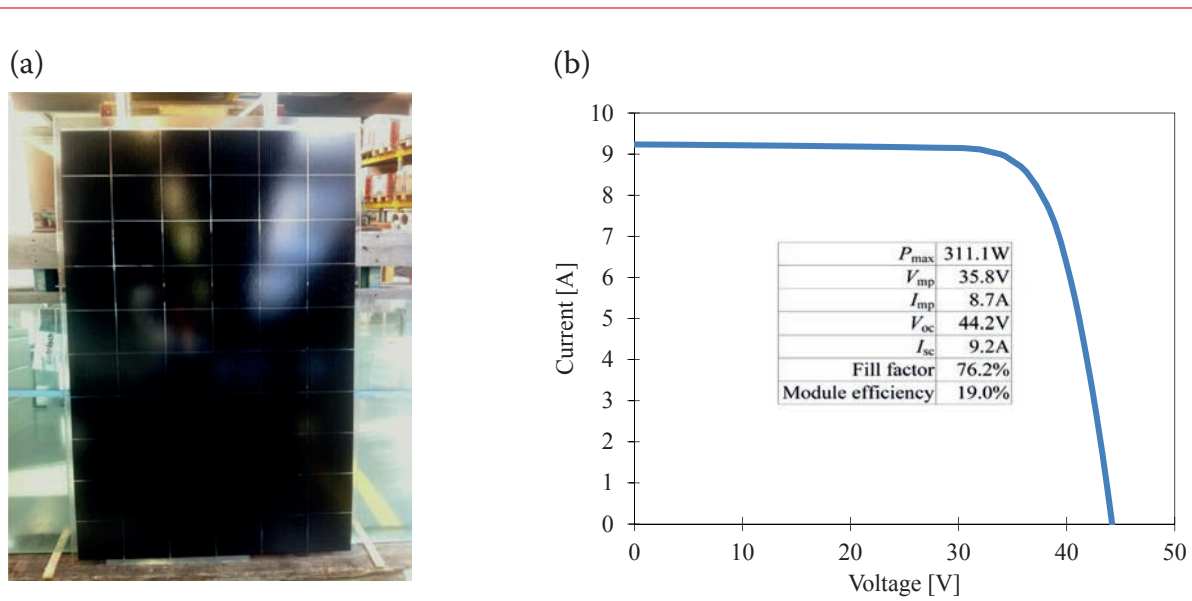

Figure 4. (a) 2mm-GG PV module with SWCT and HJT bifacial cells (CIC) produced by Meyer Burger; (b) measured *I–V* curve at standard test conditions (STC), using a PASAN sun simulator with a black housing to avoid parasitic reflection on the back side of the module.

SOLAR MEDIA

2015 WORLDWIDE EVENTS

Business critical events for the solar industry

SOLAR ENERGY EAST AFRICA

Sarova PanAfric Hotel, Nairobi, Kenya
10-11 March
eastafrica.solarenergyevents.com

SOLAR FINANCE & INVESTMENT

- **London, Grange Tower Bridge Hotel**
  10-11 March
  finance.solarenergyevents.com
- **Singapore (venue tbc)**
  July (date tbc)
  solarenergyevents.com
- **New York (venue tbc)**
  29-30 September
  financeusa.solarenergyevents.com

SOLAR & OFF-GRID RENEWABLES WEST AFRICA

Mövenpick Ambassador Hotel, Accra, Ghana
21-22 April
westafrica.solarenergyevents.com

LARGE-SCALE SOLAR UK

Thistle Bristol City Centre, Bristol, UK
28-30 April
largescale.solarenergyevents.com

DOING SOLAR BUSINESS UK

Platzl Hotel, Munich, Germany
9 June
uk.dsb.solarenergyevents.com

ROOFTOP SOLAR & STORAGE

London, UK
27 June
rooftops.solarenergyevents.com

SOLAR ENERGY UK

The NEC, Birmingham, UK
13-15 October
uk.solarenergyevents.com

SOLAR POWER PORTAL AWARDS 2015

The Vox, Resort World, NEC, Birmingham, UK
13 October
sppawards.solarenergyevents.com

SOLAR ENERGY SOUTHEAST ASIA

Bangkok, Thailand
November
seasia.solarenergyevents.com

FOLLOW US:

@_SolarEnergy

'Solar Energy Events'

BOOK NOW AT seevents.co/pvi-27

thermoplastic polyolefin (**TPO**) or **thermoplastic elastomer** (**TPE**) are now starting to enter the market because of their high electrical resistivity and their hydrolysis resistance. These properties make TPO encapsulants an interesting candidate for long-lasting PV modules.

Thermoplastic silicone elastomers (**TPSEs**) combine silicone performance and thermoplastic processability. The fast curing and the additive-free physical cross-linking make TPSEs suitable for continuous lamination processing.

Belonging to the category of thermoplastic materials, **ionomers** represent a different class of photovoltaic encapsulant, demonstrating good UV stability. No formation of acetic acid has been observed during weathering and a much longer shelf life is achieved, but the production cost is very high.

Compared with standard PV module design based on GBS module lay-up and BB ribbon connection technology, the new PV module design based on a 2mm-GG lamination scheme with SWCT and new high-efficiency solar cells implies a paradigm shift in the encapsulant requirements. Even more than the technical requirements, the main driving force that governs the selection of the encapsulant material suitable for this PV module design is the intense and ever-increasing pressure to reduce module costs. From this point of view, only EVA, PVB and TPO demonstrate a cost that is affordable when considering a promising encapsulant for the PV module design based on 2mm-GG with SWCT for high-efficiency solar cells.

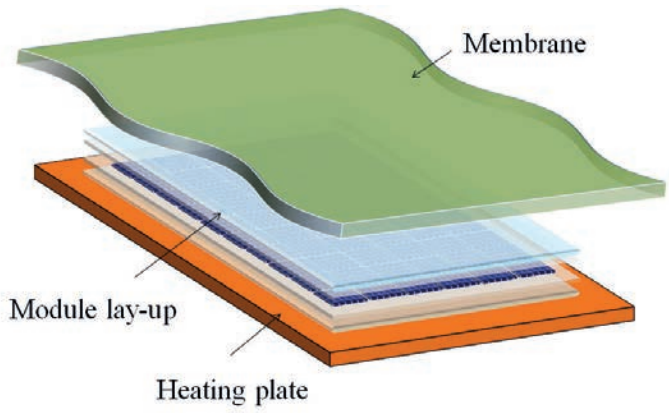

Figure 5. Schematic representation of a standard vacuum-membrane laminator.

Encapsulant	Producer Note
PVB	Outstanding UV transparency
EVA1	Fast cure EVA
EVA2	Highly light transmitting encapsulant
TPO1	Slightly cross-linking TPO
TPO2	Non-cross-linking TPO

Table 1. Selection of the most cost-effective encapsulants tested in terms of compatibility with the lamination process of the novel module design.

Lamination process for the new module design

The lamination of PV modules is most frequently carried out using a vacuum-membrane laminator with a single heating plate (Fig. 5) and a typical process based on three main steps [18].

In the first step, after the module lay-up has been loaded into the laminator, air and other volatile organic compounds (VOCs) are removed by vacuum while the module lay-up is heated until the encapsulant softening

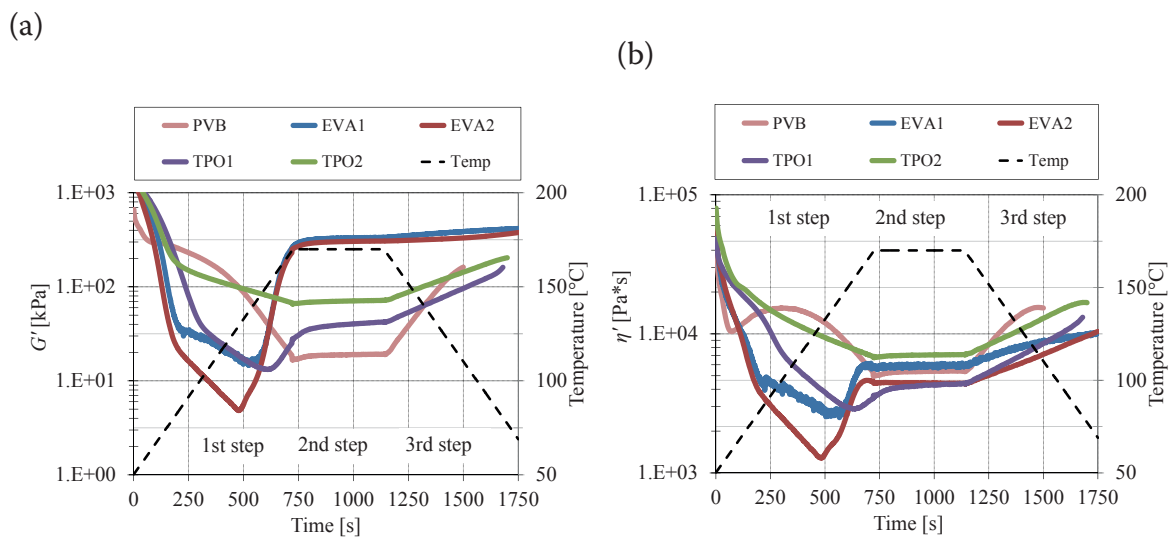

Figure 6. DMA results for the encapsulants in Table 1 (oscillatory frequency = 1Hz; strain = 10%; pressure = 2.5bar) as a function of a given temperature profile: (a) shear modulus (*G'*); (b) viscosity (*η'*).

point is reached. Under the effect of the heat, the VOCs are mainly released from the encapsulant as a result of the chemical reactions of their additives (including impurities). If VOCs are not properly removed during this first step of the lamination process, they could lead to bubbles in the final module [19]. In the second step, the flexible membrane is pressed on the module lay-up to ensure an optimal adhesion between the encapsulant and the other layers of the module lay-up. Finally a controlled cooling step terminates the induced chemical reactions and makes the PV module ready for the next processing steps.

Encapsulants (such as cross-linked EVA) with a large number of additives that cause a significant number of VOCs are not well suited to the lamination of PV modules based on 2mm-GG lay-up and SWCT. In order to promote the interconnection process during the lamination, while keeping the polymeric foil with the wires in good contact with the cells as the encapsulant melts, a slight pressure must be applied during the first vacuum phase. Pressing the module lay-up onto the heating plate results in an improved heat transfer (from the heating plate to the module lay-up), which speeds up the chemical reactions and hence the release of VOCs. In this phase, the applied pressure obstructs the removal of air and VOCs, consequently increasing the likelihood of bubble formation.

With regard to GBS, the lamination of a 2mm-GG module presents more critical aspects because of the stiffness of the glasses. It is well known that encapsulants are viscoelastic, thus exhibiting both elastic (spring-like) and viscous (dashpot-like) behaviour. Knowledge of how the elastic modulus and viscosity of an encapsulant under pressure vary with the temperature helps in choosing which encapsulant is more suitable for the lamination of a 2mm-GG PV module.

The complex shear modulus ($G^* = G' + iG''$) and the complex viscosity ($\eta^* = \eta' - i\eta''$) for a polymer material can be calculated using dynamic mechanical analysis (DMA); here, the quantities G' and η'' are a measure of the energy storage portion, while G'' and η' are a measure of the energy loss portion [20]. For a selection of the most cost-effective encapsulants (Table 1), Fig. 6 shows the measured values of G' and η' as a function of a specific temperature profile resembling the temperature variation during a standard lamination process.

The PVB encapsulant demonstrates a full thermoplastic behaviour, with both G' and η' following the temperature profile.

For the two EVA encapsulants, G' and η' quickly reach a minimum at approximately 125°C (melted encapsulant); they then increase significantly, indicating the initiation of the cross-linking process. The formation of a cross-linked network implies an elastic-like material behaviour (high value of G') that is maintained when the temperature goes down.

The two TPO encapsulants yield significantly different behaviours. The G' and η' profiles of TPO1 resemble those of the two EVA encapsulants, with cross-linking around 150°C; however, a reduced elastic behaviour (low value of G') during the second step of the lamination process is observed. In the case of the TPO2 encapsulant, G' and η' are instead closer to the thermoplastic trend of PVB, but with a higher value of G' (more elastic-like behaviour) during the second step of the lamination process.

In a 2mm-GG configuration, the flowing of the encapsulant into the space between the cells is strongly related to its viscous properties during the lamination process. Encapsulants with a high viscosity (in the first step of the lamination process), such as PVB and TPO2, need more time to flow and fill the gaps between the cells. Any remaining unlaminated patches (incomplete melting of the encapsulant) between the cells might then lead to a delamination issue. To avoid this issue, process times of over 30–40 minutes are necessary with these encapsulants.

On the other hand, the use of encapsulants that exhibit low viscosity and low elastic behaviour (e.g. TPO1) may cause, in a 2mm-GG configuration, other issues relating to excessive compression of the edges of the glasses. During the lamination process, the encapsulant may flow out as the membrane bends down the edges of the top glass (Fig. 7(a)). The difference in GG laminate thickness measured at the centre of the first cell close to the edge (d_1) and at the glass edges (d_2) can also be up to 0.8–1.0mm after the lamination process (Fig. 7(b)). The compression of the edges causes glass breakage when the module is stressed during thermal cycles. Using a frame of the same thickness as the GG lay-up or taping the edges of the module before lamination helps in reducing this effect but complicates the lamination process.

To avoid the issue of unlaminated patches between the cells, as well as the issue of edge compression, without the inconveniences of long lamination processes and/or using taping or a frame, a laminator with a symmetrical structure (two heating plates without any vacuum membrane) like the one recently developed by Meyer Burger can be employed for the lamination of a PV module with a 2mm-GG lay-up and SWCT (Fig. 8). The advantages of such a laminator concept lie mainly in the fact that with two heating plates, the PV module lay-up is heated symmetrically from the top and the bottom sides, resulting in a faster heat transfer towards the encapsulant. The

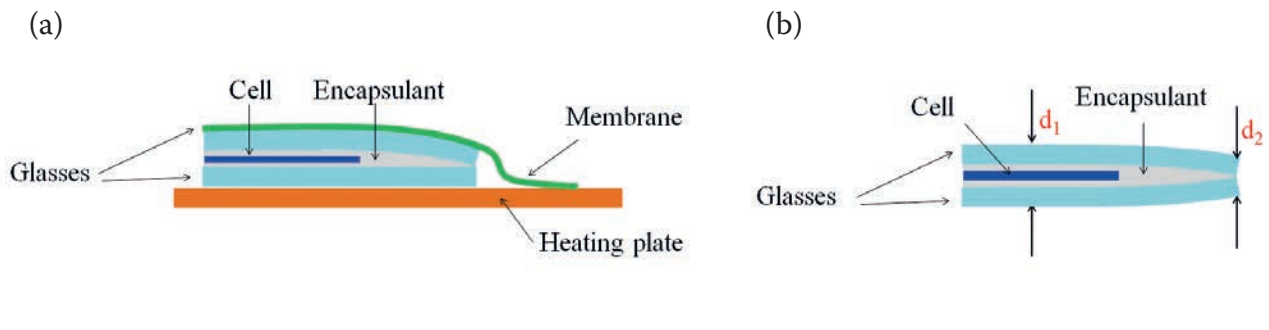

Figure 7. (a) Edge compression in 2mm-GG laminate for encapsulants with low viscosity and using a vacuum-membrane laminator; (b) difference in thickness of the 2mm-GG laminate at the centre of the first cell close to the edge and at the glass edges.

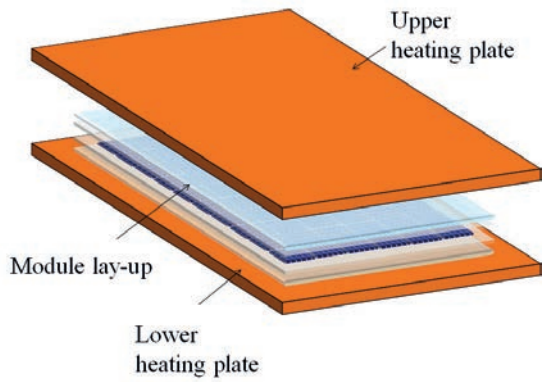

Figure 8. Schematic representation of a symmetrical laminator for GG PV module production.

Encapsulant	WVTR [g/(m²·24h)]	Water absorption [%]
PVB	>25	~0.5
EVA	15–25	~0.3–0.5
TPO	<5	<0.1

Table 2. Typical WVTR and water absorption for different types of encapsulant.

	GG-TPO	GG-EVA	GBS-EVA
ΔP_{max}	–0.4%	–19.5%	–42.0%
ΔI_{sc}	–0.7%	–1.5%	–25.0%
ΔV_{oc}	0.3%	–1.3%	0.0%
ΔFF	0.0%	–16.8%	–17%

Table 3. DH test results for a GG module (SWCT) laminated with TPO, compared with GG and GBS modules (ribbon connection technology) laminated with EVA.

encapsulant flows rapidly between the cells, and a GG PV module without unlaminated patches can be obtained within a short process time for high-viscosity encapsulants as well.

"To avoid the issue of unlaminated patches between the cells, as well as the issue of edge compression, a laminator with a symmetrical structure can be employed."

A process time under eight minutes in a single chamber GG laminator has been obtained by Meyer Burger for a 2mm-GG PV module based on SWCT using TPO1. Moreover, because the pressure is applied by the two metallic heating plates, the edge compression, without using any frame or tape, is kept lower (in the range 0.4–0.6mm) compared with the values observed in a membrane laminator (up to 1mm). The combination of such a laminator with a non-cross-linked (or only slightly cross-linked) TPO is therefore the appropriate solution for the lamination of PV modules based on a 2mm-GG lay-up and SWCT.

The investment costs (normalized per generated MW after seven years of operation) of 2mm-GG PV modules with a symmetrical laminator have been estimated to be up to 30% lower than the costs of using a standard vacuum-membrane laminator, and will be competitive with the investment costs of standard GBS modules using a standard laminator.

Reliability of GG module design

As stated earlier, an important factor influencing a PV module's reliability is the moisture ingress into the module. Even if humidity ingress is drastically reduced in a GG configuration, encapsulants with low water diffusivity and absorption are preferable for long-lasting PV modules. Water vapour transmission rate (WVTR) and water absorption values for the most cost-effective encapsulants available on the market are presented in Table 2 [21–24].

From the data listed in Table 2, for improving module reliability TPO encapsulants are therefore the more promising materials compared with EVA and PVB, as they demonstrate low values for both WVTR and water absorption. In particular, low values of water absorption are essential for preventing corrosion mechanisms that can be activated by the presence of additives (including impurities) in the encapsulant [25]. For the same reason, non-cross-linked (or only slightly cross-linked) TPO is also more promising than highly cross-linked EVA.

In damp-heat conditions (DH: 85°C, 85% RH), GG PV modules (incorporating HJT cells) with SWCT and a TPO encapsulant (TPO1 in Table 1) endure 7000h (seven times the IEC test standard) without noticeable power degradation. In contrast, PV modules (standard ribbon connection technology) laminated with EVA encapsulant (EVA1 in Table 1) for GG and GBS lay-ups exhibit power losses of 19.5% and 40%, respectively, after the same length of time in DH conditions (Table 3).

An electroluminescence analysis revealed degradation due to moisture ingress and corrosion of the cells for the module with the EVA encapsulant, while no degradation issues were observed for the module with the TPO encapsulant (Fig. 9). The lower power loss of the GG module with EVA (GG-EVA) compared with that of the GBS-EVA module is proof of the improvements realized by replacing the polymer-based insulating backsheet with a glass. However, it is only with the use of TPO encapsulants with low water absorption and no (or few) cross-linking additives that very long-lasting PV modules can be produced.

GG PV modules (incorporating HJT cells) with SWCT and TPO encapsulant (TPO1 in Table 1) also achieve successful results in extended thermal-cycling tests (TC: –40°C/+85°C), with a power output degradation of only 2.5% after 800 cycles (eight times the IEC standard) (see Table 4).

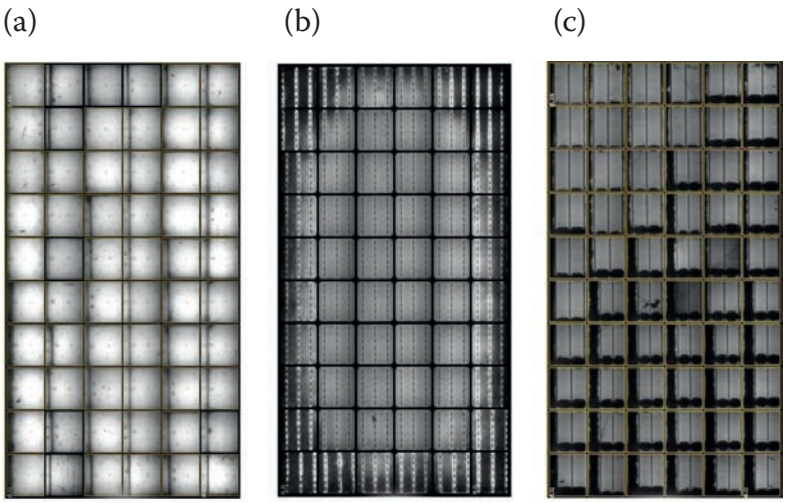

Figure 9. Electroluminescence analysis after DH: (a) GG module (SWCT) laminated with TPO; (b) GG module with ribbon connection technology laminated with EVA; (c) GBS module with ribbon connection technology laminated with EVA.

	TC200	TC600	TC800
ΔP_{max}	–0.4%	–1.5%	–2.6%
ΔI_{sc}	–0.4%	0.0%	0.7%
ΔV_{oc}	0.1%	0.5%	0.8%
ΔFF	–0.5%	–2.2%	–3.4%

Table 4. Thermal-cycling test results for a GG module (SWCT) with a TPO encapsulant.

The good results obtained for extended DH and TC testing substantiate the high reliability of PV modules based on a module design with GG and SWCT when a slightly cross-linked TPO encapsulant (TPO1 in Table 1) is used. Moreover, the lower volume resistivity of TPO encapsulants ($\rho v = 10^{14}$–$10^{17}\Omega cm$, compared with $\rho v = 10^{14}\Omega cm$ for EVA) also guarantees lower PID [26,27]. The cross-linking additionally offers an increased resistance to long-term creeping of the encapsulant at high service temperatures.

"In combination with bifacial HJT cells, the novel module design enables PV modules with a maximum power of up to 311Wp to be obtained."

Conclusions

A novel high-efficiency and long-lasting PV module design based on a thin, 2mm-GG encapsulation scheme and SWCT has been presented. In combination with bifacial HJT cells, the novel module design enables PV modules with a maximum power of up to 311Wp to be obtained. As well as high power, the bifaciality of such a module would produce a 10–30% higher energy yield.

Non-cross-linked (or slightly cross-linked) TPO encapsulants yield the best results (no bubbles, limited edge compression and a short process time) with regard to processability of the GG module design when a symmetrical laminator is used. Thanks to the high-reliability properties of TPO encapsulants (low water absorption and small number of additives), more-reliable PV modules passing extended IEC tests (7000h in DH and 800 cycles in TC) can be obtained.

Acknowledgements

The authors thank the Swiss Commission for Technology and Innovation (14567.1 PFIW-IW project), the Swiss Federal Office of Energy (Swiss Inno-HJT project), the European Union's Seventh Programme (608498 HERCULES project) and Choshu Industry Corporation for their support.

References

[1] IEA-PVPS 2014, "Review of failures of PV modules", Report T13-01.
[2] Chaberlin, C.E. et al. 2011, "Comparison of PV module performance before and after 11 and 20 years of filed exposure", *Proc. 37th IEEE PVSC*, Seattle, Washington, USA.
[3] Jordan, D.C. et al. 2013, "Photovoltaic degradation rates – An analytical review", *Prog. Photovolt.: Res. Appl.*, Vol. 21, No. 1, pp 12–29.
[4] Kempe, M.D. et al. 2007, "Acetic acid production and glass transition concerns with ethylene-vinyl acetate used in photovoltaic devices", *Solar Energy Mater. & Solar Cells*, Vol. 91, No. 4, pp. 315–329.
[5] Ketola, B. et al. 2011, "Degradation mechanism investigation of extended damp heat aged PV modules", *Proc. 26th EU PVSEC*, Hamburg, Germany, pp. 3523–3528
[6] Berghold, J. et al. 2010, "Potential induced degradation of solar cells and panels", *Proc. 25th EU PVSEC*, Valencia, Spain, pp. 3753–3759.
[7] Kempe, M.D. 2006, "Modeling of rates of moistures ingress into photovoltaic modules", *Solar Energy Mater. & Solar Cells*, Vol. 90, pp. 2720–2738.
[8] Kopecek, R. et al. 2014, "Bifaciality: One small step for technology, one giant leap for kWh cost reduction", *Photovoltaics International*, 26th edn, pp. 32–45.
[9] Schletter 2012, OptiBond Product Sheet [available online at http://www.schletter.de/files/addons/docman/solarmontage/produktblaetter/OptiBond_-_product_sheet_V5_I400051GB.pdf]
[10] Schneider, A. et al. 2006, "Solar cell efficiency improvement by new metallization techniques – The Day4 electrode concept", *Proc. 4th IEEE WCPEC*, Waikoloa, Hawaii, USA, pp. 1095–1098.
[11] Söderström, T. et al. 2013, "Smart Wire Connection Technology", *Proc. 28th EU PVSEC*, Paris, France, pp. 495–499.
[12] Faes, A. et al. 2014, "SmartWire solar cell interconnection technology", *Proc. 29th EU PVSEC*, Amsterdam, The Netherlands, pp. 2555–2561.
[13] Kobayashi, E. et al. 2014, "Rear-emitter silicon heterojunction solar cells cerium oxide-doped indium oxide", *Proc. 29th EU PVSEC*, Amsterdam, The Netherlands, pp. 472–474
[14] Bassi, N. et al. 2014, GRID^{TOUCH}: Innovative solutions for accurate

IV measurements of busbarless cells in production and laboratory environments", *Proc. 29th EU PVSEC*, Amsterdam, The Netherlands, pp. 1180–1185
[15] Peike, C. et al. 2013, "Overview of PV module encapsulation materials", *Photovoltaics International*, 19th edn, pp. 85–92.
[16] Oreski, G. 2014, "Encapsulant materials and degradation effects – Requirements for encapsulants, new materials, research trends", IEA Task 13 Open Workshop, Freiburg, Germany.
[17] Kempe, M.D. et al. 2010, "Types of encapsulant materials and physical differences between them", NREL Presentation [available online at http://www1.eere.energy.gov/solar/pdfs/pvrw2010_kempe.pdf].
[18] Lange, F.M. et al. 2011, "The lamination of (multi)crystalline and thin film based photovoltaic modules", *Prog. Photovolt.: Res. Appl.*, Vol. 19, No. 2, pp. 127–133.
[19] Perret-Aebi, L.-E. et al. 2010, "Insights on EVA lamination process: Where do the bubbles come from?", *Proc. 25th EU PVSEC*, Valencia, Spain, pp. 4036–4038.
[20] Menard, K.P. 2008, *Dynamic Mechanical Analysis: A Practical Introduction*. Boca Raton, FL, USA: Taylor & Francis.
[21] Velderrain, M. 2012, "Designing low permeability, optical-grade silicone systems: Guidelines for choosing a silicone based on transmission rates for barrier applications", *Proc. SPIE* (Vol. 8280: Advances in Display Technologies II), San Francisco, California, USA.
[22] Ketola, B. et al. 2008, "Silicones for photovoltaic encapsulation", *Proc. 23rd EU PVSEC*, Valencia, Spain, pp. 2969–2973.
[23] Hülsmann, P. et al. 2014, "Temperature-dependent water vapour and oxygen permeation through different polymeric materials used in photovoltaic-modules", *Prog. Photovolt.: Res. Appl.*, Vol. 22, pp. 415–421.
[24] Swonke, T. et al. 2009, "Impact of moisture on PV module encapsulants", *Proc. SPIE* (Vol. 7412: Reliability of Photovoltaic Cells, Modules, Components, and Systems II), San Diego, California, USA.
[25] Ketola, B. et al., "The role of encapsulant moisture permeability in the durability of solar photovoltaic modules", Dow Corning Presentation [available online at http://www.dowcorning.com/content/publishedlit/The_Role_of_Moisture.pdf]
[26] Nanjundiah, K. et al. 2012, "Improved performance encapsulation film based on polyolefin", *Proc. 27th EU PVSEC*, Frankfurt, Germany, pp. 3384–3387.
[27] Liciotti, C. et al. 2014, "Temperature dependence of encapsulant volumetric resistivity and influence on potential induced degradation of c-Si modules", *Proc. 29th EU PVSEC*, Amsterdam, The Netherlands, pp. 3093–3099

About the Authors

Gianluca Cattaneo obtained his M.Sc. in electronic engineering in 2004 from the Polytechnic of Milan and joined the IMT PV-Lab of EPFL in Neuchâtel in 2012. Since 2014 he has been working in the modules and systems sector at the CSEM PV-Center.

Antonin Faes received a master's in material science from the Swiss Federal Institute of Technology Lausanne (EPFL) in 2005, and then investigated solid oxide fuel cells, for which he received his Ph.D. He joined the CSEM PV-Center in 2012, where he is responsible for the metallization and interconnection of c-Si cells.

Heng-Yu Li received his Ph.D. from EPFL in 2013. Since 2009 he has been working on the encapsulation process and reliability of PV modules at IMT PV-Lab at EPFL. In 2014 he joined the CSEM PV-Center, where he focuses on developing reliable PV modules for various applications, including BIPV.

Federico Galliano obtained his Ph.D. from the University of Florence in 2001. Since 2013 he has been working in the modules and systems sector at the CSEM PV-Center, with a main focus on PV module reliability and building integration.

Maria Gragert received her Diploma in chemistry (with Honours) from the Martin-Luther university Halle-Wittenberg in 2010, and her Ph.D. from Imperial College London in polymerization catalysis. Since 2014 she has been working in the R&D department of Meyer Burger AG, focusing on process optimization for module lamination.

Yu Yao received her Ph.D. from the University of New South Wales (UNSW), with a thesis topic involving crystalline silicon solar cells. She joined Meyer Burger AG in 2014 as an R&D project manager, where she focuses on the development of SmartWire Connection Technology.

Rainer Grischke graduated in 1999 from the University of Kassel, Germany, in electrical engineering, with a main focus on renewable energy. Since 2014 he has been with Meyer Burger AG as a member of the R&D team working on module improvements relating to the novel SmartWire module concept.

Thomas Söderström received a master's in 2005 from EPFL and a Ph.D. in 2009 from the University of Neuchâtel (UNINE, Switzerland), with a focus on thin-film silicon solar cells. He is currently head of the transfer process and innovation module department at Meyer Burger AG, working on the development and industrialization of heterojunction SmartWire bifacial module technology.

Matthieu Despeisse received his degree in electrical engineering in 2002 from INSA in Lyon, and a Ph.D. in 2006 for his work on amorphous silicon radiation sensors vertically integrated onto integrated circuits. Since 2013 he has led research activities on crystalline silicon solar cells development at CSEM PV-Center, with a particular focus on silicon heterojunction technology, passivation contacts and metallization.

Christophe Ballif received his M.Sc. and Ph.D. degrees in physics from EPFL in 1994 and 1998, focusing on novel photovoltaic materials. He is currently Director of the IMT PV-Lab at EPFL and, since 2013, has also been Director of the CSEM-PV-Center. His research interests include thin-film silicon, high-efficiency heterojunction crystalline cells, module technology, contributing to technology transfer, and industrialization of novel devices.

Laure-Emmanuelle Perret-Aebi obtained her Ph.D. in chemistry in 2004 from the University of Fribourg, Switzerland. She is currently section head of the modules and systems sector at the CSEM PV-Center, where her main research activities focus on the development of innovative and highly reliable PV modules for various applications, such as building, mobile and ground-based power plants.

Enquiries

Gianluca Cattaneo
CSEM, PV-Center
Jaquet-Droz 1
2000 Neuchâtel
Switzerland

Tel: +41 32 720 5553
Fax: +41 32 718 3201
Email: gianluca.cattaneo@csem.ch

Market Watch

News

Obama proposes permanent extension of solar's ITC

President Obama has proposed a permanent extension of the investment tax credit (ITC) for solar energy projects in his 2016 budget.

The extension of the ITC and wind production tax credit (PTC) would be continued under his proposals. The announcement also includes an increased budget of US$7.4 billion for clean energy and a new US$4 billion fund to encourage states to accelerate their carbon reduction plans. Clean energy would be one potential use of the finance.

The US ITC is scheduled to drop from 30% to 10% at the end of 2016. Although solar enjoys bipartisan support, lobbying against the ITC extension has begun in earnest.

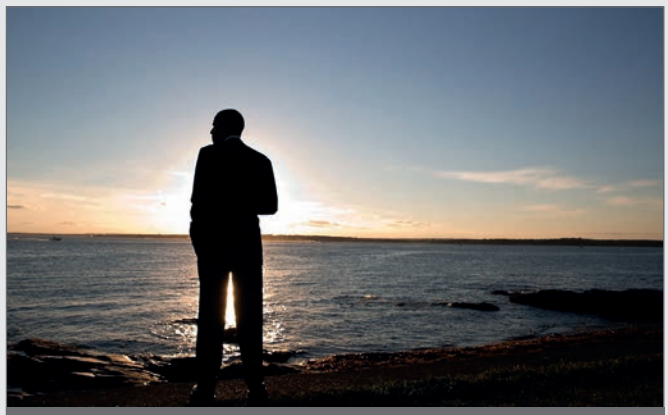

Source: Flickr/White House/Pete Souza

President Obama has proposed a permanent extension to the solar investment tax credit.

National PV market updates

Germany installed less than 1.9GW of solar in 2014

Germany installed just 1.89GW of solar power capacity in 2014, according to official figures released by the country's Federal Network Operator.

The figure falls below the 2.5GW cap introduced by the German government for 2015 onwards.

In 2013 Germany installed 3.3GW after the market slumped from 2012's 7.6GW total. Cumulative capacity has now edged past 38GW.

December saw 3,951 new installations totalling 107.6MW, up, just, from November's 105.9MW. December 2013 saw 166MW installed. Only 13 of last month's installations were more than 1MW in size.

China's NEA calls 2014 deployment at 10.6GW

China installed 10.6GW of solar in 2014, according to official data released by the country's National Energy Administration (NEA), but the final figure could in fact be higher after provinces report full-year connections, expected to be confirmed in the early part of the second quarter of 2015.

The figure includes 2.05GW of distributed PV and represents a 60% increase on the previous year.

A figure over 10.5GW had been anticipated after a meeting of the NEA in late December.

China had set an informal ambition to install 13GW in 2014, down from initial targets of 14GW with 8GW attributed to distributed generation (DG) but in mid-year that target was dropped.

Late spurt for US utility solar takes 2014 total to 3.13GW - FERC

Seventeen utility-scale PV plants totalling 618MW came online in the US in December 2014, taking the country's annual total to 3,139MW across 277 projects, official figures show.

According to the latest 'Energy Infrastructure Update' published monthly by the US Federal Energy Regulatory Commission, the US now has 11.17GW of utility solar online, representing 0.96% of the country's operating capacity.

FERC's figures show a slight drop in overall utility-scale solar installs in 2014 compared to 2013, when 364 projects totalling 3,828MW were completed.

But December 2014 saw almost double the amount of new solar capacity than the previous month, when 315MW came online, and almost 100MW more than the 519MW added in December 2013.

IHS lowers Saudi Arabia's PV forecast after push-out of renewable energy plans

Market research firm IHS has significantly lowered its PV demand forecast for Saudi Arabia in response to the country pushing back its renewable energy plans by eight years in the wake of plummeting oil prices.

IHS said that it had halved the five-year outlook for PV installations in Saudi Arabia from 1.6GW to just 800MW. Worse is that IHS expects the country to deploy the bulk of new PV capacity in the period from 2020 to 2040, with only 1GW expected to be deployed through 2020.

Saudi Arabia had previously been expected to install around 41GW of PV by 2032.

Source: SunPower Corporation

US utility-scale PV installations hit 3.13GW in 2013, according to official figures, taking the total to 11.17GW.

PV module shipments from top 20 suppliers topped 8.8GW in Q4 2014 – IHS

The top 20 PV module manufacturers shipped 8.8GW in the fourth quarter of 2014, generating an estimated US$5.9 billion in revenue, according to market research firm IHS.

Leading PV manufacturers were said to have strengthened their position in the global market last year, emphasized by a 12% increase in fourth quarter revenue, compared to the prior year period. IHS said that these suppliers accounted for 68% of global PV module demand in 2014, compared to only 60% in 2011. Based on its latest global installation forecast for 2014, shipments from the top 20 suppliers would exceed 30GW.

Japan and US to lead inverter sales in 2015 and 2016

Japan and the US will be the two largest markets for PV inverters in 2015 and 2016, according to IHS.

Despite China being the largest market for solar deployment, low prices mean it will account for 14% of inverter revenue in each of the next two years with many global suppliers opting out of the market.

IHS puts the global inverter market in 2015 and 2016 combined at US$13.2 billion. Japan is expected to continue to be the largest market by revenue capturing a quarter of the US$13.2 billion tally. The US represents 21% of this revenue during the two year period.

Despite interest from international firms in tapping into the high prices offered in the Japanese market, IHS said it continues to be dominated by domestic firms citing "a strong preference for local products and complex certification requirements".

Tough times ahead for inverter market despite steady growth: GTM

Inverter manufacturers face a growing but increasingly tough market over the next four years characterized by cost pressures and ever tighter margins, GTM Research claims.

According to the market research firm's new report, "The global PV inverter market 2015: technologies, markets and prices", global shipments of inverters will exceed 50GW this year after reaching 38.7GW AC in 2014, and then grow 13.1% annually to 2018.

But because inverter prices are expected to fall by an average 9% annually between 2014 and 2018, GTM's projected market value by that time of US$7.1 billion will represent a growth rate of only 2.8%.

"We believe the market will grow in 2015 and 2016 after declining each of the last two years," said report author and GTM Research solar analyst, Scott Moskowitz.

According to the report, a strategy by developers of lowering balance of system costs by using distributed inverters will continue to put the squeeze on central inverters.

"As the market shifts toward distributed architectures, microinverters and three-phase string inverters are gaining market share and will experience the fastest growth rates among all inverter types," said Moskowitz.

Source: SMA Solar

The US and Japan will be the two largest inverter markets this year and next year, according to IHS.

Solar took half of all renewables investment in 2014, says BNEF

Solar energy took almost half of all renewable energy investment in 2014, according to the latest figures from Bloomberg New Energy Finance (BNEF).

Investment in all renewables grew 16% in 2014 to US$310 billion. It is the first annual increase for three years but falls short of 2011's peak of US$317.5 billion. The figures include venture capital, private equity, public financing and research investment.

Asset finance for project development made up US$170.7 billion of this year's total.

Investment in the solar industry as a whole was US$149.6 billion, a 25% increase on 2013.

Solar cements status as low-risk investment in 2014

Solar's emerging status as a low-risk investment choice has been underlined by analysis revealing a 175% surge in corporate funding to the global solar industry last year.

Annual analysis by consultancy Mercom of venture capital (VC), debt and public market financing to solar reported an increase from US$9.6 billion in 2013 to US$26.5 billion in 2014.

"The big story coming out of 2014 was the revival of capital markets – solar companies were able to access funding through multiple avenues like VC, public markets, IPOs and debt in record numbers, while the quest for lower cost of capital continued with yield cos and securitisation deals," said Raj Prabhu, CEO of Mercom Capital Group. "The solar sector has come a long way from being perceived as a speculative high risk investment to attracting investors based on low risk attractive dividend yields."

According to Mercom, global VC investments performed particularly strongly last year, more than doubling to US$1.3 billion in 85 deals, compared to US$612 million across 98 deals in 2013. Mercom said downstream solar companies saw the largest amount of VC funding in 2014 with US$1.1 billion across 44 deals, accounting for 85% of venture funding.

Europe's PV researchers stake future on the power of joined-up thinking

Ben Willis, Head of Content, Solar Media

ABSTRACT

Sophia, a four-year European Commission-funded project to promote coordination across the EU's PV research community came to an end in January. With 20 partners drawn from industry and academia, the project appears to have fulfilled its aims of fostering greater collaboration. But with Europe's PV manufacturing industry facing a dire predicament in the face of competition from Asia, is it too little, too late?

What does the future hold for European PV research and development when the continent's solar manufacturing industry appears to be in the final throes of being lost altogether to foreign competitors? This question was the proverbial elephant in the room during a two-day series of events held at France's national solar institute, INES, at the end of January 2015 to mark the winding up of the Sophia project, a four-year European Commission-funded programme to promote collaboration between the continent's many PV research establishments.

The occasion was a useful opportunity to reflect on what the project had achieved over its lifetime. But during an extensive briefing for journalists at INES followed the next day by a symposium for Sophia participants, the biggest topic for discussion was not so much how the project had pushed forward the state of the art in photovoltaic technology, rather how the continent's R&D community would continue to define its place in the world when Asia is fast emerging as the dominant force in PV manufacturing.

European R&D collaboration

Launched in 2011, Sophia was awarded a €9 million grant under a European Union funding programme aimed at improving Europe's research capabilities. Its founding principle was that although a lot of good work goes on across Europe's many PV research institutes, in an age of increasing competition, efforts to improve coordination and avoid duplication were increasingly crucial to maximise its impact.

"Coordination is a key issue for EU research in general, not just for PV, to avoid overlap between all the member states," said Philippe Malbranche, incoming director general of INES and the Sophia project coordinator. "Competition is fierce worldwide and there's no use to compete between European member states and not to do the maximum to be able to compete on the international scene."

Malbranche explained how the proposal for funding for Sophia to the EU sought to

The four-year Sophia project set out with the aim of improving coordination across Europe's PV research community.

Source: CEA-INES.

engender a spirit of collaboration across Europe's PV research community by gathering together as many of the relevant organisations in the field as possible: "If there were to be two competing proposals in this field, it would have meant that some partner would be against the other. So you have to show a real willingness to coordinate everybody."

Eventually, the project secured the participation of 20 partners – 17 research bodies and three industry associations. It set out with the aim of exploring eight main research topics, covering the whole PV value chain (see box for details of partners and research topics), through three main areas of activity: networking, encompassing workshops and webinars; so-called 'transnational access', which offered industry and research centres free-of-charge access to use 48 test platforms offered by the Sophia partners, covering the project's main research topics; and joint research activities.

The latter category took place under four main themes: quicker lifetime prediction of PV modules; greater accuracy of rated power and energy output prediction of PV modules and systems; improved PV material characterisation, covering c-Si, thin-film and organic solar cells; and better modelling of PV materials, cells and modules, as well the performance of the entire PV system. In total, 50 research projects were carried out under this strand of the programme.

Malbranche said the joining up of the research efforts of a number of previously disparate entities was one of the Sophia project's first big challenges, but ultimately one of its successes.

"For instance, when you measure a PV module, one centre is going to measure it every second, the other every five seconds, another one every 10 or 30 seconds. And then when you want to compare things, it's not so simple at all," Malbranche explained. "The way to go further with collaboration is to get trust and confidence in the figures that you get and the measurements you get from one side to another if you want to compare things. And maybe you are aimed at measuring the same thing but not using the same equipment, so you need to organise a round robin and check which equipment is quickest or the most accurate. You can learn a lot from just reviewing the data; first reviewing, then exchanging and then starting to work together on some specific issues in an organised and coordinated way."

The full breadth of the joint research activities that took place under the Sophia banner and the results they generated are beyond the scope of this article to summarise. Among the highlights, Malbranche and other stakeholder colleagues in the project cited the transnational access component of Sophia as one of its great successes. The webinars too were flagged up as another of the project's highlights, in some cases attracting up to 250 viewers at a time for the more popular topics.

In terms of specific pieces of research, Malbranche pointed to the collaborative work the Sophia partners undertook in the area of accelerated ageing tests for modules as being particularly significant. "More and more you have PV modules that are passing the quality test, but which can present some defects two years after. That was not occurring so much in the past, but due to the fierce competition in which you are trying to reduce the amount of material you are trying to use in the PV module, it becomes more sensitive," he said.

"So we know the conventional test sequence which you use in the standard and we deliberately tested additional test sequences – or superimposing several constraints at the same time, which is not the case with the conventional standard. We have a complete test plan in which we tested 15 ways of degrading PV modules, not following the IEC test sequence."

Pressed on what else the project had specifically achieved in terms of advancing PV technology, Malbranche stressed that this was not the point of the project. "I understand the need of journalists to have big announcements, and for that the best thing would be to say we have developed a new cell and it has an efficiency of 25%, 45%, it's a world record, perfect. This was not at all the aim [of Sophia]. Measuring coordination is not very easy; it's little step by little step, people gradually getting to know each other."

European market difficulties

A further question that persistently arose concerned Sophia's relevance in the bigger-picture context of Europe's PV market. During the Sophia press conference, Malbranche voiced his frustration at the knock-on effect of the recent decline in the European solar market on the PV research community.

"The European market has been hit by the Asian competition, so the number of PV manufacturing companies in Europe has been decreasing a lot, which means that the equipment supplier industry is not in good shape. So that it makes at least European investors reluctant to invest [in new innovations]," he said. "If you don't have the market, then you don't have the industry, and you don't have anyone to pay for your research, even if you have some public funding."

The same issue had been graphically illustrated earlier that day during a tour of the INES laboratories, led by the institute's outgoing director general, Jean-Pierre Joly. After proudly showing off

SOPHIA partners and research topics

Partners:
CEA-INES
Fraunhofer (ISE & IWES)
ECN
IMEC
Joint Research Centre, European Commission
HZB (Helmhotz Zentrum Berlin für Materialen und Energie)
Jülich
Risö DTU (Danmarks Tekniske Universitet)
UPM
ENEL (Agenzia Nazionale per le Nuove Tecnologie, l'Energie e lo Sviluppo Economico Sostenibile)
CREST (Loughborough University)
ENEA
VTT
SINTEF (Stiftelsen Sintef)
Austrian Institute of Technology
European Photovoltaic Industry Association
EUREC (European Renewable Energy Centres Agency)
TECNALIA (Fundacion Tecnalia Research & Innovation)
DERLAB (European Distributed Energy Resources Laboratories)

Research topics:
Silicon material
Thin films
Organic PV
Modelling
Concentrating PV
Building-integrated PV
PV module lifetime
PV module and system performance

one of the advanced heterojunction solar cell prototypes developed at INES, the question of where the cell was destined for was posed. "We need to find a big investor in Europe for this, but the market is not so good," came Joly's rueful response.

And the issue erupted with some force again the next day during the Sophia project's valedictory symposium. Three representatives of Europe's declining PV manufacturing industry – from toolmaker, Meyer Burger, from Photowatt, one of Europe's few remaining integrated ingot, cell and module manufacturers, and from production system supplier, Manz – were invited to offer their views on the interplay between Europe's declining solar manufacturing industry and its research and development operation. Their assessments were not encouraging.

Sylvère Leu, chief innovation officer at Meyer Burger, urged the R&D community to "wake up", highlighting the "very, very tough" time equipment manufacturers were experiencing in the face of competition, primarily from China, where the domestic industry is sourcing more and more materials and equipment locally, effectively limiting China as a potential export market for European equipment specialists.

Leu said that for Europe to compete, it needed to build "gigawatts" of capacity to generate competitive economies of scale, meaning the R&D sector needed to produce innovation "that is ready to use".

"This is the task. I invite you to fight with us in this hard environment. We have to wake up. I have seen here a lot of strategies, a lot of technologies, but we cannot implement such a lot of tools. We need one focus. There are a lot of ideas, but the problem is choosing one idea and making it happen – this is our requirement."

Vincent Bes, chief executive of Photowatt, went a step further, warning the Sophia symposium audience that European R&D community needed "systemic" change in order to weather the storm from China. He even suggested a complete overhaul of the way Europe's PV research machine is structured.

"We won the first battle, which was to create a solar industry," Bes said, in reference to Europe's early pioneering work in PV technology. "We lost the second battle and China won everything – not because they were smarter than us, just because they were richer than us and will continue to be.

"In the next battle, if we want to survive, why don't we merge all the research centres in Europe? There are billions spent [on PV R&D] every year, but if there is no industry, what is the point? There is no point. Specialise each lab in one specific area – one lab in Switzerland could do the ingot, another one the wafer, another the cells."

Bes also urged, as a matter of necessity,

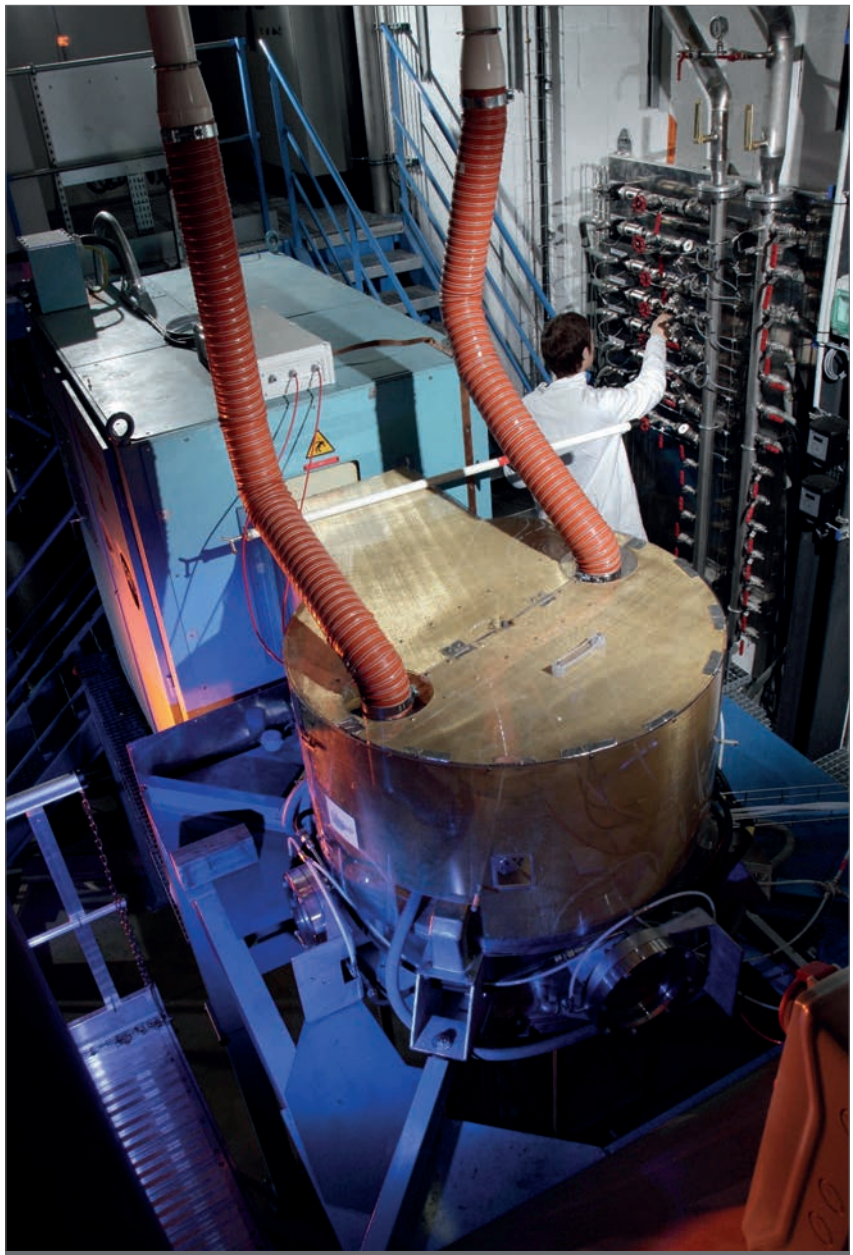

Source: CEA-INES.

The Sophia project focused on topics reflecting the whole PV value chain, from materials through to power generation.

Source: CEA-INES.

Europe's PV market decline has made industrialization of advanced PV cell designs a challenging business.

LARGE-SCALE SOLAR UK

Bristol, UK, 28-30 April 2015

MAINTAINING PROFITABILITY IN A DEVELOPING MARKET

NEW FOR 2015!

Energy Managers' Forum
Introducing 2 half-day workshops aimed exclusively at Heads of Energy and Sustainability of UK businesses. Build your contact base in this area with premier shared networking throughout the event.

Business critical sessions include:
- CfDs & government policy
- Commercial rooftops & car-park canopies
- Project finance & secondary markets
- Planning applications & the appeal process
- Grid capacity & storage solutions

For best rate tickets, confirmed speakers and attending organisations, go to **largescale.solarenergyevents.com**

Organised by: SOLAR MEDIA

Headline sponsor: LIGHTSOURCE

O&M Partner: SILVERSTONE Green Energy

Gold sponsor: Trinasolar Smart Energy Together

Brand Partner: SUNGROW

Silver sponsors: British Solar Renewables, CONERGY, BayWa r.e. renewable energy, DUPONT, JA SOLAR, UX ENERGY SERVICES, Statkraft

Supporting sponsors: S&C, LDA DESIGN, Viking

Lunch sponsor: JinKO Solar

Source: CEA-INES.

INES near Chambery, France, the coordinating institute for the Sophia project.

closer working between Europe's R&D centres and European PV equipment manufacturers. "All the ideas you have in your heads, come and work with these people, because if your ideas can't be transferred into tools, it's useless – it's academic, hopeless. I respect schools and academies, but that's wishful thinking to create jobs in the future," Bes said.

He added that without urgent action, Europe's solar R&D community would soon face a similar problem to the one experienced over the past few years by its PV manufacturers, who have seen 85% of their jobs disappear. "How many jobs have been lost in R&D over last three years? I think it increased 25, 30%, so there is a big question mark: our situation is just a mirror of what your situation will be in the coming years. So if we don't want that to happen – and I don't want that to happen, because we need you – we need systemic change, and that has to be done by the European Commission."

Influencing policymakers

In the context of these macro-scale issues, which are of course inextricably linked to European energy and industrial policy, not to mention global trade forces, it was difficult not to wonder whether despite its laudable aims, the Sophia project amounted to little more than tinkering around the edges. And yet, the collaborative spirit apparently engendered by the project could prove to be the very platform needed to help the European solar industry survive.

Responding to the challenge to the European Commission laid down by Vincent Bes, Paul Verhoef, head of the renewable energy unit in the commission's directorate general of research and development, and another panellist at the Sophia symposium, said there was a job for the European PV industry to communicate what it needs in order for the commission to respond in the right way.

"One can go to politicians either in Brussels or nationally to say we have a problem and we need help, but the first reaction you're going to get is fine, we've seen it, so what do you want help for, what are you going to try new, what is your plan, what can we support? I don't see the plan," he said.

"So let's see if we can get some sharp analysis and proposals on the table with which we can collectively go to politicians and say we've learned from the past, this is the way we're tying to reshape it, this is what we want to do, and move forward on that basis. Because otherwise I don't think you're going to get a very good reaction," Verhoef said.

Although Verhoef implied that policymakers in Europe were prepared to listen, he made it clear there would be no free meal tickets and that it would be up to the PV industry to communicate with one voice exactly what it wanted. In that context, the relevance of Sophia's legacy of closer relationships across Europe's PV community looks very different.

Future collaboration

The good news is that a successor project to Sophia is already up and running: Cheetah, the somewhat stretched acronym for 'Cost-reduction through material optimisation and Higher EnErgy outpuT of solAr pHotovoltaic modules'. Cheetah will have many of the same partners as Sophia and even some new ones, and focus on many of the same topics. Less encouraging is that Cheetah will not, as things stand, carry on exactly the same activities as Sophia.

One source of disappointment is that Cheetah is not expected to continue the policy of free access to partners' research facilities instigated under Sophia. The continuation of this was one of a number of recommendations in a 'Strategic Vision on Photovoltaic Research Infrastructure' document published by the Sophia partners to mark the project's conclusion.

"The fee access [will end] but the staff exchange may go on, which is important," said Malbranche. "One of the successful things within the Sophia project was the workshops and especially the webinars. These will go on. The coordination of testing procedures.... All these, which were activities within the Sophia project, are still activities within the Cheetah project. The free access to some facilities – that was something specific from Sophia, and it's something that's currently not designed in the type of project such as Cheetah."

Also unclear is the fate of other proposals in the Sophia strategic vision document, such as the concept of establishing a number of large-scale pilot production lines to test-manufacture new PV technologies at meaningful volumes ahead of full industrial transfer. "When a manufacturer wants to check on real capacity, the yield and efficiency that you get using this equipment and this process, we could imagine some kind of coordination of several pilot lines at a European level. This is something which is not existing," said Malbranche.

Another recommendation made in the report is the necessary 'e-infrastructure' to link databases drawn from collaborative research work and make them readily accessible to researchers. "PV is going to be used in millions or tens of millions of installations, and it's good to be able to have as quickly as possible some feedback on the performance of a new technology," said Malbranche. "The idea is to have the tools to be able to do the same thing we have done within Sophia but within a more systematic way and organise the databases a user-friendly way."

Such proposals clearly have resource implications, and as such will most likely require backing from the commission. But as Verhoef made clear, such support will only be forthcoming if the argument for it is made coherently and by an industry speaking with one voice. Sophia would seem to have begun that process. The question now is whether it will be continued with sufficient vigour to prevent Europe's PV research community suffering the same fate as its manufacturers.

A full description of the activities and research projects carried out as part of the SOPHIA project can be found at http://www.sophia-ri.eu/fileadmin/SOPHIA_docs/documents/Communication/EUREC_SOPHIA-Booklet_2014_v5.pdf

Photovoltaics International

Advertisers & Web Index

ADVERTISER	WEB ADDRESS	PAGE NO.
ASYS Auto GmbH	www.asys-solar.com	49
Heraeus Precious Metals	www.pvsilverpaste.com	OBC
Intersolar	www.intersolarglobal.com	5
JA Solar Holdings Co., Ltd	www.jasolar.com	IFC
Lamers High Tech Systems BV	www.lamershts.com	13
Large-Scale Solar UK	largescale.solarenergyevents.com	97
MacDermid Inc	photovoltaics.macdermid.com	47
Manz AG	www.manz.com	71
Meco Equipment Engineers B.V.	www.besi.com	51
PV-Tech Power	pv-tech.org/power	60
Rena GmbH	www.rena.com	47
Schmid Group	www.schmid-group.com	19
SNEC	www.snec.org.cn	IBC
Solar Media Events	www.solarenergyevents.com	85
SoLayTec BV	www.solaytec.com	13
Tempress Systems	tempress.nl	51
Von Ardenne GmbH	www.vonardenne.biz	75
Wuxi Suntech Power Co Ltd	www.suntech-power.com	3

To advertise within Photovoltaics International, please contact the sales department: Tel +44 (0) 20 7871 0122

Lightweight module durability: Working to address a market barrier

According to the US Department of Energy 2012 SunShot Vision Study, 85% of the worldwide PV module market consists of a single product design: 60-cell and 72-cell crystalline silicon glass modules with an aluminium frame. These conventional modules follow a similar design and installation process that satisfies many solar consumers' needs; however, for sites with weight constraints and high supply chain costs, lightweight modules may be preferable.

The idea of producing lightweight modules is not new. What comes to mind first when people think about lightweight PV is often thin-film PV, which has so far struggled to be competitive with traditional crystalline silicon wafer modules in cost and in efficiency.

The strategy of several new players in the market is to focus on the use of crystalline silicon-based absorbers, while replacing the glass front sheet with a thin transparent polymer sheet and using a back panel for structural stability. By removing the glass and aluminium frame the weight can be reduced by as much as 85% compared to a typical PV module. The lightweight modules developed using this approach have the following benefits:

- A lower module weight enables PV on weight-constrained buildings due to the reduced roof load.
- Transportation costs decrease drastically.
- The use of high-efficiency crystalline silicon solar cells leads to a superior power-to-weight performance.
- The fluoropolymer front sheet has typically over 95% optical transparency and lowers the glare, allowing use where glare is a critical safety issue, e.g. around airports or military bases.
- Innovative mounting approaches (such as adhesive mounts) minimize roof penetration, reduce the weight of installation even further, are less susceptible to wind loads and are generally more aesthetically favourable to the customer.

Despite this set of benefits, before lightweight modules are broadly adopted it is important that module durability questions are addressed. The differences in the structural make-up and assembly of lightweight modules mean that the long-term effect of the design changes on module durability is unknown, which results in market uncertainty.

In today's market, conventional modules are certified to established standards including IEC 61215 for crystalline silicon modules, IEC 61646 for thin-film modules and IEC 62108 for CPV modules. These qualification tests have the purpose of identifying design, materials and process flaws, which can lead to premature field failures.

These same qualification tests are currently being used to test lightweight modules, and the absence of testing standards that are specifically targeted to lightweight non-glass modules represents a major barrier to market growth. Therefore, more work is needed to determine what changes to the current qualification test protocols are appropriate for lightweight module testing. Below we explore two specific types of tests that should be adapted to account for the differences in lightweight modules.

Stress Testing: A module certification testing protocol must address both degradation and damage caused by potential stresses during installation as well as operation. Specifically, a module durability standard must include testing under typical mechanical loads that the module would experience on a rooftop, as well as the loads experienced during handling and transportation. The threshold parameters for these tests relate in part to module weight and, therefore, are different for lightweight modules compared to conventional modules.

Source: Fraunhofer CSE

Fraunhofer researchers installing a prototype lightweight PV module in a trial funded by the US Department of Energy.

Hail Testing: Many conventional glass modules show no degradation due to the hail test, and if a glass module fails the hail test it is commonly due to the front glass shattering. However, glassless modules cannot shatter. Studies conducted by Saint-Gobain Solar have shown that the module power reduction after the hail impact testing is well below 5%, which is the pass/fail criterion for the power decrease in the IEC61215 standard. Testing by D2Solar that the mechanical impact results in substantial cracking of the c-Si solar cells.

It is unclear whether subsequent field exposure over many years would cause the opening of tightly closed cracks or crack propagation and thus cause further unacceptable power degradation. In order to evaluate whether the hail damage will lead to further power reduction a subsequent thermal cycling sequence on the hail-tested modules should be performed.

At the Fraunhofer Center for Sustainable Energy Systems, researchers are working to address these issues by developing durability and robustness tests specifically designed to assess glassless and frameless module performance. Their work is evaluating vulnerabilities specific to lightweight modules that affect performance in durability testing, including:

- Cracks in solar cells and ribbons due to shocks during manufacturing, handling and installation, mechanical impact from hail and increased thermal stresses.
- Corrosion due to increased moisture permeation through the polymeric front-sheet and the lack of a frame.
- Encapsulant degradation due to increased moisture ingress

Thorough work to establish an appropriate durability standard for lightweight modules is an important next step in supporting this technology's entry into the market. If the industry can deliver lightweight modules with demonstrated durability, at low cost to the consumer, the PV market will expand even more dramatically.

This is an edited version of a blog post that first appeared on www.pv-tech.org.

Dr Cordula Schmid is a PV scientist at the Fraunhofer Center for Sustainable Energy Systems CSE in Boston, USA.

SNEC 9th (2015) International Photovoltaic Power Generation Conference & Exhibition

SNEC 2015
PV POWER EXPO
Dialogue & Conference & Exhibition

www.snec.org.cn

180,000sqm	1,800+	5,000+	150,000
Exhibition Space	Exhibitors	Professionals	Visitor Attendances

28-30 April 2015

Shanghai New International Expo Center

(2345 Longyang Road, Pudong District, Shanghai, China)

member of GLOBAL SOLAR ALLIANCE

Tel: +86-21-64276991 +86-21-33561099

Fax: +86-21-33561089 +86-21-64642653

For exhibition: info@snec.org.cn

For conference: office@snec.org.cn

Heraeus

efficiency

Wisdom creates efficiency.

Our Research and Development team is constantly thinking about paste. We are committed to developing leading-edge solutions, which improve the power output and performance of solar cells at a lower cost per watt. We are always mindful of the current and future technology needs of our customers, and are driven to deliver results. So when you think of paste...think of Heraeus.

Leadership through R&D. Breakthroughs via innovation. Achievement by tradition.

Visit us at:
SNEC I Hall W3, Booth 660 I April 28th - 30th

Heraeus Photovoltaics Business Unit
www.pvsilverpaste.com
China I Singapore I Taiwan I Europe I America I Japan